Cover Page

Universiteit Leiden



The handle http://hdl.handle.net/1887/20555 holds various files of this Leiden University dissertation.

Author: Putten, Maaike van
Title: The influence of low dystrophin levels on disease pathology in mouse models for Duchenne Muscular Dystrophy
Issue Date: 2013-02-26

The influence of low dystrophin levels on disease pathology in mouse models for Duchenne Muscular Dystrophy

Maaike van Putten

Cover: Dystrophin distribution in the quadriceps of a 16-week-old *mdx-Xist*$^{\Delta hs}$ mouse.
Layout: Maaike van Putten and Bas Brunink
Printing: Off Page, Amsterdam
ISBN: 978-94-6182-239-0

The studies described in this thesis were financially supported by grants from the Dutch Duchenne Parent Project, the Dutch organization for scientific research (NWO/ZonMW) grant numbers 43200002 and 95100102, FP6 funded TREAT-NMD network of excellence (LSHM-CT-2006-036825) and the FP7 BIO-NMD project (FP7-HEALTH-241665).

Columbus Instruments and Prosensa Therapeutics B.V. are gratefully acknowledged for covering part of the printing costs.

Copyright © 2013 M. van Putten, All right reserved. No part of this thesis may be reproduced or transmitted in any form or by any means, without the prior permission in writing of the author.

The influence of low dystrophin levels on disease pathology in mouse models for Duchenne Muscular Dystrophy

Proefschrift

ter verkrijging van
de graad van Doctor aan de Universiteit Leiden,
op gezag van Rector Magnificus prof.mr. C.J.J.M. Stolker,
volgens besluit van het College voor Promoties
te verdedigen op dinsdag 26 Februari 2013
klokke 13:45 uur

door
Maaike van Putten
geboren te Haarlem
in 1984

Promotiecommissie:

Promotor:	Prof.dr. G.J.B. van Ommen
Co-promotor:	Dr. A.M. Aartsma-Rus
Overige leden:	Prof.dr. S.M. van der Maarel Prof.dr. J.J.G.M. Verschuuren Prof.dr. A. De Luca[1] Dr. L. van der Weerd

[1]) Department of Pharmacobiology, University of Bari, Bari, Italy

Contents

		Page
Chapter 1.	**General Introduction**	
1.1.	**Duchenne Muscular Dystrophy**	
1.1.1.	Clinical phenotype	11
1.1.2.	The *DMD* gene and dystrophin	12
1.1.2.1.	The *UTRN* gene and utrophin	14
1.1.3.	Muscle pathology	16
1.1.4.	Antisense-mediated exon skipping	19
1.1.4.1.	The concept of exon skipping	20
1.1.4.2.	Clinical trials	25
1.1.4.3.	Hurdles to overcome	27
1.2.	**Mouse models for DMD**	
1.2.1.	The *mdx* mouse	29
1.2.1.1.	Skeletal muscle histopathology	29
1.2.1.2.	Neuromuscular junction and skeletal muscle pathology	31
1.2.1.3.	Pathology of the heart	34
1.2.1.4.	Limitations of the *mdx* mouse	35
1.2.2.	The *mdx*$^{2\text{-}5cv}$ mouse models	36
1.2.3.	The *mdx52* mouse	38
1.2.4.	The *mdx/utrn* $^{-/-}$ mouse	39
1.2.5.	The *mdx/utrn* $^{+/-}$ mouse	42
1.3.	**Low dystrophin levels in human and mice**	
1.3.1.	DMD and BMD carriers	44
1.3.2.	BMD patients	45
1.3.3.	Mouse models expressing low dystrophin levels from birth	45
1.3.4.	Treated *mdx* mice expressing low dystrophin levels	47
1.3.5.	The *mdx-Xist*$^{\Delta hs}$ mouse	48
1.3.5.1.	X-inactivation	48
1.3.6.	The *mdx/utrn* $^{-/-}$ */Xist*$^{\Delta hs}$ mouse	50
1.4.	**Outcome measures**	
1.4.1.	Functional tests	51
1.4.2.	Heart function	53
1.4.3.	Serum and gene biomarkers	55

		Page
Chapter 2.	A 3 months mild functional test regime does not affect disease parameters in young *mdx* mice (*NMD 2010, 20, 273-280*)	57
Chapter 3.	Comparison of skeletal muscle pathology and motor function of dystrophin and utrophin deficient mouse strains (*NMD 2012, 5, 406-417*)	71
Chapter 4.	Serum Matrix Metalloproteinase-9 (MMP-9) as a biomarker for monitoring disease progression in Duchenne Muscular Dystrophy (DMD) (*NMD 2011*, *21, 569-578*)	89
Chapter 5.	The effects of low levels of dystrophin on mouse muscle function and pathology (*PLoS One 2012, 7, e31937*)	105
Chapter 6.	Low dystrophin levels in heart are sufficient to delay heart failure in *mdx* mice (*Submitted*)	127
Chapter 7.	Low dystrophin levels increase survival and improve muscle pathology and function in dystrophin/utrophin double knockout mice (*Submitted*)	143
References		165
Discussion		181
Summary		183
Samenvatting voor niet ingewijden		185
Bibliography		187
Curriculum Vitae		188
Acknowledgements		189

Chapter 1.

General Introduction

1.1. Duchenne Muscular Dystrophy

1.1.1. Clinical phenotype

Edward Meryon, an English physician, was the first to publish on an inherited disorder we now refer to as Duchenne muscular dystrophy (DMD). In 1852, he described the clinical manifestations of eight affected boys from three families in great detail (Meryon 1852). At the time, Meryon already observed that the progressive muscle wasting and weakness was restricted to muscle and did not affect the nervous system. The disorder was later named after Guillaume Benjamin Amand Duchenne who was the first to study DMD patient biopsies (Duchenne 1868).

Muscle fibers of DMD patients are vulnerable to exercised-induced damage and despite efforts to regenerate, muscle mass is gradually lost resulting in progressive muscle weakness. In DMD patients, the first symptoms become apparent between the age of two and five years and consist of pseudohypertrophy of the calf muscles and difficulties in running, jumping and climbing stairs. Eventually, patients lose muscle coordination, have difficulties walking and rise from the ground by using their arms to climb up their body, which is known as Gower's sign (Gowers 1879). Early in the second decade, patients become wheelchair dependent due to loss of strength in the lower limb muscles. Subsequently, progressive weakness of the shoulder girdle and arms results in loss of function in all extremities (Blake et al. 2002).

Also the heart is affected in more than 90% of the DMD patients. Cardiac involvement is already found in 25% of patients under the age of six. This is recognizable by minor electrocardiographic (ECG) and echocardiographic signs, in the absence of symptoms. Clinical cardiomyopathy is observed from the age of 10 onwards and is first characterized by myocardial hypertrophy in which the interventricular septum is thickened followed by dysrhythmias. Infiltration of fibrotic tissue starts at the left ventricular wall and progressively spreads throughout both ventricles. It eventually results in cardiomyopathy in which chambers are dilated and ventricles have poor contractility resulting in a decreased ejection fraction. The left ventricular posterobasal and lateral walls are predominantly affected (Finsterer and Stollberger 2003).

Patients also develop thoracolumbar scoliosis, for which they can undergo spinal stabilisation surgery (Eagle et al. 2007;Kohler et al. 2005). This deformity of the spinal cord is thought to result from asymmetric weakening of the muscles that support the spinal column (Oda et al. 1993). In the late teens, they develop respiratory impairment and need assisted ventilation first primarily at night, but in more advanced stages in a chronic manner (Lo Mauro et al. 2010). With smooth muscles being affected as well, DMD patients often suffer from bloating, feeling of fullness and constipation (Borrelli et al. 2005). Also cases of acute gastric dilatation and intestinal pseudo-obstruction have been reported. As a consequence of their immobility, body composition is altered with a low bone mineral density, lower lean tissue and higher fat mass compared to healthy age-matched boys. At the age of 13, 44-54% of DMD patients become obese, but the same percentage of boys is underfed when they are 18 years old, primarily resulting from swallowing difficulties (Martigne et al. 2011).

The function of the retina is affected as well. Especially boys that lack the dystrophin isoform Dp260 (see below) often have difficulties in red-green discrimination (Pillers et al. 1999;Costa et al. 2007). The average IQ is one standard deviation below the mean and 20% of the patients have an IQ of less than 70. Learning disabilities, involving dyslexia and dyscalculia are common. However these non-muscle related symptoms are not of a progressive nature (Billard et al. 1992;Emery 1993).

Although improved health care has increased the life expectancy in the Western world, most DMD patients die in their third or fourth decade due to heart or respiratory problems (Eagle et al. 2007).

1.1.2. The *DMD* gene and dystrophin

With an incidence of 1 in 3500 newborn boys, DMD is the most common inherited neuromuscular disorder. It is caused by mutations in the *DMD* gene which is located on the short arm of the X-chromosome (Xp21). It is the biggest known human gene (2.4 Mb) and is also extremely large in other organisms like the mouse, zebra fish and drosophila. The majority of the gene consists of intronic regions, since the coding sequence, ~14 kb spread over 79 exons, only accounts for 0.6% in man (Koenig et al. 1987;Muntoni et al. 2003;Roberts et al. 1993).

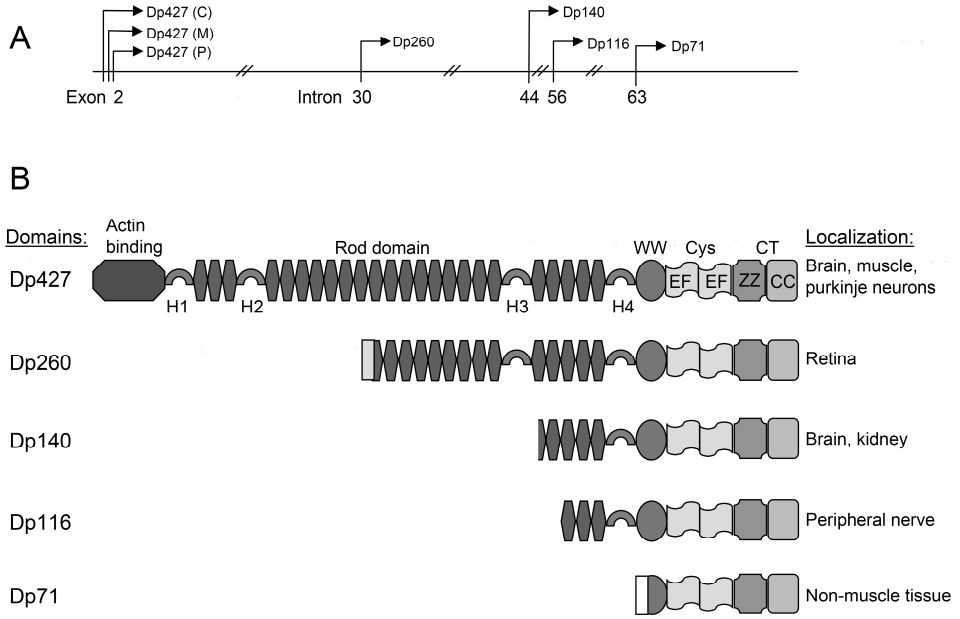


Figure 1. Schematic overview of the different dystrophin isoforms.
A. Five different promoters spread throughout the *DMD* gene ensure transcription of seven dystrophin isoforms; three full-length and four shorter proteins. **B**. Full-length dystrophin is composed of an actin-binding domain, four hinge sites (H1-4), a central rod domain, a WW domain, a cysteine-rich domain (consisting of 15 cysteines, two EF hand motifs and a ZZ domain) and a C-terminal domain (consisting of two coiled coil-domains). None of the smaller isoforms contains the N-terminal actin-binding domain and most lack great parts of the central rod domain. Dp71 even lacks the central rod domain entirely (Figure is based on Willmann et al. NMD 2009).

The *DMD* gene codes for the protein dystrophin of which different isoforms are expressed in several tissues. The isoforms originate from seven promoters spread along the gene (Figure 1). Full-length dystrophin is synthesized from three promoters located before the common exon 2. The isoforms are named after the molecular weight of the protein and the tissue of origin. The Dp427m isoform is synthesized in skeletal and cardiac muscle (Gorecki et al. 1992;Muntoni et al. 2003). The cortical neurons and the hippocampus of the brain synthesize Dp427c, while Dp427p is found in cerebellar Purkinje cells and in lower levels in skeletal muscle. Full-length 427m

dystrophin consists of 3685 amino acids. It takes approximately 12 hours to transcribe 1,770 kb, extrapolating to a transcription time of ~16 hours for the entire gene (Tennyson et al. 1995). It is expressed in very low levels in muscle (0.002% of total muscle protein). Full-length dystrophin contains four domains (Koenig et al. 1988). The N-terminal actin-binding domain is the first distinctive domain. This domain contains two actin-binding sites and facilitates binding of dystrophin to filamentous actin (F-actin) in the subsarcolemmal cytoskeleton. This domain is followed by the central rod domain which consists of 24 triple-helical repeats making it the largest domain. These repeats are interspersed by 4 proline-rich hinge regions (H1-4) (Koenig and Kunkel 1990). The rod domain provides flexibility and elasticity to the protein.

An additional actin-binding domain is located between repeat unit 11-17 (Rybakova et al. 1996) and a neuronal nitric oxide synthase (nNOS) binding domain is present in repeat unit 16-17 (Lai et al. 2009).

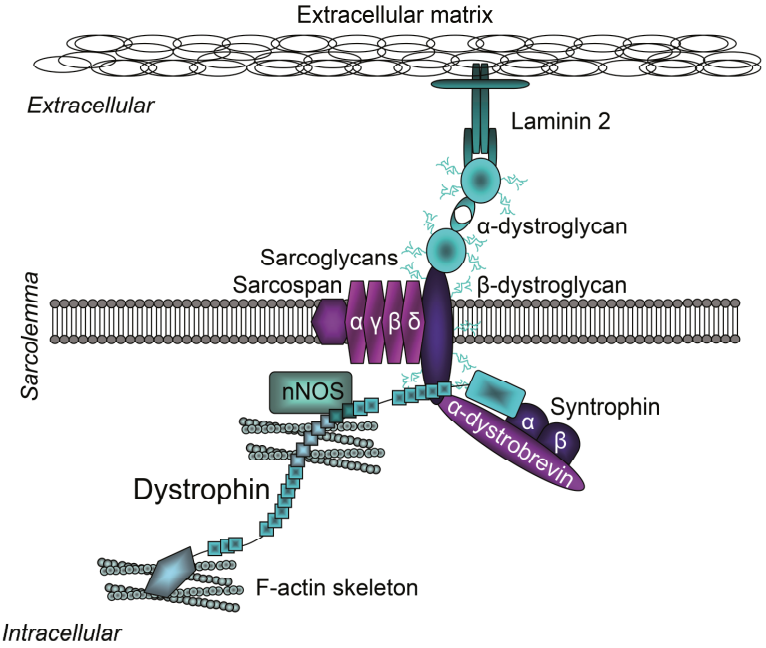


Figure 2. Dystrophin-glycoprotein complex in skeletal muscle.
Dystrophin binds with the N-terminus to the F-actin skeleton of the cell and with the C-terminus to the DGC which is linked to the extracellular matrix. The DGC consists of multiple proteins. Several muscular disorders are caused by the absence of some of these proteins.

The last two domains are the cysteine-rich domain, which includes 15 cysteines, two EF hand motifs and a ZZ domain, and the C-terminal domain that consists of two stretches that form X-helical coiled coil-domains (Koenig et al. 1988). The cysteine-rich domain promotes binding to and localization of the dystrophin-glycoprotein complex (DGC) and contains the domain that binds to β-dystroglycan.

Internal promoters allow the production of four smaller isoforms called Dp260 (retina), Dp140 (brain, kidney, blood vessels and retina), Dp116 (Schwann cells of the peripheral nerves) and Dp71 (most non-muscle tissues). Those proteins lack the actin-binding domain and part of the central rod domain. Dystrophin is located underneath the membrane of muscle fibers, where

the N-terminus binds the intracellular F-actin of the cytoskeleton while the C-terminus connects with the transmembranal DGC that is in turn connected to the extracellular matrix (ECM) (Figure 2). In this way, dystrophin provides stability to muscle fibers during contractions, but it also plays a role in cell signaling. The DGC is a large protein complex that contains, amongst others, sarcoglycans, sarcospan, dystroglycans, syntrophins and dystrobrevins (Ehmsen et al. 2002). Various muscle disorders have been linked to the absence of some of these proteins, where the absence of sarcoglycans or the improper glycosylation of dystroglycans result in various types of Limb girdle muscular dystrophy (Sciandra et al. 2003;Muntoni et al. 2008). In the absence of dystrophin, expression of these proteins is largely reduced and localization at the sarcolemma is lost.

1.1.2.1. The UTRN *gene and utrophin*

In addition to the dystrophin isoforms, also three dystrophin homologues have been described. These share homology with large proportions of dystrophin and are called utrophin (first referred to as dystrophin related protein 1), dystrophin related protein 2 and dystrobrevin. Utrophin is most similar to dystrophin and is the most relevant homologue for the DMD field (Love et al. 1989b). It is transcribed from the *UTRN* gene (0.9Mb) located on chromosome 6 and contains 74 exons. The full length protein is 395kDa and consists of an N-terminal actin-binding domain, a central rod domain, a cysteine-rich and C-terminal domain (Figure 3). Compared to dystrophin, utrophin lacks repeat units 15 and 19 and hinge regions 1 and 3 (Blake et al. 2002;Winder et al. 1995).

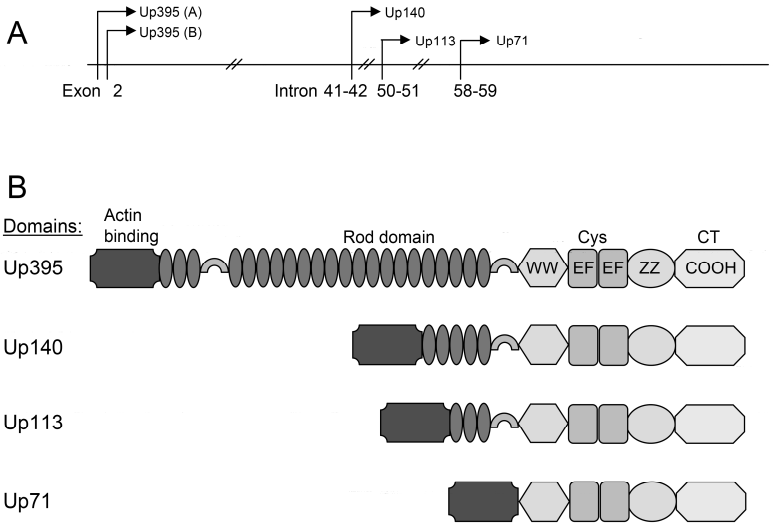


Figure 3. Utrophin isoforms.
A. Representation of the *UTRN* gene with two different promoters giving rise to full-length utrophin A and B, which are expressed at the neuromuscular junction and in vascular endothelial cells respectively. Downstream of the gene, three additional promoters synthesize shorter isoforms. **B**. Schematic representation of full-length utrophin and the three shorter isoforms. The protein structure of full-length utrophin is largely identical to that of dystrophin (Figure design is based on Willmann et al. NMD 2009).

Full-length utrophin is transcribed from two independent promoters; *Utrn-A* and *Utrn-B*, resulting in distinct proteins that differ at the initial 5' ends and in localization as utrophin A is expressed at the neuromuscular junction (NMJ) while utrophin B is expressed at the vascular

endothelium. Like dystrophin, utrophin also has three shorter isoforms; Up140, Up113 (G utrophin) and Up71 (Perronnet and Vaillend 2010;Burton et al. 1999;Dennis et al. 1996;Wilson et al. 1999). Similar to how dystrophin links actin to the DGC complex in muscles, utrophin links actin to a DGC-like complex present at the synaptic membrane, which contains agrin, rapsin and acetylcholine receptors (AChRs) in addition to proteins found in the DGC complex found for dystrophin (Figure 4) (Apel et al. 1995;Haenggi and Fritschy 2006). The expression of utrophin and dystrophin at the synaptic membrane does not overlap.

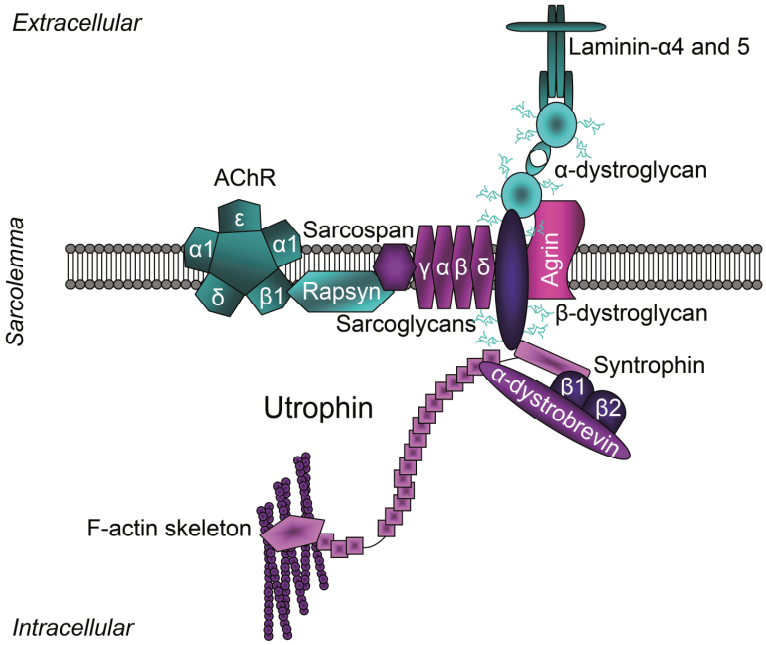


Figure 4. Utrophin-glycoprotein complex at the synaptic membrane.
Utrophin binds with the N-terminus to the F-actin skeleton and with the C-terminus to the DGC. The composition of the synaptic DGC is slightly different from that found at the muscular sarcolemma, e.g. at the synapse, laminin α4 and 5, syntrophin β1 and 2 are expressed whereas laminin α2 and syntrophin α1 and β1 are found at the muscular sarcolemma. Also additional proteins like agrin, rapsyn and the acetylcholine receptors are present at the synaptic membrane.

In heart, utrophin is localized at intercalated discs and microvasculature smooth muscle (Hainsey et al. 2003). During development, in both healthy and DMD foetuses, utrophin A is expressed in developing and regenerating muscle fibers along the entire sarcolemma. In maturing fibers, it is replaced by dystrophin at the sarcolemma and is then solely expressed at the NMJ where it colocalizes with AChRs. It participates in postsynaptic membrane maintenance and AChR clustering (Nguyen et al. 1991;Clerk et al. 1993). In DMD patients and the *mdx* mouse however, overexpression of utrophin A is observed at the sarcolemma in mature muscle fibers compensating for the absence of dystrophin. Although this, to some extent, partially rescues the dystrophic phenotype in mice, overexpression is too low to prevent muscle degeneration in DMD patients. However, the degree in which utrophin is expressed, correlates with disease severity (Kleopa et al. 2006). Mice that lack utrophin (*utrn* $^{-/-}$) but express dystrophin appear healthy and show no muscle pathology, whereas mice that lack both proteins (*mdx/utrn* $^{-/-}$) are very severely affected.

1.1.3. Muscle pathology

In DMD patients, the absence of functional dystrophin leads to a series of events, which finally result in replacement of muscle fibers by fibrotic and fat tissue. The exact cause of initiation of this pathological cascade is not fully understood, but several hypotheses have been proposed to explain why the absence of dystrophin results in vulnerable fibers and degeneration (Figure 5).

As mentioned before, dystrophin links the actin filaments to the DGC, maintains fiber integrity during eccentric contractions and plays a role in signaling. In the absence of dystrophin, muscle contractions result in disruptions of the membrane and thereby increased membrane permeability. The presence of these membrane tears is evident by elevated serum creatine kinase (CK) levels. CK is an enzyme that catalyses the conversion of creatine into phosphocreatine turning adenosine triphosphate (ATP) into adenosine diphosphate (ADP). Muscles consume ATP in large amounts and CK is mainly found in this tissue. Upon fiber damage, CK leaks through tears in the membrane into the bloodstream resulting in very high levels of 20,000 to 50,000 U/L (normal human values <200 U/L) (Emery and Muntoni 2003). This process is known to be exacerbated by exercise. Even in healthy individuals, CK levels are elevated after a bout of strenuous exercise as a consequence of membrane disruptions.

Through the same membrane tears from which CK leaks out of the fibers, extracellular Ca^{2+} passively enters. In addition, Ca^{2+} enters the fibers actively through mechanosensitive stretch-activated (SAC) channels. DMD patients have increased numbers of SAC channels and they are also more active than those in healthy individuals. The increased Ca^{2+} level causes a disruption of the intracellular Ca^{2+} homeostasis (Allen et al. 2010;Deconinck and Dan 2007). The Ca^{2+} also activates proteases like calpain, which degrade a wide range of skeletal muscle proteins, causing more membrane damage and also activate the SAC channels further, enabling more Ca^{2+} to enter and thereby creating a feedback loop of Ca^{2+} entering the fiber, eventually resulting in fiber death. To some extent, excessive intracellular Ca^{2+} will be taken up by mitochondria (Blake et al. 2002;Chen et al. 2000). However, due to the chronic nature of the disease, mitochondria get structurally damaged, inducing the downregulation of several important genes. This results in malfunction of mitochondria, leading to impaired oxidative phosphorylation and thereby a loss of energy. In addition, damaged mitochondria cause reactive oxygen species (ROS), produced by inflammatory cells like neutrophils and macrophages (Whitehead et al. 2006). ROS promote activation of transcription factor nuclear factor NF-κB, which regulates the expression of pro-inflammatory cytokines like TNF-α and Interleukine (IL)-1B. NF-κB itself inhibits muscle cell differentiation and thus the regeneration process. ROS levels are further increased via a positive feedback loop in which TNF-α exacerbates inflammation. The elevated ROS levels can be scavenged by nitric oxide (NO). NO is formed by nNOS and functions as an endogenous messenger molecule and induces vaso-dilatation. In healthy individuals nNOS is recruited to the membrane by dystrophin. In DMD patients, the absence of dystrophin results in de-localization of nNOS, forcing it to freely float in the cytoplasm (Lai et al. 2009). Since nNOS levels are decreased in DMD patients, NO levels are also largely reduced which disallows fibers to decrease ROS levels and thereby exacerbates continuous fiber damage by ROS.

The pathological cascade initiated by disrupted calcium homeostasis eventually results in fiber necrosis, which induces a chronic inflammatory response that triggers fibrosis. The immune response consists of numerous components including leukocyte adhesion, chemokine signaling, diapedesis, invasive cell type specific markers and complement system activation. The inflammatory cells produce cytokines and other toxins that further damage the muscle fibers.

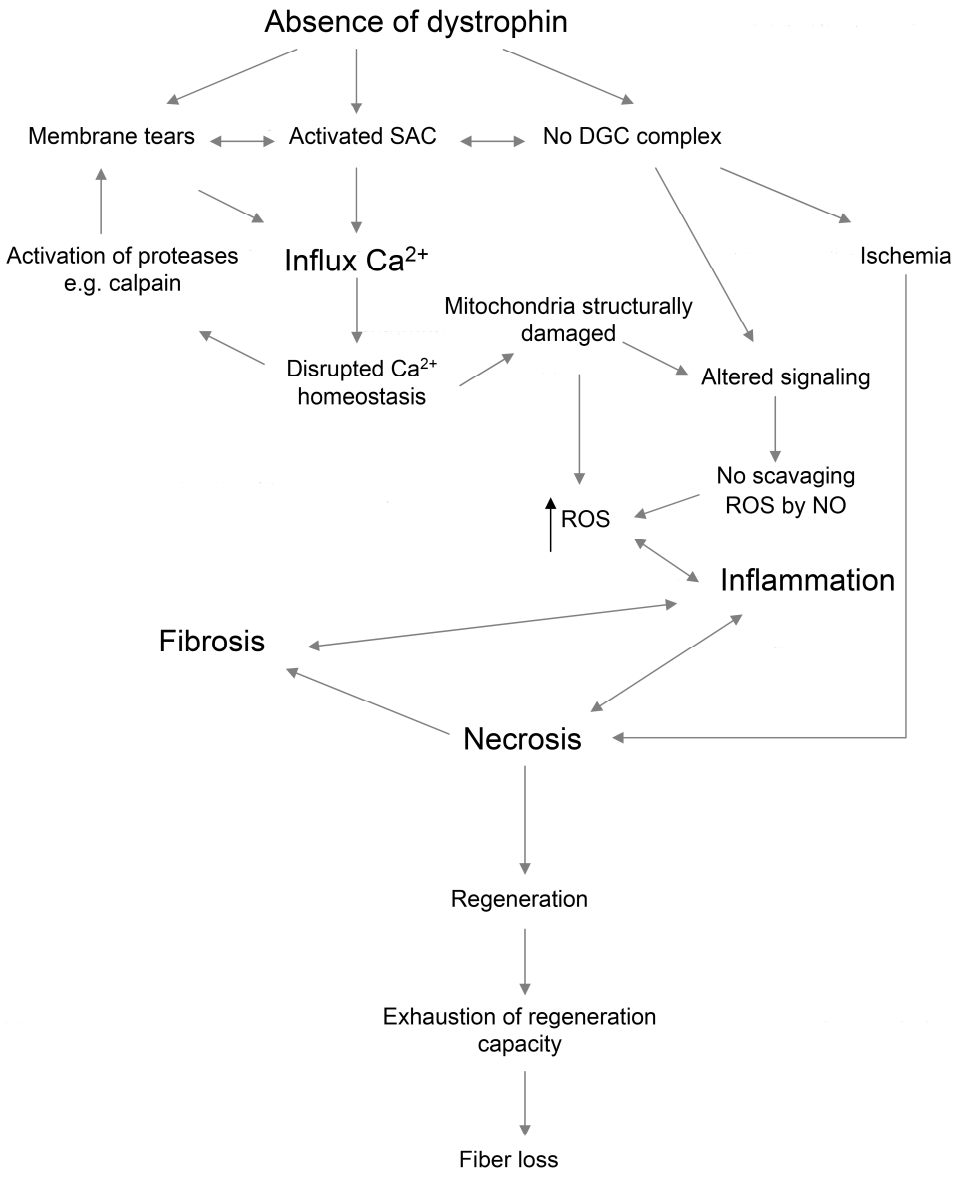


Figure 5. Schematic overview of pathogenesis in skeletal muscles of DMD patients.
In absence of dystrophin an extensive cascade of pathological events is chronically triggered that eventually results in the replacement of muscle fibers by connective and fat tissue leading to loss of muscle function.

Blood vessel abnormalities, including impaired vasodilatation resulting from low NO levels, have been reported in DMD patients. Especially during exercise, when the need of oxygen is higher, muscle ischemia may occur (Miike et al. 1987;Saito et al. 2005;Sander et al. 2000). In skeletal muscle, degenerated fibers are replaced through regeneration. This does not occur in heart as cardiomyocytes do not contain satellite cells (Blake et al. 2002;Deconinck and Dan 2007).

Regenerated fibers are characterized by central nucleation which originates from the differentiation and fusion process of myoblasts into myotubes. Additionally, to compensate for the loss of force-generating capacity, muscles increase in mass by undergoing hypertrophy (Karpati et al. 1988;Narita and Yorifuji 1999). Upon exhaustion of the regenerative capacity, fibers are gradually replaced by connective and adipose tissue. With decreased numbers of muscle fibers from which CK leaks out, serum CK levels drop. The described pathological hallmarks are clearly visible in DMD patient biopsies, which contain groups of necrotic or degenerated fibers, fibrotic and fatty tissue.

Although muscle sections of DMD patients are essentially dystrophin negative, in about 50% of patients ~1-10% of the fibers express some dystrophin. Those so-called 'revertant' fibers express dystrophins that can lack up to 30 exons of the rod-domain in mice. Revertant fibers originate most probably from secondary mutations which re-frame the transcript enabling synthesis of truncated but functional dystrophin (somatic reversion). It is hypothesized that this happens in a specific subset of myogenic stem cells that proliferate in response to degeneration. Revertant fibers are most often found in small clusters and have the same deletion within a cluster, while this often differs per cluster. This indicates that fibers within a cluster inherit the secondary mutation from the same myogenic stem cells (Hoffman et al. 1990;Thanh et al. 1995;Klein et al. 1992).

The degree in which individual skeletal muscles and the heart are affected differs. Some muscles like the diaphragm are severely affected, while others like the soleus are partly spared. Extraocular muscles even appear to entirely escape from the pathological events. Also the order in which muscles are affected and fibrosis and fatty tissue infiltrations are observed is chronological (Torriani et al. 2011;Marden et al. 2005). The exact cause(s) for both phenomena are unclear, however several hypotheses exists. Most often, severely affected muscles are the ones that are constantly used and therefore undergo more stress than those which are rarely used. As exercise exacerbates disruption of the intracellular Ca^{2+} homeostasis this might underlie differences in severity. However, although the soleus is often used during movements, it is largely protected from pathology. It has been hypothesized that this muscle is spared until late in the disease because it mainly consists of slow muscle fibers.

Individual fibers contain functionally distinct isoforms of myosin heavy chain (MyHC) (Gregorevic et al. 2008). Based on the different MyHC isoforms, several fiber types have been identified, which differ in their functional properties. There are two types of muscle fibers. Slow twitch (type I) fibers are efficient at using oxygen (aerobic) and therefore stand muscle contraction over a long time. Fast twitch (type II) fibers use glycogen (anaerobic) and are better at generating short bursts of strength than slow muscles, however they fatigue quicker. Type II fibers can be further grouped into type IIa, IIb and IId/x fibers (Schiaffino et al. 1989). Type IIa fibers are intermediate fast twitch fibers that can use both an aerobic and anaerobic metabolism for energy supply, making them more a combination of type I and II fibers. Type IIb and IId/x fibers only use an anaerobic metabolism. Type II fibers have a larger diameter than type I fibers and are subjected to the greatest mechanical stress during muscle contraction. Most often muscles containing primarily fast fibers are more vulnerable to mechanical damage and earlier affected than muscles that mainly consist of slow fibers (Table 1). Muscles can primarily consist of slow or fast fibers or of a mixture of both types. Depending on the demand of muscles, fiber type compositions can change over time, which happens in a distinct order: type IIb → type IId/x → type IIa → type I. Exercise-induced fiber type switches have been described in mice, as well as differences in composition between mouse strains that differed in disease severity.

Muscle	Fiber type composition	Severity pathology
Quadriceps	Mixed	Moderate
Gastrocnemius	Mixed	Moderate
Tibialis anterior	Fast	Moderate
Soleus	Slow	Mild
EDL	Fast	Moderate
Triceps	Mixed	Moderate
Biceps	Mixed	Moderate
Diaphragm	Fast	Severe

Table 1. Overview of fiber type composition and the degree of histopathology.
The table is based on several studies in *mdx* mice of which fiber type composition of several muscles was determined. Fiber types and the timing of onset of pathological symptoms closely correlate, however multiple other factors play a role as well (Table is adapted from Willmann et al NMD 2012).

In healthy muscle, individual fibers express only one MyHC isoform. Expression of multiple different MyHC isoforms is found in dystrophin negative fibers (Willmann et al. 2011;Emery and Muntoni 2003;Johnson et al. 1973;Webster et al. 1988).

However, fiber type composition is not the only factor that influences the order of initiation of muscle pathology (Emery and Muntoni 2003). Other factors are the number of SAC channels per muscles, differences in regeneration capacity, muscle fiber diameter and length, mitochondrial content, growth rate during development and expression levels of utrophin and members of the DGC (Lewis and Ohlendieck 2010;Porter 1998;Grounds and Shavlakadze 2011). Differences in embryonic origin might play a role as well as muscles derived from the somatic mesoderm are more severely affected than those derived from the paraxial mesoderm. It has also been speculated that some muscles have improved ability to regulate Ca^{2+} homeostasis and that they possess mechanical properties that make them more resistant to damage (Khurana et al. 1995;Wiesen et al. 2007). For example the functional properties of extraocular muscles are more advanced as they display faster peak contraction rates, higher fatigue resistance profiles and have smaller motor units which are less prone to damage (Thomas et al. 2008).

1.1.4. Antisense-mediated exon skipping

In order to synthesize dystrophin protein, a pre-mRNA transcript is generated from the *DMD* gene. During splicing, all introns are spliced out and exons joined so that mRNA is formed. This mRNA is used as a template for protein synthesis, where every three consecutive nucleotides contain the information for one amino acid. DMD patients have mutations that disrupt the reading frame, e.g. a deletion of an exon that contains a number of base pairs that is not divisible by three. This leads to a shift in the reading frame, inclusion of aberrant amino acids and generally a premature stop codon (UAA, UGA or UAG) and untimely truncation of protein translation. Since dystrophin forms a flexible bridge-like connection between the intracellular F-actin filaments and the ECM, and only one bridge-head remains in DMD patients, this function is lost, resulting in the previously described pathogenesis.

Mutations that maintain the reading frame in the *DMD* gene lead to Becker muscular dystrophy (BMD) which affects 1:20,000 men (section 1.3.2). In these patients, a shorter, internally deleted, but partly functional protein is synthesized. The bridge-like connection is maintained in these patients (albeit with an altered connecting domain) and proteins of the DGC

are expressed to some extent. These fibers are supposed to be less vulnerable to exercise-induced damage which leads to a less pronounced pathology and better life expectancy. Some of these patients even lack over two thirds of the central rod domain, indicating that large parts of this domain can be missed (England et al. 1990;Love et al. 1989a).

1.1.4.1. The concept of exon skipping

With no causal treatment available for DMD, effort has been put into attempting to restore the disrupted reading frame (Aartsma-Rus 2010). With the use of antisense oligonucleotides (AONs), which are modified, small pieces of DNA or RNA (~6-8 kDa), signals that are required for inclusion of an exon can be hided from the splicing machinery, so that this exon and its flanking introns are spliced out during pre-mRNA splicing. In this way, the reading frame is restored and internally deleted BMD-like dystrophin proteins are synthesized. As shown in the example of Figure 6, a deletion of exon 52 disrupts the reading frame and causes protein synthesis to stop prematurely. With AONs directed to exon 51, this exon will be skipped, thereby restoring the reading frame enabling the synthesis of a BMD like dystrophin protein.

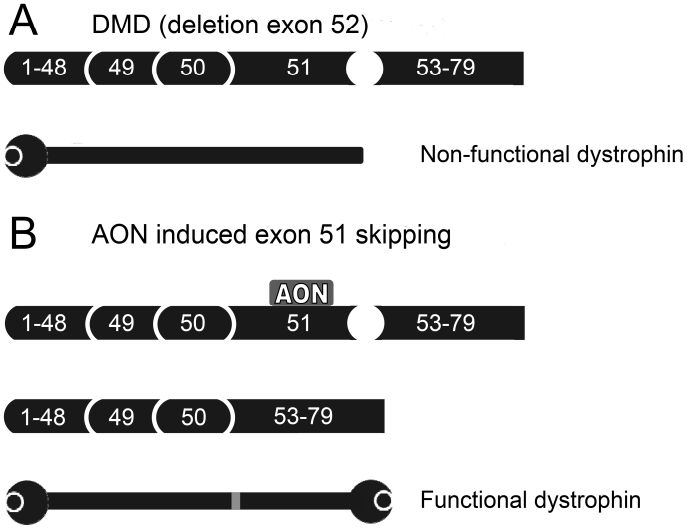


Figure 6. Antisensense oligonucleotide mediated exon 51 skipping.
A. In DMD out-of-frame deletions lead to premature stop codons and truncated, non-functional dystrophins.
B. Using AONs, an exon can be hidden from the splicing machinery, restoring the open reading frame and allowing the production of internally deleted, partly functional dystrophins. The synthesized protein has an unnatural transition (represented by the grey bar) resulting from the lack of the skipped exon (From van Putten et al. Expert Opin. Biol. Ther.).

Mutations found in DMD patients can occur anywhere across the entire gene, but a major hotspot is present between exon 45 and 53 (den Dunnen et al. 1989). Exon skipping is a mutation specific approach, as for different mutations different exons have to be skipped to restore the reading frame. However, skipping of some exons benefits larger groups of patients with different mutations. Exon skipping can be applied to all reading frame disrupting exons of the central rod domain and theoretically might benefit over 90% of the DMD patients. Only a small proportion of all mutations (5-10%) cannot be addressed with this approach. These consist of mutations in the two outer exons; 1 and 79 as these exons cannot be skipped, and mutations

that also result in DMD while they maintain the open reading frame, e.g. mutations that remove either all actin-binding domains or the cysteine-rich domain (Aartsma-Rus et al. 2009).
In the majority (65%) of DMD patients one or more exons are deleted. Here, often skipping one or two flanking exons corrects the reading frame. Skipping two exons, so-called double exon skipping, is feasible by using a combination (cocktail) of AONs targeting the two exons. *In vitro* transfection of patient-derived cell cultures using an AON cocktail to induce double exon skipping results in only slightly lower amounts of dystrophin expressing cells compared to single exon skipping (Aartsma-Rus et al. 2004a).



Figure 7. Overview of the exons of the *DMD* gene.
Light grey bars represent in-frame exons, which can be deleted without disrupting the reading frame. Black exons represent out-of-frame exons and deletions of these exons disrupt the reading frame resulting in DMD. For these exons one or multiple neighbouring exons need to be skipped to restore the reading frame. (Based on Aartsma-Rus et al. Hum. Mut 2008 used with kind permission of John Wiley and Sons).

Small mutations (nonsense mutations, small deletions or insertions and splice site mutations) are found in 28% of the patients. For these patients the reading frame can generally be corrected by only skipping the mutated exon when this is an in-frame exon, or together with an adjacent exon in case of an out-of-frame exon (Figure 7). Duplications, found in 7% of the patients, are more challenging to address with exon skipping (Aartsma-Rus et al. 2007). AONs are sequence specific and cannot distinguish between the original and duplicated exon as they both contain the same sequence. In case of single exon duplications either that exon or the original exon can be skipped to restore the reading frame. However, when skipping efficiency it too high (i.e. close to 100%), both the original and duplicated exon are skipped, which is reading frame disrupting. By skipping an additional exon in addition to the duplication this can sometimes be remedied. The duplication of exon 2 is the most common and makes up 12.7% of all duplications. When the duplication consists of multiple exons, exon skipping becomes very complex and restoration of the reading frame has not been feasible to date for these mutations. Based on data of the Leiden Open Variation Database, it is known that the largest group of patient (13%) would benefit from exon 51 skipping. Therefore skipping this exon is the current focus of clinical development (Aartsma-Rus et al. 2009). As shown in Table 2, 41% of the patients will benefit from AONs skipping 10 exons.

RANKING	EXON(S)	ALL MUTATIONS	DELETIONS SMALL	MUTATIONS SINGLE	EXON DUPLICATIONS
1	51	13.0%	19.1%	0.3%	3.0%
2	45	8.1%	11.8%	0.2%	2.2%
3	53	7.7%	11.4%	0.1%	1.5%
4	44	6.2%	8.8%	0.4%	2.7%
5	46	4.3%	6.2%	0.2%	1.6%
6	52	4.1%	5.7%	0.5%	2.3%
7	50	4.0%	5.6%	0.2%	1.9%
8	43	3.8%	5.3%	0.2%	2.6%
9	6 and 7	3.0%	3.6%	0.1%	6.3%
10	8	2.3%	2.3%		8.0%
11	55	2.0%	2.7%	0.8%	0.2%
12	2	1.9%	1.3%		12.7%
13	69 and 70	1.4%		5.6%	
14	19 and 20	1.1%		4.6%	
15	45 and 51	1.1%	1.7%		
16	58 and 59	1.1%		4.5%	
17	17	1.0%	1.1%	0.1%	3.1%
18	7	1.0%	1.4%		0.8%
19	65 and 66	1.0%		3.9%	
20	43 and 44	0.9%		3.5%	
21	12	0.8%	1.0%	0.3%	1.4%
22	23	0.8%		3.1%	
23	18	0.9%	1.0%	0.1%	2.5%
24	20	0.8%	1.0%	0.2%	1.2%
25	21	0.8%	0.5%	1.2%	1.6%
26	17 and 18	0.8%		3.1%	
27	11 and 12	0.7%		2.9%	
28	68 and 69	0.7%		2.9%	
29	19	0.6%	0.5%	0.4%	1.8%
30	22	0.6%	0.6%	0.1%	1.8%
31	45 and 53	0.6%	0.9%		
32	41	0.6%		2.3%	
33	14	0.6%		2.2%	
34	54 and 55	0.6%		2.2%	
35	20 and 21	0.5%		2.1%	
36	35	0.5%		2.1%	
37	54	0.5%	0.6%		1.0%
38	24	0.5%		2.0%	
39	40	0.5%		2.0%	
40	34	0.4%		1.8%	
41	56	0.4%	0.6%		0.5%
42	11	0.4%	0.3%	0.2%	2.3%
43	16	0.4%		1.7%	
44	39	0.4%		1.7%	
45	62 and 63	0.4%		1.5%	
46	64	0.4%		1.6%	
47	7 and 8	0.4%	0.4%	0.5%	0.2%
48	26	0.4%		1.5%	
49	10	0.4%		1.4%	
50	51 and 52	0.4%		1.4%	
51	6	0.4%	0.3%		1.6%

RANKING	EXON(S)	ALL MUTATIONS	DELETIONS SMALL	MUTATIONS SINGLE	EXON DUPLICATIONS
52	52 and 53	0.3%		1.4%	
53	74	0.3%		1.4%	
54	3	0.3%		1.2%	0.5%
55	13	0.3%		1.3%	
56	21 and 22	0.3%		1.3%	
57	32	0.3%		1.3%	
58	48	0.3%		1.3%	
59	55 and 56	0.3%		1.3%	
60	69	0.3%		1.3%	
61	30	0.3%		1.3%	
62	44 and 45	0.3%		1.3%	
63	47	0.3%		1.1%	0.3%
64	25	0.3%		1.1%	
65	60	0.3%		1.0%	0.3%
66	75 and 76	0.3%		1.2%	
67	5	0.3%		1.0%	
68	27	0.3%		1.0%	
69	50 and 51	0.3%		1.0%	
70	50 and 55	0.3%	0.4%		
71	56 and 57	0.3%		1.0%	
72	57	0.3%	0.2%	0.2%	0.9%
73	28	0.2%		1.0%	
74	4	0.2%		0.9%	
75	29	0.2%		0.9%	
76	38	0.2%		0.7%	0.5%
77	52 and 55	0.2%	0.3%		
78	33	0.2%		0.8%	
79	36	0.2%		0.8%	
80	37	0.2%		0.8%	
81	68	0.2%		0.7%	
82	70	0.2%		0.7%	
83	9	0.2%		0.7%	
84	61	0.2%	0.03%		1.6%
85	15	0.2%			
86	43 and 53	0.2%	0.2%		
87	63	0.1%	0.1%	0.3%	0.2%
88	43 and 51	0.1%	0.2%		
89	59 and 60	0.1%	0.2%		
90	65	0.1%		0.5%	
91	66	0.1%	0.03%	0.4%	
92	6 and 8	0.1%	0.1%	0.2%	
93	45 and 46	0.1%		0.4%	
94	58	0.1%	0.1%	0.1%	0.5%
95	61 and 62	0.1%			1.1%
96	2 and 11	0.1%			0.9%
97	8 and 11	0.1%			0.9%
98	31	0.1%		0.3%	
99	62	0.1%	0.03%	0.2%	0.3%
100	2 and 7	0.1%	0.1%		
101	68 and 69	0.1%	0.1%		
102	12 and 19	0.04%			0.5%

RANKING	EXON(S)	ALL MUTATIONS	DELETIONS SMALL	MUTATIONS SINGLE	EXON DUPLICATIONS
103	17 and 22	0.04%	0.1%		
104	42	0.04%		0.2%	
105	53 and 54	0.04%	0.03%		0.2%
106	57 and 58	0.04%	0.1%		
107	59	0.04%	0.03%	0.1%	
108	59 and 63	0.04%	0.1%		
109	67	0.04%			0.5%
110	73	0.04%		0.2%	
111	2 and 6	0.02%			0.2%
112	2 and 17	0.02%			0.2%
113	8 and 17	0.02%			0.2%
114	11 and 22	0.02%	0.03%		
115	17 and 20	0.02%	0.03%		
116	18 and 46	0.02%			0.2%
117	21 and 44	0.02%	0.03%		
118	22 and 43	0.02%			0.2%
119	44 and 52	0.02%			0.2%
120	46 and 52	0.02%			0.2%
121	49	0.02%		0.1%	
122	52 and 57	0.02%	0.03%		
123	58 and 62	0.02%			0.2%
124	62 and 68	0.02%	0.03%		
125	66 and 68	0.02%		0.1%	
126	71	0.02%		0.1%	
127	72	0.02%		0.1%	
128	75	0.02%	0.03%		
129	77	0.02%		0.1%	
130	78	0.02%			0.2%

Table 2. Applicability of the exon skip approach.
This table gives an overview of the proportions of patients that benefit from single or double exon skipping (From Aartsma-Rus et al. Hum. Mut 2008, reprinted with kind permission of John Wiley and Sons).

Several different AON chemistries are available to induce exon skipping, but only the 2'O-methyl phosphorothioate (2OMePS) and phosphorodiamidate morpholino oligomers (PMO) have so far been tested in clinical trials for DMD. These specific chemistries are favoured above others for their specificity and good safety profile in humans. The structure of 2OMePS AONs is similar to that of RNA, but contains two modifications. Instead of the non-bridging oxygen atom found in RNA, 2OMePS AONs contain a sulphur (atom) in the phosphate backbone, thereby forming a phosphorothioate (PS) backbone. This enhances stability by inhibiting breakdown by endo- and exonucleases. The PS backbone also facilitates low affinity binding to serum proteins, thereby preventing rapid clearance by liver and kidney upon systemic injection. This leads to a relatively long serum half-life of approximately 29 days (Goemans et al. 2011). The second modification consists of a methyl group at the 2'-OH position of the ribose sugar which renders 2OMePS AONs resistant against RNase-H mediated knockdown, and also results in higher affinity to the target RNA (Aartsma-Rus et al. 2004b).

PMOs contain six-membered morpholine rings that are connected through phosphorodiamidate linkages (Summerton and Weller 1997). They have a non-ionic backbone at physiological pH, which minimizes protein interactions and non-specific antisense effects, and increases binding capacity to mRNA. Unfortunately, their uncharged nature makes them hard to

transfect in tissue culture and results in a short half-life of ~1.6-3.6 hours upon systemic injection as they are rapidly filtered out by the kidney (Amantana and Iversen 2005;Cirak et al. 2011).

The first *in vitro* proof of concept studies were performed with 2OMePS AONs on patient-derived cell cultures carrying a variety of different mutations throughout the *DMD* gene. AON transfections resulted in the skip of the targeted exon, subsequent restoration of the reading frame and synthesis of dystrophin (Takeshima et al. 2001;van Deutekom et al. 2001;Aartsma-Rus et al. 2003). Both chemistries have also been locally administered in the *mdx* mouse where a skip of exon 23 restores the murine *Dmd* reading frame (Dunckley et al. 1998;Wilton et al. 1999). These experiments showed that also in the mouse model restoration of the reading frame resulted in dystrophin synthesis. Systemic administration revealed that dystrophic muscle is an easier AON target than healthy muscle, since 10-fold higher AON levels were detected in dystrophic compared to healthy muscles (Heemskerk et al. 2010). This is thought to results from the damaged membranes that facilitate AONs to enter the target tissue. Treated *mdx* mice had improved muscle pathology and function in the absence of toxicological side effects (Lu et al. 2003;Alter et al. 2006). PMOs were also successfully tested in some GRMD-dogs, where a double skip of exon 6 and 8 results in the correction of the reading frame and consequent dystrophin synthesis (Yokota et al. 2009).

1.1.4.2. Clinical trials

With these encouraging data, AONs targeting exon 51, which would benefit the largest group of patients, have been tested in clinical trials for both chemistries. Trials with 2OMePS AONs (PRO051/GSK2402968) were initiated by Prosensa Therapeutics, later joined by GlaxoSmithKline (GSK), while those with PMOs (AVI-4658) were undertaken by AVI-BioPharma in collaboration with the MDEX consortium. The first-in-man trial involved a single local intramuscular injection with 0.8 mg PRO051/GSK2402968 in the tibialis anterior of four DMD patients (NTR712). Biopsies taken one month later revealed that targeted exon 51 skipping resulted in 67-97% dystrophin positive fibers at levels of 17-35% of wild type (van Deutekom et al. 2007).

Later, intramuscular injections in the extensor digitorum brevis (EDL) of DMD patients with 0.09 mg (n = 2) and 0.9 mg (n = 5) AVI-4658 were performed by AVI-BioPharma and the MDEX consortium (NCT00159250) (Kinali et al. 2009). Biopsies were taken three and four weeks after administration. In all patients receiving the high dose, dystrophin restoration was found in 44-79% of the fibers at intensities ranging from 22-32% of wild type. The low dose only resulted in specific exon 51 skipping but no dystrophin synthesis. These trials showed that AON-mediated exon skipping with both chemistries was effective and safe.

The human body consists of 434 different muscles which account for 30-40% of its content. Since all these should be targeted, systemic AON delivery is crucial. Thus, after the encouraging results obtained with local administration for both chemistries and optimization of systemic treatment in animal models (Alter et al. 2006;Heemskerk et al. 2009;Heemskerk et al. 2010;Lu et al. 2005;Malerba et al. 2009), systemic trials were initiated. An open-label Phase I/II trial was undertaken for PRO051/GSK2402968 (NTR1241). Four cohorts, each consisting of three patients, received five weekly subcutaneous injections of either 0.5, 2, 4 or 6 mg/kg (Goemans et al. 2011). Biopsies revealed a dose-dependent recovery of dystrophin expression in almost all patients, of up to >80% of the fibers in patients receiving the highest dose. Maximum dystrophin signal intensity compared to wild type was 15.6% after treatment, while no adverse effects were reported. Thereupon, at the beginning of 2010, all patients enrolled in a still ongoing open label extension study (NCT01480245), receiving weekly injections of the highest (6mg/kg) dose. No serious adverse effects have been reported so far. The mild or moderate side effects so far are

reactions at the injection site, proteinuria and increased urinary α_1-microglobulin levels. After 12 weeks, this resulted in a trend of functional improvement in the 6-minute walk test in most of the patients, contrasting the anticipated decline. Results should be interpreted with caution due to the open-labelled nature of the trial and the lack of a placebo group. Therefore, to elucidate the effectiveness of the compound, as well as long term safety and tolerability, a double-blind placebo-controlled Phase III trial has been initiated involving weekly GSK2402968 administration of 6 mg/kg in 180 patients (NCT01254019). Another double-blind placebo-controlled trial, undertaken for the same compound is a Phase II trial elucidating the effects of different dosing regimens (once versus twice weekly 6 mg/kg) (NCT01153932). In addition, a Phase I trial assessing the pharmacodynamic profile of a single injection of different doses (3, 6, 9 and 12 mg/kg) in non-ambulant patients has been initiated (NCT01128855). Finally, a phase II, placebo controlled study has been initiated assessing two doses (3 and 6 mg/kg/week) in ambulant patients (NCT01462292).

AVI-BioPharma performed an open-label dose escalation Phase Ib/II trial, in which 19 DMD patients received weekly intravenous injections with 0.5, 1, 2, 4, 10 or 20 mg/kg AVI-4658 for a period of 12 weeks (NCT00844597). Exon 51 skipping was detected in biopsies from all patients, leading to a variably dose-dependent dystrophin synthesis in patients receiving 2 mg/kg or more. The maximum proportion of dystrophin positive fibers found was 55% obtained in a patient of the highest dosing cohort, while maximum fiber intensity compared to wild type levels was 27% post-treatment. As AVI-4658 also appeared to be well tolerated, a double blind placebo-controlled Phase II study has been undertaken to assess efficacy, pharmacokinetics, safety and tolerability (Cirak et al. 2011). Patients received a 60-minute intravenous infusion of 30 mg/kg (n = 4), 50 mg/kg (n = 4) or placebo (n = 4) once weekly (NTC01396239). Exon 51 skipping was detected in all patients receiving 30 mg/kg for 24 weeks, resulting in increased dystrophin levels. In biopsies from patients receiving 50 mg/kg for 12 weeks exon 51 skipping did not result in increment of dystrophin synthesis (www.avibio.com). Clinical outcome measures (6-minute walk test, Gower's maneuver, 10 meter run) did not change in any of the treatment groups. As no serious side-effects were reported, all patients enrolled in an open-label extension study. Patients belonging to the placebo group are now also receiving AVI-4658.

Although no apparent differences in efficiencies regarding both proportion of dystrophin positive fibers and their expression levels were observed between the two chemistries upon intramuscular injection, these were observed upon systemic administration. Compared to the PRO051/GSK2402968 trial where doses dependent dystrophin expression (in up to 80% of the fibers) was observed in roughly all (10 out of 12) patients, the AVI-4658 trial reported to observe restored dystrophin expression in 55% of the fibers or less in only a few (7 out of 19) patients. This might be due to technical differences in immuno-histochemical protocols, reference samples and analysis methods used in the two studies. On the other hand, biological factors might underlie this difference. As previously mentioned, the serum half-life of 2OMePS (<4 to 28 days) and PMOs (1.6 to 3.6 hours) differs significantly. Since PMOs are quickly cleared by the liver and kidney, the chances of being taken up by muscle are lower for PMO than for 2OMePS AONs. Possibly, and consistent with the greater variability observed for PMO, the much lower effective muscle exposure with PMO leads to variable uptake of AONs dependent on the physical integrity of specific fibers, with recently disrupted/repaired fibers taking up more AON. Further studies are needed to elucidate the exact cause for the differences in dystrophin expression found upon systemic administration.

Effort is also put in the development of AONs targeting other exons. Currently, Prosensa Therapeutics conducts a dose escalation trial with 2OMePS AON targeting exon 44 (PRO044) which would apply to 6% of patients (NCT01037309). This open-label Phase I/IIa trial consists of weekly subcutaneous injections of 0.5, 1.5, 5, 8, 10 and 12 mg/kg PRO044 for 5 weeks. Pre-clinical investigations for AONs targeting exon 45, 53, 52 and 55 are ongoing and it is anticipated that exon Phase I/IIa trials for exon 45 and 53 will be initiated in 2012.

1.1.4.3. Hurdles to overcome

Even though AON-mediated exon skipping results in restoration of dystrophin expression and is well tolerated, there are still several hurdles to overcome. As previously mentioned, skeletal muscle fibers of DMD patients have an uptake advantage as AONs can easily enter the fibers through disruptions of the membrane. However, mouse studies indicate that large amounts are still taken up by liver and kidney. To improve delivery to muscle, AONs may be bound to sugar groups or cell-penetrating peptides. The efficiency of the latter has been investigated to enhance uptake of PMOs in mouse models. Cell-penetrating, arginine-rich peptides were conjugated to PMOs (PPMO) and injected in *mdx* and *mdx/utrn* $^{-/-}$ mice. This resulted in increased intracellular PPMO levels and very efficient dystrophin restoration, leading to improved functional performance and life span in the severely affected *mdx/utrn* $^{-/-}$ mouse. No adverse effects were observed in both models (Goyenvalle et al. 2010;Yin et al. 2008;Moulton et al. 2009). Based on these encouraging results, PPMOs targeting exon 50 (AVI-5038) were further tested in primates in preparation for a clinical trial. Unfortunately, the toxicity observed after systemic administration has precluded further development of this specific compound (Sazani et al. 2009). As differences in chemistry might resolve the toxicity issue, pre-clinical investigations aim at identification of non-toxic peptides that enable targeted AON uptake (Yin et al. 2009;Yin et al. 2010;Yin et al. 2011).

Additionally, also the heart is more challenging to target (Heemskerk et al. 2010). This is probably due to differences in architecture of cardiomyocytes, which are not as permeable as skeletal muscle fibers and thus have a more limited AON uptake. The consequences of AON-induced dystrophin expression in skeletal muscle in the absence of expression in heart are unknown. It is speculated that as dystrophin expression in skeletal muscle will result in increased activity levels, a higher workload will be projected to the heart, which might worsen heart disease progression (Malerba et al. 2011a;Townsend et al. 2008). Other reports indicate that dystrophin correction of diaphragm itself is already beneficial for heart function in dystrophic animal models (Crisp et al. 2011). As more than 90% of DMD patients develop dilated cardiomyopathy, applying some form of cardiac therapy is essential. In principle, heart transplantation is an option but this may not always be a viable approach dependent on organ availability, condition and histocompatibility status. Thus preferably also the heart would need to be targeted.

As yet, it remains unknown which levels of dystrophin are needed to protect muscles against damage and prevent or delay disease progression. From case reports, and studies in BMD and DMD patients and BMD carriers it has been speculated that ~20% already results in a mild phenotype (Hoffman et al. 1988;Hoffman et al. 1989;Neri et al. 2007). With new mouse models expressing variable, low dystrophin levels more insight in this issue has been gained (Chapters 4, 5 and 6).

As AON-mediated exon skipping is a personalized approach leading to the production of dystrophins that internally lack different sequences, it can only be speculated whether these proteins differ in performance. It might be that deletion of specific parts differentially affects the

ability to protect against fiber damage, protein stability or secondary pathology (eg. brain involvement). Additional factors might also play a role as differences in severity within BMD families have been reported (Melis et al. 1998). Upcoming clinical trials will probably give more insight in these issues.

Finally, DMD is a rare disease affecting only 1:3500 newborn boys and mutations are present throughout the entire gene. To treat all patients that might theoretically benefit from this approach 130 combinations of single and double exon skipping are needed targeting more than 50 different exons (Aartsma-Rus et al. 2009) (Table 2).

1.2. Mouse models for DMD

1.2.1. The *mdx* mouse

The most commonly used mouse strain in DMD research is the *mdx* mouse. This is a natural model which arose from the C57BL/10ScSnJ (wild type) strain. It was first described in 1984 under the official name C57BL/10ScSn-*Dmd*^{mdx}/J (Bulfield et al. 1984), where *mdx* stands for: X-linked muscular dystrophy. *Mdx* mice have a point mutation in exon 23 of the *Dmd* gene (A>T at base 3185 replacing a glutamine codon (CAA) with a termination codon (TAA)). This premature stop codon prevents synthesis of full-length dystrophin (Sicinski et al. 1989). Even though only 15% of the DMD patients have a nonsense mutation, this model has been of great importance for proof of concept studies of potential therapeutic approaches like exon skipping and compounds targeting premature stop codons.

Although both DMD patients and *mdx* mice lack full-length dystrophin, the pathology of *mdx* mice is less severe (see below), enabling them to almost live as long as wild type mice and making homozygous breeding possible. The mean age of wild type mice is 27 and 26.5 months for females and males respectively, whereas this is 22.5 and 21.5 months for female and male *mdx* mice respectively (a reduction of 17% for females and 19% for males) (Chamberlain et al. 2007). In addition, slightly higher (~3.5 fold) mortality levels have been observed in *mdx* pups. Also the number of young *mdx* mice that die before the age of seven days is 45% higher than wild type mice (Torres and Duchen 1987). These rates seem to be independent of litter size, but as *mdx* mice are very susceptible to stress, mortality can be reduced by reducing animal handling and regular cage cleaning.

1.2.1.1. Skeletal muscle histopathology

The initiation of muscle pathology in *mdx* mice is essentially identical to that in DMD patients. However, in *mdx* mice, pathogenesis occurs in waves and is not a continuum like in DMD patients. Until weaning, only minor pathological changes have been reported (Grounds et al. 2008). From the age of 3-4 weeks onwards, an acute onset of degeneration followed by regeneration is present, which lasts for five weeks and then subsides (Bulfield et al. 1984). The cause for the acute onset instead of a more gradual one is unknown. As a result, loss of muscle fibers is slow in adult *mdx* mice, with regenerated fibers being more resistant to necrosis. More severe muscle weakness is only found in old *mdx* mice with the diaphragm being the most severely affected muscle. Replacement of fibers by fat tissue is rare (Chamberlain et al. 2007;Stedman et al. 1991;Bulfield et al. 1984;Deconinck et al. 1998;Karpati et al. 1988;Weller et al. 1990).

For obvious reasons, pathological events in mice can be studied in more detail than in DMD patients, where generally only biopsies are available (Figure 8). Histopathology is characterized by increased numbers of small, newly regenerated fibers, as well as big hypertrophic fibers and by large patches of fibrosis and necrosis (Marshall et al. 1989). Like DMD patients, *mdx* mice also have revertant fibers and these increase in number with age from ~11 fibers in one month old to >100 in one year old mice. *Mdx* mice that are irradiated with 18 Gy have significantly reduced muscle regeneration and consequently a reduced expansion of their revertant fibers. Revertant fibers in heart do not increase in number over time (Yokota et al. 2006;Lu et al. 2000).

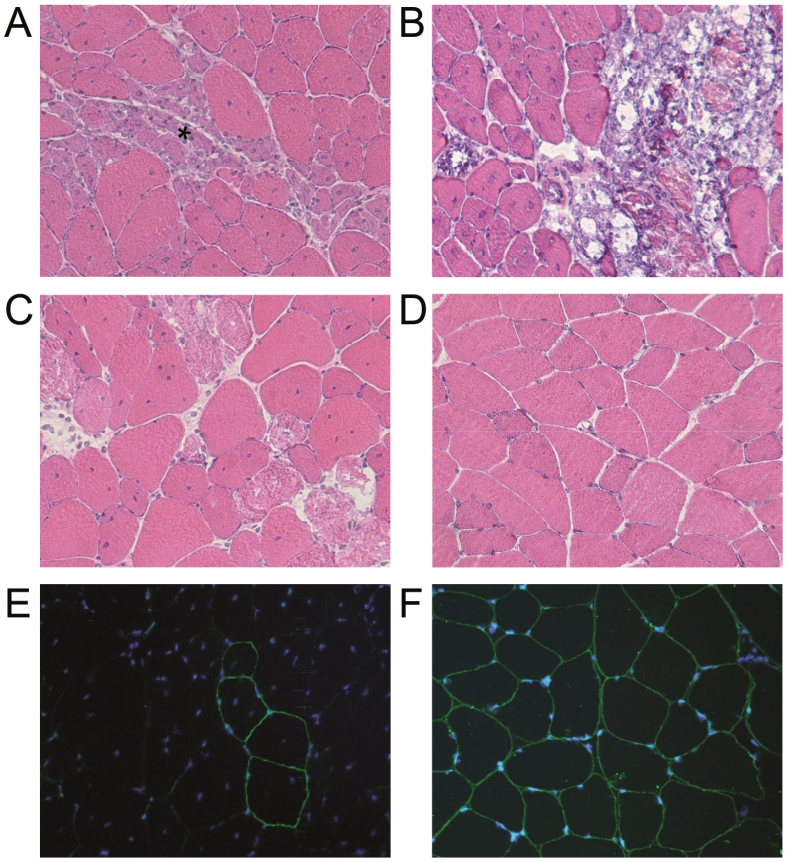


Figure 8. Cross sections of the quadriceps of an *mdx* and a C57BL/10ScSnJ (wild type) mouse.
A. The *mdx* mouse section shows a lot of variation in fiber size, with small, newly regenerated fibers and enlarged hypertrophic fibers. Most fibers have centralized nuclei, indicating recent regeneration events. Newly regenerated fibers are indicated with an arrow. **B**. Pathology in an *mdx* mouse involving an area with fibrosis and infiltration of inflammatory cells. **C**. Fibers undergoing necrosis in a section of an *mdx* mouse. **D**. C57BL/10ScSnJ mouse reveals muscle fibers that are evenly sized and with nuclei at the membrane. No pathological features are evident. **E**. Revertant fiber in an *mdx* cross section. **F**. Dystrophin expression of a C57BL/10ScSnJ mouse.

Muscle fibers of *mdx* mice also have an abnormal architecture as they can have one or multiple branches (Head et al. 1992;Lovering et al. 2009). Different types of branches have been found; fibers being totally split in two (Y-shape), having one or multiple small branches on the side (╣ shape), or having a small split in the middle while remaining intact at either side. It is hypothesized that branches originate from imperfect fusion of myogenic cells during regeneration. Branched fibers are more susceptible to exercise-induced damage. The number and complexity of the branches increases with age as in young *mdx* mice (6-8 weeks old) 17% of the fibers have branches, while this increases to 89% in old (27-31 weeks old) mice. Only in old *mdx* mice these branches result in a significantly increased drop in maximum tetanic force upon repeated eccentric contractions of 58% in *mdx* compared to 25% in wild type mice. Fibers of wild type mice rarely have branches (Chan et al. 2007;Chan and Head 2011).

1.2.1.2. Neuromuscular junction and skeletal muscle pathology

Mdx mice have abnormalities in the anatomy of the NMJ and show functional deficits in muscle. To better appreciate the significance of these abnormalities and those observed in other DMD mouse models, the situation in wild type mice is discussed first, followed by that in *mdx* mice.

Muscle contractions are coordinated by the central nervous system, from which nerve pulses are sent to the NMJ (Figure 9). When these reach the synaptic end bulb, acetylcholine (ACh) is released from vesicles and diffuses across the synaptic cleft to bind ACh receptors (AChR) at the motor end plate of the muscle. This causes ion channels to open which allow entrance of Na^+ into the muscle fiber resulting in an action potential. The action potential travels across the sarcolemma and initiates the muscle to contract (see below). ACh is then broken down by acetylcholinesterase (AChE) in choline and acetate in the synaptic cleft. Dystrophin and utrophin colocalize with the Na^+ channels at the base of the folds and with the AChRs respectively. Although utrophin compensates for the lack of dystrophin in the muscular sarcolemma, compensation for each others absence does not happen in the NMJ. The DGC is involved in the maturation and cluster formation of AChRs, in the regulation of ACh release and maintenance during NMJ differentiation (Deconinck et al. 1997a;Grady et al. 1997a;Miike et al. 1989;Pilgram et al. 2010;Grady et al. 2000).

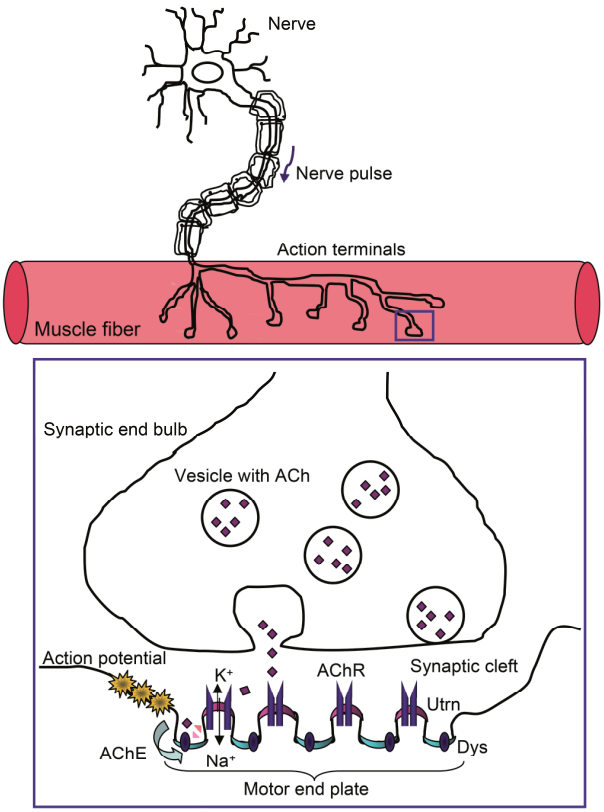


Figure 9. The neuromuscular junction.
Nerve pulses excited by the central nervous system ensure release of ACh in the synaptic cleft. Uptake of ACh by AChR results in an influx of Na^+ in the motor end plate of the muscle provoking an action potential which eventually ensures muscle contraction. (Figure adapted from http://www.educarer.com).

In comparison to wild type mice, the NMJ motor end plate of *mdx* mice displays varying decrease of postsynaptic folding, whith ~30% of the area completely lacking folding. Additionally, AChRs and AChEs are abnormally distributed from the age of 4-6 weeks onwards. α-Bungarotoxin staining (visualizing AChRs) reveals that synapses of *mdx* mice consist of distinct boutons whereas continuous branches are present in wild type mice (Lyons and Slater 1991;Ferretti et al. 2011). Electrophysiological properties of the NMJ are not impaired as the total number of AChRs and AChEs remains similar. Interestingly, all these pathological hallmarks are only observed in regenerated fibers, indicating that the lack of dystrophin itself has minor direct consequences. However, during regeneration in the absence of dystrophin, utrophin clustering is altered which results in remodelling of the pre- and postsynaptic components (Lyons and Slater 1991;Ferretti et al. 2011).

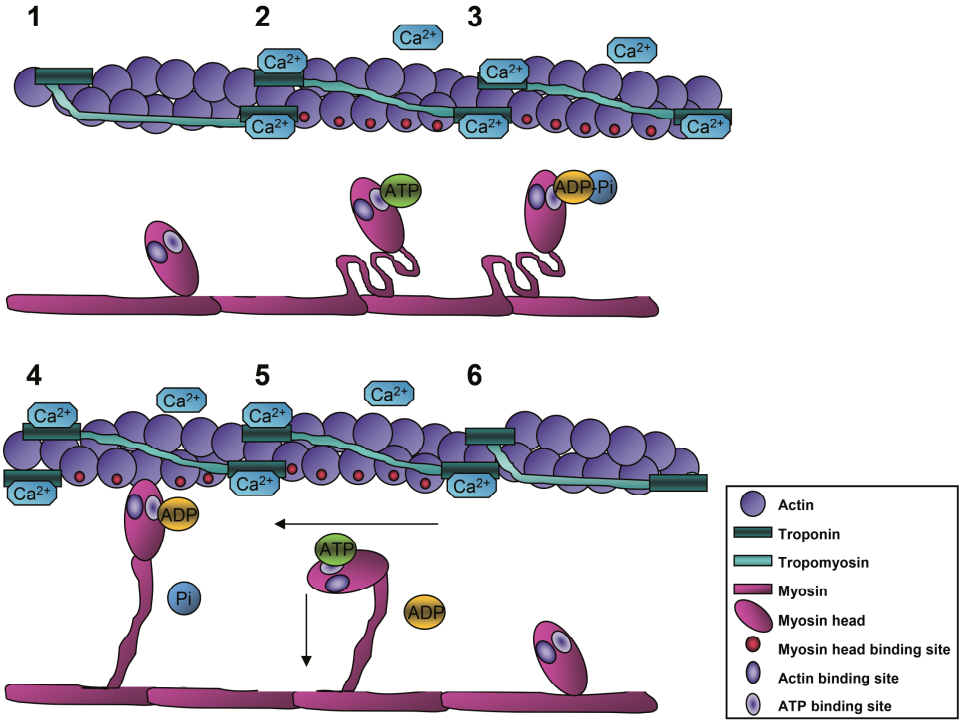


Figure 10. Molecular mechanisms of a muscle contraction.
1. Upon arrival of the action potential in the T-tubules, Ca^{2+} is released from the sarcoplasmic reticulum and binds to Troponin C in the myofibril. **2.** This ensures a conformational change of tropomyosin exposing the myosin head binding sites. **3-5.** Cycles of ATP triggered binding and release of the myosin head to actin, bring them in close proximity of each other resulting in contraction of the muscle. **6.** Upon depletion of Ca^{2+}, the conformational change of actin will be reversed, making myosin head binding sites inaccessible. Thereupon, actin slides back in its original position resulting in muscle relaxation.

The action potential from the NMJ is transported over the sarcolemma and ends up in the T-tubules located in the core of the muscle fibers. This triggers opening of voltage sensitive proteins and thereby release of Ca^{2+} from the sarcoplasmic reticulum in the cytosol. Within the myofibril, Ca^{2+} binds to Troponin C in the actin filaments of the sarcomere, changing the conformation of tropomyosin ensuring exposure of myosin head binding sites (Figure 10 step 1). Contractions start with the binding of ATP to the myosin head (step 2), which contains the

enzyme adenosine triphosphatase (ATPase) which splits ATP into ADP, phosphate and energy (step 3). This triggers the myosin head to bind to the actin filament. This initial binding is tightened by release of the phosphate molecule (step 4). Conformation of proteins in the myosin head lead to their repositioning and thereby pulls the actin filament along the myosin. Upon binding of another ATP molecule to the myosin head it moves back to starting position and the ATP is broken down into ADP and phosphate (step 5). Binding of a new ATP molecule will repeat this procedure, but leads to a more proximal binding so that the myosin and actin filaments are brought towards each other resulting in muscle contraction. In the absence of new Ca^{2+}, tropomyosin will move back in its original conformation. This depletes the number of myosin head binding sites, forcing actin to slide back in its previous location leading to muscle relaxation (step 6) (Holmes 1996).

The myotendinous junction (MTJ) is located at the distal sides of a muscle where it is connected to the tendon. In wild type mice, the MTJs are extensive finger-like projections of the sarcolemmal membrane, which serve to increase the area of attachment between the muscle fiber and the tendon. They also ensure force transmission between muscle and tendon. Like the NMJ, also in the MTJ a marked reduction in the number of foldings is observed in *mdx* mice (Law and Tidball 1993;Deconinck et al. 1997b).

There are three main types of muscle contractions; isotonic (muscle shortens as force generated is greater than the load), isometric (load is greater than force generated, muscle length remains similar) and isokinetic (same speed) contractions. Isotonic contractions can be divided into two groups; concentric and eccentric contractions. During concentric contractions muscle contract and shorten in length, eccentric contractions result in lengthening of the muscle. In the latter case, muscles not only contract to build force but also slide alongside each other to lengthen. Muscle contractions in *mdx* mice have been studied in individual fibers and whole muscles. The most often used outcome measures are twitch force (force generated upon a single stimulation), tetanic force (force generated upon summation of individual twitches) and muscle fatigue initiated by multiple eccentric contractions.

Acute weakness of the proximal followed by the distal muscles is observed in young *mdx* mice during the cycles of degeneration and regeneration (Muntoni et al. 1993). Although hypertrophic fibers generate higher twitch force than wild type mice, the relative force normalized for cross sectional area is significantly decreased in both young and old *mdx* mice. Force generating capacity of 21 months old *mdx* mice differs between fast and slow muscles. Fast muscles have significantly decreased twitch and tetanic force as well as decreased resistance to eccentric contractions, whereas slow muscles only have a significant decreased tetanic force compared to wild type muscle (Bobet et al. 1998;Lynch et al. 2001;Raymackers et al. 2003). Muscle force also differs between male and female mice as in females tetanic force is significantly less impaired at the age of six months (Hakim and Duan 2012). Impaired muscle function of *mdx* mice results in significantly reduced voluntary activities and bad overall motor performance (section 1.4.1.5.) (Hara et al. 2002;van Putten et al. 2012). However, chronic voluntary wheel running activities improve tetanic force of the EDL by 28% (Call et al. 2010). On the other hand, muscle pathology can also be negatively influenced by chronic horizontal treadmill running, which puts increased strain on the muscles. Especially downhill running in which muscles are mainly challenged by eccentric contractions result in very severe pathology (Wooddell et al. 2010).

1.2.1.3. Pathology of the heart

Like DMD patients, *mdx* mice also develop dilated cardiomyopathy resulting from an identical pathological cascade. Heart function has been primarily studied by ECG and MRI (section 1.4.2.). In mice, the first pathological hallmarks are observed from the age of 2-3 months onwards. These involve uptake of Evans blue dye by cardiomyocytes, lower levels of nNOS and increased strain and tension (van Erp et al. 2010;Bia et al. 1999). In a proportion of *mdx* mice abnormal S-waves are observed. Mice aged 6 months have significantly higher levels of fibrosis and macrophage infiltrations than wild type mice, and these increase in proportion with age. Fibrosis is not restricted to a particular region, but is distributed in a patchy manner over both ventricles (Li et al. 2009). In parallel, elevated levels of markers involved in ECM remodeling and fibrosis (amongst others; CTGF, TIMP-1, MMP-9 and TGF-β1) are found as well (Au et al. 2011). Additionally, hypertrophy of the heart involving in particular the left ventricle has been described. ECGs of these mice are characterized by polyphasic R-waves and decreased S/R ratios. More extensive impairment of heart function is present from the age of 7-8 months onwards. First a decrease in right ventricular ejection fraction is observed accompanied by a decreased end diastolic volume and increased end systolic volume. In slightly older mice, a decreased left ventricular ejection fraction is observed as well (Figure 11). Some articles have reported a decreased cardiac output of both ventricles in 9-10 months old mice. A decreased S and R wave amplitude and increased heart rate is present at the age of 12 months.

Discrepancy exists in literature regarding the age of onset of dilated cardiomyopathy, as some studies report these changes at an early age (Verhaart et al. 2011;Zhang et al. 2008;Crisp et al. 2011) while others do not observe major functional abnormalities in 10 months old *mdx* mice (Li et al. 2009).

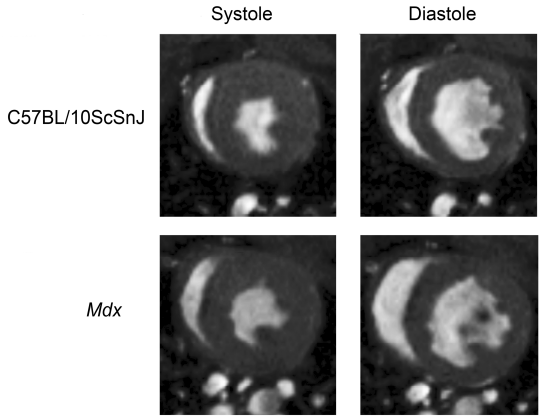


Figure 11. MRI scans of the heart of a C57BL/10ScSnJ and *mdx* mouse.
MRI scans of the systolic and diastolic phase of the heart contraction from a wild type and *mdx* mouse aged 10 months. At this age, *mdx* mice show severe dilatation of both the left and right ventricles, involving decreased stroke volume and ejection fraction.

The exact cause for this is unknown, but it might be due to differences in the wild type strains used (C57BL/10ScSnJ versus C57BL/6). Also gender is known to influence heart function as this is more severely impaired in 22 months old female compared to male *mdx* mice (Bostick et al. 2010).Forced treadmill exercise or voluntary wheel running has been found to negatively influence heart function most likely by putting an increased workload and strain on the heart (Costas et al. 2010;Nakamura et al. 2002).

1.2.1.4. Limitations of the mdx mouse

Although *mdx* mice and DMD patients share the genetic defect that hampers the expression of functional dystrophin, pathology is less severe in mice. In contrast to DMD patients, motor function of *mdx* mice is only slightly reduced, they do not lose the ability to walk and life span is only slightly shorter. These differences can primarily be explained by differences in body size and architecture. The time-scale in which mice grow and mature is much shorter than that of humans, as mice directly go from childhood into adulthood, while humans spend a significant period of their life in puberty. This means that only 5% of a mouse's total life span has passed before they become sexually mature, while this is 20% for humans. Developmental milestones of DMD patients have been compared with *mdx* mice based on hormonal and physiological changes (Table 3) (Grounds et al. 2008). This clearly showed that the time-frame in which *mdx* mice undergo major pathological changes is extremely short in comparison to DMD patients. Mice also have a much smaller body size and distribute their body weight over four limbs instead of two. Taken together, this reduces the workload and stress on the muscles, preventing damage.

Human	Mouse
Newborn	1 week
~3 months	2 weeks
~6 months	3 weeks
~10 months	4 weeks
~16-18 years	6 weeks
~20 years	8 weeks
~25 years	12 weeks

Table 3: Developmental comparison between human and *mdx* mouse.
Based on hormonal and physiological changes, Grounds et al. published this comparison between DMD patients and the *mdx* mouse. It can be appreciated from the table that most of the DMD pathology falls within the first eight weeks of the mouse's live (From Grounds et al. Neurobiol. Dis. 2008; reprinted with permission of Elsevier)

The less severe pathology observed in *mdx* mice results from multiple additional factors. *Mdx* mice have an incredible regeneration capacity for exceeding that of DMD patients. Furthermore, expression of transcription factors like Myod is upregulated, which enhances regeneration. Muscles of *mdx* mice are also better protected against damage since they are more efficient in overexpressing the dystrophin homologue utrophin that can functionally compensate for the loss of dystrophin. Also in DMD patients, utrophin is overexpressed between 2 and 10-fold compared to healthy controls, and these levels do positively correlate with disease severity (Kleopa et al. 2006). However, compensation in mice is more effective than that in human. This might be caused by differences in fiber diameter between human and mouse. As the surface-to-volume ratio is smaller in human, the sarcolemma of these fibers experiences more stress and therefore they might require more utrophin (Grady et al. 1997b). It is not known whether the compensatory mechanisms of mice will generate similar protective effects in human, as overall size and forces placed on muscles are different.

1.2.2. The *mdx*$^{2\text{-}5cv}$ mouse models

In addition to the naturally occurring *mdx* mouse, several other mice with mutations in the *Dmd* gene have been generated to make more extensive studies possible (Chapman et al. 1989). Male C3H.X$_{25}$ x C57BL/6Ros mice were intraperitoneally treated with the chemical *N*-ethylnitrosourea (ENU). This chemical is a powerful mutagen inducing point mutations to progeny at a frequency of 1 mutation per 700 loci. Crossings of ENU treated males with C57BL/10 x *mdx* females resulted in female progeny which were selected according to their CK level. This resulted in four *mdx* models with mutations throughout the *Dmd* gene, called *mdx*^{2cv}, *mdx*^{3cv}, *mdx*^{4cv} and *mdx*^{5cv}. Mutations of these mice, consisting of one nonsense and three affecting mRNA splicing were found to be spread over the gene, making these mice an ideal object to study the effect of mutation position on pathology (Cox et al. 1993;Im et al. 1996).

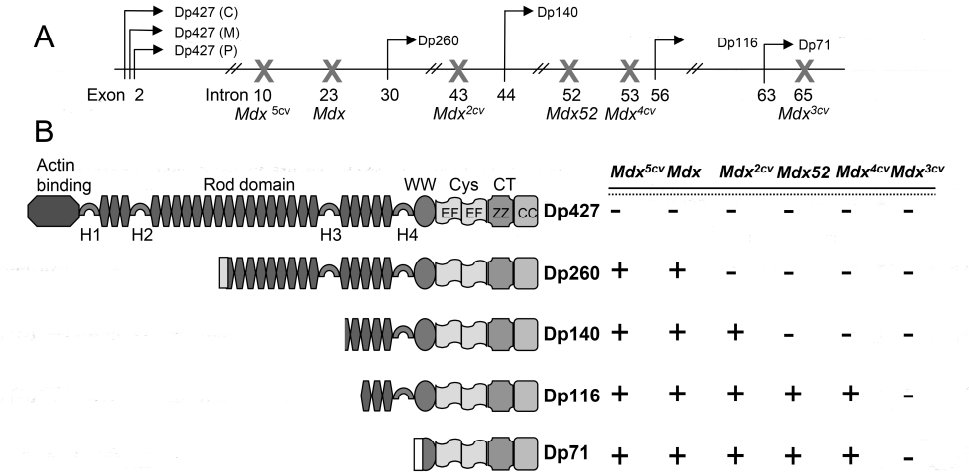


Figure 12. Dystrophin isoforms in different *mdx* mouse models.
A. Representation of the *Dmd* gene in which the induced or natural mutations of the *mdx*^{cv}, *mdx52* and *mdx* mouse models are indicated by a cross. **B**. This schematic overview summarizes which isoforms are expressed in the *mdx*^{cv}, *mdx52* and *mdx* models. (Figure is based on Willmann et al. NMD 2009).

The *mdx*^{2cv} mouse has a single base mutation (A>T) in the acceptor splice site of exon 43 (which lies in intron 42) of the *Dmd* gene. This mutation results in a complex pattern of aberrant splicing that generates multiple transcripts, of which none has an intact reading frame, so that the synthesis of functional full-length dystrophin synthesis is prevented. The smaller isoforms Dp140, Dp116 and Dp71 are normally expressed in these mice (Figure 12). The *mdx*^{3cv} mouse carries a T>A mutation in intron 65 (14 base pairs proximal to exon 66), which introduces a cryptic splice site and frame-shift that prevents completion of all dystrophin isoforms. This makes *mdx*^{3cv} mice exceptional since all other known *mdx* substrains express Dp71 and one or multiple additional short dystrophin isoforms. *Mdx*^{4cv} mice have a C>T transition (CAA to TAA) at position 7916 in exon 53, which results in a premature stop codon, preventing dystrophin synthesis. These mice express only the dystrophin isoforms Dp116 and Dp71 (Im et al. 1996). *Mdx*^{5cv} mice have an A>T mutation at position 1324 of exon 10. This mutation introduces a cryptic splice donor site (GTGAG) that generates a frame shift and prevents the synthesis of dystrophin (Im et al. 1996). As this mutation is close to the N-terminus of the protein, these mice only lack full-length dystrophin and express all the short dystrophin isoforms, like *mdx* mice.

Initially, it was thought that pathology of the *mdx*$^{2\text{-}5cv}$ mice greatly corresponded with that of *mdx* mice, therefore only mice younger than six months were studied. However, detailed investigations carried out in non-muscle tissues revealed phenotypical differences resulting from the absence of specific dystrophin isoforms. As the *mdx*^{3cv} mouse does not express any dystrophin isoform, this model has been most intensively studied. *Mdx*^{3cv} mice appeared hard to breed and survival chances of pups were smaller than that of *mdx* mice. Also the litter size is much smaller, which is not the case for the other *mdx*^{cv} models (Cox et al. 1993). Mouse spermatozoa contain Dp71. Spermatozoa lacking Dp71 have abnormally shaped flagella and altered distribution of ion channels and signalling proteins. Although the short utrophin isoform Up71 is upregulated and redistributed and levels of α-syntrophin and voltage dependent Na^+ and K^+ channels are increased in *mdx*^{3cv} mice, this does not prevent the phenotype (Hernandez-Gonzalez et al. 2005).

Besides differences in fertility, *mdx*^{3cv} mice also differ on a histological level from the other *mdx*^{cv} mice. Danko et al. compared the number of revertant fibers between the *mdx*^{cv} and *mdx* mice (Danko et al. 1992). He observed that *mdx*^{3cv} mice do not express revertant fibers while *mdx* mice and the other three *mdx*^{cv} strains do. In contrast, *mdx*^{3cv} express a nearly full-length dystrophin (415kDa) at very low levels (~5% of normal levels) in all skeletal muscle fibers, but not in heart. These dystrophin proteins result from alternative splicing of the transcript, and lack the cysteine-rich domain sequences encoded by exon 65 and 66. Among the other *mdx*^{cv} mice differences in the number of revertant fibers and the amount of increment of fiber numbers over time are found. *Mdx*^{2cv} mice express 10 times more revertant fibers in skeletal muscle at the age of two and six months in comparison to *mdx*^{4cv} and *mdx*^{5cv} mice. With age, the number of revertant fibers increases 7.4 times, while increases of 4 and 4.6 times are found in *mdx*^{4cv} and *mdx*^{5cv} mice respectively. In this perspective, *mdx*^{2cv} mice are most comparable to *mdx* mice. Also in heart, the highest numbers and biggest clusters of revertant fibers are found in *mdx*^{2cv} mice. *Mdx*^{3cv} mice express revertant fibers in heart at the age of six but not two months.

Muscle function of the majority of the *mdx*^{cv} models is indistinguishable from *mdx* mice. The *mdx*^{5cv} mouse is an exception as a recent publication showed that they have functional deficits exceeding those observed in *mdx* mice. *Mdx*^{5cv} mice perform significantly worse on the rotarod and have more severe strength deficits in the diaphragm. No differences in force generation have been observed for the EDL and histopathology is also comparable between the two strains (Beastrom et al. 2011). Differences in genetic background probably underlie these findings, as differences in e.g. functional tests have been described before between different wild type strains (Connolly et al. 2001).

More distinct phenotypes have been observed in non-muscle tissues. The dystrophin isoforms Dp427, Dp260, Dp140 and Dp71 are expressed in the retina of both mouse and human. The function of the retina can be measured with an electroretinogram (ERG) which measures the electrophysiological response of the retina to light stimulation. DMD and BMD patients have abnormal ERG waveforms characterized by a reduced scoptopic b-wave. Severity of ERG abnormality is mutation specific; patients with mutations 3' have abnormal ERGs while these are normal in most patients with 5' mutations (Pillers et al. 1999;Pillers et al. 1995). To elucidate the correlation between position of the mutation and ERG severity, *mdx*^{cv} mice have been intensively studied. *Mdx*^{5cv} and *mdx* mice lacking only Dp427 have ERG waves comparable to those of wild type mice. All other strains that lack the retina isoform Dp260 have a phenotype, which differs in severity between them. *Mdx*^{2cv} and *mdx*^{4cv} mice show increased b-wave and oscillatory potential implicit times. *Mdx*^{3cv} mice are most severely affected and show in addition to increased b-wave and oscillatory potential implicit times also reduced b-wave amplitudes (Pillers et al. 1995). The mutation specific phenotype is caused by the different sites of expression, where Dp427, Dp260

and Dp140 are expressed at the outer plexiform layer of the retina, while Dp71 is expressed at retinal blood vessels and the inner limiting membrane (Howard et al. 1998). In addition, cones also have a higher Dp427 to Dp260 ratio than rods (Wersinger et al. 2011). As colour blindness is caused by non-functional rods, this nicely correlates to the finding that DMD patients who lack Dp260 more often present a deficit in red-green discrimination (Costa et al. 2007).

Also in brain, several dystrophin isoforms are expressed. Primarily *mdx*^{3cv} mice have been used to study the consequences of additional loss of all the other dystrophin isoforms. It was hypothesized that especially the loss of Dp140 and Dp71 might result in subtle abnormalities during brain development because these proteins are highly expressed in foetal brains (Lidov 1996). Studies investigating spatial learning abilities showed no differences in acquisition rates between *mdx*^{3cv}, *mdx* and wild type mice (Vaillend et al. 1995;Vaillend et al. 1998). Like in *mdx* mice, the retrieval of long term memory and synaptic transmission is unaltered in *mdx*^{3cv} mice, however differences in strategies to learn the task have been observed between these mice. In contrast to *mdx* mice, anxiety-related behaviour of *mdx*^{3cv} mice is enhanced, whereas locomotion is reduced compared to wild type mice (Vaillend and Ungerer 1999). Strangely, the ability of *mdx*^{3cv} mice to learn to press a bar is in the acquisition phase almost comparable to that of wild type, while *mdx* mice perform much worse. Performance in the extinction phase however is similar between all mice. The differences observed between *mdx* and *mdx*^{3cv} mice might be caused by the expression of low dystrophin levels in *mdx*^{3cv} mice and/or the different genetic backgrounds. However, more extensive research is needed to elucidate the exact mechanisms.

1.2.3. The *mdx52* mouse

As only a limited number of DMD patients carry point mutations, the *mdx52* mouse was generated to mimic a frequently found deletion in humans (Araki et al. 1997). In this mouse exon 52 of the *Dmd* gene was disrupted by means of homologous recombination on a C57BL/6J background. These mice lack, similar to *mdx*^{4cv} mice, full-length dystrophin and the shorter isoforms Dp260 and Dp140. Pathology and muscle function is similar to that of *mdx* mice. Hypertrophy of limb muscles is present in four months old mice along with variation in fiber size and central nucleation in 90% of the fibers. At this age also the diaphragm is more severely affected than the tibialis anterior and EDL. Revertant fibers are occasionally observed. There are no pathological changes in the heart and brain nor have behavioural changes been identified in 18 months old mice.

These mice have also been used to explore the applicability of exon 51 skipping. PMOs targeting exon 51 induced exon skipping resulted in synthesis of truncated but functional dystrophin in the absence of adverse effects (Aoki et al. 2010).

1.2.4. The *mdx/utrn* $^{-/-}$ mouse

Disease pathology of *mdx*, *mdx*^{cv} and *mdx52* mice is relatively mild in contrast to that of DMD patients, which is partly caused by functional compensation for dystrophin through the upregulation of utrophin. It was hypothesized that absence of both proteins would result in a more severe model, which would accelerate research. Therefore, effort was put into making a utrophin knockout mouse (*utrn* $^{-/-}$) to be used to generate a dystrophin and utrophin knockout mouse. However, as spontaneous mutations in the utrophin gene had never been found, it was believed that mice lacking this protein would not be viable (Grady et al. 1997a;Pearce et al. 1993). Despite these speculations, two independent groups successfully generated *utrn* $^{-/-}$ mice (Deconinck et al. 1997a;Grady et al. 1997a).

In 1997, Deconinck et al. made a construct in which an NH2 terminal exon of the *Utrn* gene, which is located in the actin-binding domain, was missing. They transfected embryonic stem (ES) cells with this construct and generated *utrn* $^{+/-}$ mice which were crossed to obtain *utrn* $^{-/-}$ mice. The mutation led to the complete loss of full-length utrophin (Deconinck et al. 1997a). Simultaneously, Grady et al. generated *utrn* $^{-/-}$ mice in which the COOH-terminal cysteine-rich region of the *Utrn* gene was removed, which is needed for binding to the DGC (Grady et al. 1997a). To do so, ES cells with this mutation generated by homologous recombination were implanted and resulted in germ line chimeras. *Utrn* $^{-/-}$ mice were again produced from crossings of *utrn* $^{+/-}$ mice. Despite the slight difference in the way utrophin expression was abolished, both models were phenotypically normal. Therefore, phenotypes of both mice will be discussed together, without making any distinctions.

Despite expectations, *utrn* $^{-/-}$ mice appeared to be viable and able to produce normal litter sizes. They did not develop any dystrophic phenotype or behavioural abnormalities and even two year old mice were indistinguishable from age-matched wild type mice in prospect of muscle function. As utrophin normally clusters with AChRs of the NMJ, a subtle phenotype was expected. Although synapses of *utrn* $^{-/-}$ mice had a normal architecture, AChRs density was 30% lower than that of *utrn* $^{+/-}$ mice, postsynaptic currents were altered and the number of postsynaptic folds of the NMJ was lower in *utrn* $^{-/-}$ mice than these of *mdx* and *utrn* $^{+/-}$ or $^{+/+}$ mice. Although utrophin was missing from the synaptic sites, the synaptic DGC complex was maintained and no decrease in levels of any of the proteins was observed, probably as a consequence of dystrophin somehow making up for the utrophin absence. As discussed in section 1.1.2.1, the distribution of utrophin and dystrophin does not overlap in the NMJ. It was assumed that the DGC complex would be unaffected in the *utrn* $^{-/-}$ mice as a result of replacement of utrophin by dystrophin. Investigations however revealed that this was not the case as dystrophin was evenly distributed with no synaptic enrichment. Dystrophin did also compensate for utrophin in several other organs like brain, kidney and heart (Deconinck et al. 1997a;Grady et al. 1997a).

As *utrn* $^{-/-}$ mice were viable and free from any dystrophic phenotype, both research groups crossed them with *mdx* mice to obtain mice lacking both dystrophin and utrophin. These mice were called *mdx/utrn* $^{-/-}$ or double knockout (dko) mice (Deconinck et al. 1997b;Grady et al. 1997b). Extensive studies have been carried out, elucidating the consequences of the lack of both proteins in mice. In accordance with the two *utrn* $^{-/-}$ mouse models, no phenotypical differences have been described for the two *mdx/utrn* $^{-/-}$ strains. Therefore no distinction will be made between the two from now on.

Mdx/utrn $^{-/-}$ mice are much more severely affected than *mdx* mice and closely mimic the phenotype of DMD patients. At birth, *mdx/utrn* $^{-/-}$ pups have a similar appearance as *mdx* and

wild type pups. However, from weaning onwards, *mdx/utrn* $^{-/-}$ mice are significantly smaller than *mdx* mice and develop joint contractures and kyphosis leading to abnormal breathing patterns. They show difficulties walking and have an abnormal posture of the hindlimbs as they are not able to spread them like *mdx* or wild type mice (Figure 13). Mice die prematurely between 4 and 20 weeks. Only 50% is still alive at the age of eight weeks, and they rarely survive 12 weeks. Life span can be slightly extended by feeding the mice wet food or sunflower seeds, but it never exceeds 20 weeks. The primary cause of death is unknown, but is most often related to respiratory and heart failure combined with swallowing difficulties, so it might be generalised weakness and conditional loss.

Even though *mdx/utrn* $^{-/-}$ mice have a significantly reduced life span, muscle pathology does not dramatically differ from that observed in *mdx* mice. It is hypothesized that the absence of severe histopathology is caused by the lack of time for pathology to develop due to their short life span. The most dramatic difference in histopathology is seen in the extraocular muscles which are spared from pathology in *mdx* mice, but are severely affected in the *mdx/utrn* $^{-/-}$ mice, indicating that the upregulation of utrophin in particular prevents pathogenesis in *mdx* mice (Porter et al. 1998).



Figure 13. Phenotypical characteristics of *mdx/utrn* $^{-/-}$ mice.
A. Pictures of a C57BL/10ScSnJ mouse which is able to spread its hindlimbs upon handling by the tail and which does not show any malformations of the back. **B**. The *mdx/utrn* $^{-/-}$ mouse is unable to spread it hindlimbs normally as they contract upon handling. In addition, severe kyphosis is visible.

Subtle differences are seen in the onset of degeneration and development of necrosis which is already observed in six day old *mdx/utrn* $^{-/-}$ mice whereas at that time this is not yet observed in *mdx* mice. At the age of three weeks, when repeated cycles of degeneration and regeneration start in *mdx* mice, both strains have similar amounts of fibrosis, necrosis and inflammation. Although pathology in skeletal muscle but not diaphragm subsides in older *mdx* mice, this does not occur in *mdx/utrn* $^{-/-}$ mice, resulting in more intensive fibrosis and necrosis in 10 week old mice. Nevertheless, severity of histopathology at time of death is significantly less

compared to that seen in 18 months old *mdx* mice. Contrastingly, severity of the diaphragm is indistinguishable between the two models. In several muscles of *mdx/utrn* $^{-/-}$ mice fiber types tend to shift towards type I fibers. Although *mdx/utrn* $^{-/-}$ mice are much smaller than *mdx* mice, relative body weight to muscle mass does not significantly differ. Muscles of *mdx/utrn* $^{-/-}$ mice also seem to have problems to mature. Normally, only regenerating and immature fibers express developmental proteins like embryonic myosin heavy chains (eMHC) and neural cell adhesion molecule (N-CAM) and lose this expression upon maturing. Surprisingly, in a substantial group of large calibre fibers in *mdx/utrn* $^{-/-}$ mice eMHC and N-CAM expression remains present in contrast to *mdx* and wild type mice (Deconinck et al. 1997b;Deconinck et al. 1998;Grady et al. 1997b;Rafael et al. 1998).

With minor pathological changes of the NMJ in *utrn* $^{-/-}$ mice, extensive research has been carried out on the NMJ of *mdx/utrn* $^{-/-}$ mice. The axon of the synaptic terminal of the NMJ is similar to that of *mdx* mice, however, it almost completely lacks folding in the postsynaptic motor end plate regions. As previously mentioned, the synapse end plate of *utrn* $^{-/-}$ mice is identical to wild type mice, whereas a proportion of those seen in *mdx* mice are broken up to some extent and not as continuous. All synapses of *mdx/utrn* $^{-/-}$ mice are broken up into multiple boutons. No differences have been observed in intensities of AChRs detected by α-bungarotoxin staining between *mdx* and *mdx/utrn* $^{-/-}$ mice (Deconinck et al. 1997b;Grady et al. 1997b;van Putten et al. 2012). Like in the NMJ of *mdx/utrn* $^{-/-}$ mice the MTJ has significantly less foldings compared to *mdx* mice, which might be detrimental to force transmission. This causes marked increases in forces placed on individual contact areas between fiber membrane and the connective tissue matrix of the tendon resulting in membrane damage in these regions. A causative defect from nerves or synapses was ruled out after an experiment demonstrated that muscles that were repetitively stimulated had a similar time for tension to fall 50% as wild type mice, indicating that the impaired muscle function solely has a muscular basis (Grady et al. 1997b;Deconinck et al. 1997b).

In *mdx/utrn* $^{-/-}$ mice, the synaptic DGC complex is partly maintained despite the lack of both utrophin and dystrophin. This strengthened the observation that dystrophin expression is not upregulated in utrophin negative synapses. In *mdx/utrn* $^{-/-}$ mice levels of β-dystroglycan and α-sarcoglycans are comparable to those of *mdx* mice, while β_2-syntrophin and dystrobrevin are nearly undetectable. Even though expression of utrophin, dystrophin and a majority of the synaptic DGC proteins is altered in *mdx/utrn* $^{-/-}$ mice, expression of laminin-β2, agrin and rapsyn is unaffected. This indicates that synaptic development does not depend on these proteins, but that structural stabilization and maintenance do (Deconinck et al. 1997b;Grady et al. 1997b).

Muscle force is also more severely impaired in *mdx/utrn* $^{-/-}$ mice compared to *mdx* mice. *In vitro* electrophysiology showed that twitch tension is significantly reduced in steromastoid muscle, EDL, soleus and diaphragm. Relaxation time was also found to be greatly prolonged especially in the diaphragm. Time to peak tension, on the other hand, does not differ between *mdx/utrn* $^{-/-}$ and *mdx* mice in the steromastoid muscle, EDL, soleus and diaphragm. Interestingly, although force is greatly reduced in *mdx/utrn* $^{-/-}$ mice, repeated stimulation of the soleus did result in the same level of fatigue compared to *mdx* and wild type muscle, as force remained relatively stable. Apparently, where 40-50% of the soleus consists of fatigable type II fibers in *mdx* and wild type mice, in *mdx/utrn* $^{-/-}$ mice the soleus mainly consists of type I fibers (Deconinck et al. 1998;Grady et al. 1997b). The drop in force described can be partly addressed by administration of several compounds (Call et al. 2011;Yue et al. 2006).

Heart function of *mdx/utrn* $^{-/-}$ mice has been studied both by ECG and cine-MRI analysis. Before the age of five weeks, no visual abnormalities are present in cardiomyocytes.

From the age of seven weeks onwards, Evans blue dye uptake is significantly elevated and large patches of degenerating cardiomyocytes, inflammation and fibrosis has been reported in some studies (Chun et al. 2012;Hainsey et al. 2003;Verhaart et al. 2011;Grady et al. 1997b). Other studies did not find histopathology in 10 week old mice (Deconinck et al. 1997b). The onset of cardiomyopathy in *mdx/utrn* $^{-/-}$ is significantly earlier than that in *mdx* mice as first abnormalities are already observed at the age of five weeks consisting of a significantly decreased heart rate. Discrepancy in literature exists about the heart rate in eight week old mice as both a decrease and increase in heart rate has been described. Abnormal ECG patterns have been found with significantly decreased S- to R-wave ratios and depressed contractile function of the right ventricular muscles (Bia et al. 1999;Chun et al. 2012;Janssen et al. 2005). In depth cine-MRI revealed a diminished left ventricular function with a significantly decreased cardiac output, stroke volume, end diastolic volume and cardiac mass while ejection fraction remained comparable to age-matched wild type mice. These findings correspond to cardiomyopathy seen in DMD patients which also display a decreased stroke volume, resulting from hypertrophy of the left ventricle (Maciver and Townsend 2008). With declining heart function one would expect an increase in end diastolic volume, however, in *mdx/utrn* $^{-/-}$ mice the end diastolic volume is decreased probably due to the decreased cardiac mass. The right ventricular function of *mdx/utrn* $^{-/-}$ mice is less severely affected, with only a decreased ejection fraction. This probably results from their severe respiratory impairment which decreases the work load for the right ventricle, but to compensate for the low oxygen supply increases the work load for the left ventricle (Chun et al. 2012;Verhaart et al. 2011). With ECG, decreased thickness of the left ventricular posterior wall and intraventricular septum was found in 10 week old *mdx/utrn* $^{-/-}$ mice. The decreased ejection fraction and end diastolic volume seen already in eight week old mice with cine-MRI was observed by ECG in 15 weeks old mice, accompanied by end systolic volume and fractional shortening. This difference probably reflects the difference in sensitivity between the two techniques used.

1.2.5. The *mdx/utrn* $^{+/-}$ mouse

Only recently, more attention has been drawn to the *mdx/utrn* $^{+/-}$ mouse (Huang et al. 2011;Zhou et al. 2008;Rafael-Fortney et al. 2011;Verhaart et al. 2011;van Putten et al. 2012). Previously, this mouse model was only used for breeding purposes to obtain *mdx/utrn* $^{-/-}$ mice. A limitation of the latter model is the short life span making long-term experiments impossible. The *mdx/utrn* $^{+/-}$ mouse expresses utrophin from only one allele and has a life span comparable to that of *mdx* mice. It was postulated that the phenotype of *mdx/utrn* $^{+/-}$ mice would be more severe than that of *mdx* mice and therefore would mimic the human phenotype better, without premature death.

Zhou et al. described that the quadriceps and diaphragm of three and six months old *mdx/utrn* $^{+/-}$ mice had more pronounced inflammation and fibrosis respectively, compared to age-matched *mdx* mice (Zhou et al. 2008). The diaphragm was more severely affected than the quadriceps for both strains. This results in impairment of respiratory function at the age of three and six months in both strains, measured with whole body pleismography (method to measure respiratory rate and amplitude in conscious mice) (Huang et al. 2011). Only at the later time point, *mdx/utrn* $^{+/-}$ mice performed significantly worse than *mdx* mice. Our own study addressed functional performance of these mice and directly compared it to that of *mdx/utrn* $^{+/+}$ and $^{-/-}$ mice, revealing severely affected motor function (Chapter 3). Heart function of both 2, 5, 6 and 10 months old *mdx/utrn* $^{+/-}$ mice is however not more severely impaired than that of age-matched *mdx* mice, as both strains show a mild decrease in left ventricle function and a large decrease in

right ventricle function at the latter time point (Verhaart et al. 2011;Rafael-Fortney et al. 2011). Further research is needed to elucidate why the heart is spared in these mice. It might be that this is caused due to differences in physical abilities, causing less strain on the heart of *mdx/utrn* $^{+/-}$ mice, or due to differences in genetic background.

The first article in which the phenotype of *mdx/utrn* $^{+/-}$ mice was partly corrected by compound administration was published by Rafael-Fortney et al. They showed that *ex vivo* function of cardiac, limb and diaphragm was partly corrected by lisinopril and spironolactone administration starting at four or eight weeks of age (Rafael-Fortney et al. 2011). Also tetanic force of the EDL and diaphragm was significantly impaired in 20 week old *mdx/utrn* $^{+/-}$ mice compared to wild type mice. Direct comparison with *mdx* mice is impossible as these were not included.

As functional compensation for dystrophin by monoallelic expression of utrophin seems to be insufficient in *mdx/utrn* $^{+/-}$ mice, AON treatment was assumed to have a more pronounced effect in these mice compared to *mdx* mice. Upon subcutaneous administration of 2OMePS for six months, we observed that AON uptake, exon skip levels and functional improvement was significantly higher in *mdx/utrn* $^{+/-}$ than in *mdx* mice (Tanganika-de Winter et al. manuscript submitted).

Based on these studies, it can be concluded that the *mdx/utrn* $^{+/-}$ mouse is a more severely affected model. This suggests that the functional compensation of dystrophin by heterozygous expression of utrophin is incomplete. Taken together, this underlines that the *mdx/utrn* $^{+/-}$ mouse is a better model than the *mdx* or *mdx/utrn* $^{-/-}$ mouse for long term experiments.

1.3. Low dystrophin levels in human and mice

1.3.1. DMD and BMD carriers

Although no therapy is available for DMD yet, different potential therapeutic approaches aiming to restore dystrophin synthesis are currently tested in clinical trials. These trials result in the expression of low dystrophin levels. However, it is not yet known how these levels affect disease pathology and which levels are needed to maintain or improve muscle integrity, to prevent against exercise-induced damage or to improve muscle function. In addition, it is unknown whether the percentage of dystrophin that is needed for these outcome measures will be similar for skeletal muscle and heart, or whether different muscles need different levels.

The first hints to answer these questions were obtained from DMD and BMD carriers. Symptoms in these females vary from mild muscle pain and cramps, to severe muscle weakness leading to wheelchair dependency. Muscle weakness is proximally distributed first affecting the legs and later the shoulder girdle. The age at onset ranges from the first to the fourth decade. Generally, onset before the age of 15 results in a severe phenotype (Hoogerwaard et al. 1999). The majority of DMD and BMD carriers (76% and 81% respectively) express ~50% of dystrophin early in life, based on random X-inactivation levels and these females are not affected. This indicates that these levels are sufficient to maintain skeletal muscle function and prevent pathology (Pegoraro et al. 1995;Schmidt-Achert et al. 1993). Non-random X-inactivation results in a mild dystrophic phenotype in rare cases. Despite muscle weakness being absent or only very mild, a small percentage (~8%) of the carriers develops DMD-associated dilated cardiomyopathy (Ogata et al. 2000;Hoogerwaard et al. 1999).

Manifesting carriers have also been described which express <50% of dystrophin. The prevalence of clinically manifesting DMD and BMD carriers in the female population is 1:45,000 and 1:100,000 respectively. Several mechanisms are known to cause symptoms in these carriers. The majority of manifesting carriers are the consequence of unfortunate, skewed X-inactivation (section 1.3.4.1.). In this case, the intact X-chromosome is predominantly inactivated, so that the X-chromosome with the *DMD* mutation is active in the majority of the cells. Disease severity in these carriers depends on the degree of inactivation of the intact X-chromosome. Examinations of biopsies from carriers reveal a mosaic pattern of fibers that do express dystrophin at normal intensities and fibers that lack dystrophin expression (Azofeifa et al. 1995;Pegoraro et al. 1995;Soltanzadeh et al. 2010). Some manifesting carriers however, have gross chromosomal rearrangements involving translocations between the X-chromosome and an autosome. These translocations lead to almost complete inactivation of the normal X-chromosome with the intact *DMD* gene, resulting in much decreased dystrophin levels (Lindenbaum et al. 1979;Boyd et al. 1986). Alternatively, a few rare cases have been described of females who suffered from Turner's syndrome (patients with this syndrome lack one X-chromosome) and also carried mutations in their *DMD* gene. In these patients, lack of dystrophin resulted in the typical DMD phenotype (Ferrier et al. 1965;Bjerglund and Nielsen 1984;Chelly et al. 1986). Also a number of monozygotic twins have been described with heterozygous mutations in their *DMD* gene. In all these cases one of the twins was phenotypically normal while the other had severe DMD-like symptoms. The affected twin showed unfortunate skewed X-inactivation resulting in low dystrophin levels. It is hypothesized that the twinning process directly relates to the observed low dystrophin levels, as no reports exists on cases in which both twins are manifesting. In rare occasions, during random X-inactivation, the maternal derived X-chromosome (Xm) is inactivated in particular clumps of cells while the paternal derived X-chromosome (Xp) is inactivated in other clumps. These clumps

might define each other as 'foreign' which initiates them to separate 3-8 days post fertilization (Richards et al. 1990). One article also reported a twin in which the unaffected girl had random X-inactivation while the affected girl had unfortunate skewed X-inactivation. This resulted from asymmetric splitting of the inner cell mass (ICM) (Lupski et al. 1991).

1.3.2. BMD patients

As mentioned in section 1.1.4., BMD patients express low levels of truncated but partly functional dystrophin. In these patients, disease severity varies from very mild, in which patients remain asymptomatic until later in life, till quite severe where patients are diagnosed in childhood and lose ambulation in the early to late teens. The clinical outcome depends primarily on the amount of dystrophin expressed. Patients expressing <3% of normal on average become wheelchair dependent before the age of 11 years. Levels between 3 and 10% lead to wheelchair dependence between the age of 13 and 20 years whereas levels >20% delay wheelchair dependence till the second decade (Hoffman et al. 1988;Hoffman et al. 1989). Most patients lose ambulation between 20-30 years after diagnosis. Life span of mildly affected patients is near normal, whereas severely affected patients die between the age of 40 and 50 years. Some BMD patients also suffer from dilated cardiomyopathy, which can be the main symptom in the less severely affected patients. Other patients only have very mild symptoms of either skeletal muscles and/or heart (Helderman-van den Enden et al. 2010). A case report of one BMD patient expressing 29% of dystrophin in a uniform manner revealed that this already completely prevented muscle pathology (Neri et al. 2007). Another study described patients expressing <10% dystrophin that were more severely affected than the patient that expressed ~20% of dystrophin (Beggs et al. 1991). Taken together, expression of dystrophin correlates with disease severity and even levels of ~30% can largely prevent pathogenesis.

1.3.3. Mouse models expressing low dystrophin levels from birth

With only limited access to tissues from DMD and BMD carriers and BMD patients, in-depth research was warranted in animal models expressing low dystrophin levels. Experiments in heterozygous *mdx* mice revealed that also in mice ~50% of dystrophin completely prevents skeletal muscle pathology. Additionally, they revealed that the number of dystrophin positive fibers increases over time due to their survival advantage over dystrophin negative ones. Surprisingly, these mice do not develop any heart pathology, while this is observed in ~8% of the DMD and BMD carriers. The cause for this difference is poorly understood (Bostick et al. 2008;Tanaka et al. 1990).

From the early nineties onwards, transgenic mice expressing full-length or truncated dystrophin of murine or human origin were generated to study the applicability of gene therapy for DMD (Dunant et al. 2003;Lee et al. 1993;Phelps et al. 1995;Rafael et al. 1994;Wells et al. 1995). The majority of these lines expressed dystrophin at intensities exceeding wild type levels or at both moderate and high intensities. Interestingly, some of these mice expressed <50% dystrophin as assessed by Western blot in a uniform or mosaic manner (Table 4). The way in which dystrophin was expressed and at which intensities differed per line. Within an individual mouse differences in expression between muscles and/or fiber types were observed, with fast fibers predominantly expressing dystrophin (Lee et al. 1993). These differences resulted most likely from the autosomal location of the transgene and the promoter by which it is driven.

Studies in these transgenic mice indicate that the beneficial effect of different types of dystrophins (full-length versus truncated) and the manner in which it is expressed (uniform versus mosaic) varies. Complete restoration of disease pathology was observed in mice uniformly expressing full-length dystrophin (mouse line 852 diaphragm) at intensities of ~20% of wild type levels. Expression of 40% of truncated dystrophin (mouse line 12157 quadriceps) did not completely restore pathology, although it dramatically reduced symptoms. This was confirmed by others: an incomplete restoration of pathology was observed upon uniform expression of 20-30% of truncated dystrophin (lacking exon 17-48), while no pathology was seen in mice expressing similar amounts of full-length dystrophin (Wells et al. 1995). This suggests that fibers expressing truncated dystrophin are more vulnerable to damage than those expressing full-length dystrophin (Chamberlain 1997;Phelps et al. 1995;Wells et al. 1995).

Author	Transgenic model	Dystrophin pattern	Histopathology
Lee 1993	Full-length murine	Mosaic (only dys positive in fast fibers) Western blot 20% in 1 month while 60% in 4 month old mice	Improved
Rafael 1994	Truncated murine lack 71-74	Mosaic 50% dys positive fibers in Qua (intensities from 1 to >100%) 10-20% dys positive fibers in Dia	Qua: improved fibrosis Dia: no improvement
Phelps 1995	Full-length murine Line 8487	Mosaic Western blot 15% dys in Qua Western blot <5% dys in Dia	Qua: partial reduction CN Dia: reduction fibrosis and inflammation
Phelps 1995	Full-length murine Line 852	Uniform (U)/Slightly variable (Sv) Western blot >70% dys in Qua (U) Western blot 20% dys in Dia (Sv)	Qua: prevented all pathology Dia: prevented all pathology
Phelps 1995	Truncated murine lack 17-48 Line 12157	Uniform (U)/Mosaic (M) Western blot 40% dys in Qua (U) Western blot 20% dys in Dia (M)	Qua: dramatic reduction of pathology Dia: no improvement
Wells 1995	Human full-length	Uniform Western blot 20-30% dys in Dia	Prevented all pathology
Wells 1995	Human mini-dys lack 17-48	Uniform Western blot 20-30% dys in Dia	Nearly prevented all pathology still some CNs
Hauser 1997	MCK promoter driven expression	Uniform Western blot 20% of wild-type in Dia	Nearly prevented all pathology
Hauser 1997	MCK promoter driven expression	Mosaic Levels not mentioned in article	Improvement depended on % dys positive fibers
Dunant 2003	MCK promoter driven expression	Mosaic (only dys positive in fast fibers) In ~50% of the fibers	Improved
Stillwell 2009	Wild-type ES-cell incorporation	Mosaic Western blot 60-100% or <5% of wild-type	Dose dependent improvement
Li 2008	*Mdx*^{3cv} mouse	Uniform Western blot ~5% of wild-type	Some improvement in young not old mice

Table 4. Overview of *mdx* mice generated that express <50% dystrophin.
This table summarizes some of the transgenic *mdx* mice that express low levels of full-length or truncated dystrophin from murine or human origin. Dystrophin expression is either in a mosaic or uniform manner. The amount of dystrophin expressed correlates with histopathology. CN= centralized nuclei, Dia= diaphragm, Qua= quadriceps.

Mosaic expression of dystrophin clearly protects fibers to damage to a smaller extent than homogenous expression, as higher total protein levels are needed to prevent pathology. While full-length dystrophin expressed at 20% of wild type uniformly, completely prevented pathology

(as stated above), mosaic expression only partly decreased the percentage of centralized nuclei (line 8487). However, mosaic expression of 20% of truncated dystrophin (line 12157), did not improve histopathology at all (Phelps et al. 1995). This indicates that the uniformity of dystrophin expression might be more relevant than the level of expression in protecting muscle fibers against pathogenesis. This observation was confirmed in an independent study generating different transgenic mouse lines (Hauser et al. 1997).

Although decreases in numbers of centralized nuclei were found in the majority of these lines, no clear correlation was observed between dystrophin expression in a particular fiber and the presence of nuclei located at the periphery or the center of that fiber (Rafael et al. 1994). However, others observed that dystrophin negative fibers neighbouring dystrophin positive ones were more likely to have nuclei at the periphery, than those surrounded by dystrophin negative fibers (Dunant et al. 2003). An increment in dystrophin positive fibers over time, which was observed in heterozygous *mdx* mice, was found in some (Lee et al. 1993), but not all transgenic models (Dunant et al. 2003;Rafael et al. 1994). This might be caused by the different ways in which these models were generated, or due to the young age of the mice at time of assessment.

Besides transgenic mice, alternative approaches have also been undertaken to generate mice expressing low dystrophin levels. Stillwell et al. injected wild type ES cells into *mdx* blastocytes (Stillwell et al. 2009). Depending on the incorporation of the ES cells, mice expressed dystrophin in either a very high (60-100%) or low (<5%) percentage of the muscle fibers at wild type intensities. The percentage of dystrophin positive fibers in these mice also differed per muscle. A dose-dependent restoration of muscle pathology was observed. This approach of generating animals for further investigations is less favourable as it is labour intensive and results in mice with dystrophin levels on both extremes of the scale only.

The final model expressing very low dystrophin levels is the *mdx*^{3cv} mouse. As described earlier, these mice express dystrophin in all fibers but at ~5% of the intensity of wild type mice. Li et al. observed that these levels resulted in some improvements in young but not in older mice. The EDL of young mice was partially protected from eccentric contraction-induced injury and had a significant higher tetanic force compared to *mdx*^{4cv} mice (Li et al. 2008). Also the forelimb grip strength of the *mdx*^{3cv} mice was slightly increased. No difference in CK was detected, nor did histopathology differ between *mdx*^{3cv} and ^{4cv} mice.

1.3.4. Treated *mdx* mice expressing low dystrophin levels

Despite the lack of a good mouse model to assess the effect of low dystrophin levels on disease pathology, knowledge could still be obtained from mice that expressed low dystrophin levels upon treatment with AONs, AAV-U1 and gentamycin. These studies primarily focussed on the effect of low dystrophin levels on functional and biomarker outcome measures. Intramuscular PMO administration revealed that dystrophin expression in ~20% of the fibers (resembling ~10% assessed by Western blot) largely protects muscles against eccentric contraction induced injury. The functional improvement correlated more strongly to the number of dystrophin positive fibers than to levels assessed by Western blot, which again indicates that the total number of fibers expressing dystrophin is most relevant (Sharp et al. 2011). The same compound was also systemically injected in *mdx* mice at a low (5mg/kg) and high (50mg/kg) dose for 20 or 50 weeks. Short term treatment resulted in 23% (5mg/kg, resembling 20% on Western blot) and 27% (50mg/kg, 40% on Western blot) of dystrophin positive fibers in the tibialis anterior, expressing dystrophin at intensities slightly lower and higher than wild type for the low and high dose respectively. This resulted in improved grip strength and resistance to eccentric contractions.

Treatment for 50 weeks with the same doses resulting in ~60% of dystrophin in the tibialis anterior improved voluntary activities and grip strength, but not resistance to eccentric contractions. Histopathology in all mice was only slightly improved (Malerba et al. 2011b). Uniform dystrophin at intensities of 20% of wild type, induced by gentamycin treatment has been found to partly protect muscles even while chronically challenged with horizontal treadmill exercise twice weekly. In these mice, histopathology and CK levels were reduced, however higher levels were needed to restore altered calcium homeostasis (De Luca et al. 2008). Very low dystrophin levels (<10%) resulting from exon skipping either induced with 2OMePS or AAV-U1 have been shown to reduce the expression of some mRNA and miRNAs involved in various aspects of disease pathology (Verhaart et al. 2012;Cacchiarelli et al. 2010).

1.3.5. The *mdx-Xist*$^{\Delta hs}$ mouse

Despite the fact that transgenic mice and mice treated with potential therapeutic compounds provided us with important information regarding the effects of low dystrophin expression on muscle pathology, these approaches are not ideal for more in-depth research. The disadvantages of the transgenic lines are the big differences in dystrophin intensities between individual fibers as well as fiber type specific dystrophin expression which are not favoured. An obvious disadvantage of treating mice is that treatment is quite expensive, stressful to the mice and labour intensive. With this in mind, we generated the *mdx-Xist*$^{\Delta hs}$ mouse model, which expresses low levels of dystrophin from birth onwards based on intentionally skewed X-inactivation.

1.3.5.1. X-inactivation

In all animals in which there is an imbalance in the amount of sex-chromosomes (e.g. female humans and mice carry two X-chromosomes, while males only carry one X-chromosome), compensation is ensured by sex chromosome inactivation (generally X-inactivation in mammals) resulting in equal transcript levels between females and males (Lyon 1961). This is a critical event as failure results in significant copy number variation of around 1000 genes resulting in embryonic lethality or malformations. Although X-inactivation was discovered 50 years ago, the exact mechanism, which differs between species, is still poorly understood. Two distinct cycles of X-inactivation (imprinting and random X-inactivation) have been described in mice, whereas only the latter occurs in humans. In mice, at the 2-4 cell stage, equal levels of both the Xp and the Xm are active (Figure 14). From this stage onwards, Xp is inactivated via imprinting, ensuring Xm being active in all extra-embryonic tissues. Maternal germ line cells are protected against inactivation by an imprint which represses *Xist* expression (see below). The inactive state of Xp is reversed again in the ICM of the blastocytes. Thereafter, either Xp or Xm is inactivated in each cell during random X-inactivation. All descendants of these cells inherit the same inactivation pattern which is maintained throughout life. Only in the female germ line, the inactivation pattern is reversed ensuring that all oocytes have an active X-chromosome (Xa) (Ng et al. 2007).

Both imprinted and random X-inactivation rely on one single locus; the X-inactivation center (Xic). The Xic expresses many regulatory elements which mediate in the inactivation process. At the onset of random X-inactivation, the X-pairing region ensures pairing of the X-chromosomes. Subsequently, the number of X-chromosomes rerlative to the number of autosome is counted. This is done based on levels of *Rnf12*, which is expressed from the Xic.

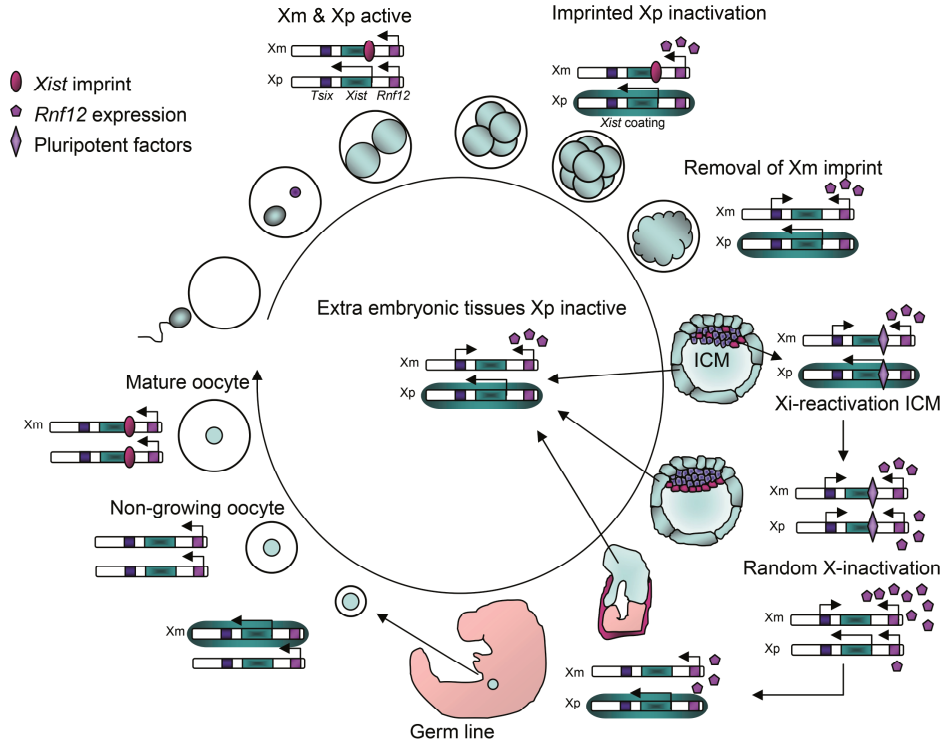


Figure 14. The mechanism of random X-inactivation in mice.
In mice the paternally derived X-chromosome (Xp) is inactivated in all extra-embryonic tissue from the 2-4 cell stage onwards. The maternally derived X-chromosome (Xm) is protected from X-inactivation by an imprint. In the blastocytes, upon reversion of the inactive state of the Xp, either the Xp or Xm are inactivated in a random manner. At initiation of random X-inactivation both Xp and Xm express high levels of *Rnf12*, *Tsix* and pluripotency factors. In one of the two chromosomes, *Rnf12* and *Tsix* expression decrease initiating overexpression of *Xist* on the other X-chromosome. The *Xist* expression leads to coating of that X-chromosome which makes it transcriptional inactive. The active or inactive state of the X-chromosomes is maintained throughout life. Only the X-chromosomes in the germ line remain active and become imprinted (Picture based on by Augui et al 2011 Nat. Rev. Genet.).

Females express twice as much *Rnf12* compared to males. Regardless of the number of X-chromosomes present, only one of them remains active. This decision is made during an interplay between the main players *Rnf12*, *Tsix*, *Jpx* and *Xist*, but the pluripotency factors NANOG, OCT4 and SOX2 are thought to play a role as well (Augui et al. 2011). *Xist* and *Tsix* are two long non-coding RNAs which are expressed from partly the same location of the Xic in sense and antisense direction respectively. At initiation of X-inactivation, both X-chromosomes express *Rnf12* and *Tsix* and thereby trigger the expression of *Xist*. Later on, downregulation of *Rnf12* and *Tsix*, and upregulation of *Jpx* on the future inactive X-chromosome (Xi) lead to a monoallelic upregulation of *Xist* (Tian et al. 2010;Lee et al. 1999). This results in coating of this X-chromosome, initiating its inactivation. Consequently, Polycomb protein complexes are recruited which ensure packaging of the DNA by histone modifications into heterochromatin thereby making it transcriptionally inert. In this way, a discrete body in the nucleus called the Barr body is formed. As previously mentioned the inactive state of Xi is inherited by daughter cells and maintained throughout life. Some regions located on the short arm of the X-chromosome, escape inactivation.

These regions are called pseudoautosomal regions and contain genes that are also present on the Y-chromosome, obviating the need for dosage compensation (Carrel and Willard 2005).

To study the mechanism of X-inactivation, many mouse models have been generated each lacking an important modulator of X-inactivation on one or both alleles (Barakat et al. 2011;Shin et al. 2010;Tian et al. 2010;Penny et al. 1996). We used one of these models (*Xist*$^{\Delta hs}$ mouse) for the generation of two new innovative mouse models for DMD, which are described in Chapters 5, 6 and 7 of this thesis. As previously mentioned, in these models the phenomenon of skewed X-inactivation, as seen in some female symptomatic DMD and BMD carriers, was used as a concept. The mouse model used had a PGKneo cassette inserted immediately upstream of the *Xist* promoter P_1 (Newall et al. 2001). The authors observed that in heterozygous *Xist*$^{\Delta hs}$ females, targeting this locus resulted in preferential inactivation in ~80-90% of X-chromosomes carrying the mutation in *Xist*. We crossed *Xist*$^{\Delta hs}$ females with *mdx* males in our lab. In the female pups, the mutated *Xist* gene was heterozygously expressed, resulting in preferential inactivation of the X-chromosome with the mutation in the *Xist* gene. As these X-chromosomes do not carry a mutated *Dmd* gene, their preferential inactivation causes a preponderance of active X-chromosomes from the *mdx*-background on overall deficit of dystrophin positive cells in female progeny. Therefore, female *mdx-Xist*$^{\Delta hs}$ offspring typically express dystrophin levels between 3-47% depending on their X-inactivation ratio. Detailed information regarding their phenotype can be found in Chapters 5 and 6 of this thesis.

1.3.6. The *mdx/utrn* $^{-/-}$ */Xist*$^{\Delta hs}$ mouse

In *mdx* mice utrophin very effectively compensates for the lack of dystrophin resulting in a very mild phenotype. It is therefore of interest to study the effects of low dystrophin levels in a utrophin negative background. Due to the severe phenotype of *mdx/utrn* $^{-/-}$ mice, this model is more suitable to assess the dystrophin levels needed for improved life expectancy as well as pathology and muscle function.

Several labs have put effort in generating such a mouse over time, unfortunately without any success as none of the models expressed a variety of low dystrophin levels. The first attempt was made in 1999, in a paper focussing on the role of dystrophin and utrophin in non-muscle tissues but no protective effects were observed for the low dystrophin levels expressed (Rafael et al. 1999). Several years later, Li et al. generated utrophin negative *mdx*^{3cv} mice (Li et al. 2010). For these mice, a significantly improved life span has been reported (in contrast to the findings of Rafael et al). The difference might result from differences in backgrounds of the strains among others.

Exploiting the principle of skewed X-inactivation patterns like we did for the *mdx-Xist*$^{\Delta hs}$ mice, we generated *mdx/utrn* $^{-/-}$ mice expressing low dystrophin levels. To utilize these mice, *utrn* $^{-/-}$ *Xist*$^{\Delta hs}$ males were needed. These mice were generated by crossing *Xist*$^{\Delta hs}$ females with *utrn* $^{-/-}$ *hDMD* $^{+/-}$ males. The *hDMD* mouse has an intact and functional copy of the human dystrophin gene on a C57BL/6 background. This mouse model was generated earlier in our group ('t Hoen et al. 2008). The *hDMD* gene functionally compensates for the absence of mouse dystrophin. In the pups we selected against the *hDMD* gene so that we obtained *utrn* $^{-/-}$ *Xist*$^{\Delta hs}$ mice. These mice were further crossed with *mdx/utrn* $^{+/-}$ females to generate *mdx/utrn* $^{-/-}$ */Xist*$^{\Delta hs}$ female pups. This model is the first in its kind expressing dystrophin levels that are between 1 and 38% and extensive research is described in Chapter 7 of this thesis.

1.4. Outcome measures

1.4.1. Functional tests

Preventing or delaying the onset of progressive loss of muscle function is the ultimate goal of clinical trials currently ongoing for DMD. Therefore, muscle function is the most important outcome measure in pre-clinical screening of potential therapeutic approaches and compounds. To determine motor function pre-clinically in mouse models of DMD, several different functional tests have been designed. As they do not interfere with disease progression, they can be used to either assess the course of natural history of the disease, or the effects of compounds on disease progression (Chapter 2) (van Putten et al. 2010). Examples of non-invasive functional tests are the grip strength, the rotarod and hang tests (Figure 15A-E). Using the grip strength test, strength of either the forelimbs or hindlimbs can be tested based on the instinct of a mouse to grasp an object (Connolly et al. 2001). The rotarod is used to test muscle function and coordination and involves walking on a rotating tube that increases in speed in the first minute (Chapillon et al. 1998). Balance, coordination and muscle condition can be tested with hanging tests. A distinction can be made between two types of hanging tests in which either only the forelimbs of all four limbs are used at start of the test. The start position with two limbs allows direct distinction in the functional abilities of a mouse to also start using its hindlimbs and tail thereby reducing the maximum load per leg. Contrastingly, in the hang test in which all limbs are used from the start onwards equal chances are given to all mice (Raymackers et al. 2003;van Putten et al. 2010). With dystrophin negative fibers being vulnerable to damage caused by exercise, the type, load and duration must be correctly chosen in these cases.

On the other hand, forced treadmill exercise can be chronically used to intentionally exacerbate disease progression and to determine the protective effect of compounds more thoroughly in *mdx* mice (Figure 15F). Horizontal treadmill running increases muscle necrosis of the quadriceps, gastrocnemius and triceps, whereas the diaphragm and tibialis anterior are affected to a lesser extent. Also an increase in the number of centrally nucleated fibers, the proportion of fast fibers and serum CK levels is found, whereas muscle strength decreases (De Luca et al. 2005;Payne et al. 2006;Radley et al. 2008;Pierno et al. 2007). Besides horizontal treadmill running, also downhill running can be applied. As *mdx* fibers are especially vulnerable to eccentric contractions, this type of exercise induces major pathology. Muscles mostly affected by this exercise are the diaphragm and triceps, while the tibialis anterior and EDL only show minor damage (Brussee et al. 1997). Alternatively, the treadmill can also be used to measure the ability of *mdx* mice to run on a horizontal treadmill and encouraged to run till exhaustion. Six months old *mdx* mice exhaust earlier (after ~12 min) than age-matched wild type mice (~after 60 min) (Brunelli et al. 2007;Minetti et al. 2006).

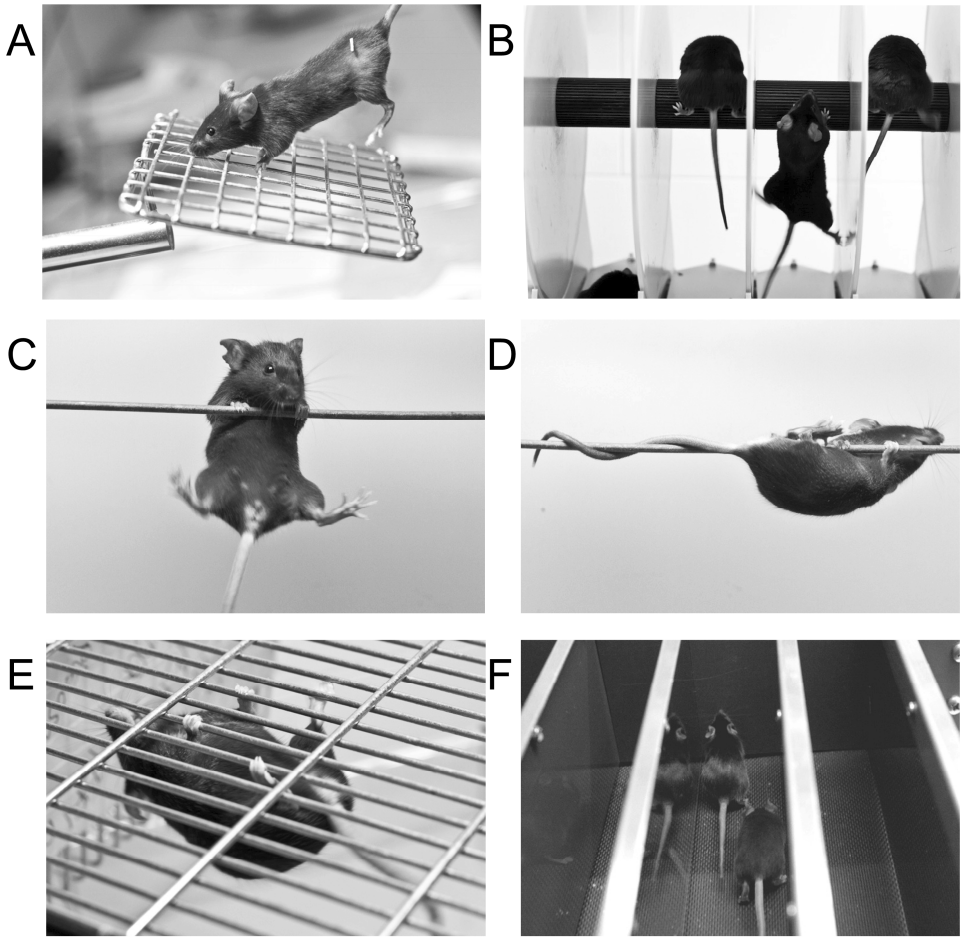


Figure 15. Overview of the most often used functional tests.
A. Grip strength device used to monitor strength of the extremities. **B**. Rotarod running device, used to measure the ability of a mouse to run on a rotating rod. **C-D**. Two limb hanging wire test. In this test, the begin position is with the two forelimbs. Mice that perform well can be distinguished by their ability to use their hindlimbs and tail additionally. **E**. Hanging wire test in which the start position is with four limbs. **F**. Treadmill device used in experiments to either exacerbate disease progression or to assess running abilities.

Interestingly, voluntary running exercise results in improved muscle function. Voluntary wheel running is assessed in mice that are individually housed in a cage enriched with a metal wheel and is used to determine neuromuscular impairment. Studies assessing the direct consequences of this exercise on muscle pathology in *mdx* mice showed that within 24-48 hours post exercise necrosis is doubled in the quadriceps, while the tibialis anterior remained spared. Also the EDL is more affected than the plantaris and soleus muscles (Archer et al. 2006;Radley and Grounds 2006). Long term voluntary running exercise has beneficial effects on muscle quality of *mdx* mice (Dupont-Versteegden et al. 1994;Carter et al. 1995;Landisch et al. 2008;Hara et al. 2002;Hayes and Williams 1996). Accumulation of dirt increases the resistance of the wheel rotation which is likely to influence outcomes, as even mild resistance already influences skeletal and heart muscle physiology in wild type mice (Konhilas et al. 2005). Interestingly, increased

workload does not negatively impact pathology in *mdx* mice. It does however force *mdx* mice to run less when the load is 13% of their body weight. This is only observed in wild type mice when the load is 25% of their body weight (Call et al. 2010). Alternatively voluntary activity can also be assessed in cages equipped with multiple photocell receptors and emitters that monitor horizontal and vertical movements (Spurney et al. 2009).

To summarize; major differences in the impact of different exercise types on disease pathology have been described ranging from extremely detrimental to beneficial. Generally, treadmill running is detrimental to *mdx* mice, voluntary exercise is beneficial and other functional tests do not have a distinct impact on muscle pathology. Exercise-induced histopathology does differ between muscles, as type II fibers are more prone to damage than type I fibers. Additionally, the likelihood that specific muscles get damaged depends on the recruitment of these muscles during the specific exercise. Also age influences the impact with young *mdx* mice being more vulnerable to exercise than old mice (Faist et al. 2001). When exercise is applied, physiological, metabolic and vascular adaptations can be observed (Kobayashi et al. 2008). It has been reported that these response can differ between dystrophic and wild type strains, which in turn might affect drug absorption and metabolism. A high degree of standardization in the methodology is essential to enable comparisons between experiments and labs. In a collaborative effort of the TREAT-NMD network of excellence and the Wellstone Center, numerous standard operating procedures for functional tests to be used in *mdx* mice are now available (http://www.treat-nmd.eu/resources/research-resources/dmd-sops/). Eventually extended knowledge on the influence of exercise on disease pathology is important to better advise DMD patients.

1.4.2. Heart function

In mice, heart function can be measured by ECG or MRI. During an ECG-scan, the heart's electric activities are recorded, which is visualised by waves and peaks (Figure 16). To do so, the mouse is anesthetized, after which two fine needle electrodes are subcutaneously inserted at the ventral junction between the chest and the right and left forelimbs. Additionally, one needle is inserted at the junction between the lower abdomen and left hindlimb (Bia et al. 1999). Recordings provide information regarding the heart rate, the rhythm of the heart beat and the strength and timing of the electrical signals. The cycle starts with spontaneous depolarization in the sinoatrial node located at the top of the right atrium, transmitting an electric signal that spreads from the right to the left atrium and results in contraction of the atria. The signal ends up in the atrioventricular node while the blood is pumped to the ventricles. This atrial depolarization is characterized in the ECG by the P-wave. The duration of this (PR interval) is an estimation for atrioventricular node function. The signal is further directed to the His bundle and the Purkinje cells. Both ventricles are depolarized when the signal is redirected back to the atria. This results in contraction (systole) of the ventricles pumping blood through the aorta and is reflected by the QRS complex. Relaxation of the atria and ventricles is ensured upon repolarisation of the ventricles (T-wave) which enables the heart to fill with blood (diastole). The QT interval reflects the de and repolarisation of the ventricles e.g. the time it takes for the ventricles to fully contract and relax. The ST segment is the period of depolarization of the ventricles (Bia et al. 1999;Hurst 1998).

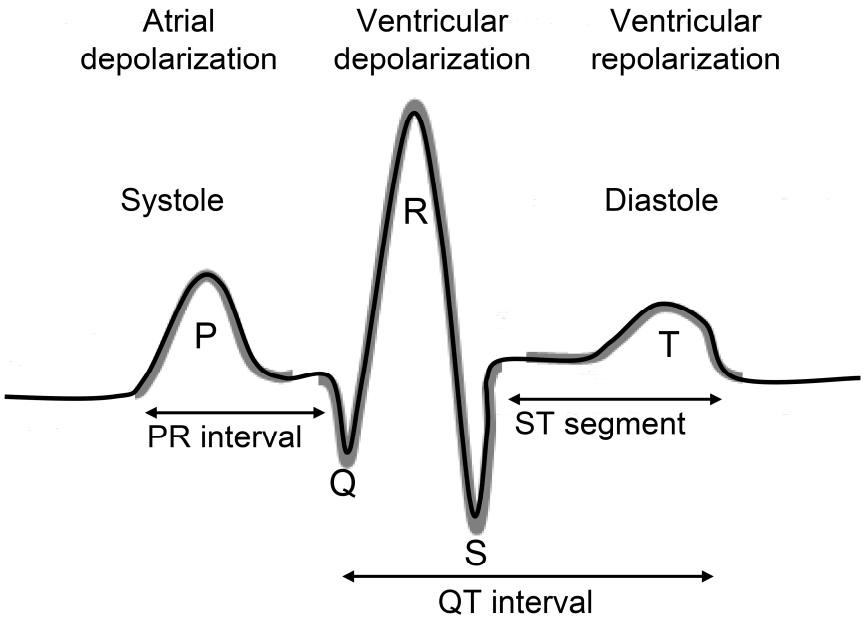


Figure 16. Electrocardiogram of the heart.
The ECG consists of a P-wave indicating atrial depolarisation, the QRS peak which resembles ventricular depolarisation whereas repolarisation of the ventricles is resembled by the T-wave. The PR interval reflects the time of the signal leaving the sinoatrial node to it ending up in the AV node. The QT interval is a reflection of the de and repolarization of the ventricles, so the total time for the ventricles to fully contract and relax. The ST segment is the period of depolarization of the ventricles. Heart failure is characterized by alterations in amplitude and timing of the waves and peaks.

The major disadvantage of the ECG is that it only provides indirect information regarding the ventricular contractions. Additionally, ECG measurements are significantly hampered in severely affected mouse models like the *mdx/utrn* $^{-/-}$ mice in which the position of the heart varies per individual due to severe kyphosis. Here, reliable data can still be obtained with MRI as this technique enables more in-depth and accurate assessments of the heart function (Verhaart et al. 2011). An MRI machine has an extremely powerful magnetic field, which forces all the hydrogen atoms in the body to align to the direction of this field. Upon generation of extremely strong radiofrequency waves, the nucleus of the hydrogen atoms in the body move slightly. When this is turned off, these atoms regain their position, sending out radiofrequency waves themselves which are detected and used to generate a picture. Hydrogen atom rich areas (i.e. blood) appear much brighter in these images then areas containing less hydrogen atoms (muscle) (Bothwell and Griffin 2011). Although mice are scanned in a vertical position in the coil of the MRI this does not affect heart function (Schneider et al. 2003). Pictures obtained cover the entire heart beat cycle and can be used to precisely determine contractions. The most often used outcomes measures are: the end diastolic volume and end systolic volume which represent the volume in the ventricle prior contraction and after ejection respectively. The stroke volume is the difference between those two parameters and represents the volume of blood which is pumped from a particular ventricle within a heart beat. The ejection fraction is the amount of blood which leaves the heart at every heart beat. The cardiac output is the volume of blood pumped by a particular ventricle within one minute (Crisp et al. 2011;Verhaart et al. 2011;Zhang et al. 2008).

1.4.3. Serum and gene biomarkers

Although functional tests are extremely valuable outcome measures, subtle changes cannot easily be detected. For potential upcoming therapies like AON-induced exon skipping, chronic administration will be necessary. Timing of these administrations will probably be patient dependent and monitoring disease progression with the use of serum biomarkers will be critical. Biomarkers are biological measurable parameters that offer a way to monitor normal and abnormal processes in e.g. body fluids that replace invasive biopsies (Nadarajah et al. 2011). One would aim for the use of robust biomarkers that are stable (not influenced by life style and dietary changes), specific (to a disease, pathway or genotype) and can repeatedly be quantified in which different analysis and laboratories obtain similar results. To date, serum CK has been used as a biomarker for diagnostic screenings of DMD patients. As CK leaks out of damaged muscle fibers, levels are low in more advanced stages of the disease when fibers are largely replaced by fibrotic and fat tissue. Additionally, CK levels increase upon activity, even in healthy controls. This reduces the utility of this biomarker, requiring the discovery of more robust biomarkers that can be used to monitor disease progression throughout the patient's life. In this thesis, several serum and gene expression biomarkers were assessed. To identify potential biomarkers, targeted (based on literature) and non-targeted (screening serum from DMD, BMD and controls to identify which proteins are differentially expressed) approaches were used for the gene and serum biomarkers respectively. The biomarkers used in this thesis were identified by the targeted approach and are important players in either maintenance of the ECM, inflammation, fibrosis, regeneration, heart and mitochondrial function.

Chapter 2

A 3 months mild functional test regime does not affect disease parameters in young mdx mice

M. van Putten, C.L. de Winter, W.M. van Roon-Mom, G.J.B. van Ommen, P.A.C. 't Hoen, A.M. Aartsma-Rus

Neuromuscular Disorders 2010; 20, 273-280

Abstract

To assess the effect of potential therapeutic agents in dystrophic mice it is useful to have a functional test regime that does not affect the natural disease progression of *mdx* mice with dystrophinopathy. We determined the effect of a 12 week test regime consisting of fore limb grip strength, rotarod analysis and two and four limb hanging wire tests on the disease progression of 4-week-old *mdx* mice. Mice performed the different functional tests on consecutive days on a weekly basis. No difference was found in serum creatine kinase levels between functionally active and sedentary mice. The percentage of fibrotic/necrotic areas assessed in a semi-automated way with colour deconvolution of skeletal muscles, heart and diaphragm did not vary within muscles or between groups, nor did the gene expression levels of disease-related genes. We conclude that this test regime may be suitable for short-term functional evaluation of therapeutic approaches in the *mdx* mouse.

Introduction

Duchenne Muscular Dystrophy (DMD) is an X-linked, severely progressive, muscle wasting neuromuscular disorder, which is caused by frame-shifting or nonsense mutations in the *DMD* gene. Translation of the disrupted reading frame results in the synthesis of truncated, non functional dystrophin protein (Hoffman et al. 1987). Intact dystrophin anchors the intracellular cytoskeleton of muscle fibers to the extracellular matrix and thereby protects the fibers from disruption during contraction. It also controls the calcium (Ca^{2+}) homeostasis, which is essential for normal fiber function (Blake et al. 2002). In dystrophin-negative muscles the Ca^{2+} homeostasis is disturbed due to an excessive influx through stress-activated channels and membrane tears. This leads to altered mitochondrial metabolism and down regulation of several mitochondrial genes, the activation of proteases, such as calpain, and the production of reactive oxygen species, resulting in more fiber damage and more Ca^{2+} uptake (Chen et al. 2000;Whitehead et al. 2006). This Ca^{2+} induced cascade leads to fiber necrosis, which attracts inflammatory cells that trigger fibrosis. Regeneration of fibers compensates for the lost muscle fibers, but eventually the regenerative capacity of the fibers becomes exhausted resulting in the replacement of healthy fibers by connective and adipose tissue (Deconinck and Dan 2007). In most patients, this causes profound muscle weakness leading to wheelchair dependency in the early teens and death due to respiratory and heart failure in their mid twenties.

The *mdx* mouse carries a nonsense mutation in exon 23 of the mouse *Dmd* gene (Sicinski et al. 1989). It is the most commonly used mouse to study the pathogenesis of DMD and to test putative therapeutic approaches (Grounds et al. 2008). Despite the similarity in gene defects, *mdx* mice are functionally less severely affected than DMD patients and their life expectancy is only slightly reduced compared to healthy mice. Muscle degeneration appears in cycles, the most pronounced acute phase lasts from 3 to 8 weeks of age, followed by relatively successful regeneration. In contrast to skeletal muscles, the diaphragm and tongue reflect the severe pathology found in DMD patients (Chamberlain et al. 2007). The less severe phenotype of *mdx* mice is thought to result from a combination of improved regeneration and, to some extent, functional compensation by the dystrophin homologue utrophin, although other yet unidentified factors may play a role as well (Blake et al. 2002;Perkins and Davies 2002).

Nonetheless, as a consequence of the genetic defect, *mdx* mouse muscle fibers cannot produce functional dystrophin resulting in fibers that are, like human DMD fibers, more vulnerable to contraction-induced injury and degeneration. Serum creatine kinase (CK) levels are elevated and the muscle fibers exhibit the same pathology resulting in fibrosis and necrosis in all

skeletal muscles including the heart in aging *mdx* mice (De Luca et al. 2008;Perkins and Davies 2002;Spurney et al. 2008).

Due to the pathology, transcription levels are altered for genes involved in immunological and tissue remodelling pathways. Microarray analyses of a series of dystrophic mice has resulted in several biomarkers that correlate with disease severity and progression, and that normalize upon therapeutic intervention ('t Hoen et al. 2006). These biomarkers are thus a useful tool to follow the natural course of the disease and monitor therapeutic effects over time.

Phenotypic severity in *mdx* mice can be exacerbated by exercise and eccentric contraction regimes (De Luca et al. 2008). The effect of a mild exercise regime on disease progression is less well understood. Several studies revealed beneficial effects, while other studies point towards harmful effects on disease progression (Dupont-Versteegden et al. 1994;Radley et al. 2008).

To determine whether genetic or pharmacologic treatment strategies are effective, more insight in the functional, histological and biomarker levels during the natural history of the disease in *mdx* mice is needed. To achieve this, a functional test regime that is not detrimental to the phenotype is needed. Therefore, we here assessed the effect of a 12 week functional test regime, consisting of four functional tests, on young *mdx* males. We monitored functional performance over time, and compared levels of previously identified fibrotic and immunologic RNA biomarkers between functionally challenged and unchallenged mice. In addition, we assessed the percentage of necrotic, fibrotic and regenerating cells using histological staining followed by a new semi-automatic analysis method based on the principle of colour deconvolution (Ruifrok et al. 2003). This analysis provides a more accurate, unbiased and faster method to analyze histopathology in whole muscle sections.

Materials and methods

Animal care

Mdx mice (C57BL/10ScSn-mdx/J) were bred at the animal facility of the LUMC. Mice were housed in individually ventilated cages with 12-h light–dark cycles. Standard mouse chow and water was given *ad libitum*. All experiments were approved by the Animal Experimental Commission (DEC) of the LUMC.

Functional tests

Four week old male *mdx* mice were randomly assigned to a functionally challenged or unchallenged group, each consisting of five mice. Functionally challenged mice underwent a 12 week test regime, consisting of four different functional tests, each addressing different muscle groups and/or coordination. Mice performed the four tests in the afternoon on consecutive days on a weekly basis (Supplementary Table 1). When possible, standardized operating procedures from the TREAT-NMD network were implemented (http://www.treat-nmd.edu/activities/treatment/html). Both groups were weighed at the beginning and end of each week.

Creatine kinase level analysis

Blood was collected weekly on Monday mornings from all mice in a Minicollect tube (0.8 ml Lithium Heparin Sep, Greiner bio-one, Austria) through a small cut at the end of the tail. CK levels were determined in sera with Reflotron CK test strips in the Reflotron plus machine (Roche diagnostics Ltd., UK).

Forelimb grip strength test

The forelimb grip strength test was performed with a home-made grid attached to an isometric force transducer that measures peak force of the forelimbs (Ugo Basile, Italy). Mice were suspended above the grid, which they instinctively grasped, and then pulled backwards. Mice were tested five times, with three consecutive measurements per trial (15 in total), and a two minute interval between trials. The three highest measured values were averaged to calculate absolute strength, which was divided by the body weight in grams. The degree of fatigue was measured by comparing the average of the first two and the last two trails as described previously (Connolly et al. 2001).

Rotarod

With the Rotarod (Ugo Basile, Italy) coordination, balance, muscle strength and condition was tested. Mice were placed on the rod that accelerated from 5 to 45 rotations per minute within 15 s. When a mouse ran for 500 s without falling from the rod, the test session was ended. Mice that fell off within 500 s were given a maximum of two more tries. The longest running time was used for analysis.

Two limb hanging wire test

Overall body coordination and strength was tested by a two limb hanging wire test. Mice were suspended above a metal cloth hanger secured 30 cm above a cage. The mouse was released a few seconds after instinctively grasping the wire with its forelimbs. Depending on the functional ability of the mouse, all limbs and the tail were used during a 10 min hanging session. Mice that fell down before the 10 min time limit were given two more tries. The longest hanging time was used for further analysis.

Four limb hanging wire test

Mice were placed on a grid where it stood using all four limbs. Subsequently, the grid was turned upside down 15 cm above a cage. Mice that fell down before the 10 min time limit were given two more tries. The longest hanging time was used for further analysis.

Histological examination

Mice were euthanized by cervical dislocation at an age of 16 weeks. Quadriceps, gastrocnemius, tibialis anterior, triceps, heart and diaphragm muscles were dissected and snap frozen in 2-methylbutane (Sigma–Aldrich, The Netherlands) cooled in liquid nitrogen. Sections of 8 µm were cut with a Shandon cryotome (Thermo Fisher Scientific Co., Pittsburgh, PA, USA) on Superfrost Plus slides (Thermo Fisher Scientific, Menzel-Gläser, Germany) along the entire length of the muscle with an interval of 240 µm between the sections. The excess tissue belonging to the 240 µm intervals was collected in MagNa Lyser Green Beads tubes (Roche diagnostics Ltd., UK) for total RNA isolation. Sections were fixed for five minutes with ice-cold acetone and stained with Harris haematoxylin and eosin (H&E) (Sigma–Aldrich, The Netherlands) according to conventional histological procedures. The diaphragm was stained with the Masson's trichrome staining (Sigma–Aldrich, The Netherlands). Sections were examined with a light microscope (LeicaDMLB, Leica Microsystems, The Netherlands) at a 2.5 times magnification at five locations in the muscle. Images were captured with a Leica DC500 camera and Leica IM50 software (Leica Microsystems, The Netherlands). Blending and background correction was performed with Adobe Photoshop CS3 version 10.0.1. Freely available ImageJ software with the

haematoxylin/eosin (H&E) colour deconvolution plugin (Rasband, W.S., ImageJ, US National Institutes of Health, Bethesda, Maryland, USA, http://rsb.info.nih.gov/ij/, 1997–2008) was used to determine the fibrotic/necrotic percentage of the entire cross section. This plugin provides a number of "built in" stain vectors to provide an accurate stain separation of the green, blue and red component, which is based on the primary and secondary three-dimensional colour space (RGB and CYM) (http://www.dentistry.bham.ac.uk/landinig/software/cdeconv/cdeconv.html). Based on this linear description, ImageJ plugins have been created for different histological stainings (Ruifrok et al. 2003). The total tissue area was determined on the original picture while the area of healthy cells was determined using ImageJ's automatic threshold on the eosin component, obtained after H&E colour deconvolution. For the diaphragm, (Masson's trichrome staining) the haematox component of this plugin was used. This allowed calculation of the percentage of fibrosis/necrosis ((whole area minus healthy area) divided by whole area).

Biomarker analysis

Total RNA was isolated using RNA-Bee (Tel-Test, Bio-Connect, Huissen, The Netherlands) and purified with the NucleoSpin RNA II kit according to the manufacturer's instructions including a DNAse digestion (Bioke, The Netherlands). The RNA concentration was measured on a Nanodrop (Nanodrop Technologies, DE, USA) and integrity was checked with a total RNA nano assay on a labchip assay (Agilent, The Netherlands). cDNA was synthesised with random hexamer primers and gene expression levels were determined for *CD68*, *Lgals3* (influx of macrophages and immune cells), *Tnnt2*, *MyoG* (regeneration), *Bgn* (extra cellular matrix) *Nox2*, *Nox4*, *Lox* (fibrotic), *GLUT 4* and *PGC-1α* (exercise induced genes) by Syber Green based Real Time qPCR (95 °C 10 s, 60 °C 30 s, 72 °C 20 s 45 cycli and melting) on the Roche Lightcycler 480 (Roche diagnostics Ltd., UK). *GAPDH* was used as a reference gene, since the expression of this gene did not differ between different muscles or over time. The C_p values were obtained with the second derivative maximum method and analyzed with genex (http://www.gene-quantification.com/download.html).

Statistics

Statistical analyses were performed with statistical software in the R package 2.5.1 (http://www.Rpackage.org). The two-tailed homoscedastic student's *t*-test was conducted for comparison between the groups on the weight, CK levels, histological and gene expression data. $P<0.05$ was considered significant for all tests, however to the gene expression data a Bonferroni correction was applied to correct for multiple testing, therefore a $P<0.01$ was considered significant. The Spearman correlation test, which is not affected by differences in the distribution of values for the different measured parameters, was used for comparisons of all data from both the functionally challenged and unchallenged mice. The data obtained in the last week of functional testing were used to determine a possible correlation between the functional performance and histology, gene expression and creatine kinase levels. For the correlation analysis $P<0.05$ was considered significant.

Results

Functional tests

A group of 5 four week old male *mdx* mice was subjected to a 12 week functional test regime that consisted of four different functional tests performed on consecutive days on a weekly basis. The functional tests consisted of grip strength analysis, Rotarod running and two and four limb hanging wire tests. Each functional test was performed only once a week at the same time in the

afternoon and addressed different muscle groups and/or coordination. A group of five unchallenged *mdx* males was used as a control group.

Body weight was assessed at the beginning and the end of every week. No significant differences were found for average body weight at any time point or over time between functionally challenged and unchallenged mice. Notably, in the functionally challenged mice, a clear trend of a fluctuating body weight was seen that can be related to their functional test regime. After each weekend, when no functional tests were performed, there was an increase in body weight while a decrease in body weight occurred during the week, when the functional tests were performed (Fig. 1A).

Serum CK levels were elevated compared to C57BL/10ScSnJ mice (<500 U/L, De Luca et al. 2008), but did not differ significantly between the functionally challenged and unchallenged mice at any time point or over time (Fig. 1B). For each functional test, mice performed badly in the first week of testing. This is partly a learning effect, but may also be due to the decreased strength that correlates to the re-, and degenerating cycles which are present at the age of 4 weeks. Forelimb grip strength corrected for body weight decreased gradually over time from 5 to 15 weeks of age. This result is in consensus with a decreased forelimb strength found in *mdx* mice (5–12 weeks of age) that did not perform other functional tests beside the grip strength test De Luca et al. 2008).

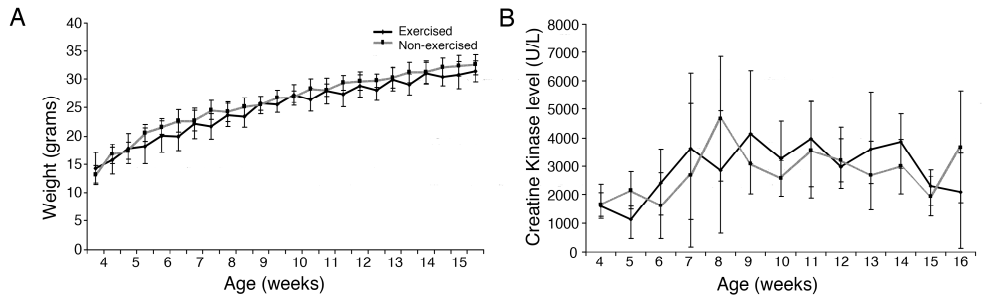


Fig. 1. Effect of the functional test regime on body weight and serum CK levels over time. (**A**) Body weight values of functionally challenged and unchallenged mice. Notably, a drop in weight can be observed during the week when tests were performed, while weight increases occurred during the weekends when no tests were performed.
(B) Serum CK levels of both groups over time. For both the body weight and serum creatine kinase levels, no significant difference was found between the two groups at any time point or over time. The error bars reflect the standard deviation of the average.

This decrease is mainly due to the increase in weight, as uncorrected strength remained virtually unchanged (Fig. 2A and B). No indications of fatigue were found at any time point (data not shown). On the Rotarod, the mice showed an average peak in their running time of 368 s at an age of seven weeks (i.e. after three weeks of testing). From then on, their performance declined to an average running time of around 200 s, which remained constant until the end of the test regime (Fig. 2C). This again is in agreement with previously reported data (Turgeman et al. 2008). Similar to the Rotarod peak performance, a peak at seven weeks was also observed with the two different hanging tests. However, the longest hanging time of both tests remained constant till an age of 12 weeks after which it dropped by 50% for both hanging tests (Fig. 2D and E), while the Rotarod performances dropped after the peak observed at an age of 7 weeks. For the Rotarod and both hanging wire tests no effect of body weight was found (data not shown).

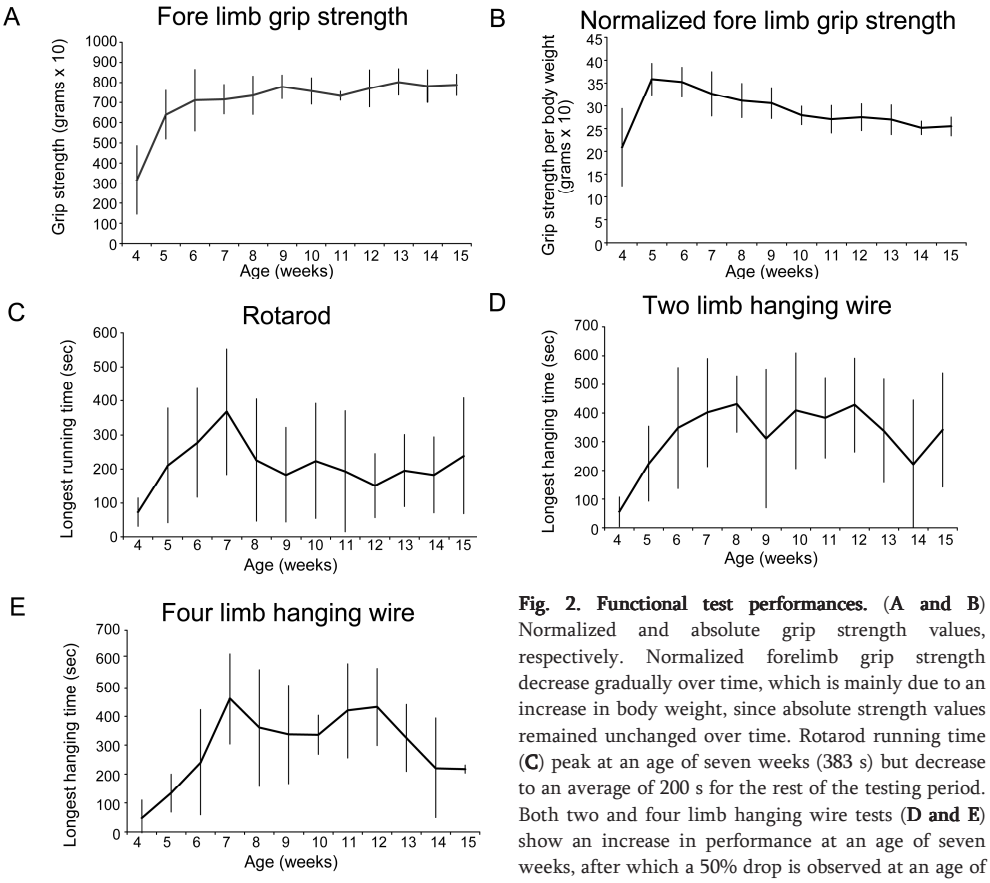


Fig. 2. Functional test performances. (**A and B**) Normalized and absolute grip strength values, respectively. Normalized forelimb grip strength decrease gradually over time, which is mainly due to an increase in body weight, since absolute strength values remained unchanged over time. Rotarod running time (**C**) peak at an age of seven weeks (383 s) but decrease to an average of 200 s for the rest of the testing period. Both two and four limb hanging wire tests (**D and E**) show an increase in performance at an age of seven weeks, after which a 50% drop is observed at an age of 14 weeks.

Histological examination

The quadriceps, gastrocnemius, tibialis anterior, triceps, heart and diaphragm were isolated from the functionally challenged and unchallenged mice at the age of 16 weeks. To determine levels of fibrosis, necrosis, connective tissue and recently regenerated tissue, a colour deconvolution based, semi-automatic analysis was set up on compiled pictures covering the entire cross sections. The haematoxylin/eosin plugin divides the picture in an eosin, haemotoxylin and background component. The eosin component represented the healthy area of the muscle examined. This area excluded fibrotic, necrotic, connective and recently regenerating tissue (Fig. 3).

In order to determine whether fibrotic/necrotic cells were equally distributed throughout the muscle (from tendon to tendon) the percentage of fibrotic/necrotic cells was determined at five levels along each muscle. For both the hind-, and forelimb muscle the proximal part was referred to as the beginning of the muscle (A) and the distal part as the end (E). The areas in between were referred to as B, C and D respectively. For the diaphragm, the dorsal part was designated the beginning (A) and the ventral part the end (E), while for the heart the cranial and caudal parts were beginning (A) and end (E), respectively. No significant differences in fibrotic/necrotic cell percentages were found between the five locations for any of the analyzed muscles (Fig. 4A).

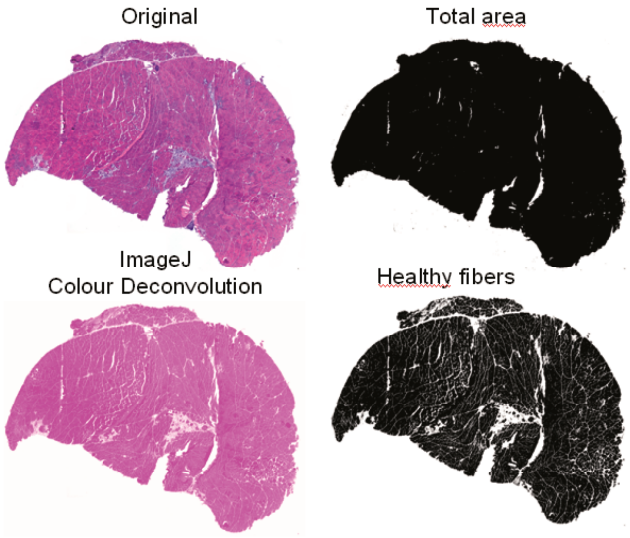


Fig. 3. Example of the semi-automatic histopathological determination using the colour deconvolution ImageJ plugin. The eosin component obtained with ImageJ after the haematoxylin/eosin colour deconvolution plugin represents the healthy area of the total cross section. Using this method, the percentage of necrotic, fibrotic, connective and recently regenerated tissue can be calculated from the total and the healthy fiber area.

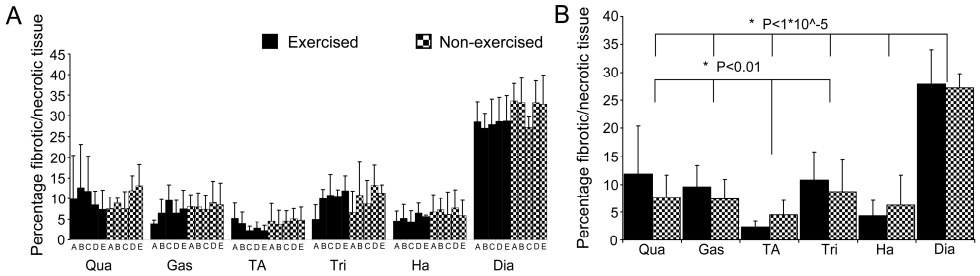


Fig. 4. Histopathology between different areas within a muscle (A) and comparison of histopathology between functionally challenged and unchallenged *mdx* mice for different muscles (B). (**A**) In four different skeletal muscles, the heart and diaphragm, the percentage of damage was determined at five locations from tendon to tendon. No significant difference was found between different areas within one muscle, or between functionally challenged and unchallenged mice. (**B**) A clear, significant difference in histopathological severity was found between different muscles; the tibialis anterior and the diaphragm were the least and most severely affected muscles respectively.

Therefore, for further comparisons only the middle section (C) of the muscle was analyzed. This revealed that the level of fibrosis and/or necrosis did not differ significantly between the functionally challenged and unchallenged mice in any of the muscles (Fig. 4B). This indicates that the functional test regime had no effect on tissue composition in *mdx* males. A clear difference in muscle damage severity was found between the different muscles. The tibialis anterior was significantly less affected (3.5%) than the gastrocnemius (8.5%), the quadriceps and the triceps (10% and 10.6%). The diaphragm was significantly more affected (30.3%) than all other muscles examined. The triceps was significantly more affected than the heart (5.9%). This is in accordance to previous studies based on several arbitrary fields (Turgeman et al. 2008) and an indication that the methodology used in the current study accurately detects changes in histological markers of muscle damage.

Biomarker analysis

The expression levels of several previously identified biomarkers that correlate with disease severity were assessed in the different muscles of the functionally challenged and unchallenged mice (Fig. 5) ('t Hoen et al. 2006;Baar et al. 2002;Spurney et al. 2009). The genes tested were *CD68*, *Lgals3* (influx of macrophages and immune cells), *Tnnt2*, *MyoG* (regeneration), *Bgn* (extra cellular matrix) *Nox2*, *Nox4*, *Lox* (fibrotic), *GLUT 4* and *PGC-1α* (exercise induced genes). When $P<0.05$ was considered significant, the expression of *Lox* differed between the groups in the diaphragm ($P = 0.027$), *Nox2* ($P = 0.038$) and *PGC-1α* ($P = 0.022$) in the tibialis anterior and *MyoG* ($P = 0.039$) and *GLUT 4* ($P = 0.010$) in the Triceps. However, after we conducted a Bonferroni correction, none of the tested genes were significantly differentially expressed between functionally challenged and unchallenged mice for any muscle.

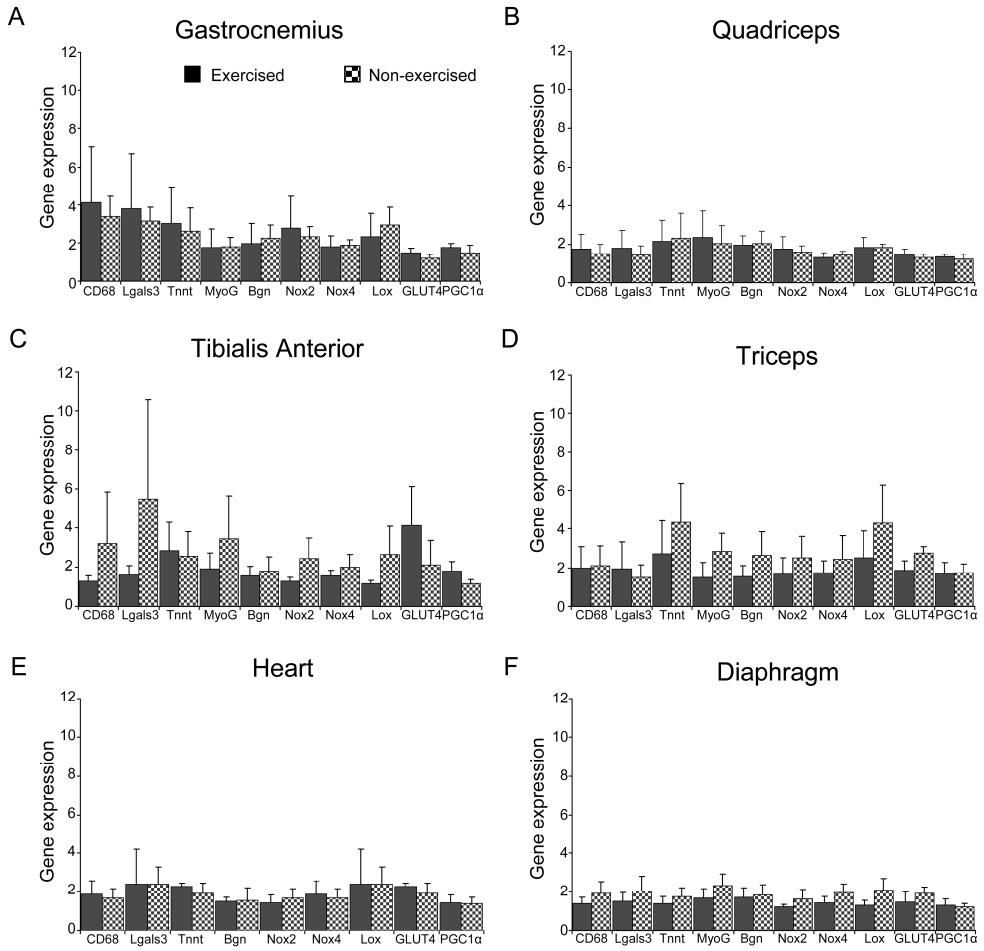


Fig. 5. Expression of genes involved in influx of macrophages and immune cells, regeneration, extracellular matrix stability, fibrosis and exercise. (**A**) Quadriceps, (**B**) gastrocnemius, (**C**) tibialis anterior, (B) triceps, (**E**) heart, (**F**) diaphragm. No significant difference was found between the functionally challenged and unchallenged mice for all the muscles examined.

Correlation between muscle function, histology and biomarker levels

Spearman correlation analysis was conducted to test for correlations between the functional performance, histological results and relative RNA levels of the genes examined in the current study. In addition we determined the correlation between genes (Table 1). No significant correlation was found between performance and histology, or between performance and serum CK levels. A positive correlation was observed between forelimb grip strength and the four limb hanging wire test ($P = 0.016$). Elevated serum CK levels correlated positively to the severity of fiber damage in the diaphragm ($P = 0.026$). A significant positive correlation was found between the percentage of fibrosis and both immunological genes (*CD68* $P = 0.011$ and *Lgals3* $P = 0.006$) in the tibialis anterior, indicating that the expression of these genes was increased in mice that had more fibrosis. In the gastrocnemius a significant positive correlation was found between histology and gene expression of *CD68* ($P = 0.013$), *MyoG* ($P = 0.006$), *Nox2* ($P = 0.033$) and *Lox* ($P = 0.003$). *GLUT 4* was positively correlated with histopathology in the quadriceps ($P = 0.042$) and *Bgn* was positively correlated with histopathology in the diaphragm (positive, $P = 0.017$) and *PGC-1α* (negative, $P = 0.021$). Almost all examined muscles showed a correlation between the immunological and fibrotic genes. In addition, correlations between genes involved in macrophage and immune cells influx, fibrosis and regenerative genes were found in some muscles. *Bgn* was correlated to immunologic and fibrotic genes in the quadriceps and triceps. Most correlations between genes were found in the quadriceps (21) and the fewest in the heart (6).

	Histology	CD68	Lgals3	Tnnt 2	MyoG	Bgn	Nox4	Lox	GLUT4	PGC-1α	Grip strength	Rotarod	2 LHW	4 LHW	CK
Histology															
CD68	TA G														
Lgals3	TA	TA G T D													
Tnnt 2		G T	G Q												
MyoG	TA G	TA G T D	TA G Q	G Q D											
Bgn	D	Q T H	Q T	Q T	Q T										
Nox2	G	TA G Q T D	TA Q	Q	G Q T D	Q T									
Nox4		Q H D		Q	G Q T D	Q H									
Lox	G	TA G Q T D	TA Q H		G T D	Q T	T D								
GLUT4	Q	**TA** D	**TA**	I D	I D	I		D							
PGC-1α	**D**			D											
Grip strength			D				G								
Rotarod										TA					
2 LHW								G							
4 LHW			D				G				TA G Q T H D				
CK	D					D				D					

Table 1 Significant correlations between histology, biomarkers and muscle function. Both tissue dependent positive and negative correlations were found between genes. Functional performance did not correlate to gene expression or histopathology, but some tests results did correlate to other tests. Fiber pathology did correlate to serum CK levels in the diaphragm. TA, tibialis anterior; G, gastrocnemius; Q, quadriceps; T, triceps; H, heart; D, diaphragm; LHW, limb hanging wire. Normal and bold abbreviations resemble positive and negative correlations, respectively. All correlations have P values <0.05.

Discussion

There is an increasing interest to gain more insight into the natural progression of the phenotype of the *mdx* mice on a functional, histological and biomarker level, since multiple studies aim to assess the efficacy of genetic or pharmacologic treatment strategies. Recently, effort was put into the standardization of pre-clinical testing in *mdx* mice with an emphasis on functional testing (Grounds et al. 2008;Spurney et al. 2009;Willmann et al. 2009). Due to inconsistencies in the experimental methods used, such as differences in outcomes measures, initiation age of the animals and exercise intensity and duration, discrepancies in the effects of exercise on disease progression are often seen in literature. Whether beneficial or detrimental effects will be found is largely influenced by the type of exercise. A delay in pathology progression can be found after voluntary exercise, such as swimming or wheel running (Carter et al. 1995;Dupont-Versteegden et al. 1994;Hayes and Williams 1998), while forced horizontal treadmill exercise results in muscle damage and is an often used protocol to enhance the pathogenic phenotype (De Luca et al.

2003;De Luca et al. 2008;Granchelli et al. 2000). In addition, age dependent effects have been found within an experimental protocol, where detrimental and beneficial effects were found in young (4 weeks) and old (16 weeks) animals, respectively (Faist et al. 2001). In pharmacological studies, treadmill exercise is often used to aggravate the pathogenic phenotype, after which grip strength analysis is used to monitor functional improvement (De Luca et al. 2008). Until now, the effect of a combination of several functional tests addressing different muscle groups and/or coordination on disease progression of *mdx* mice has not been studied.

We here assessed the effects of a 12 week functional test regime consisting of four functional tests, not including the treadmill, on disease progression. Our objective was to have a functional testing regime of which the outcome parameters would not interfere with the normal disease progression. We determined differences in histopathology and expression levels of previously identified fibrotic and immunologic RNA biomarkers between functionally challenged and unchallenged mice. The functional test regime used is intense and requires prolonged daily mouse handling. As this is an unavoidable part of functional testing, we actually compared the combination of functional testing and handling-induced stress to unchallenged mice that were handled only twice weekly for a short period to assess weight and CK. The fluctuations in body weight found in the present study might be caused by the functional test regime, however it cannot be ruled out that differences in handling time play a role as well.

Our functional test regime was chosen to assess which of the tests showed the lowest variation between mice over time, without interfering with disease pathology, thereby providing the most reliable outcome parameter(s). The current study included five male *mdx* mice per group, which is small. However, in a similar set up using dystrophic mice of different severities, we were able to pick up significant differences (unpublished data). To optimally use the *mdx* mouse for the efficient development of novel therapies to be used in humans, it is crucial to perform long-term blinded controlled studies in young and old mice, which thoroughly assess and compare the clinical phenotype of active versus placebo-treated animal cohorts. For these studies even longer term functional test regimes are needed.

The obtained grip strength and Rotarod data showed an age dependent performance decrease that is in accordance with previous data in sedentary *mdx* mice (mice that did not perform treadmill running prior to the functional test). The grip strength data obtained with the Ugo Basile meter are not comparable to those obtained by a Columbus meter by others. Preliminary data obtained with the Columbus meter in our *mdx* mice indicate that approximately two fold lower values are obtained with the Ugo Basile meter. Exercise, especially eccentric contraction, is known to directly cause an intensity dependent increase in serum CK level (Vilquin et al. 1998). Our functional test regime had no influence on the serum CK levels of the mice, which indicates that the functional test regime was mild. Carter et al. also found no effect on serum CK in mice that were exposed to voluntarily wheel running, while treadmill running is known to increase CK levels in *mdx* mice (Carter et al. 1995;De Luca et al. 2008). Both hanging wire test designs have not been reported before and the performances could therefore not directly be compared with results obtained by others. However, an age dependent de cline in hanging performance was earlier obtained with a different hanging wire test design (Golumbek et al. 2007).

Histological examination found no difference in pathology along the muscles. This indicates that the pathological features were equally distributed throughout the muscle. No difference in severity of muscle damage was found between the functionally challenged and unchallenged mice, which is in consensus with earlier data obtained after mild exercise (Carter et al. 1995). The percentage of damaged muscle differed between muscles, with the highest

percentage found in the diaphragm, which is known to be the most severely affected muscle in these mice (Ishizaki et al. 2008).

The here described semi-automatic procedure to determine histopathology provides an unbiased, accurate and fast method to determine the severity of histopathology in entire muscle cross sections. The main advantage of this methodology is that it provides an objective measure of fibrotic tissue but also of necrotic tissue, in contrast to other analysis in which only a collagen specific staining is used to determine the fibrosis percentage (Ishizaki et al. 2008). Furthermore, for this analysis the entire cross section of the muscle is used and not only a subsection, as was done in previous studies (Turgeman et al. 2008). Finally, the analysis software is freely available. This all together makes it an attractive method to determine histopathology in *mdx* mice.

In addition to comparing the functionally challenged and unchallenged mice on a histological level, we also looked at expression levels of several RNA biomarkers, but found no difference. *Lox* is known to be significantly increased in *mdx* mice compared to wild type mice (Spurney et al. 2009). A decreased *Lox* expression was expected in the heart upon a beneficial effect of exercise. However, no difference was found for this gene. This may be because the functional test regime was too mild to have an effect on the heart. Upon exercise the expression of genes like *PGC-1α* and *GLUT 4* were expected to increase, which is in contrast to our findings. However, the time gap between the last exercise and dissection was four days while in the study of Baar et al. this period was limited to 6 h (Baar et al. 2002). Therefore, by the time we analyzed the muscles, expression levels probably had already normalized. Comparison of gene expression levels between the different muscles was impossible due to the experimental design, which was aimed at comparing functionally challenged and unchallenged mice.

With the Spearman analysis, muscle dependent correlations between immunologic, fibrotic and regenerative genes were found. These correlations were in accordance to the pathogenic cellular events, in which necrotic fibers initiate immune responses and will be replaced by newly generated fibers (Deconinck and Dan 2007). Elevated serum CK levels correlated positively to the severity of fiber damage in the diaphragm. Due to a relative small sample size and high variation in biomarkers and other variables possible existing correlations might have been missed. A correlation between functional performance, histopathology and gene expression was not found. Possible correlations are likely to become undetectable due to high individual variations, but might be detected after a forced treadmill running protocol, which enhances the pathological phenotype.

Our findings indicate that our functional test regime is a useful tool to monitor muscle function and/or coordination in young *mdx* mice over time without accelerating the disease progression. Combined with our histological assay, this provides a convenient and accurate tool to functionally monitor the natural course of the disease in *mdx* mice.

Acknowledgement

We are grateful to J.M. Ross for her expert assistance with Image J analysis. This work is supported by the FP6 funded TREAT-NMD network of excellence and ZonNW.

Supplementary figure 1. Functional test regime.

Weight	•	•	•	•	•	•	•	•	•	•	•	•	•
CK	•	•	•	•	•	•	•	•	•	•	•	•	•
Grip strength	•	•	•	•	•	•	•	•	•	•	•	•	•
Rotarod	•	•	•	•	•	•	•	•	•	•	•	•	•
Hanging wire 2 limbs	•	•	•	•	•	•	•	•	•	•	•	•	•
Hanging wire 4 limbs	•	•	•	•	•	•	•	•	•	•	•	•	•
Age in weeks	4	5	6	7	8	9	10	11	12	13	14	15	16

Chapter 3

Comparison of skeletal muscle pathology and motor function of dystrophin and utrophin deficient mouse strains

M. van Putten, D. Kumar, M. Hulsker, W.M.H. Hoogaars, J.J. Plomp, A. van Opstal, M. van Iterson, P. Admiraal, G.J.B. van Ommen, P.A.C. 't Hoen, A.M. Aartsma-Rus

Neuromuscular Disorders 2012; 5, 406-417

Abstract

The genetic defect of *mdx* mice resembles that of Duchenne muscular dystrophy, although their functional performance and life expectancy is nearly normal. By contrast, mice lacking utrophin and dystrophin (*mdx/utrn* $^{-/-}$) are severely affected and die prematurely. Mice with one utrophin allele (*mdx/utrn* $^{+/-}$) are more severely affected than *mdx* mice, but outlive *mdx/utrn* $^{-/-}$ mice. We subjected *mdx/utrn* $^{+/+}$, $^{+/-}$, $^{-/-}$ and wild type males to a 12 week functional test regime of four different functional tests. *Mdx/utrn* $^{+/+}$ and $^{+/-}$ mice completed the regime, while *mdx/utrn* $^{-/-}$ mice died prematurely. *Mdx/utrn* $^{+/-}$ mice performed significantly worse compared to *mdx/utrn* $^{+/+}$ mice in functional tests. Creatine kinase levels, percentage of fibrotic/necrotic tissue, morphology of neuromuscular synapses and expression of biomarker genes were comparable, whereas *mdx/utrn* $^{+/-}$ and $^{-/-}$ mice had increased levels of regenerating fibers. This makes *mdx/utrn* $^{+/-}$ mice valuable for testing the benefit of potential therapies on muscle function parameters.

Introduction

Duchenne muscular dystrophy (DMD) is an X-linked, severe, muscle wasting neuromuscular disorder leading to death in the early thirties in the Western world. Due to frame shifting or nonsense mutations in the *DMD* gene, truncated, non functional dystrophin proteins are synthesised. Intact dystrophin is part of the dystrophin–associated protein complex that connects the extracellular matrix to the cytoskeleton thereby providing muscle fibers with stability during contraction. In the absence of dystrophin, fibers are more injury-susceptible and eventually the regenerative capacity of the fibers becomes exhausted resulting in the replacement by connective and adipose tissue (Hoffman et al. 1987).

The *mdx* mouse, which carries a nonsense mutation in exon 23 of the mouse *Dmd* gene, is the most commonly used mouse strain for DMD research. Despite the resembling genetic defects, their functional performance and life expectancy is nearly normal, which is thought to result from a combination of improved regeneration, upregulation of muscle transcription factors like myoD and functional compensation by upregulation of the dystrophin homologue utrophin (Deconinck et al. 1997c;Sicinski et al. 1989).

During development, utrophin is predominantly found at the sarcolemma of developing and regenerating fibers before dystrophin is expressed (Perronnet and Vaillend 2010). In mature muscle fibers, dystrophin replaces utrophin, which is in this phase only present at the neuromuscular junction (NMJ) where it colocalizes with acetylcholine receptors and is involved in post-synaptic membrane maintenance and acetylcholine receptor clustering (Ohlendieck et al. 1991;Pons et al. 1993). In DMD patients, female DMD carriers and the *mdx* mouse, the expression of utrophin at the extra-synaptic sarcolemma is dramatically increased in dystrophin negative fibers (Kleopa et al. 2006;Mizuno et al. 1993). In *mdx* mice, muscles with the greatest upregulation of utrophin exhibit the least pathological changes and are most resistant to injury (Tinsley et al. 1996). Also in DMD patients, a negative correlation between utrophin upregulation and disease severity has been described (Kleopa et al. 2006). Moreover, overexpression of a truncated or full length utrophin in *mdx* mice improves dystrophic pathology in a utrophin concentration dependent manner (Baban and Davies 2008;Deconinck et al. 1997c;Squire et al. 2002;Tinsley et al. 1998;Tinsley et al. 1996). Mice lacking only one or both utrophin alleles are viable and fertile and display only a mild (subclinical) congenital myasthenia, which was concluded to result from effective replacement of utrophin by dystrophin at the NMJ (Deconinck et al. 1997b;Grady et al. 1997b).

By contrast, mice deficient for both dystrophin and utrophin (*mdx/utrn* $^{-/-}$) are severely affected, develop pronounced scoliosis and kyphosis, have impaired mobility, difficulty breathing and a

reduced life expectancy of around 3 months, thus more closely resembling the DMD patient phenotype (Deconinck et al. 1997b;Grady et al. 1997b). Unfortunately, since *mdx/utrn* $^{-/-}$ mice are short lived and difficult to breed and maintain, they are not an ideal animal model for the study of long term effects of potential therapeutic compounds. In addition, on a histological level, *mdx/utrn* $^{-/-}$ mice are comparable to *mdx* mice, possibly because they do not live long enough to develop a more severe dystrophic and/or fibrotic phenotype (Deconinck et al. 1997b). *Mdx* mice with haploinsufficiency of the utrn gene (*mdx/utrn* $^{+/-}$) have an almost normal life span, but show more pronounced skeletal inflammation and fibrosis at an age of 3 and 6 months, respectively (Zhou et al. 2008). At 6 months of age, they also show a more severe impaired respiratory function and fibrosis of the diaphragm than *mdx* mice (Huang et al. 2011). This suggests that the functional compensation of dystrophin by utrophin is incomplete when expressed in a heterozygous manner in *mdx* mice.

To assess how heterozygous expression of utrophin in *mdx* mice affects disease progression, muscle function and histology, *mdx/utrn* $^{-/-}$, *mdx/utrn* $^{+/-}$, *mdx/utrn* $^{+/+}$ and C57BL/10ScSnJ (wild type) mice were subjected to a previously developed 12 week functional test regime addressing strength and coordination of different muscle groups (van Putten et al. 2010). We show here that *mdx/utrn* $^{+/-}$ mice perform significantly worse than *mdx/utrn* $^{+/+}$ mice, while levels of fibrosis and mRNA biomarkers are comparable at 4 months of age. We propose that the *mdx/utrn* $^{+/-}$ model is a more suitable mouse model for testing potential therapies for DMD.

Materials and methods

Animal care

All studied mouse strains were bred at the animal facility of the LUMC where they were housed in individually ventilated cages with 12-h light–dark cycles. Mice were given standard chow and water *ad libitum*. Breeding pairs of *mdx* mice heterozygous for a utrophin knockout mutation (*mdx/utrn* $^{+/-}$) gave birth to *mdx* mice with two (*mdx/utrn* $^{+/+}$), one (*mdx/utrn* $^{+/-}$) and zero (*mdx/utrn* $^{-/-}$) utrophin alleles. Genotyping was performed on DNA obtained from tail tips by PCR analysis (primers and PCR condition on request). All experiments were approved by the Animal Experimental Committee (DEC) of the LUMC.

Functional tests

Four week old male *mdx/utrn* $^{+/+}$, $^{+/-}$, $^{-/-}$ and C57BL/10ScSnJ mice (n = 6 per group) were subjected to a 12 week functional test regime consisting of four different functional tests, each addressing different muscle groups and/or coordination (van Putten et al. 2010). Mice performed the tests in the afternoon on consecutive days on a weekly basis. Body weight was assessed at the beginning and end of each week. Where possible, standard operating procedures from the TREAT-NMD network were implemented (http://www.treat-nmd.eu/resources/research-resources/dmd-sops/).

Fore limb grip strength test

Fore limb grip strength was assessed by means of a grip strength meter (Columbus Instruments, USA). Mice were suspended above a grid which they instinctively grasped. Mice were then pulled backwards so that they released the grid. This was repeated five times in a row. The average of the three highest measured values was used to calculate the absolute strength, which was divided by the body weight in grams to obtain the normalized strength.

Rotarod

Mice were placed on the Rotarod (Ugo Basile, Italy) that accelerated from 5 to 45 rotations per minute within 15 s. The test session ended when a mouse ran for 500 s without falling. Two more tries were given to mice that fell off within 500 s. The longest running time was used in all analyses.

Two limb hanging wire test

Mice were suspended above a metal cloth hanger which was secured above a cage with bedding and released a few seconds after instinctively grasping the wire with the fore limbs. Depending on the functional ability of the mouse, all limbs and the tail were used during a 10 min hanging session. Mice that fell down before the 10 min time limit were given two more tries. The longest hanging time was used for further analysis.

Four limb hanging wire test

The start position of this test was with all four limbs. To this end, mice were placed on a grid, which was then turned upside down above a cage filled with bedding. The session ended after a hanging time of 10 min was achieved or otherwise after three sessions. The maximum hanging time was used for further analysis.

Creatine kinase level analysis

Blood was collected weekly on Monday mornings via a small cut at the end of the tail in a Minicollect tube (0.8 ml Lithium Heparin Sep, Greiner bio-one, Austria). Creatine kinase (CK) levels were determined in plasma with Reflotron CK test strips in the Reflotron plus machine (Roche diagnostics Ltd., UK).

Histological examination

After performing the functional test regime for 12 weeks, mice (aged 16 weeks) were euthanized by cervical dislocation and the tibialis anterior, triceps and quadriceps were dissected and snap frozen in 2-methylbutane (Sigma–Aldrich, The Netherlands) cooled in liquid nitrogen. Sections of 8 μm were cut on Superfrost Plus slides (Thermo Fishes Scientific, Menzel-Gläser, Germany) with a Shandon cryotome (Thermo Fisher Scientific Co., Pittsburgh, PA, USA) along the entire length of the muscle with an interval of 240 μm between the sections. The excess tissue belonging to the 240 μm intervals was collected in MagNa Lyser Green Beads tubes (Roche diagnostics Ltd., UK) for total RNA isolation. Sections were fixed for 5 min with icecold acetone and stained with Harris Haematoxylin and Eosin (H&E) (Sigma–Aldrich, The Netherlands) according to conventional histological procedures. Sections were examined with a light microscope (Leica DM LB, Leica Microsystems, The Netherlands) at a 5 times magnification and images were captured with a Leica DC500 camera and Leica IM50 software (Leica Microsystems, The Netherlands) from the middle section of the muscles. Blending and background correction was performed with Adobe Photoshop CS3 version 10.0.1. Freely available ImageJ software with the H&E color deconvolution plugin (Rasband, W.S., ImageJ, U. S. National Institutes of Health, Bethesda, Maryland, USA, http://rsb.info.nih.gov/ij/) was used to determine the fibrotic/necrotic percentage of the entire cross section by two individuals in a double blinded manner, as described previously (van Putten et al. 2010).

Fiber size and the proportion of centrally nucleated fibers were determined with Mayachitra Imago 1 (http://www.mayachitra.com/imago/) on whole muscle cross sections of the

tibialis anterior. Sections were stained with a laminin antibody, (ab11575, dilution 1:50, Abcam, USA), goat-anti-rabbit Alexa 594 (dilution 1:1000, Invitrogen, The Netherlands) and DAPI. Sections were examined and the middle section of the muscle was captured with a fluorescent microscope (Leica DM 5500B) and a Snapshot camera (Photometrics Coolsnap K4) at a 5 times magnification. Images were mozaiked with the Mayachitra Imago 1 (http://www.mayachitra.com/imago/) and preprocessed with ImageJ to obtain an even illumination of laminin. Pictures were segmented by the Mayachitra Imago software based on the staining intensity difference between the membranes and the cytoplasm. Of these segmented fibers, the area (μm^2), fiber density and the percentage of central nucleation were determined. Fibers were assessed for presence of centralized nuclei based on the maximum intensity (from the blue channel) of the cytoplasm. Objects smaller than 200 μm^2 were excluded from analysis. Fiber density was determined by dividing the total number of fibers by the total area of the cross section.

Utrophin and dystrophin expression was analyzed for the quadriceps stained with utrophin (MANCHO7, dilution 1:50, Santa Cruz, Germany), dystrophin (C-20, dilution 1:50, Santa Cruz, Germany), donkey-anti-goat Alexa 594 (dilution 1:1000, Invitrogen, The Netherlands) and DAPI with use of the mouse on mouse (MOM) kit (Vector Laboratories, UK). Sections were examined with a fluorescent microscope (Leica DM RA2) at a 16 times magnification and captured with a Leica DC350FX Snapshot camera.

Morphology of the NMJ was assessed on whole-mount diaphragm muscles of two mice per genotype. The snapfrozen diaphragm was thawed in PBS, pinned out on a silicone-rubber lined Petri dish and fixated with 1% paraformaldehyde in PBS for 30 min after it was washed with PBS (30 min). Incubation with Alexa Fluor 488 α-bungarotoxin (1 μg/ml, Molecular Probes, The Netherlands) lasted 2.5 h and was followed by PBS washing (30 min). All incubations were performed at room temperature (20–22 °C). Muscle strips were mounted with Citifluor AF-1 (Citifluor Ltd., UK) and covered with a cover slip which was secured with nail polish. Slides were examined with an Axioskop 2FS microscope equipped with fluorescence optics (Zeiss, Jena, Germany) at a 400 times magnification and pictures were taken using Zeiss Axiovision (Kaja et al. 2007).

Western blot analysis

Muscles were homogenized using treatment buffer (100 mM Tris–HCl pH 6.8 and 25% SDS) using MagNa Lyser green beads in the MagNa Lyser (Roche Diagnostics, The Netherlands). Protein concentration was determined with the BCA protein assay kit (Thermoscientific, IL, USA), according to the manufacturer's instructions. Subsequently, the homogenate was complemented to contain 75 mM Tris–HCl pH 6.8, 15% SDS, 5% β-mercaptoethanol, 20% glycerol and 0.001% bromophenol blue. Samples (50 μg) were boiled for 5 min and 75 μl was loaded on a 4–7% gradient polyacrylamide gel and run overnight at 4 °C. Gels were blotted to nitrocellulose BA83 (Whatman, Schleicher & Schuell, Germany) for 6 h at 4 °C and blocked with 5% non-fat dried milk (Campina Melkunie, The Netherlands) in TBS. Primary utrophin antibody 8A4 (dilution 1:100, Santa Cruz, Germany) was incubated over night at 4 °C. The fluorescent IRDye 800CW goat-anti-mouse IgG (dilution 1:5000, Li-Cor, NE, USA) was used as a secondary antibody. Blots were visualized and quantified with the Odyssey system and software (Li-Cor, NE, USA) as described previously (Heemskerk et al. 2009).

Biomarker analysis

cDNA was synthesised from 1 µg of total RNA with random hexamer primers and expression levels of genes involved in regeneration (*Myog, Myh3*), inflammation (*Lgals3, Cd68*) and fibrosis (*Col1a1, Lox*) were determined by Sybr Green based Real Time qPCR (95 °C 10 s, 60 °C 30 s, 72 °C 20 s, 45 cycles followed by melting curve analysis) on the Roche Lightcycler 480 (Roche diagnostics Ltd., UK). *Gapdh* was used as a reference gene, since the expression of this gene did not differ between different strains, different muscles or over time. Primer efficiencies were determined and analysis was performed with LinREgPCR version 11.1 (Ramakers et al. 2003). The average expression levels of C57BL/10ScSnJ mice were set to one.

Statistics

Statistical analyses were performed with statistical software in R (version R2.11.1). Figs. 1 and 2 summarize the data, i.e. showing the mean and standard deviation per genotype and age. To overcome applying separate tests for each age between genotypes, which suffers from multiple testing and ignores the age trend, we applied an analysis of covariance (ANCOVA) to the data. ANCOVA was applied to temporal functional performance, body weight and CK level data with age as continuous and genotype as a categorical variable. In choosing the appropriate model we applied the principle of parsimony. Given the application of tests for several different variables, we considered $P<0.01$ as significant.

The two-tailed homoscedastic Student's *t*-test was conducted for comparison of the single time point histological and gene expression data. $P<0.05$ was used to determine significance for the histopathology, while $P<0.01$ was used for the gene expression data to correct for multiple testing.

Results

Functional tests

Four week old male *mdx/utrn* $^{+/+}$, *mdx/utrn* $^{+/-}$, *mdx/utrn* $^{-/-}$ and wild type mice followed a 12 week functional test regime consisting of four different functional tests on consecutive days on a weekly basis (van Putten et al. 2010). The test regime consisted of fore limb grip strength, rotarod running and two and four limb hanging wire tests. *Mdx/utrn* $^{-/-}$ mice were humanely sacrificed when their body weight had dropped >15% within 2 days, which was the case between 6 and 9 weeks of age for all mice (Fig. 1A). All *mdx/utrn* $^{-/-}$ developed severe kyphosis and showed difficulties moving and breathing. Once a week, body weight and plasma CK levels were assessed. When body weight was compared between groups over time, *mdx/utrn* $^{-/-}$ mice were significantly ($P<0.01$) lighter compared to the other strains (Fig. 1B). By contrast, *mdx/utrn* $^{+/-}$ mice were significantly ($P<0.01$) heavier than both *mdx/utrn* $^{+/+}$ and wild type mice. Plasma CK levels were significantly ($P<0.01$) elevated for all mouse strains compared to wild type (<500 U/L), but no differences were found between the dystrophic strains (Fig. 1C).

Wild type mice outperformed ($P<0.01$) all the dystrophic mouse strains in the fore limb grip strength test with an average normalized fore limb strength of 5.4. No difference was observed between the *mdx/utrn* $^{+/+, +/-}$ and $^{-/-}$ mice ((5.0, 4.9, 4.2, respectively) Fig. 2A). On the rotarod, the wild type mice ran, with an average highest running time of 224 s, significantly ($P<0.01$) longer than the other strains.

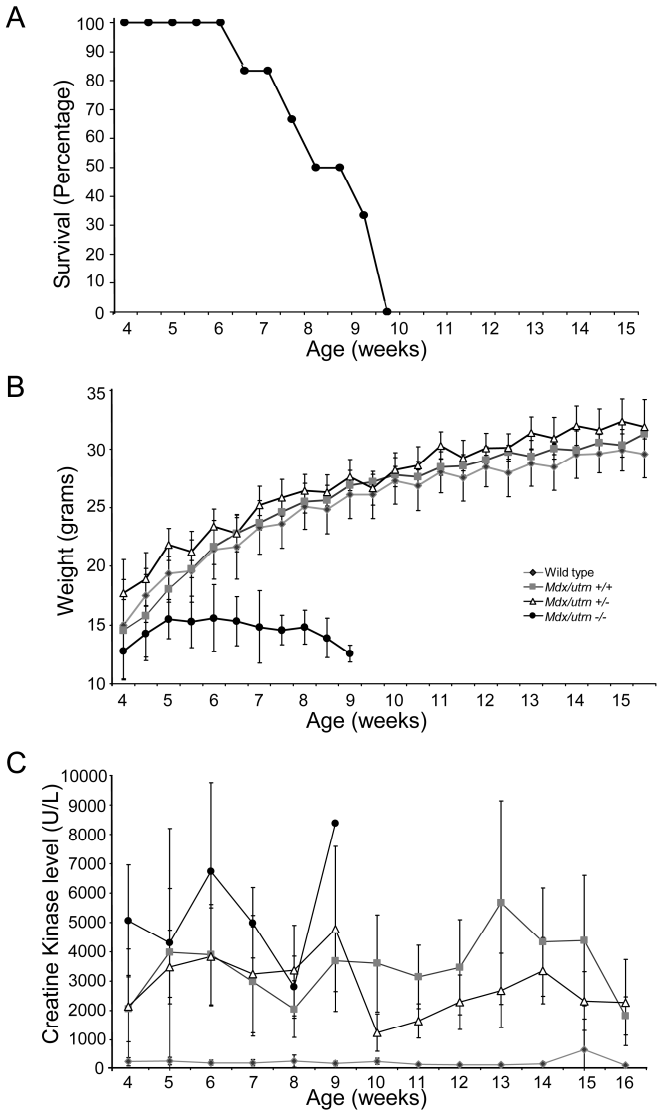


Fig. 1. Survival, body weight and plasma CK levels of the different mouse strains over time. (**A**) Survival curve of the *mdx/utrn* $^{-/-}$ mice. All mice died before the age of 10 weeks. (**B**) Body weight of *mdx/utrn* $^{-/-}$ mice was significantly lower than that of all other mouse strains. *Mdx/utrn* $^{+/-}$ mice were significantly heavier than *mdx/utrn* $^{+/+}$ and wild type mice. (**C**) CK levels of the wild type mice were significantly lower (<500 U/L) when compared to the three dystrophic mouse strains, which did not differ among themselves. Data represent the mean and standard deviation per time point.

Up to an age of 10 weeks, no difference between the dystrophic mouse strains was observed. However, from 11 weeks on, running times for *mdx/utrn* $^{+/+}$ increased and mice ran significantly (P<0.01) longer (140 s) than age-matched *mdx/utrn* $^{+/-}$ mice (average 77 s), which performance did not increase and remained as poor as the *mdx/utrn* $^{-/-}$ mice did when they were still alive (Fig. 2B). For the hanging wire tests the maximum hanging time was used as outcome measure which did not differ between wild type and *mdx/utrn* $^{+/+}$ mice for both the two and four limb hanging wire tests (Fig. 2C and D). *Mdx/utrn* $^{+/-}$ mice hang for a significantly shorter time period of 141 and 135 s, for the two and the four limb hanging test, respectively. The two limb hanging test performance of the *mdx/utrn* $^{-/-}$ mice was as bad as that of the *mdx/utrn* $^{+/-}$ mice, whereas they performed better in the four limb hanging test. This is because of the survival of only the good performing mice.

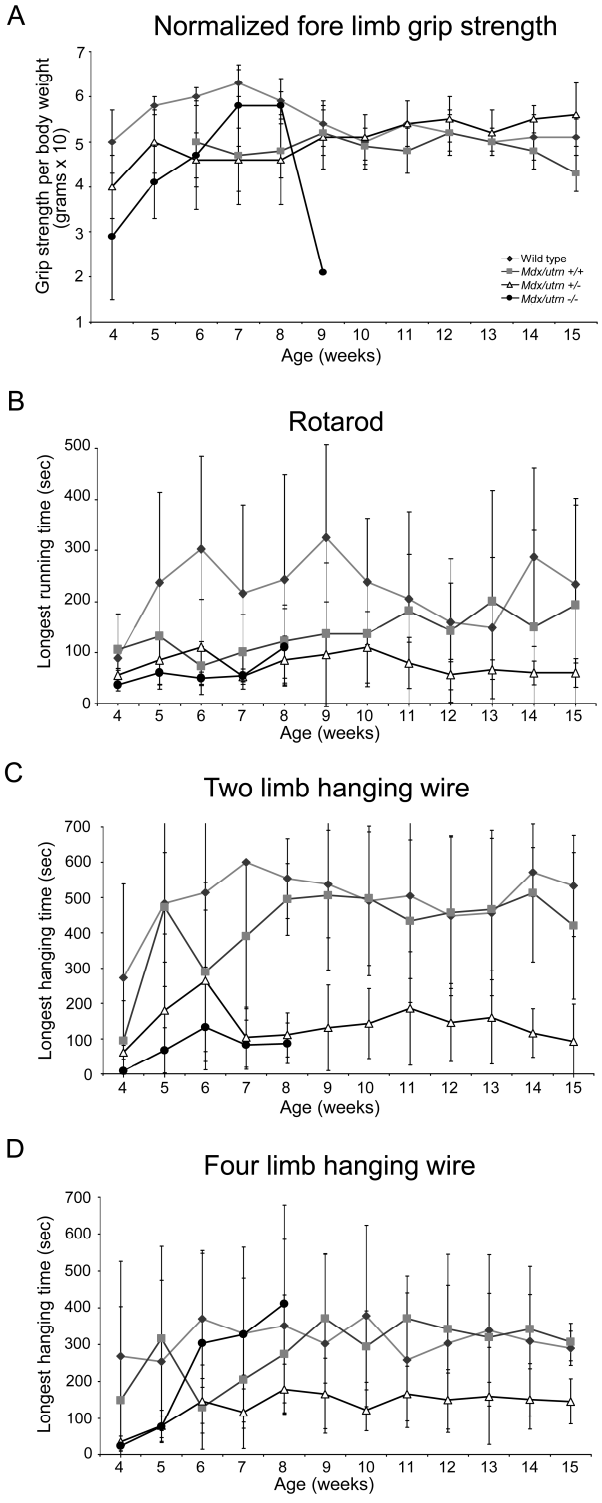


Fig. 2. Functional test performance of the different mouse strains over the 12 week functional test regime. (**A**) Normalized grip strength was significantly higher in wild type mice when compared to the dystrophic mouse strains, but did not differ between them. (**B**) Rotarod running times of wild type mice were significantly longer (224 s) than that of *mdx/utrn* $^{+/+}$ mice. From an age of 10 weeks, *mdx/utrn* $^{+/-}$ mice ran significantly shorter (77 s) than *mdx/utrn* $^{+/+}$ mice (140 s), but running times did not differ from *mdx/utrn* $^{-/-}$ mice. (**C**) Two limb hanging wire performance was best for wild type and *mdx/utrn* $^{+/+}$ mice. *Mdx/utrn* $^{+/-}$ and $^{-/-}$ performed significantly worse. (**D**) In the four limb hanging wire test, wild type and *mdx/utrn* $^{+/+}$ mice had a significantly longer hanging time than *mdx/utrn* $^{+/-}$ mice. For all mice except for the *mdx/utrn* $^{-/-}$ mice maximum hanging time was longer in the two limb hanging tests than the four limb hanging test (compare C versus D). Data represent the mean and standard deviation per time point.

Histological examination

After the mice completed the 12 week functional test regime, they were sacrificed and skeletal muscles were isolated. Cryosections of the quadriceps stained for utrophin and dystrophin showed a strong dystrophin staining in the wild type mice, whereas utrophin staining was weak. By contrast, fibers were clearly utrophin positive in the *mdx/utrn* $^{+/+}$ and $^{+/-}$ mice (Fig. 3A). As anticipated, *mdx/utrn* $^{-/-}$ mice lacked both dystrophin and utrophin. These results were confirmed by western Blot analysis, which showed an upregulation of utrophin in *mdx/utrn* $^{+/+}$ mice and to a lesser extent in the *mdx/utrn* $^{+/-}$ mice of approximately 2.2- and 1.8-fold, respectively (Fig. 3B).

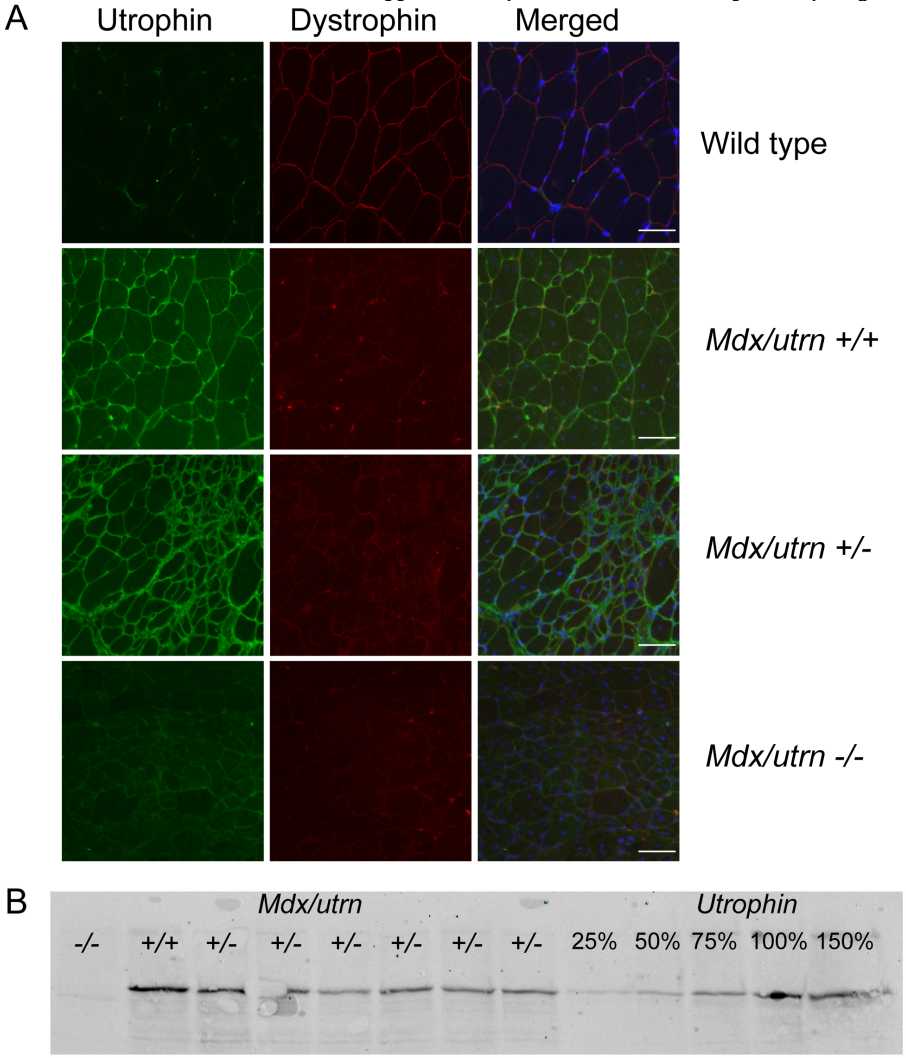


Fig. 3. Utrophin and dystrophin immunostaining and western blot analysis of the quadriceps. (**A**) Fibers of wild type mice expressed dystrophin whereas utrophin was hardly detectable. Fibers of *mdx/utrn* $^{+/+}$ and $^{+/-}$ mice were strongly positive for utrophin staining, while dystrophin staining was negative. In *mdx/utrn* $^{-/-}$ mice, fibers were negative for both utrophin and dystrophin. (**B**) Utrophin western blot of the quadriceps. Utrophin was upregulated in both *mdx/utrn* $^{+/+}$ and $^{+/-}$ mice, but to a larger extent for *mdx/utrn* $^{+/+}$ mice. Each lane represents an individual mouse. *Mdx/utrn* $^{-/-}$ mice did not express utrophin. Scale marker is 64 µm.

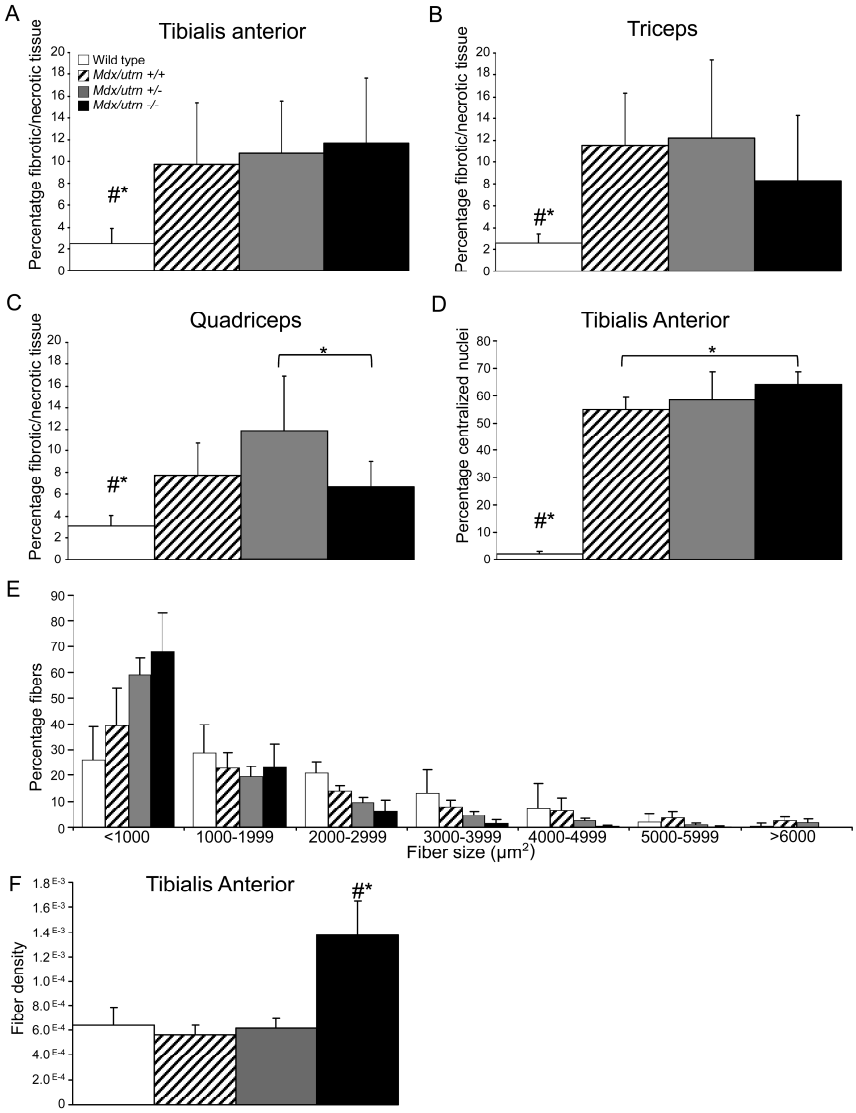


Fig. 4. Percentage of fibrotic/necrotic area, central nucleation, fiber size and density. (**A–C**) For the tibialis anterior and triceps no significant difference in the percentage of fibrosis/necrosis was observed between the dystrophic mouse strains. In the quadriceps, the level significantly differed between *mdx/utrn* $^{+/-}$ and $^{-/-}$ mice. The levels in the wild type mice were significantly lower (P<0.05) than the other mouse strains as indicated by the #. Single asterisks indicate a P<0.05. (**D–E**) The fiber size and percentage of central nucleation was automatically determined with Mayachitra Imago, which segments the fibers into individual objects. Based on the maximum intensity (from the blue channel) of the cytoplasm, fibers were assessed for presence of centralized nuclei. The percentage of centralized nuclei was significantly increased in the dystrophic mouse strains compared to the wild type. The *mdx/utrn* $^{-/-}$ mice had significantly more central nucleated fibers than the *mdx/utrn* $^{+/+}$ mice. (**E**) Especially the *mdx/utrn* $^{+/-}$ and $^{-/-}$ mice had a large number of small regenerated fibers (<1000 µm²). No hypertrophic fibers were found in the *mdx/utrn* $^{-/-}$ mice. (**F**) Fiber density was comparable between wild type, *mdx/utrn* $^{+/+}$ and $^{+/-}$ mice. Significantly higher densities were observed in the *mdx/utrn* $^{-/-}$ mice, which corresponds to the high number of small regenerated fibers found in these mice.

The percentage of fibrotic/necrotic tissue was assessed in all mouse strains for the tibialis anterior, triceps and quadriceps on H&E stained complete cross sections obtained from the middle part of the muscle. The proportion of fibrosis, necrosis, connective tissue and freshly regenerated tissue was determined with a color deconvolution plugin of Image J as described previously (van Putten et al. 2010). Wild type mice had significantly less fibrotic/necrotic tissue (~2%) than the dystrophic mouse strains, for which the histopathological severity did not significantly differ between the strains and varied between 8% and 13% for the different muscles (Fig. 4A–C). Only for the quadriceps, a significant difference (P<0.05) between mice with 1 and 0 utrophin alleles was observed.

Fiber size distribution, fiber density and the percentage of centralized nuclei was determined on the middle section of the tibialis anterior stained for laminin and DAPI. Pictures were automatically analyzed with Mayachitra Imago which segmented the image and defined fiber area based on the number of pixels within an object and centralized nuclei based on the maximum intensity of fibers (Fig. 4D and E). The percentage of centrally nucleated fibers was 2% in wild type mice, while it was over 50% in the dystrophic mouse strains. A clear trend was observed, in which the number of utrophin alleles of the mice correlated to the number of centrally nucleated fibers, which reached significance when comparing mice with two or zero utrophin alleles. In line with this trend, we also observed a higher number of small regenerated fibers (<1000 μm²) in the more severely affected *mdx/utrn* $^{+/-}$ and $^{-/-}$ mice. No hypertrophic fibers were observed for the *mdx/utrn* $^{-/-}$ mice, while they were present in the sections of the *mdx/utrn* $^{+/-}$ mice and to a bigger extent in *mdx/utrn* $^{+/+}$ mice. The fiber size distribution of the *mdx/utrn* $^{+/+}$ mice matched that of the wild type mice more than those of the *mdx/utrn* $^{+/-}$ and $^{-/-}$ mice. Fiber density (number of fibers per μm²) was determined for all mice by dividing the total number of fibers by the total area of the whole cross section. We observed no significant difference between any of the mouse strains (Fig. 4F). Since *mdx* mice are known to have hypertrophic muscle and we observed that *mdx/utrn* $^{+/-}$ mice also have hypertrophic muscle to some extent, their muscle mass to body weight (muscle mass divided by body weight) of the quadriceps and gastrocnemius was compared (n = 4–6). Muscle mass to body weight ratio of *mdx/utrn* $^{+/+}$ mice (quadriceps mean 0.0080, SD 0.0009 and gastrocnemius mean 0.0062, SD 0.0006) did not significantly differ from that of *mdx/utrn* $^{+/-}$ mice (quadriceps mean 0.0081, SD 0.0016 and gastrocnemius mean 0.0062, SD 0.0011) as was previously reported (Deconinck et al. 1997b). It should be noted, however, that the *mdx/utrn* $^{+/-}$ mice were significantly heavier than the *mdx/utrn* $^{+/+}$ mice.

To qualitatively assess the effect of expression of one, two or zero utrophin alleles in *mdx* mice on the morphology of NMJs, the diaphragm of two mice per genotype was stained with Alexa Fluor 488 α-bungarotoxin and viewed with fluorescence microscopy (Fig. 5). NMJs of wild type mice generally had continuous branches of acetylcholine receptor while most synapses of the dystrophic mouse strains showed discontinuous, more punctuate staining (Ferretti et al. 2011;Ghedini et al. 2008;Grady et al. 1997b;Lyons and Slater 1991). This punctuate pattern was observed to more or less equal extent in all dystrophic genotypes, the current quantitative analysis not allowing to discriminate amongst them.

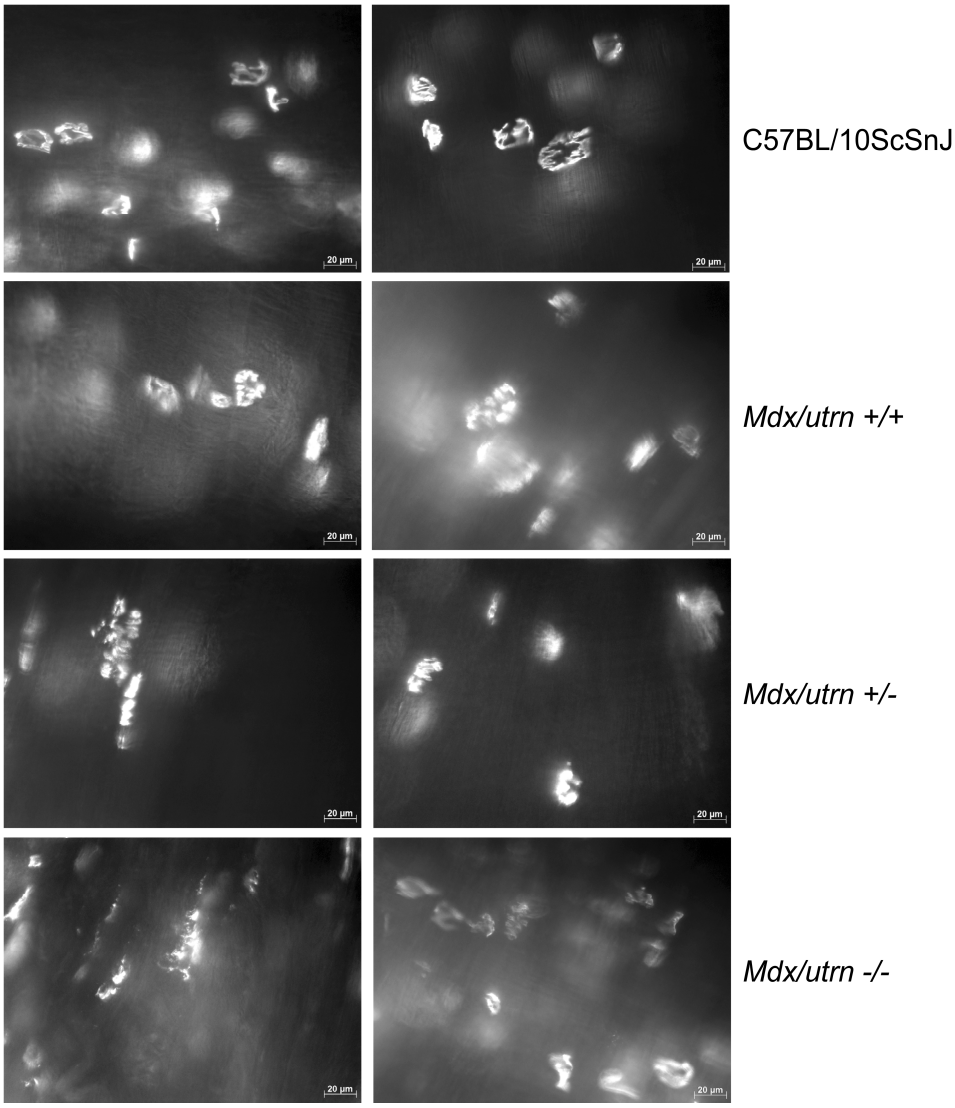


Fig. 5. Diaphragm NMJs stained with Alexa Fluor 488 α-bungarotoxin, which labels acetylcholine receptors. Representative pictures of synapses of two different mice per genotype. Clear distinctions in morphology are visible between wild type and dystrophic mice. The majority of wild type synapses are intact and show continuous acetylcholine receptor area branches that are arranged in an elliptical manner. Most synapses of the dystrophic mouse strains had a more disorganized, punctuate structure with discontinuous branches, with apparent qualitative similarity between *mdx/utrn* $^{+/+, +/-}$ and $^{-/-}$ mice. Scale marker is 20 µm.

Biomarker analysis

The expression of some potential biomarker genes known to be involved in different pathological processes was determined in the quadriceps of mice of the four strains that underwent the functional test regime. For each gene, expression was upregulated in the three dystrophic mouse strains compared to wild type levels (Fig. 6). In concordance with the histological analysis, no significant difference was observed between *mdx/utrn* $^{+/+}$ and $^{+/-}$ mice, although a trend of higher levels in the *mdx/utrn* $^{+/-}$ mice was found. The *mdx/utrn* $^{-/-}$ levels were increased or comparable to *mdx/utrn* $^{+/-}$ levels. As the *mdx/utrn* $^{-/-}$ mice were younger than the other strains (8–9 weeks versus 16 weeks) due to their premature death, we also checked the expression levels in the gastrocnemius of 6 week old mice for the four strains, to exclude that the observed differences were age related. Also in these young mice, a significant lower expression was found in wild type mice than in the dystrophic mouse strains. Between the dystrophic mice, a clear disease severity-related trend was observed for all genes, except for *Col1a1*, with the *mdx/utrn* $^{-/-}$ mice showing the highest levels, followed by *mdx/utrn* $^{+/-}$ and *mdx/utrn* $^{+/+}$ mice. For *Lgals3* and *Myh3* the difference between *mdx/utrn* $^{+/+}$ and $^{-/-}$ mice reached significance.

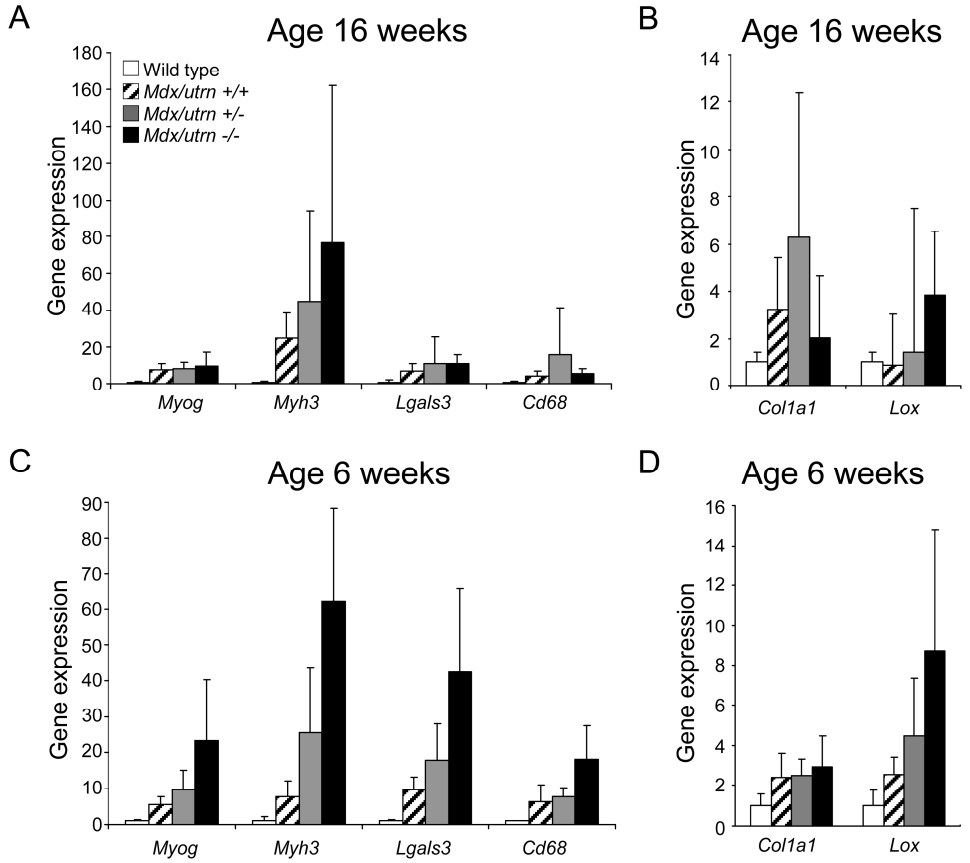


Fig. 6. Biomarker gene expression in 16 and 6 weeks old mice. (**A and B**) Expression of genes involved in regeneration (*Myog*, *Myh3*), inflammation (*Lgals3*, *Cd68*) and fibrosis (*Col1a1*, *Lox*) was elevated in 16 weeks old *mdx/utrn* $^{+/-}$ mice compared to the other mouse strains. Note that the *mdx/utrn* $^{-/-}$ mice were sacrificed between the age of 6 and 9 weeks as a consequence of their severe phenotype. (**C and D**) For all genes in the age-matched mice, the expression level was the highest in *mdx/utrn* $^{-/-}$ mice, followed by the *mdx/utrn* $^{+/-}$ and the $^{+/+}$ mice. Expression values shown have been normalized with *Gapdh* expression and are shown relative to wildtype values.

Discussion

Pre-clinical research on DMD pathology and the development of potential therapies has primarily made use of the *mdx* mouse, which resembles the genetic defect found in DMD patients (Willmann et al. 2009). Unfortunately, since the *mdx* mouse's functional ability and lifespan is only slightly reduced and none of the skeletal muscles except the diaphragm show severe histopathology, the mouse does not resemble the pathology observed in DMD patients. One of the underlying causes of the improved phenotype is upregulation of utrophin which is less pronounced in patients than it is in *mdx* mice. The *mdx/utrn* $^{-/-}$ mouse more closely resembles the natural history of the disease with their short life span, kyphosis and walking difficulties (Deconinck et al. 1997b). Unfortunately, their fragility and limited life expectancy prevents long term treatment studies in these mice. With pre-clinical research focusing on the effect of potential therapeutic compounds on functional performance and fiber integrity, a mouse model more severely affected than the *mdx* mouse, but with a longer lifespan than the *mdx/utrn* $^{-/-}$ mouse would be very helpful.

In this study, we tested how mono-allelic expression of utrophin affects muscle function, histopathology and disease progression. *Mdx* mice with two, one or zero utrophin alleles were subjected to a 12 week functional test regime. The performance of *mdx/utrn* $^{+/-}$ mice in the functional tests was as bad as that of *mdx/utrn* $^{-/-}$ mice and significantly worse than that of *mdx/utrn* $^{+/+}$ and wild type mice for rotarod and two and four limb hanging wire tests. Since the performance of the *mdx/utrn* $^{+/+}$ mice closely matched that of wild type mice, assessing functional improvement in *mdx/utrn* $^{+/+}$ mice upon treatment is challenging. Using the functionally more hampered *mdx/ utrn* $^{+/-}$ mouse would enable better monitoring of functional improvement upon treatment. Only grip strength did not differ between *mdx/utrn* $^{+/-}$ and $^{+/+}$ mice. Performance of *mdx/utrn* $^{+/+}$ mice matched that of C57BL/10ScSnJ-DMDmdx/J mice (i.e. *mdx* mice on a pure BL10 background) tested with the same functional test regime (van Putten et al. 2010). An exception was the rotarod performance where C57BL/10ScSnJ-DMDmdx/J mice peaked at an age of 7 weeks, while *mdx/utrn* $^{+/+}$ mice did not. This might result from the difference in background between the two strains, an observation which has been described previously for grip strength performance of two wild type strains (Connolly et al. 2001). For the four limb hanging wire test, *mdx/utrn* $^{-/-}$ mice even outperformed the *mdx/utrn* $^{+/-}$ mice, but this is caused by the survival of only the mouse which performed best in this test, while the mice that did not perform well died earlier. The bad functional performance of the *mdx/utrn* $^{-/-}$ mice is in line with previous findings of lower twitch and tetanus force, which is observed to a lower extent in *mdx/utrn* $^{+/+}$ mice (Deconinck et al. 1998). No differences in CK levels between the dystrophic strains were observed over time but levels were significantly elevated for the dystrophic mouse strains compared to wild type as expected. When strains are compared for over half a year, *mdx/utrn* $^{+/-}$ mice have significantly higher CK levels than *mdx* mice (Tanganyika–de Winter et al., submitted for publication).

Histopathology did not differ in severity between the three dystrophic mouse strains at an age of 4 months. This is in concordance with Zhou et al., who observed no difference in Collagen III immunostaining in quadriceps between *mdx* and *mdx/utrn* $^{+/-}$ mice aged 3 months (Zhou et al. 2008). Histopathology is known to increase in severity over time, as indicated by more pronounced fibrosis in 6 months old *mdx/utrn* $^{+/-}$ compared to *mdx* mice. The *mdx/utrn* $^{-/-}$ mice did have a significantly lower percentage of fibrotic/necrotic tissue in the quadriceps than the *mdx/utrn* $^{+/-}$ mice. The number of centrally nucleated fibers was increased in the *mdx/utrn* $^{+/-}$ and $^{-/-}$ compared to the *mdx/utrn* $^{+/+}$ and wild type mice. The significant difference observed between *mdx/utrn* $^{+/+}$ and $^{-/-}$ is in concordance with previous published work (Rafael et al. 1998).

The high number of fibers with central nuclei observed in the *mdx/utrn* $^{+/-}$ and $^{-/-}$ mice nicely overlaps with that of small regenerated fibers in these mice. This indicates that the regeneration can still keep up in these more severe mice, which is in contrast to DMD patients, which usually have a lower regenerative capacity. Fiber density was significantly higher in *mdx/utrn* $^{-/-}$ compared to *mdx/utrn* $^{+/+}$ and $^{+/-}$ mice, which corresponds to their high number of regenerated and low number of hypertrophic fibers. No significant difference was found between *mdx/utrn* $^{+/+}$ and $^{+/-}$ mice, although fiber density was slightly lower in *mdx/utrn* $^{+/+}$ mice. This slight difference is caused by the large proportion of hypertrophic fibers of the *mdx/utrn* $^{+/+}$ that exceeded that of *mdx/utrn* $^{+/-}$ and wild type mice. On the other hand, the proportion of small regenerated fibers of *mdx/utrn* $^{+/-}$ exceeded that of *mdx/utrn* $^{+/+}$ and wild type mice. Hypertrophy was not observed in the *mdx/utrn* $^{-/-}$ mice, which might be due to their short lifespan, during which damaged fibers are continuously replaced by newly regenerated fibers. Muscle mass to body weight ratio showed no significant difference between *mdx/utrn* $^{+/+}$ and $^{+/-}$ mice. Previously, a similar comparison has been made between *mdx* and *mdx/utrn* $^{-/-}$ mice, for which no significant difference was found too (Deconinck et al. 1997b). However, one should keep in mind that *mdx/utrn* $^{+/-}$ and $^{-/-}$ mice are much heavier and lighter than *mdx/utrn* $^{+/+}$ mice, respectively. This indicates that the capacity for hypertrophy appears to be unaffected by either partial or total utrophin deficiency. The differences observed in central nucleation and muscle fiber size probably also account to some degree for the reduced performance in the *mdx/utrn* $^{+/-}$ and $^{-/-}$ mice, which have been described previously for *mdx/utrn* $^{-/-}$ mice (Grady et al. 1997b).

We also analyzed whether the bad motor performance observed in the *mdx/utrn* $^{+/-}$ mice might be partly caused by fatigability resulting from loss of acetylcholine receptors at the NMJ due to the mono-allelic utrophin expression. In *mdx* mice, the NMJ is remodelled in both its pre- and postsynaptic components due to continuous cycles of re- and degeneration (Ferretti et al. 2011;Lyons and Slater 1991). Previous studies in *utrn* $^{-/-}$ and $^{+/-}$ mice, that do not have a behavioral or skeletal muscle phenotype, revealed that the overall structure of their NMJs is qualitatively normal (Deconinck et al. 1997a;Grady et al. 1997a). NMJs of *mdx/utrn* $^{-/-}$ mice do not qualitatively differ from those of *mdx* mice, although in these mice re- and degeneration is more pronounced (Grady et al. 1997b;Rafael et al. 2000). We showed with α-bungarotoxin staining of the diaphragm that neuromuscular synapses of the *mdx/utrn* $^{+/+}$, $^{+/-}$ and $^{-/-}$ mice have more punctuate, discontinuous acetylcholine receptor area, while synapses of wild type mice generally have an area of continuous branches. Although our quantitative analysis does not allow for detection of subtle distinctions between the strains, we at least can conclude that massive acetylcholine receptor loss at the NMJ does not underlie muscle weakness of *mdx/utrn* $^{+/-}$ mice. To elucidate whether NMJ dysfunction contributes to fatigability of *mdx/utrn* $^{-/-}$ mice more detailed (physiological) investigation is needed.

Expression levels of genes involved in regeneration, inflammation and fibrosis were tested in mice which underwent the functional test regime and were sacrificed at an age of 16 weeks as well as in non-exercised 6 weeks old mice. For the older mice, a less pronounced trend was observed, which might be caused by the age difference of *mdx/utrn* $^{-/-}$ mice and the other strains. To test this, expression was also assessed in young mice, revealing that for all genes this was higher in *mdx/utrn* $^{-/-}$ mice compared to age-matched *mdx/utrn* $^{+/-}$ and $^{+/+}$ or C57BL/10ScSnJ mice. The expression of the *mdx/utrn* $^{+/-}$ mice was higher than that of the *mdx/utrn* $^{+/+}$ mice for all genes, although no significant difference was found. Given that the fibrosis of *mdx/utrn* $^{+/-}$ mice worsens after 6 months we anticipate larger difference at later ages. However, this was beyond the scope of this study.

Additional factors that might result in bad motor function of the *mdx/utrn* $^{+/-}$ mice are i.e. behavioral, force transmission and respiratory function related. Motor function tests performed in this study are not a reflection of a sole neuromuscular defect, such as fatigue or strength, but an integrated result of the whole body performance. As such, outcomes are also influenced by behavioral and coordination components, which might be altered in dystrophic mice to certain extents since both dystrophin and utrophin are expressed in the central nervous system, although expression does not overlap (Knuesel et al. 2000). *Mdx* mice suffer from behavioral abnormalities, however for *mdx/utrn* $^{-/-}$ mice this is unknown, because behavioral studies are hampered by their immobility and poor survival. Mice lacking one or two utrophin alleles *in the presence* of dystrophin at least show no behavioral abnormalities (Deconinck et al. 1997a;Grady et al. 1997a).

To determine whether individual muscles suffer from fatigue or loss of strength, experiments assessing e.g. specific forces and resistance to eccentric contractions should be performed. *Mdx* mice have decreased specific forces and resistance to eccentric contractions (Consolino and Brooks 2004;Deconinck et al. 1998;Dellorusso et al. 2001). To which extent the overall performance of the *mdx/utrn* $^{+/-}$ mice is affected by reduced muscle forces needs special attention and should be monitored aside motor function tests. In addition, the structure of the myotendinous junction, which is involved in force transmission from myofibrils across the muscle membrane to the extracellular matrix, might also play a role. The number of foldings in this structure is reduced in *mdx* mice, but to a greater extent in *mdx/utrn* $^{-/-}$ mice (Deconinck et al. 1997b). Future studies should address this in the *mdx/utrn* $^{+/-}$ mice. Finally, decreased respiratory function disables functional performance as well. A recent paper indicates that respiratory function in older (6 months) *mdx/utrn* $^{+/-}$ mice is impaired compared to *mdx* mice, while no difference is found at the age of 3 months (Huang et al. 2011). The mice used in this study might already experience respiratory impairment resulting in a lower functional performance. To which extent respiratory function disabled *mdx/utrn* $^{+/-}$ mice in their performance needs to be further elucidated.

In conclusion, our findings indicate that *mdx/utrn* $^{+/-}$ mice have significantly impaired functional performance compared to *mdx/utrn* $^{+/+}$ mice. *Mdx/utrn* $^{+/-}$ mice have a high life expectancy and develop a more severe histopathology when aging, which is already initiated at 4 months, based on the increased mRNA muscle pathology biomarkers. This makes the *mdx/utrn* $^{+/-}$ mouse a better study subject to determine the benefits of potential therapeutic compounds than the *mdx/utrn* $^{-/-}$ and *mdx/utrn* $^{+/+}$ mouse.

Acknowledgments

This work is supported by the FP6 funded TREATNMD network of excellence (number 036825), the FP7 BIO-NMD Project (number 241665), the Dutch Organization for Scientific Research (NWO/ZonMW), and the Dutch Duchenne Parent Project. The work utilized the infrastructure of the Center for Biomedical Genetics (The Netherlands) and the Center for Medical Systems Biology (The Netherlands). We are grateful to Jiyun Byun for her help with Mayachitra Imago.

Chapter 4

Serum matrix metalloproteinase-9 (MMP-9) as a biomarker for monitoring disease progression in Duchenne Muscular Dystrophy (DMD)

V.D. Nadarajah, M. van Putten, A. Chaouch, P. Garrood, V. Straub, H. Lochmüller, H.B. Ginjaar, A.M. Aartsma-Rus, G.J.B. van Ommen, J.T. den Dunnen, P.A.C. 't Hoen

Neuromuscular Disorders 2011; 8, 569-578

Abstract

To identify serum biomarkers that allow monitoring of disease progression and treatment effects in Duchenne muscular dystrophy (DMD) patients, levels of matrix metalloproteinase-9 (MMP-9), tissue inhibitors of metalloproteinase-1 (TIMP-1) and osteopontin (OPN) were determined in 63 DMD patients on corticosteroid therapy. These proteins were selected for their role in the pathogenesis of muscular dystrophy. Levels of MMP-9 and TIMP-1 were significantly higher in sera of DMD patients compared to healthy controls, whereas the OPN levels showed no significant difference. MMP-9 levels were also observed to be significantly higher in older, nonambulant patients, compared to ambulant patients. Longitudinal data from a smaller cohort of DMD patients followed up for over 4 years showed that MMP-9, but not TIMP-1 increased significantly with age. Hence, MMP-9 is a potential DMD biomarker for disease progression. Future studies have to confirm whether serum MMP-9 levels can be used to monitor therapeutic response.

Introduction

Clinical biomarkers can be used to diagnose, monitor aetiology and progression of diseases and guide therapeutic decisions (Rifai et al. 2006). The serum biomarker currently used primarily as a first diagnostic hint for Duchenne muscular dystrophy (DMD), is creatine kinase (CK), where high levels of CK reflect muscle damage and/or disease. There are, however, several drawbacks to the CK test: levels may fall when disease progresses, probably due to the loss of muscle tissue (Emery and Muntoni 2003), and CK levels are also increased in normal individuals due to exercise, exertion or trauma to the skeletal muscle. Other available tests to monitor the progression of DMD pathology have limitations as well. Muscle biopsies have diagnostic value, but are laborious and invasive, and provide only local information on muscle quality, which may not be reflective for the state of all muscles. Muscle strength assessments are less of a burden to the patient and have prognostic applications, but are subject to extensive intra- and inter-patient variability (Mazzone et al. 2009). As such, there is no single test that can be used for diagnosis, prognosis, the recognition and/or prediction of potential complications and response to treatment. However, it might be feasible to achieve this with a group of serum biomarkers. Considering the various clinical treatments and trials currently ongoing for DMD (Angelini 2007;Bushby et al. 2009;Malik et al. 2010;van Deutekom et al. 2007), the identification of serum biomarkers to assess the effect of these treatments would be invaluable, since functional improvement cannot be expected within the short treatment periods in early phase clinical trials, and monitoring through repetitive muscle biopsies is not feasible for longer trials.

Based on recent literature findings on the pathophysiology of dystrophinopathy in both men and mice (dystrophin deficient mouse, *mdx*) via gene expression analyses (Li et al. 2009;Pescatori et al. 2007;Turk et al. 2005;Vetrone et al. 2009), we selected several potential serum biomarkers for DMD: matrix metalloproteinase 9 (MMP-9), tissue inhibitor of metalloproteinase (TIMP-1) and osteopontin (OPN). MMP-9 is associated with the degradation or remodeling of the extracellular matrix and is either secreted or present as a trans-membrane proenzyme. It has recently been demonstrated that *Mmp9* gene expression is increased in *mdx* mice and inhibition of *Mmp9* reduces skeletal muscle damage, inflammation, necrosis and fibrosis (Li et al. 2009). This implies that the absence of MMP-9 in *mdx* mice reduces the effects of dystrophin deficiency in the skeletal muscle. The proteolytic activity of MMP-9 is modulated by TIMPs and it has been postulated that the maintenance of the balance between MMP-9 and TIMPs is essential to maintain tissue integrity (Raffetto and Khalil 2008). Gene expression analysis of *mdx* and DMD muscles showed an upregulation of the *TIMP-1* gene (Li et al.

2009;Malik et al. 2010), suggesting it is worthwhile to include TIMP-1 in our biomarker study. OPN, a phosphorylated glycoprotein of the bone, is also expressed in immune cells, skin and blood vessels. The functions of OPN include formation of collagen fibrils during tissue remodelling, promotion of macrophage and neutrophil migration, angiogenesis and wound healing (Vetrone et al. 2009). A recent study revealed that *mdx* mice have high OPN serum concentrations, while absence of the OPN encoding *Spp1* gene in mice reduced neutrophils and decreased TGF-β levels resulting in reduced fibrosis in *mdx* mice (Vetrone et al. 2009). Interestingly, studies on gene expression profiles of DMD muscles at various stages of the disease also demonstrated significant upregulation of *SPP1* (Haslett et al. 2002;Pegoraro et al. 2011;Pescatori et al. 2007;Turk et al. 2006).

The three selected biomarkers are suggested to have a role either in inflammation, fibrosis, or extracellular matrix degradation, which are key events in the pathogenesis of DMD. We hypothesize that these biomarkers will be elevated in the DMD sera since DMD muscle fibres are leaky and continuously degenerating. Furthermore, as these markers are indicative for the disease pathophysiology, we suggest that they have potential as prognostic biomarkers. Our study examined serum levels of the selected biomarkers in *mdx* mice and in sera of corticosteroid treated DMD patients. The animal and patient studies reinforced each other, as mouse studies are better controlled but cannot be directly extrapolated to humans. Based on comparisons with control samples and correlations with other patient information, we suggest that MMP-9 and TIMP-1 in combination can be used as potential biomarkers for monitoring disease progression in DMD.

Materials and methods

Mice

Four week old C57BL/10ScSnJ (wt) ($N = 5$) and C57BL/10ScSn-mdx/J (*mdx*) ($N = 6$) females were subjected to forced exercise consisting of three times a week horizontal treadmill running at 12 m/min for 30 min for duration of 12 weeks to augment the severity of disease (De Luca et al. 2008). Blood was collected at the age of 8 and 14 weeks via the tail vein, allowed to clot at room temperature for 10 min and then spun at 1700 *g* for 10 min at 4 °C before pipetting the serum for storage at -80 °C, prior to use. For CK determination blood from the tail vein was collected in a Minicollect tube (0.8 ml Lithium Heparin Sep, Greiner bio-one, Austria). All mice were sacrificed at the age of 16 weeks by cervical dislocation. The quadriceps muscle was isolated, snap frozen in isopenthane, cooled in liquid nitrogen and stored at -80 °C. Quadriceps muscles from nonexercised *mdx* mice were used as controls for the gene expression studies. All experiments were approved by the Institutional Animal Experimental Commission (DEC) at LUMC.

Study participants

Sixty-three male patients with a molecular diagnosis of DMD were recruited for this study from the clinic population of the muscle service in Newcastle upon Tyne (mean age 13.1 years, age range between 2.9 and 31.2 years). As shown in Table 1, 34 of the patients were ambulant, with a mean age of 8.7 years and 29 were nonambulant, with a mean age of 18.1 years. Other clinical information such as duration of corticosteroid therapy and North Star Ambulatory Assessment (NSAA) scores were also available for these patients. Patients were on corticosteroid therapy for an average of 3.2 years and the mean NSAA score (available only for 29 ambulant patients) was 23/34.

Nine of the boys were followed up in a longitudinal study involving blood sampling at various time intervals (Garrood et al. 2009). They were on corticosteroid therapy, commenced at

a dose of 0.75 mg/kg/day of prednisolone as per international guidelines (Manzur et al. 2008). Child D8 was on deflazacort prior to and for the duration of the study due to unacceptable side effects from prednisolone (Table 2). The characteristics of the nine boys are summarised in Table 2, as the type of mutation, age of the boys, duration of corticosteroid treatment and the North Star Ambulatory Scores (NSAA) were also documented.

As part of the study four adult males (age range, 29.6–5.3 years; mean 32.4 years) and 12 healthy male children (age range, 6.25–1.9 years; mean 8.2 years) were recruited as controls. The healthy adult males ($N = 4$) were working at the Institute of Human Genetics when recruited. The control children were attending the Royal Victoria Infirmary, Newcastle upon Tyne for venepuncture for renal isotope imaging after a urinary tract infection. Any child with an abnormal renal isotope investigation was subsequently excluded from the study. Informed consent was taken from the parents after a further discussion of the study with both parents and child. The control children had no significant medical disorders and were not on any systemic medication. All elements of the human study received a favourable opinion from the local Research Ethics Committee prior to commencement.

Table 1
Clinical parameters of the independent DMD patient cohort.

	Age	Years on corticosteroid therapy	NSAA scores
Total DMD (N = 63)	13.10 ± 6.2 (2.9–31.2)	3.2 ± 3 (0–11.75)	23.33 ± 8.1# (3–33)
Ambulant (N = 34)	8.7 ± 3.3 (2.9–17.10)	2.7 ± 2.3 (0–7.5)	23.33 ± 8.1# (3–33)
Nonambulant (N = 29)	18.1 ± 4.6 (9.9–31.2)	3.8 ± 3.6 (0–11.5)	not available

±Std. deviation; () minimum and maximum values.

Table 2
Clinical parameters of the longitudinal DMD patient cohort.

Patient	Mutation (del exon)	Visit	Age	NSAA scores	Years on corticosteroid therapy
D1	47–50	1	9.40	26.00	3.25
D1		2	10.30	22.00	4.16
D1		3	11.00	11.00	4.83
D1		4	13.80	2.00	7.7
D2	53	1	9.25	32.00	3.16
D2		2	10.00	32.00	3.91
D2		3	10.80	27.00	4.83
D2		4	13.40	16.00	7.3
D3	52	1	6.40	–	0.83
D3		2	7.40	13.00	1.83
D3		3	8.10	8.00	2.5
D3		4	10.80	–	2.5
D5	52	1	7.25	22.00	0.41
D5		2	8.00	21.00	1.16
D5		3	11.25	11.00	4.35
D6	5–29	1	9.10	8.00	2.91
D6		2	9.80	10.00	3.67
D6		3	10.60	–	4.42
D6		4	13.10	–	6.85
D8	41–43	1	10.00	29.00	3.17
D8		2	10.60	29.00	3.83
D8		3	11.30	19.00	4.58
D8		4	13.80	23.00	7.2
D9	51	1	8.60	20.00	2.75
D9		2	9.30	15.00	3.50
D9		3	12.30	6.00	6.70
D10	42 Frames shift	1	6.73	27.00	2.17
D10		2	7.60	27.00	3.00
D10		3	10.00	24.00	5.60
D11	41 Nonsense	1	6.50	34.00	1.67
D11		2	7.30	33.00	2.50
Mean ± std. dev.			9.79 ± 2.12	20.25 ± 9.18	3.78 ± 1.92

Human serum samples

Blood was taken from DMD and control groups by the following method: 3–5 ml of venous blood (obtained prior to radioisotope injection for the child controls) was drawn and placed in BD-

Vacutainer (367694) tubes. The blood was allowed to clot at room temperature for 10 min and then placed in a refrigerator at 4 °C before further spinning at 2800 *g* at room temperature for 10 min. The serum supernatant was carefully removed and aliquoted for storage at -80 °C pending use.

RNA isolation and RT-PCR analysis

Total RNA of the quadriceps was isolated in Magna Lyser Green Beads tubes (Roche diagnostics Ltd., UK) using RNA-Bee (Tel-Test, Bio-Connect, Huissen, The Netherlands) and purified with the NucleoSpin RNA II kit (Bioke, The Netherlands). The RNA concentration was measured on a Nanodrop (Nanodrop Technologies, DE, USA) and integrity was checked with a lab-on-chip total RNA nano assay on a labchip assay (Agilent, The Netherlands). cDNA was generated and gene expression levels were determined for *Mmp9*, *Timp1* and *Spp1* (primer sequences available on request) by Syber Green based Real Time qPCR (95 °C 10 s, 60 °C 30 s, 72 °C 20 s, 45 cycles) on the Roche Lightcycler 480. *Gapdh* was used as a reference gene, since the expression of this gene did not differ between different muscles or over time. The C_P values were obtained with the second derivative maximum method and analysed with genex (http://www.gene-quantification.com/download.html).

Determination of MMP-9, TIMP-1 and OPN levels in mice and human serum samples

Levels of MMP-9, TIMP-1 and OPN were determined using commercially available immunoassays kits. To determine levels in mouse serum, the mouse MMP-9 (total) immunoassay kit (catalogue number MMPT90) and mouse TIMP-1 immunoassay (catalogue number MTM100) were purchased from R&D systems (Abingdon, United Kingdom), while the mouse OPN kit (code number 27351) was purchased from IBL (Hamburg, Germany). The immunoassay kits for detection in human serum were the Human MMP-9 (total) immunoassay kit (catalogue number DMP900), the Human TIMP-1 immunoassay kit (catalogue number DTM100) and the Human OPN immunoassay kit (catalogue number DOST00) all purchased from R&D systems. These kits used the quantitative sandwich enzyme immunoassay technique where only free, unbound forms of the biomarkers are detected. All experiments were carried out in duplicates using the manufacturer's instructions.

Statistical analysis

Statistical analyses were performed using the Statistical Package for the Social Sciences (SPSS), version 17. All data sets were subjected to normality testing using the Kolmogorov–Smirnov method. For comparisons between means the Student's *t*-test (two-tailed) was applied. Additionally, data on the independent study groups (DMD and controls) were presented using descriptive statistics in which the median value and interquartile range (IQR, the statistical dispersion of the middle 50% of the data) were calculated to show the distribution of the biomarker levels for each group. Pearson's Correlation was used for correlation studies and data were analysed with a 95% confidence interval and $P<0.05$ was considered significant and $P<0.01$ was considered highly significant. For the longitudinal DMD group, the statistical package from R2.9.2 was used and the linear mixed-effects model (lme4, version 0.99937538) was applied to determine the relationship of each biomarker with age and duration of corticosteroid therapy.
The fixed and random effects used in this model were as follows: for fixed it was age and duration of corticosteroid therapy and for random, it was the patient.

Results

Gene expression analysis of Mmp9, Timp1 and Spp1 in mouse quadriceps

As we had begun our study by selecting candidate biomarkers from *mdx* gene expression data, we first confirmed whether these mRNA expression changes were also present in the mice used in our study. Whereas previously reported studies on these biomarkers used sedentary mice (Li et al. 2009;Vetrone et al. 2009), the *mdx* and wt mice used for serum collection were subject to exercise to augment the severity of the disease. We therefore compared the gene expression of *Mmp9*, *Timp1* and *Spp1* (coding for OPN) between the study mice groups (exercised *mdx* and exercised wt) and nonexercised mice (*mdx*) using qPCR analysis. Fig. 1a, b and c show the gene expression data of *Mmp9*, *Timp1* and *Spp1*, respectively, from the quadriceps of 16 week old, exercised *mdx* and *mdx* compared to exercised wt. We observed no significant difference between the expression of these genes in the exercised *mdx* and *mdx* group. There was, however, a significant difference between exercised wt and *mdx*. Although gene expression in exercised *mdx* was much higher than in exercised wt mice, this difference was not significant due to a higher standard deviation (SD) observed in the exercised *mdx* group compared to the exercised wt and *mdx* group.

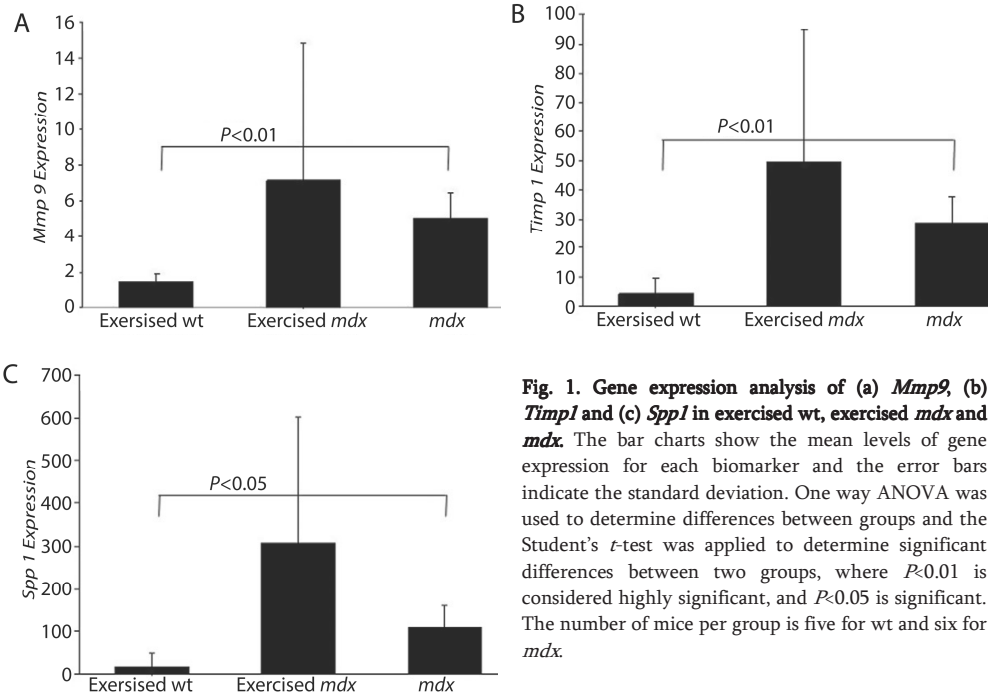


Fig. 1. Gene expression analysis of (a) *Mmp9*, (b) *Timp1* and (c) *Spp1* in exercised wt, exercised *mdx* and *mdx*. The bar charts show the mean levels of gene expression for each biomarker and the error bars indicate the standard deviation. One way ANOVA was used to determine differences between groups and the Student's *t*-test was applied to determine significant differences between two groups, where $P<0.01$ is considered highly significant, and $P<0.05$ is significant. The number of mice per group is five for wt and six for *mdx*.

Mouse serum levels of MMP-9, TIMP-1 and OPN

We then assessed serum from 8 and 14 week old exercised *mdx* and exercised wt mice. At the age of 8 weeks, a highly significant difference was observed in the serum MMP-9 levels between exercised wt and exercised *mdx* mice. The serum MMP-9 levels in exercised *mdx* mice were twofold higher than in exercised wt mice, with mean levels of 41.8 ng/ml ± 10.5 (level ± SD) for exercised wt mice and 86.52 ng/ml ± 21.07 for exercised *mdx* mice (Fig. 2a). At the age of 14 weeks, levels of MMP-9 were still elevated in exercised *mdx* mice (mean = 62.53 ng/ml ± 39.4),

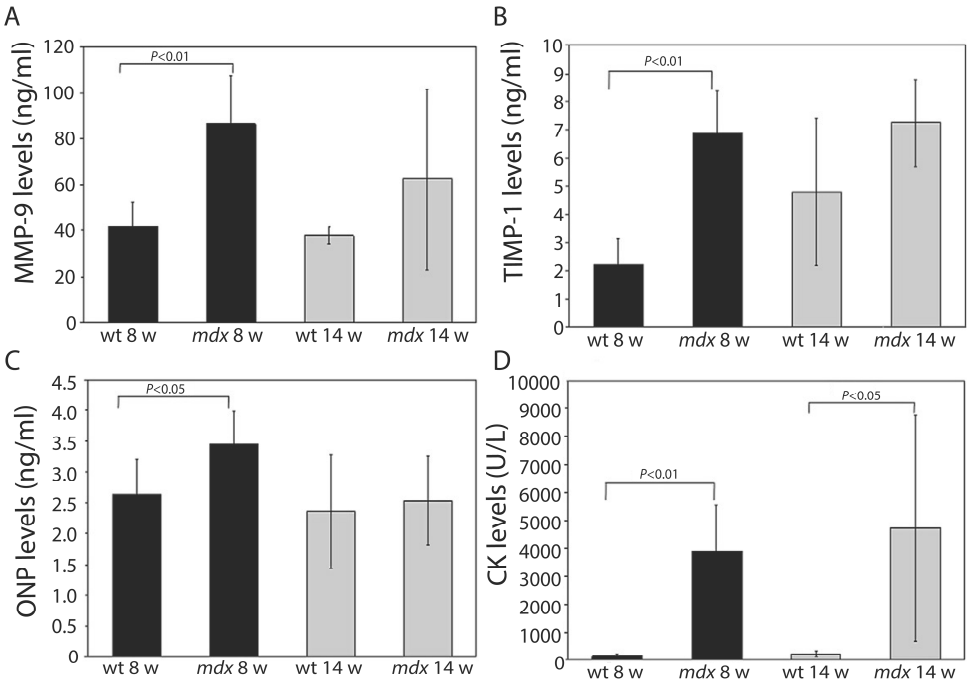


Fig. 2. Serum levels of (a) MMP-9, (b) TIMP-1, (c) OPN and (d) CK in exercised wt and exercised *mdx* at 8 and 14 weeks. The bar charts show the mean serum levels of each biomarker and the error bars indicate the standard deviation. One way ANOVA was used to determine differences between groups and the Student's *t*-test was applied to determine significant difference between two groups, where $P<0.01$ is considered highly significant, and $P<0.05$ is significant. The number of mice per group is five for wt and six for *mdx*.

however this difference was not significant when compared to exercised wt mice at the similar age group (mean = 37.85 ng/ml ± 3.50). There were no significant differences in the serum levels at the different time points for either exercised wt or exercised *mdx* mice. However in exercised *mdx* mice, a drop in serum levels of MMP-9 was noted between 8 and 14 weeks.

The levels of TIMP-1 at 8 weeks were 3-fold higher in exercised *mdx* mice (mean = 6.9 ng/ml ± 1.32) compared to exercised wt mice (mean = 2.22 ng/ml ± 0.91), and this difference was significant ($P<0.01$) (Fig. 2b). Although a difference was observed in the TIMP-1 levels in 14 week old mice, where exercised *mdx* mice (mean = 7.25 ng/ml ± 1.55) had higher levels than exercised wt mice (mean = 4.78 ng/ml ± 2.62), this difference was not significant. There was also no significant difference in the levels of TIMP-1 between 8 and 14 weeks for both strains.

Serum OPN levels were found to be higher ($P<0.05$) in 8 week old exercised *mdx* mice (mean = 3.44 ng/ml ± 0.54) compared to exercised wt mice (mean = 2.62 ng/ml ± 0.59) (Fig. 2c). At 14 weeks, the levels were similar for exercised *mdx* (mean = 2.53 ng/ml ± 0.73) and exercised wt mice (mean = 2.36 ng/ml ± 0.91).

CK levels were also determined for the 8 and 14 weeks groups (Fig. 2d) and significant differences were observed between exercised wt and exercised *mdx* for mice at both age groups. At 8 weeks, the CK levels for exercised wt were lower (mean = 142 U/L ± 100) than the CK levels for exercised *mdx* (mean = 3900 U/L ± 1631). At 14 weeks, this difference is smaller but still significant as the CK levels for exercised wt were 230 U/L ± 102 whereas they were 4773U/L ± 4024 for exercised *mdx*.

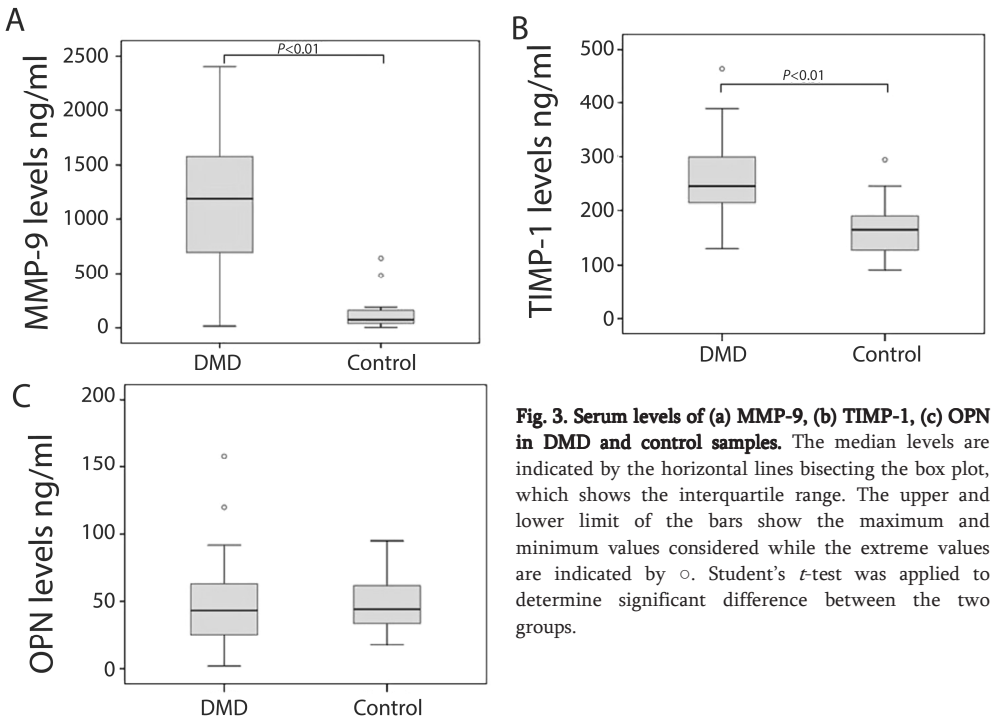


Fig. 3. Serum levels of (a) MMP-9, (b) TIMP-1, (c) OPN in DMD and control samples. The median levels are indicated by the horizontal lines bisecting the box plot, which shows the interquartile range. The upper and lower limit of the bars show the maximum and minimum values considered while the extreme values are indicated by ○. Student's *t*-test was applied to determine significant difference between the two groups.

Serum levels of MMP-9, TIMP-1, and OPN in DMD and control samples

We measured the serum levels of MMP-9, TIMP-1 and OPN in serum samples of 63 DMD boys and 16 control subjects (12 age-matched boys and 4 adult men) and statistically compared the levels with Students *t*-test. The 12 boys and 4 adults in the healthy control group were grouped together since there were no differences between biomarker levels in young and adult subjects (data not shown). As shown in Fig. 3a, serum MMP-9 levels were significantly higher in DMD (median level = 1185.34 ng/ml, IQR = 966.56) compared to control samples (median level = 73.22 ng/ml, IQR = 121.00) (P<0.001). Similarly, serum TIMP-1 (Fig. 3b) levels were significantly higher in DMD (median levels = 245.55 ng/ml, IQR = 69.57) compared to control groups (median level = 164.77 ng/ml, IQR = 62.45) (P<0.01). The serum OPN levels, however, were not significantly different between DMD (median levels = 41.24 ng/ml, IQR = 33.74) and control groups (median level = 44.19 ng/ml, IQR = 30.69) (Fig. 3c).

Further stratification of the DMD samples into ambulant and nonambulant groups (Fig. 4) showed significantly higher levels for nonambulant compared to ambulant for MMP-9 (ambulant group median levels = 927.89, IQR = 885.60; nonambulant group median levels = 1328.45, IQR = 822.95), while both groups were significantly increased compared to the control group. By contrast, similar levels were observed in ambulant and nonambulant groups for TIMP-1, which were both significantly higher than in the control group (Fig. 4b). OPN levels were similar for all three groups (Fig. 4c).

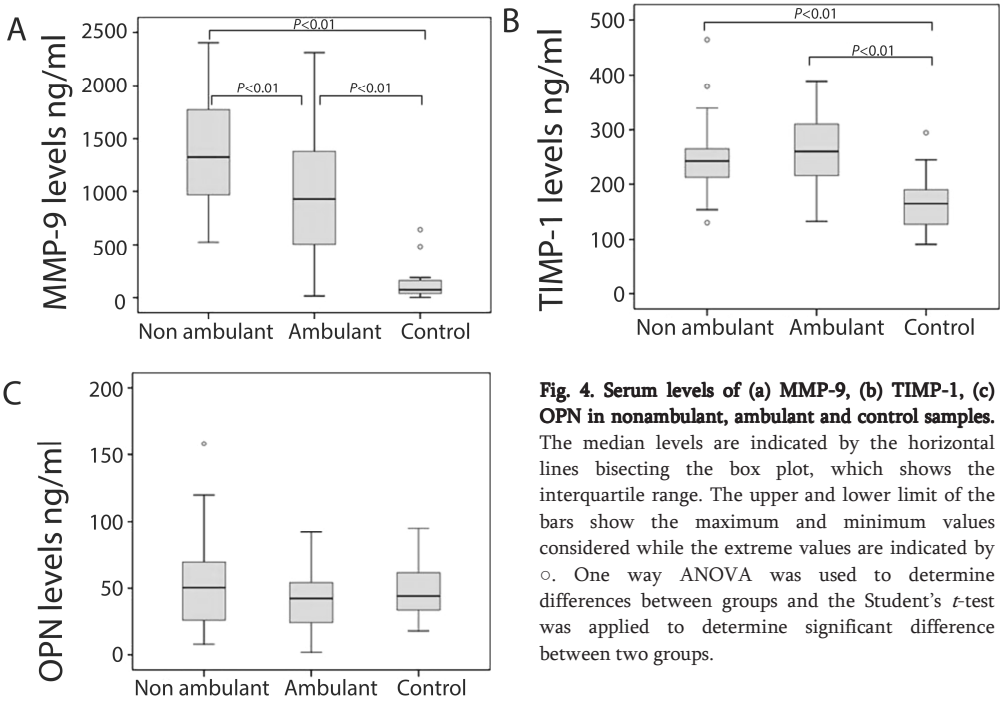


Fig. 4. Serum levels of (a) MMP-9, (b) TIMP-1, (c) OPN in nonambulant, ambulant and control samples. The median levels are indicated by the horizontal lines bisecting the box plot, which shows the interquartile range. The upper and lower limit of the bars show the maximum and minimum values considered while the extreme values are indicated by ○. One way ANOVA was used to determine differences between groups and the Student's *t*-test was applied to determine significant difference between two groups.

Correlation between levels of MMP-9, TIMP-1, OPN, age, steroid treatment and NSAA scores in DMD and control groups

Pearson correlation analysis was applied to determine the correlation coefficient between the three biomarker levels with other patient characteristics (age, years on steroid treatment and NSAA scores) in the independent DMD patient cohort (as observed from Table 3). MMP-9 levels were positively correlated with age and duration of corticosteroid therapy ($P<0.01$). There were however, no significant correlations observed between levels of MMP-9 and TIMP-1, OPN or the functional scores, NSAA (ambulant boys only). There was a significant positive correlation between age and duration of corticosteroid therapy ($P<0.05$) and although there was negative correlation (correlation coefficient of -0.241) between age and the NSAA scores, the effect was not significant. Age dependent trends were not observed for TIMP-1 and OPN. Serum OPN showed negative correlation with NSAA scores (correlation coefficient of -0.309), however this effect was not significant. In the control group, no significant correlation was observed between any of the variables (age, serum MMP-9, TIMP-1 and OPN levels).

Table 3
Correlation between levels of biomarkers and clinical parameters of the independent DMD patient cohort.

	MMP-9	TIMP-1	OPN	Age	Corticosteroid therapy
MMP-9	–				
TIMP-9	0.187 (0.142)	–			
OPN	−0.134 (0.293)	0.040 (0.757)	–		
Age	0.386** (0.002)	−0.078 (0.545)	0.118 (0.358)	–	
Corticosteroid therapy	0.403** (0.001)	0.125 (0.329)	−0.005 (0.971)	0.251* (0.047)	–
NSAA Scores	−0.028 (0.883)	−0.025 (0.900)	−0.309 (0.103)	−0.241 (0.209)	−0.145 (0.452)

() P-values.
* Correlation is significant at P < 0.05.
** Correlation is significant at P < 0.01.

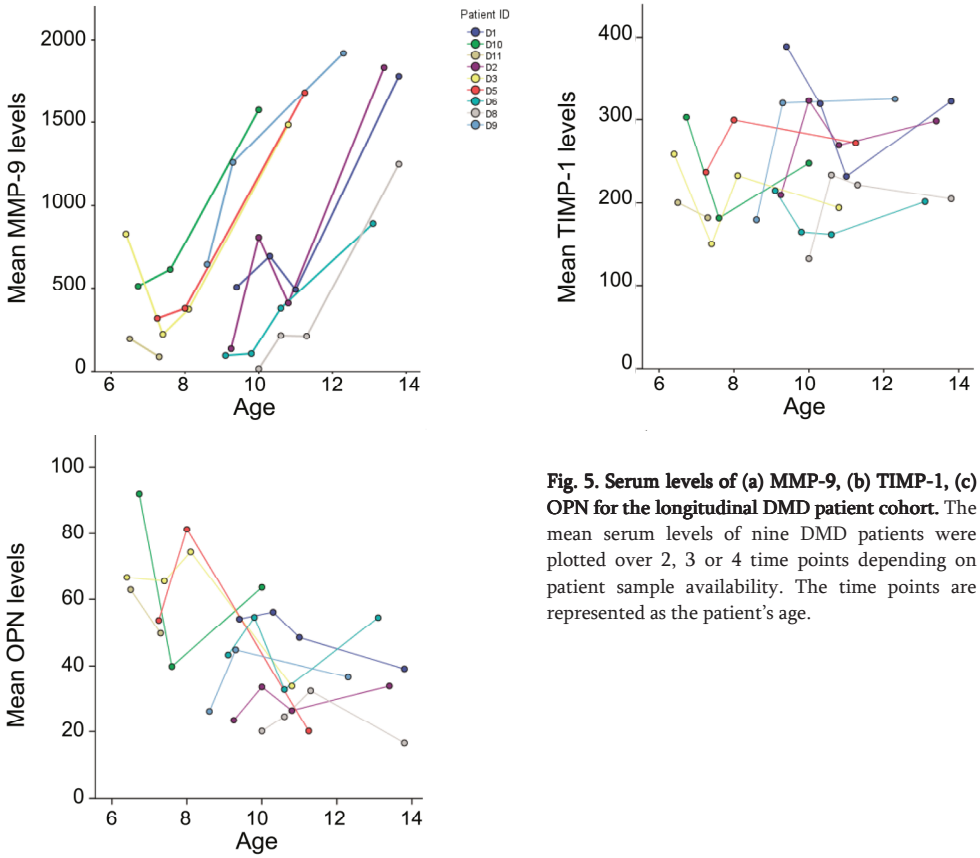


Fig. 5. Serum levels of (a) MMP-9, (b) TIMP-1, (c) OPN for the longitudinal DMD patient cohort. The mean serum levels of nine DMD patients were plotted over 2, 3 or 4 time points depending on patient sample availability. The time points are represented as the patient's age.

Longitudinal analysis of MMP-9, TIMP-1 and OPN in DMD patients

As nine patients were followed up longitudinally, there was an opportunity to determine serum levels of these biomarkers over time for the same group of patients. Fig. 4 shows the biomarker levels of the individual DMD patients followed up between two and four and a half years. The levels of MMP-9 (Fig. 5a) increased with age whereas the levels of TIMP-1 (Fig. 5b) did not demonstrate a consistent increase with age. Interestingly, the levels of OPN (Fig. 5c) seemed to decrease with age. To determine whether age and duration of corticosteroid therapy had an effect on biomarker levels, the linear mixed-effects model analysis was applied to the longitudinal data. We observed that MMP-9 shows a significant linear relationship with age (t-stat = 2.17, $P<0.01$) but duration of corticosteroid therapy does not significantly contribute to this relationship (t-stat = 0.63, $P=0.53$). OPN levels show a significant linear and negative relationship with age (t-stat = -2.77, $P<0.01$) and the duration of corticosteroid therapy does not contribute significantly to this relationship (t-stat = 1.7, $P=0.1$).

Discussion

The potential biomarkers explored in this study, were initially hinted at by recent findings in *mdx* mouse experiments. Gene expression analysis of *mdx* muscle showed that the *Timp1* gene and the *Spp1* gene (which encodes OPN) were significantly upregulated compared to muscles of healthy mice (Turk et al. 2005), while other studies have shown that both MMP-9 and OPN were elevated in serum of the *mdx* mouse compared to wild-type (Li et al. 2009;Vetrone et al. 2009). MMP-9, TIMP-1 and OPN are known to have a role as pro inflammatory markers (Castellano et al. 2008;Sun et al. 2006) and in the absence of dystrophin in mouse models, MMP-9 and OPN have been shown to have an effect in extra cellular matrix degeneration, inflammation and subsequent degeneration and regeneration of muscle fibres leading to fibrosis (Li et al. 2009;Vetrone et al. 2009). Data from our 8 week old exercised mice confirmed the findings of these previous studies. TIMP-1 levels remained elevated in 14 week old exercised *mdx* mice, but MMP-9 and OPN levels appeared to decrease with age. These latter observations were not in agreement with previous reports (Li et al. 2009;Vetrone et al. 2009), possibly as a consequence of the exercise regimen we used with our *mdx* mice. To examine whether our results differed because mice used in our study were subjected to forced exercise from the age of 4 weeks until time of blood sampling (8 weeks and 14 weeks) and sacrifice (16 weeks), we examined the gene expression of these three biomarkers in exercised *mdx* and nonexercised *mdx* mice. No significant differences in gene expression were observed between the exercised and nonexercised group for any of the biomarkers. We did however observe that inter mouse variation was higher in the exercised *mdx* group compared to the *mdx* and exercised wt. It has been suggested that the beneficial or deleterious effect of exercise on dystrophic muscles depends on the age of the animal at the start of exercise, the severity of pathology, the intensity, and the duration and type of training (Carter et al. 2002). Although in this study these parameters were similar in the exercised *mdx* group, the severity of the dystrophy for each mouse may be more variable, which could contribute to the higher variation seen in this group.

Our results in humans are in line with the mouse data: levels of MMP-9 and TIMP-1 are higher in DMD compared to controls. We also observed that MMP-9 levels were significantly higher in older, nonambulant patients compared to the younger, ambulant patients, suggesting that there is an increase in MMP-9 levels with disease progression. Results of the longitudinal study supported this observation as levels of MMP-9 increased with age for individual patients. While this study reports on both MMP-9 and TIMP-1 levels in serum of DMD patients, gene expression analysis on DMD muscle tissue has indicated a role for elevated *TIMP1* and *MMP2* in extra cellular matrix modelling at early stages of disease development (Pescatori et al. 2007), which makes it likely that MMP-9 and TIMP-1 are derived from dystrophic muscles. An earlier study to detect inflammatory proteins in muscles of symptomatic DMD patients (5–12 years) and pre-symptomatic patients (infants) showed that the transforming growth factor (TGF)-β pathway was activated in the symptomatic group (Chen et al. 2005). The study by Li et al. 2009 suggested that MMP-9 increased TGF-β levels, which in turn exacerbated muscle degeneration in dystrophic mice (Li et al. 2009). A recent study comparing plasma levels and muscle expression of TGF-β and TIMP-1 in DMD, congenital muscular dystrophy (CMD) and Becker muscular dystrophy (BMD) showed that these markers were markedly elevated in DMD and CMD compared to the less severe BMD (Sun et al. 2010). Our data on serum levels of MMP-9 and TIMP-1 confirmed the findings of earlier studies on the pathogenesis of DMD.

The Pearson correlation analysis also confirmed a significant positive correlation between MMP-9 levels, age and duration of corticosteroid treatment in the 63 DMD patients. While the positive correlation between age and MMP-9 levels reflected the observation seen in

the nonambulant and ambulant patients, the correlation between MMP-9 levels and duration of corticosteroid therapy needs further analysis. The patient cohort in our study was limited by the number of patients who were steroid naïve, and for patients that were on corticosteroid therapy, age and duration of treatment was confounded, making it difficult to discriminate between disease progression due to age and effects of steroid treatment. From the limited studies available on MMP-9 levels and corticosteroid therapy, one study on serum levels of patients with Graves ophthalmology and another on gene expression of MMP-9 in a murine model showed that MMP-9 levels were lowered after corticosteroid therapy (De Paiva et al. 2006;Mysliwiec et al. 2007) while another study of asthmatic patients on corticosteroid therapy suggests that MMP-9 levels do not differ in steroid sensitive or resistant patients (Goleva et al. 2007). There was however one study which showed a short term increase in MMP-9 levels in patients with multiple sclerosis on a high dose of intra-venous methyl-prednisolone (1000 mg/day), where MMP-9 levels were noted to be significantly elevated at day 10 before returning to pre-treatment levels at day 20 (Mirowska et al. 2004). In our study, the positive correlation between age and MMP-9 was further strengthened by the results of the linear mixed-effects analysis in the longitudinal DMD cohort as there was a significant and positive linear relationship between MMP-9 levels and age i.e. disease progression, and the duration of steroid treatment did not contribute significantly to this relationship. Thus, based on our findings and information available from the above mentioned literature, we suggest that elevated MMP-9 levels are due to disease progression rather than the effect of corticosteroid treatment.

Although we observed TIMP-1 levels to be significantly higher in DMD compared to controls, there was no significant difference in levels between ambulant and nonambulant groups or a significant correlation with age. However, due to the recent findings that plasma TIMP-1 levels are lower in less severe BMD compared to DMD (Sun et al. 2010), the reports that ratio of MMP-9 and TIMP-1 reflected the balance of pro and anti-inflammatory cytokines (Wu et al. 2008), and our own observation that TIMP-1 levels remained elevated in DMD patients, we suggest it is still useful to assess the potential of TIMP-1 as a biomarker in larger and independent cohorts from other clinical centres. OPN levels showed no significant difference between DMD and control samples or between ambulant and nonambulant groups. There was however a significant linear but negative relationship in the longitudinal cohort for OPN and age. A recent study on DMD patients with the less common G allele of the rs28357094 *SPP1* promoter, which was associated to decreased OPN mRNA expression levels, suggested that less *SPP1* leads to more muscle weakness, with lower grip strength and earlier age for loss of ambulance (Pegoraro et al. 2011). As serum OPN levels were not reported in that study, it would be of future interest to know whether blood OPN levels were lowered in the DMD patients carrying the less common G allele.

Current clinical trials on exon skipping and stop codon read-through (Aartsma-Rus and van Ommen 2010) include CK as a serum biomarker to study the effectiveness of treatment. While decreasing CK levels can be a positive prognostic indicator in some diseases (myocardiac infarction for example), in DMD patients the role of CK as a prognostic biomarker is questionable. CK levels are markedly increased before signs and symptoms of DMD are observed, confirming the useful diagnostic application at a very early stage of the disease. However as mentioned earlier (Emery and Muntoni 2003), declining CK levels in DMD are associated to decrease in ambulatory skills and disease progression. We suggest that MMP-9 and TIMP-1 levels are potentially more useful biomarkers for response to therapy, since they do not show this decreasing trend, probably as a consequence of the continued inflammatory response in DMD patients, even after substantial muscle degeneration. Effective therapy should reduce the degeneration-induced inflammatory

response. Future studies have to confirm whether MMP-9 and TIMP-1 indeed decrease after dystrophin restoration, and therefore are useful as biomarkers to monitor therapeutic responses.

Due to their role in inflammation, cell migration, angiogenesis and fibrosis (Brunner et al. 2010;Wu et al. 2008), elevated levels of MMP-9 and TIMP-1 are not specific to DMD or muscle diseases. These markers have been investigated for their role in cancers (breast, bladder and pancreas), cardiovascular diseases and in preeclampsia. In breast cancer for example, MMP-9 is used as a marker for diagnosis and prognosis, early detection and risk assessment, but also as an indicator of tumour recurrence, metastatic spread, and response to primary and adjuvant therapy (Wu et al. 2008). In coronary artery disease, the ratio of MMP-9/TIMP-1 in serum was suggested to be useful for progression of disease as it is reflective of the balance between circulating pro and anti inflammatory cytokines (Brunner et al. 2010). Hence, their diagnostic value for DMD perse may be limited. However, based on our study in mice and humans, we suggest to further evaluate MMP-9 and TIMP-1 as valuable biomarkers in DMD for the monitoring of disease progression and therapy efficacy.

Acknowledgements

This work was supported by the Dutch Organisation for Scientific Research (Medical council ZON-MW), the BIO-NMD Grant (EC, 7th FP, proposal# 241665; www.bio-nmd.eu) and the Centre for Medical Systems Biology within the framework of the Netherlands Genomics Initiative (NGI)/Netherlands Organisation for Scientific Research (NWO). The MRC Centre for Neuromuscular Diseases Biobank Newcastle is a partner of EuroBioBank (www.eurobiobank.org) and TREAT-NMD (EC, 6th FP, proposal# 036825). We wish to thank Dr Michelle Eagle and Geraldine Bailey for NSAA assessments, and Mojgan Reza and Daniel Cox for expert technical assistance.

Chapter 5

The effects of low levels of dystrophin on mouse muscle function and pathology

M. van Putten, M. Hulsker, V.D. Nadarajah, S.H. van Heiningen, E. van Huizen, M. van Iterson, P. Admiraal, T. Messemaker, J.T. den Dunnen, P.A.C. 't Hoen, A.M. Aartsma-Rus

PLoS One 2012; 7e; 31937

Abstract

Duchenne muscular dystrophy (DMD) is a severe progressive muscular disorder caused by reading frame disrupting mutations in the *DMD* gene, preventing the synthesis of functional dystrophin. As dystrophin provides muscle fiber stability during contractions, dystrophin negative fibers are prone to exercise-induced damage. Upon exhaustion of the regenerative capacity, fibers will be replaced by fibrotic and fat tissue resulting in a progressive loss of function eventually leading to death in the early thirties. With several promising approaches for the treatment of DMD aiming at dystrophin restoration in clinical trials, there is an increasing need to determine more precisely which dystrophin levels are sufficient to restore muscle fiber integrity, protect against muscle damage and improve muscle function. To address this we generated a new mouse model (*mdx-Xist*$^{\Delta hs}$) with varying, low dystrophin levels (3–47%, mean 22.7%, stdev 12.1, n = 24) due to skewed X-inactivation. Longitudinal sections revealed that within individual fibers, some nuclei did and some did not express dystrophin, resulting in a random, mosaic pattern of dystrophin expression within fibers. *Mdx-Xist*$^{\Delta hs}$, *mdx* and wild type females underwent a 12 week functional test regime consisting of different tests to assess muscle function at base line, or after chronic treadmill running exercise. Overall, *mdx-Xist*$^{\Delta hs}$ mice with 3–14% dystrophin outperformed *mdx* mice in the functional tests. Improved histopathology was observed in mice with 15–29% dystrophin and these levels also resulted in normalized expression of pro-inflammatory biomarker genes, while for other parameters >30% of dystrophin was needed. Chronic exercise clearly worsened pathology, which needed dystrophin levels >20% for protection. Based on these findings, we conclude that while even dystrophin levels below 15% can improve pathology and performance, levels of >20% are needed to fully protect muscle fibers from exercise-induced damage.

Introduction

Duchenne Muscular Dystrophy (DMD) is an X-linked recessive disorder affecting 1:3500 new born boys. It is characterized by muscle fiber wasting, functional impairment and eventual death due to respiratory and heart failure. The underlying causes are frame-shifting and nonsense mutations in the *DMD* gene, resulting in the absence of functional dystrophin protein. Intact dystrophin anchors the intracellular cytoskeleton to the extracellular matrix and thereby prevents membrane damage during muscle contraction (Aartsma-Rus et al. 2006;Hoffman et al. 1987). An allelic, less severe form of the disease, Becker muscular dystrophy (BMD) is caused by mutations that maintain the open reading frame and allow synthesis of internally deleted, partially functional dystrophin proteins (Hoffman et al. 1988;Monaco et al. 1988).

There is no cure for DMD, but many potential therapeutic compounds currently tested in clinical trials aim at restoration of (a BMD like) dystrophin (Aartsma-Rus et al. 2010;Cirak et al. 2011;Goemans et al. 2011;Hirawat et al. 2007;Kinali et al. 2009;Malik et al. 2010;Mendell et al. 2010;Ogata et al. 2000;Pegoraro et al. 1995;Schmidt-Achert et al. 1993;van Deutekom et al. 2007). These trials at best resulted in the synthesis of low levels of dystrophin protein. However, it is not yet known how these levels will affect disease pathology, and which levels are needed to maintain muscle fiber integrity, to prevent against exercise-induced damage, or to improve muscle function. In addition, it is as yet unknown whether low dystrophin levels will stabilize and/or delay disease progression (Aartsma-Rus et al. 2010). In perspective of further optimization of currently tested potential therapeutic compounds, detailed studies in this direction are necessary.

Early studies primarily involved female *DMD* carriers, heterozygous *mdx* mice and isolated BMD patients expressing less than 50% dystrophin. Female *DMD* mutation carriers

express dystrophin in approximately 50% of the fibers (when seen in a transverse cross section) due to random X-inactivation early in life (Pegoraro et al. 1995;Schmidt-Achert et al. 1993). During life, the proportion of dystrophin positive fibers increases due to positive selection. It appears that this is sufficient to maintain skeletal muscle function and fiber integrity in both human and mice. Although skeletal muscles appear to escape damage, human carriers are at risk for *DMD*-associated dilated cardiomyopathy (Ogata et al. 2000), while no heart failure is observed in heterozygous *mdx* mice (Bostick et al. 2008;Tanaka et al. 1990). Nevertheless, symptomatic carriers have been described, often expressing less than 50% of normal dystrophin levels due to either gross chromosomal rearrangements (Boyd et al. 1986), or unfortunate skewed X-inactivation in which the degree of skewedness correlated with disease severity (Azofeifa et al. 1995;Lupski et al. 1991;Pegoraro et al. 1995;Soltanzadeh et al. 2010). In addition, BMD patients generally have lower levels of dystrophin and these levels seem to correlate with disease severity, where levels <10% are observed in very severe patients and levels >20% in moderate/mild patients (Hoffman et al. 1988;Hoffman et al. 1989). Based on a case study involving one patient, it appears that dystrophin levels as low as 30% can be sufficient to largely prevent a muscle phenotype (Neri et al. 2007). The amount of revertant fibers has also been reported to correlate positively with disease severity (Nicholson et al. 1993). However, reports on BMD and skewed X-inactivation cases involve low numbers of patients and detailed analysis (e.g. assessment of dystrophin levels in various muscles) is not possible for obvious reasons. Thus, there is an increasing need for a mouse model expressing low levels of dystrophin to allow the detailed study of the effects of low dystrophin levels on disease pathology.

So far, several attempts have been made to achieve this. Unfortunately, each had limitations. First, transgenic mice expressing low levels of full-length or truncated dystrophin of murine or human origin have been generated to test whether this results in a less severe phenotype (Phelps et al. 1995;Rafael et al. 1994). However, from the 13 mouse lines generated, only two expressed dystrophin levels lower than 50% of wild type in both the quadriceps and diaphragm. The other lines had higher dystrophin levels or a combination of both higher and lower levels than wild type. From the two potential lines, one expressed low dystrophin levels (15% quadriceps and <5% diaphragm), while the other line expressed higher dystrophin levels (40% quadriceps and 20% diaphragm), thus allowing detailed analysis of only two different dystrophin levels. Dunant et al. generated *mdx* mice in which dystrophin expression was driven by a 1.35-kb MCK promoter resulting in abundant expression in fast-twitch muscles (˜50%) and very low expression in slow-twitch fibers. The heart did not express dystrophin at all (Dunant et al. 2003). The fiber type specific dystrophin expression makes this model less suitable for detailed analysis. In another study, Stillwell et al. generated chimeric mice expressing various dystrophin levels depending on the amount of wild type cells incorporated in *mdx* blastocytes. Mice expressed dystrophin in skeletal muscles in a very high (60–100%) or low (<5%) manner (Stillwell et al. 2009). This, combined with the fact that this method is extremely labour intensive, makes this approach less favourable for extended studies. The final model known to express low dystrophin levels is the *mdx*^{3cv} mouse. Studies in the *mdx*^{3cv} mouse revealed that even ˜5% of dystrophin increased specific tetanic force and partly prevented against eccentric contractions induced damage in young but not in old mice. However, it was insufficient to prevent histopathology, since severity did not differ from dystrophin negative *mdx*^{4cv} mice (Li et al. 2008). Although *mdx*^{3cv} mice are easy to generate, dystrophin levels do not exceed 5%, making studies on the effect of higher dystrophin levels e.g. 20–30% impossible.

Taken together, these models give an indication that <50% dystrophin is sufficient for improvement of many pathological aspects, however, they are not ideal to assess the effects of low

dystrophin levels on disease pathology in detail. Our study describes a mouse model expressing low dystrophin levels, based on non-random X-inactivation. In mammals, X-inactivation is regulated by the X-inactivation center in which *Xist* is the key player (Brockdorff et al. 1991;Senner and Brockdorff 2009). Mutations in the *Xist* promoter can skew the randomness of X-inactivation resulting in preferential inactivation (60–90%) of the X-chromosome containing the mutated *Xist* gene (Newall et al. 2001). Here, non-dystrophic female *Xist*$^{\Delta hs}$ mice with a mutation in the *Xist* promoter were crossed with dystrophic *mdx* males. This resulted in female *mdx-Xist*$^{\Delta hs}$ mice in which the X-chromosome containing the wild type dystrophin is preferentially inactivated, leading to a wide range of low dystrophin levels in individual mice (Figure 1). Within individual muscle fibers of these pups, a mosaic pattern of dystrophin expression was observed, in which nuclei either did or did not express dystrophin. Experiments revealed that low dystrophin levels have a beneficial effect on muscle integrity, histology, function and serum biomarkers in a dose dependent manner.

Materials and methods

Ethics statement

All experiments were approved by and performed following the guidelines of the Dier Experimenten Commissie (Animal Experimental Commission) of the Leiden University Medical Center (Permit Numbers: 08096 and 09136). Effort was put in minimizing the amount of distress caused to the animals as much as possible.

Animal care

All studied mouse strains were bred at the animal facility of the LUMC where they were housed in individually ventilated cages with 12-h light-dark cycles. The *Xist*$^{\Delta hs}$ model (Newall et al. 2001) was a kind gift from Prof Brockdorff (MRC Clinical Sciences Centre London, UK, current affiliation Department of Biochemistry, University of Oxford, UK). Mice were given standard chow and water *ad libitum* and were weighed two times a week. Breeding pairs of *mdx* (C57BL/10ScSn-mdx/J) males and *Xist*$^{\Delta hs}$ females gave birth to *mdx-Xist*$^{\Delta hs}$ females (Figure 1A). Genotyping was performed on DNA obtained from tail tips by PCR analysis to confirm the mutation in the *Dmd* and *Xist* gene (primers and PCR conditions on request).

Functional test regimes

To test the functional abilities of the different mouse strains over time, a group of 5 *mdx*, 24 *mdx-Xist*$^{\Delta hs}$ (0–15% dys n = 9, 15–30% dys n = 9 and >30% n = 6, as assessed by Western blot of quadriceps muscles at the end of the study) and 5 *Xist*$^{\Delta hs}$ females underwent a functional test regime consisting of four different functional tests starting at four weeks of age, as described previously (van Putten et al. 2010). Plasma creatine kinase (CK) levels were determined once a week at the beginning of the functional test regime. Mice were sacrificed by cervical dislocation after 12 weeks of testing and muscles were isolated.

To determine whether functional test performances could be influenced by chronic treadmill exercise, 6 *mdx*, 7 *mdx-Xist*$^{\Delta hs}$ and 5C57BL/10ScSnJ four week old females had to run 30 minutes on a horizontal treadmill at 12 m/min, directly followed by either fore limb grip strength, rotarod running or the two limb hanging wire test three times a week for 12 weeks. CK levels were determined two times a week; on Mondays before exercise and on Fridays directly after the two limb hanging wire test. At the age of 8 and 14 weeks additional blood was collected via the tail to assess several serum biomarkers (MMP-9, TIMP-1 and OPN) of which we have

determined in parallel research that these correlate with disease severity (Nadarajah et al. 2011). After the 12 week chronic exercise protocol, mice were forced to run a final time on the horizontal treadmill for 30 minutes at 12 m/min. Evans blue dye (5 μg/μl) was applied intravenously (5 μl/gram of body weight) 20–30 minutes after this exercise. Twenty four hours after the injection, mice were sacrificed by cervical dislocation and muscles were isolated. Standardized operating procedures from the TREAT-NMD network were implemented for grip strength, both hanging wire tests and treadmill running (http://www.treat-nmd.eu/resources/research-resources/dmd-sops/).

Fore limb grip strength test

Fore limb grip strength was assessed by means of a grip strength meter (Columbus Instruments, USA). Mice were tested five times, with three consecutive measurements per trial (15 in total), and a two minute interval between trials. The three highest measured values were averaged to calculate the absolute strength, which was divided by the body weight in grams.

Rotarod

Mice were placed on the Rotarod (Ugo Basile, Italy) that accelerated from 5 to 45 rotations per minute within 15 seconds. The test session ended when a mouse ran for 500 seconds without falling. Mice that fell off before 500 seconds were given a maximum of two more tries. The longest running time was used for analysis.

Two limb hanging wire test

Mice were suspended above a metal cloth hanger secured above cage and released a few seconds after instinctively grasping the wire with the fore limbs. Depending on the functional ability of the mouse, 2–4 limbs and the tail were used during a 10 minute hanging session. Mice that fell down before the 10 minute time limit were given two more tries. The longest hanging time was used for further analysis.

Four limb hanging wire test

The start position of this test was with all limbs. To this end, mice were placed on a grid, which was then turned upside down above a cage filled with bedding. The session ended after a hanging time of 10 minutes was achieved or otherwise after three sessions. The longest hanging time was used for further analysis.

Blood CK, MMP-9, TIMP-1 and OPN level analysis

For CK determination, blood was collected via a small cut at the end of the tail in a Minicollect tube (0.8 ml Lithium Heparin Sep, Greiner bio-one, Austria). Plasma CK levels were determined with Reflotron CK test strips in the Reflotron plus machine (Roche diagnostics Ltd, UK) at the day of collection.

To detect MMP-9, TIMP-1 and OPN levels, blood was collected via the tail and allowed to clot at room temperature for 10 minutes before spinning (1700 *g* for 10 minutes at 4°C). The serum supernatant was carefully aspirated and stored at -80°C, before use. To determine serum biomarker levels in mouse, the mouse MMP-9 (total) immunoassay kit (catalog number MMPT90) and mouse TIMP-1 immunoassay kit (catalog number MTM100) were purchased from R&D systems (Abingdon, United Kingdom), while the mouse OPN kit (code number 7351) was purchased from IBL (Hamburg, Germany). Experiments were performed as per manufacturer's protocol.

Histological examinations

For all 16 week-old mice the quadriceps, gastrocnemius, tibialis nterior, triceps, biceps, diaphragm and heart were dissected and snap frozen in 2-methylbutane (Sigma Aldrich, the Netherlands) cooled in liquid nitrogen. Cross-sections of 8 μm were cut on Superfrost Plus slides (Thermo Fishes Scientific, Menzel-Gläser, Germany) with a Shandon cryotome (Thermo Fisher Scientific Co., USA) along the entire length of the muscle with an interval of 240 μm between the sections. The excess tissue between the sections was collected in MagNa Lyser Green Beads tubes (Roche diagnostics Ltd, UK) for total RNA and protein isolation.

To determine the percentage of fibrotic/necrotic fibers, sections of the quadriceps were stained with Harris Haematoxylin and Eosin (H&E) (Sigma Aldrich, the Netherlands) and examined with a light microscope (Leica DM LB, Leica Microsystems, the Netherlands) at a 5 times magnification and images were captured with a Leica DC500 camera and Leica IM50 software (Leica Microsystems, the Netherlands) from the entire middle section of the muscle. Analysis was performed in a double-blinded manner, by two independent researchers on stitched pictures with the color deconvolution plugin of the ImageJ software (Rasband, W.S., ImageJ, U. S. National Institutes of Health, Bethesda, Maryland, USA, http://rsb.info.nih.gov/ij/, 1997–2008) as described previously (van Putten et al. 2010). Quadriceps, tibialis anterior, diaphragm and heart sections were stained with dystrophin (C-20, dilution 1:50, Santa Cruz, Germany) and donkey-anti-goat Alexa 488 (dilution 1:1000, Invitrogen, the Netherlands) and mounted with Vectashield mounting medium including DAPI (Vector Labs, Germany). The percentage of dystrophin positive fibers was manually and independently counted by two persons in a blinded manner for the quadriceps, stained with dystrophin and laminin (ab11575, dilution 1:50 Abcam, UK) where donkey-anti-goat Alexa 488 and donkey-anti-rabbit Alexa 594 (dilution 1:1000, Invitrogen, the Netherlands) were respectively used as a secondary antibody. To determine the dystrophin expression per nucleus, longitudinal sections of the quadriceps were cut and stained with dystrophin, spectrin (dilution 1:200, Thermo Scientific, USA) and DAPI. Co-localization of dystrophin with nNOS (H-299, dilution 1:50, Santa Cruz, Germany) and β-dystroglycan (NCL b-DG, dilution 1:50, Novocastra, UK) was determined in the quadriceps. The donkey-anti-rabbit Alexa 488 (dilution 1:1000, Invitrogen, the Netherlands) and MOM kit (Vector Laboratories, UK) were used as secondary antibody respectively.

Fiber size and the percentage of centrally nucleated fibers were determined with Mayachitra Imago 1 (http://www.mayachitra.om/imago/) on five randomly captured images of the quadriceps stained with laminin and DAPI (van Putten et al. manuscript in preparation). Fibers were segmented based on intensity differences between the membrane and the cytoplasm. The cross sectional area of each segmented fiber was computed by the software. Centrally nucleated fibers were identified based on the maximum intensity of the cytoplasm which is higher in fibers with a centralized nucleus than without. The percentage of Evans blue dye positive fibers was manually counted in a blinded manner for the quadriceps of all mice which were subjected to the chronic treadmill exercise. All fluorescent stained sections were examined with a fluorescent microscope (Leica DM RA2) at a 16 times magnification and six images were randomly captured with a Leica DC350FX snapshot camera.

Western blot analysis

Muscles were homogenized in treatment buffer (100 mM Tris- HCl pH 6.8 and 25% SDS) using MagNa Lyser green beads tubes in the MagNa Lyser (Roche Diagnostics, the Netherlands). Protein concentration was determined using the BCA protein assay kit (Thermoscientific, USA), according to the manufacturer's instructions. Subsequently, the homogenate was complemented

to contain 75 mM Tris-HCl pH 6.8, 15% SDS, 5% β-mercaptoethanol, 20% glycerol and 0.001% bromophenol blue. Samples were boiled for 5 minutes and 50 µg was loaded on a hand-made 4–7% gradient polyacrylamide gel and run overnight at 4°C. The gel was blotted to nitrocellulose BA83 (Whatman, Schleicher & Schuell, Germany) for 6 hours at 4°C. The blot was blocked with 5% non-fat dried milk (Campina Melkunie, the Netherlands) in Tris Buffered Saline (TBS) plus 0.05% Tween20 followed by an overnight incubation with NCL-DYS1 (dilution 1:125, Novacastra, UK) or MANCHO3 (dilution 1:50,Tebu-bio, the Netherlands) in TBS plus 0.05% Tween20 to detect dystrophin and utrophin respectively. Myosin (MF20 dilution 1:20000, Developmental Studies Hybridoma Bank, University of Iowa, Iowa City) was used as a loading control. The fluorescent IRDye 800CW goat anti-mouse IgG (dilution 1:5000 for dystrophin and utrophin, dilution 1:10000 for myosin, Li-Cor, USA) was used as a secondary antibody. Blots were visualized and quantified with the Odyssey system and software (Li-Cor, USA) as described previously (Heemskerk et al. 2009). For each sample, 2–9 technical replicates were performed. A standard deviation of 15% was allowed between the replicates. RT-qPCR analysis Total RNA was isolated with RNA-Bee (Tel-Test, Bio-Connect, the Netherlands) and purified with the NucleoSpin RNA II kit including a DNAse digestion (Bioke, the Netherlands) according to the manufacturer's instructions. The RNA concentration was measured on a Nanodrop (Nanodrop Technologies, USA) and integrity was checked with a total RNA nano chip assay on a labchip assay (Agilent, the Netherlands). cDNA was synthesized with random hexamer primers and gene expression levels were determined by Sybr Green based Real Time qPCR (95°C 10 sec, 60°C 30 sec, 72°C 20 sec. 45 cycles followed by melting curve determination) on the Roche Lightcycler 480 (Roche diagnostics Ltd, UK). Expression of genes involved in inflammation (*Lgals3*,*Cd68*), fibrosis (*Tnnt2*, *Itgb2*, *Timp-1*, *Nox2*, *Lox*, *Nox4*, *Mmp9*, *Spp1*)regeneration (*Myog*, *Bgn*, *eMHC*, *Ctsk*, *Thymosinβ*), heart function (*Nppa*, *Serca2a*, *Cdnk1a*) and exercise (*Glut4*, *Pgc1α*) were analysed. Gapdh was used as a reference gene, since the expression of this gene did not differ between different muscles or over time. Primer efficiencies were determined with LinREgPCR version 11.1 (Raymackers et al. 2003). The C_p values were obtained with the second derivative maximum method and analysed.

Statistics

Statistical analyses were performed with statistical software in R (version R2.11.1). *Mdx-Xist*$^{\Delta hs}$ mice were divided in three groups by k-means clustering, based on the median level of dystrophin quantified by Western blot data (n =2–9). Figures 2, 5 and 6 summarize the data, i.e. showing the mean and standard deviation per genotype and age. To overcome applying separate tests for each age between genotypes, which suffers from multiple testing and ignores the age trend, we applied an analysis of covariance (ANCOVA) to the data. ANCOVA was applied to temporal functional performance, body weight and CK level data with age as continuous and genotype as a categorical variable. In choosing the appropriate model we applied the principle of parsimony. Given the application of tests for several different variables, we considered P<0.01 as significant.

The two-tailed homoscedastic Student's t-test was conducted for comparison of the single time point histological, serum biomarker and gene expression data. P<0.05 was considered significant for all tests, while P<0.01 was used for the gene expression data to correct for multiple testing.

Results

Mdx-Xist$^{\Delta hs}$ *mice express varying levels of dystrophin*

To study whether low dystrophin levels reduce the dystrophic pathology of *mdx* mice, *mdx-Xist*$^{\Delta hs}$ mice carrying a wide range of low dystrophin levels based on non-random X-inactivation were bred (Figure 1A). For each *mdx-Xist*$^{\Delta hs}$ mouse, dystrophin levels in the quadriceps muscle were quantified by Western blot (Figure 1B). These varied between 3–47% of wild type levels (mean 22.7, stdev 12.1, $n = 24$) (Figure 1C), which correlated well (R = 0.97) with the percentages of dystrophin positive fibers in cross sections of the same muscle, as assessed by blinded manual counting (Figure 1D). Dystrophin levels of individual muscles differed (assessed in $n = 6$ *mdx-Xist*$^{\Delta hs}$ mice), with the tibialis anterior and biceps expressing slightly higher levels than the quadriceps, gastrocnemius and triceps. Lowest dystrophin levels were found in the diaphragm and heart (Figure S1A–B). The dystrophin level of the quadriceps was used to group the mice. Longitudinal sections of the quadriceps revealed that dystrophin expression along a single whole fiber was patchy, with nuclei either expressing dystrophin or not (Figure 1E). This indicates that dystrophin proteins cannot freely diffuse along the muscle fiber and that nuclei where the normal *DMD* gene is not inactivated serve only certain regional domains in the muscle fiber. Transverse cross sections of several skeletal muscles and heart revealed that dystrophin positive fibers were most often grouped together and that these small groups were spread over the muscle (Figure S1C).

Dystrophin is part of a larger complex of dystrophin-glycoprotein associated proteins, such as β-dystroglycan and nNOS. As expected, dystrophin positive fibers of the *mdx-Xist*$^{\Delta hs}$ mice were also positive for β-dystroglycan and nNOS (Figure S2A). In absence of dystrophin, the homolog utrophin can partly take over its function. Muscles of adult *mdx* mice have significantly higher utrophin levels than those of adult C57BL/10ScSnJ, as utrophin is overexpressed in the absence of dystrophin (van Putten et al. 2012b). We assessed how dystrophin expression influences utrophin expression for six *mdx-Xist*$^{\Delta hs}$ mice expressing various levels of dystrophin. In *mdx-Xist*$^{\Delta hs}$ mice with very low dystrophin levels (<15%), utrophin levels were increased as confirmed by Western blot (Figure S2B, lane 2 and 6). In contrast, *mdx-Xist*$^{\Delta hs}$ mice with intermediate dystrophin levels (>15%) had low utrophin levels (lanes 1, 3–5). We did not observe a decrease in utrophin intensity in dystrophin positive fibers analyzed by immunohistology (data not shown).

Dystrophin level dependent improvement in muscle function

To determine the effect of low dystrophin levels on functional performance, *Xist*$^{\Delta hs}$, *mdx* and *mdx-Xist*$^{\Delta hs}$ mice were subjected to a functional test regime consisting of four functional tests per week for 12 weeks, during which also body weight and creatine kinase (CK) levels were monitored. After sacrificing, quadriceps muscles were isolated and dystrophin levels were determined by Western blot. K-means clustering was used to divide *mdx-Xist*$^{\Delta hs}$ mice into three groups in an unbiased way. This resulted in the following division: <15%, 15–30% and >30% dystrophin. *Mdx* mice were significantly ($P<0.001$) heavier at the end of the functional test regime than the other mouse strains (mean weight 26, 24.5 and 18.2 gram for *mdx*, *mdx-Xist*$^{\Delta hs}$ and *Xist*$^{\Delta hs}$, respectively). An increased weight compared to wild type has been described before for *mdx* mice (Spurney et al. 2009). *Xist*$^{\Delta hs}$ mice had a stable body weight from week 11 onwards, while the other models showed a mild increase overtime. The body weights of the *mdx-Xist*$^{\Delta hs}$ mice from the three dystrophin level groups were very similar and fell in between *mdx* and *Xist*$^{\Delta hs}$ mice, but significantly ($P<0.001$) differed from both (Figure 2A).

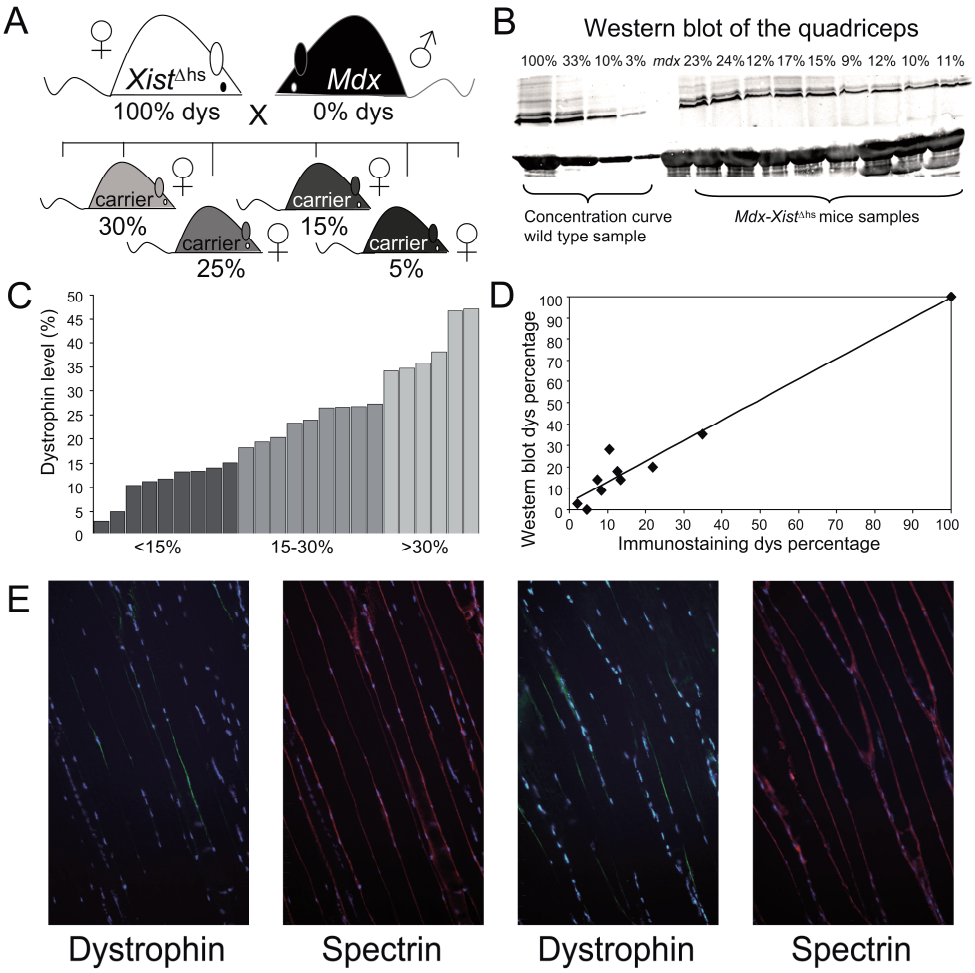


Figure 1. *Mdx-Xist*$^{\Delta hs}$ mice. A. To breed mice with low dystrophin levels, female *Xist*$^{\Delta hs}$ mice, carrying a mutation in the *Xist* promoter which coordinates X-inactivation, were crossed with dystrophin negative *mdx* males. During embryogenesis, the maternal X-chromosome encoding a functional dystrophin gene will be preferentially (60–90%) inactivated as a result of the mutated *Xist* promoter. The *Xist*$^{\Delta hs}$ mice were a kind gift from N. Brockdorff (MRC Clinical Sciences Center, London, UK, current affiliation Department of Biochemistry, University of Oxford, UK). **B**. Picture of a representative Western blot. The percentage of dystrophin was determined for the quadriceps of all *mdx-Xist*$^{\Delta hs}$ mice by Western blot (2–9 technical replicates per mouse). The percentage of individual mice was determined using a concentration curve made from wild type samples. Myosin was used as a loading control. **C**. Skewed X-inactivation resulted in dystrophin levels of 3–47% (mean 22.7, stdev 12.1, $n = 24$) (as determined by Western blot) in the female *mdx-Xist*$^{\Delta hs}$ offspring. Each bar represents the dystrophin level of an individual mouse. The dystrophin levels of the individual mice belonging to the three dystrophin groups can be appreciated from this graph. **D**. Dystrophin levels determined by Western blot and manual counting of dystrophin positive fibers demonstrate a strong correlation (R = 0.97). **E**. Longitudinal sections of a quadriceps stained with dystrophin (green) and spectrin (red). From the pictures it can be appreciated that dystrophin expression is not homogeneously expressed across the fiber but rather confined to certain nuclear domains.

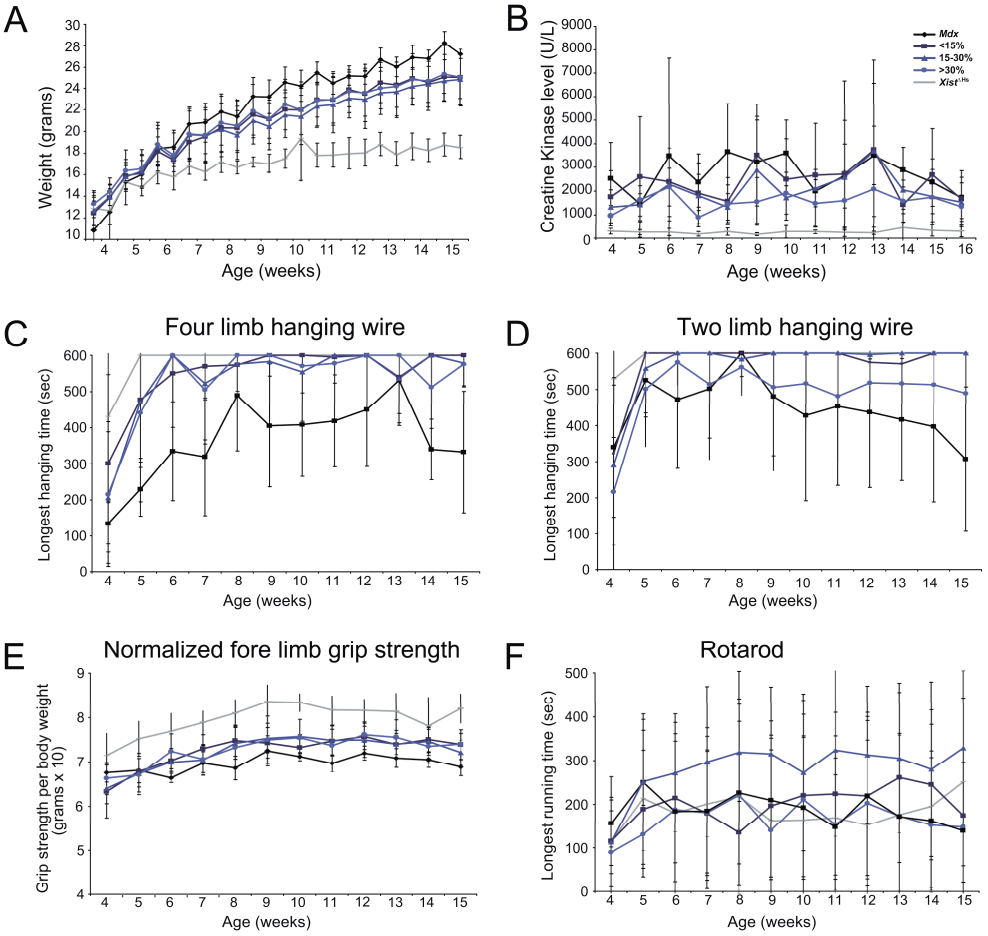


Figure 2. Body weight, CK levels and functional performance of the mouse models. A. Normalization towards wild type levels was observed for bodyweight of the *mdx-Xist*$^{\Delta hs}$ mice. At the end of the functional test regime *mdx* mice were significantly heavier (P<0.001) than the other mice. **B**. CK levels of *mdx* and *mdx-Xist*$^{\Delta hs}$ mice with low dystrophin levels were both significantly (P<0.001) higher compared to the levels of *mdx-Xist*$^{\Delta hs}$ mice with >30% dystrophin and *Xist*$^{\Delta hs}$ mice. **C**. Four limb hanging wire performance was comparable for the *Xist*$^{\Delta hs}$ and *mdx-Xist*$^{\Delta hs}$ mice, while *mdx* mice performed significantly (P<0.001) worse. **D**. The best performance on the two limb hanging wire test was obtained for the *Xist*$^{\Delta hs}$, *mdx-Xist*$^{\Delta hs}$ with <15% and 15–30% while the *mdx* and *mdx-Xist*$^{\Delta hs}$ with >30% dystrophin performed significantly (P<0.001) worse. Bad performance of *mdx-Xist*$^{\Delta hs}$ with >30% was due to the bad performance of one individual mouse. **E**. Normalized fore limb grip strength was significantly (P<0.001) higher in the *Xist*$^{\Delta hs}$ mice compared to the other strains and all the *mdx-Xist*$^{\Delta hs}$ mice were significantly (P<0.001) stronger than the *mdx* mice. **F**. No difference in rotarod running was observed, except for the *mdx-Xist*$^{\Delta hs}$ mice with 15–30% dystrophin, which performed significantly (P<0.001) better than all other groups.

CK levels are a measure for muscle condition and are <500 U/L in healthy mice. CK levels of the *Xist*$^{\Delta hs}$ mice never exceeded this threshold and were, averaging 270 U/L, significantly (P<0.001) lower than levels of the other mouse strains. *Mdx* mice had the highest CK levels (average 2700 U/L). When analyzed over the complete time course, these were significantly (P<0.001, linear regression) higher than those of *mdx-Xist*$^{\Delta hs}$ mice with >30% dystrophin (average 1570 U/L). CK levels of mice with 15–30% dystrophin generally fell between those with <15% and >30%, showing a clear correlation between CK and dystrophin levels. CK levels of mice with <15% of dystrophin were similar to *mdx* suggesting that these dystrophin levels were not enough to decrease CK levels (Figure 2B).

In the four limb hanging wire test, *mdx* mice performed significantly (P<0.001) worse compared to all the other groups (Figure 2C). *Xist*$^{\Delta hs}$ mice were able to hang for the maximum period of time for the entire testing period of 12 weeks, whereas all *mdx-Xist*$^{\Delta hs}$ mice performed nearly as well as *Xist*$^{\Delta hs}$ mice. Also in the two limb hanging wire test, *Xist*$^{\Delta hs}$ and *mdx-Xist*$^{\Delta hs}$ mice significantly (P<0.001) outperformed *mdx* mice and were able to hang for the maximum allowed time. Performance of *mdx-Xist*$^{\Delta hs}$ mice with >30% dystrophin dropped from an age of 9 weeks compared to the other *mdx-Xist*$^{\Delta hs}$ mice, but this was due to the poor performance of a single mouse. Generally, the decreased performance was more pronounced in *mdx* mice (Figure 2D). The normalized fore limb grip strength measured for *Xist*$^{\Delta hs}$ mice (7.9) was significantly (P<0.001) higher than that of *mdx* and *mdx-Xist*$^{\Delta hs}$ mice (Figure 2E). Strength was improved towards wild type levels in all *mdx-Xist*$^{\Delta hs}$ mice (6.5) and significantly (P<0.001) lower in *mdx* mice (5.9). Rotarod performance was significantly (P<0.001) better in the *mdx-Xist*$^{\Delta hs}$ mice with 15–30% dystrophin compared to all the other groups (Figure 2F). Unfortunately, we observed a high inter group variation, which makes drawing conclusions difficult for this test. Based on these analyses, even the lowest levels of dystrophin analyzed (between 3 and 14%), appear sufficient to improve hanging times and grip strength.

Dystrophin dependent improvement of histopathology and restoration of gene expression

After sacrificing the animals, the quadriceps, heart and diaphragm were dissected and cryosections were made. To determine fiber size and the percentage of centralized nuclei, the quadriceps of all mice was stained with laminin and DAPI. Five pictures were randomly captured of the middle section of the muscle and analysed with Mayachitra Imago (Figure 3A and B). Regenerating fibers (<1000 μm^2) and hypertrophic fibers (>6000 μm^2) were predominantly found in the *mdx* mice (50% and 4.8%, respectively), whereas smaller proportions were observed for the *Xist*$^{\Delta hs}$ mice (20% and 0.9%, respectively) and a dystrophin level dependent normalization towards the wild type fiber size distribution was observed for *mdx-Xist*$^{\Delta hs}$ mice. The percentage of centralized nucleated fibers was significantly higher (P<0.01) in *mdx* (51%) compared to *Xist*$^{\Delta hs}$ mice (2%). More than 15% of dystrophin was sufficient to significantly (P<0.01) reduce the amount of centralized nuclei by 40%, whereas dystrophin levels above 30% caused a reduction of around 60%.

To determine the percentage of fibrotic/necrotic fibers, sections of the quadriceps, diaphragm and heart were stained with haematoxylin & eosin. For all muscles quantified, except heart, the percentage of fibrosis was significantly higher (P<0.001) in *mdx* mice compared to *Xist*$^{\Delta hs}$ mice. In the quadriceps of *mdx-Xist*$^{\Delta hs}$ mice of the different groups no significant differences was observed, although there appears to be a dystrophin-dependent trend towards lower levels of fibrosis in the mice with moderate levels of dystrophin (Figure 3C).

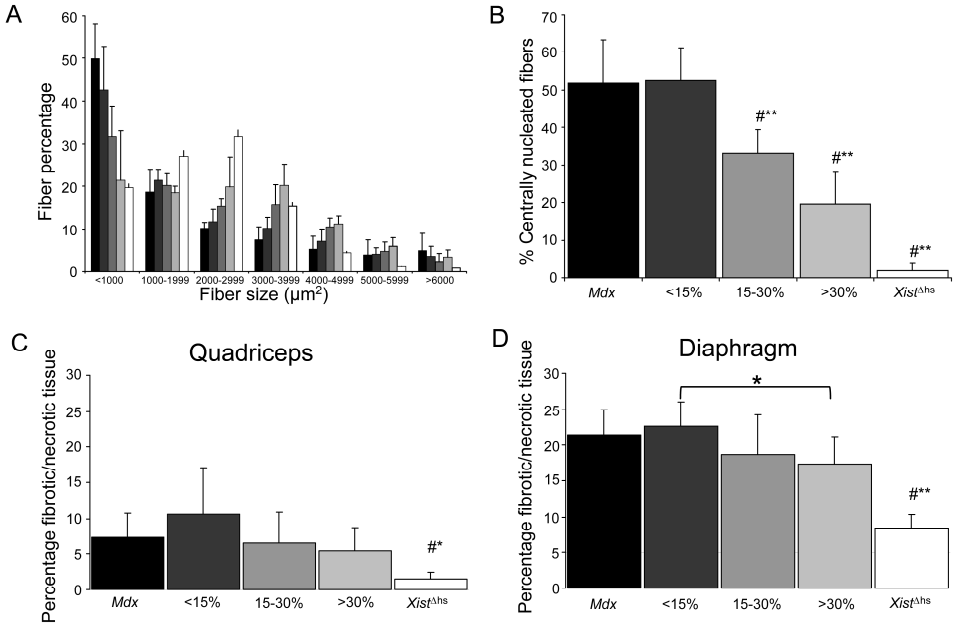


Figure 3. Muscle fiber size, degree of central nucleation and percentage of fibrotic/necrotic tissue. A. Regenerating and hypertrophic fibers were mainly observed in the *mdx* mice. A dystrophin level depend trend towards wild type distribution was observed for *mdx-Xist*$^{\Delta hs}$ mice where <15% dystrophin already resulted in improvement. **B**. Dystrophin levels between 15–30% and >30% resulted in a reduction of the percentage of centralized nuclei of 40% and 60% respectively. **C**. The quadriceps of all mice was significantly more severely affected compared to *Xist*$^{\Delta hs}$ mice. **D**. The diaphragm was the most severely affected muscle with on average 20% fibrotic/necrotic tissue in *mdx* mice. All mice were significantly more severely affected compared to *Xist*$^{\Delta hs}$ mice. *Mdx-Xist*$^{\Delta hs}$ mice with >30% dystrophin had less fibrotic/necrotic tissue than *mdx* and *mdx-Xist*$^{\Delta hs}$ mice with <15% dystrophin, but this difference was only significant between both *mdx-Xist*$^{\Delta hs}$ groups. # indicates a significant difference of that bar with all the other groups. Single asterisks indicate a $P<0.05$ and double asterisks indicate a $P<0.01$.

The diaphragm was the most severely affected muscle examined, with fibrotic/necrotic tissue percentages of 20% in both *mdx* and *mdx-Xist*$^{\Delta hs}$ mice with <15% dystrophin compared to 8% in *Xist*$^{\Delta hs}$ mice. Again, there was a dystrophin-level dependent pattern of reduced fibrotic tissue which reached significance ($P<0.05$) in mice with >30% dystrophin (Figure 3D). Fibrosis/necrosis levels in heart were below 5% in all mice, which is expected, as fibrosis in heart generally is observed in older mice (data not shown) (van Erp et al. 2010).

To determine whether low levels of dystrophin were able to normalize the expression of genes known to be involved in inflammation, fibrosis, regeneration and heart function RT-qPCR was performed on mRNA of the quadriceps, diaphragm and heart of all mice (Turk et al. 2005). The expression of most genes was significantly ($P<0.01$) elevated in *mdx* mice compared to *Xist*$^{\Delta hs}$ mice in the three muscles, and most often normalized in a dystrophin level dependent manner in the *mdx-Xist*$^{\Delta hs}$ mice (Figure 4). Notably, in the diaphragm, mRNA levels of the biomarkers for muscle regeneration (*Tnnt2*, *Bgn*) decreased in mice with <15% dystrophin, while biomarkers for inflammation (*Lgals3*, *Cd68*) only decreased in mice with >30% dystrophin. Biomarkers for fibrosis (*Timp-1*, *Nox2*) decreased in mice with <15% and >15% dystrophin, respectively. No difference in expression of heart function genes was observed, except for *Nppa*, which is due to the young age of the mice.

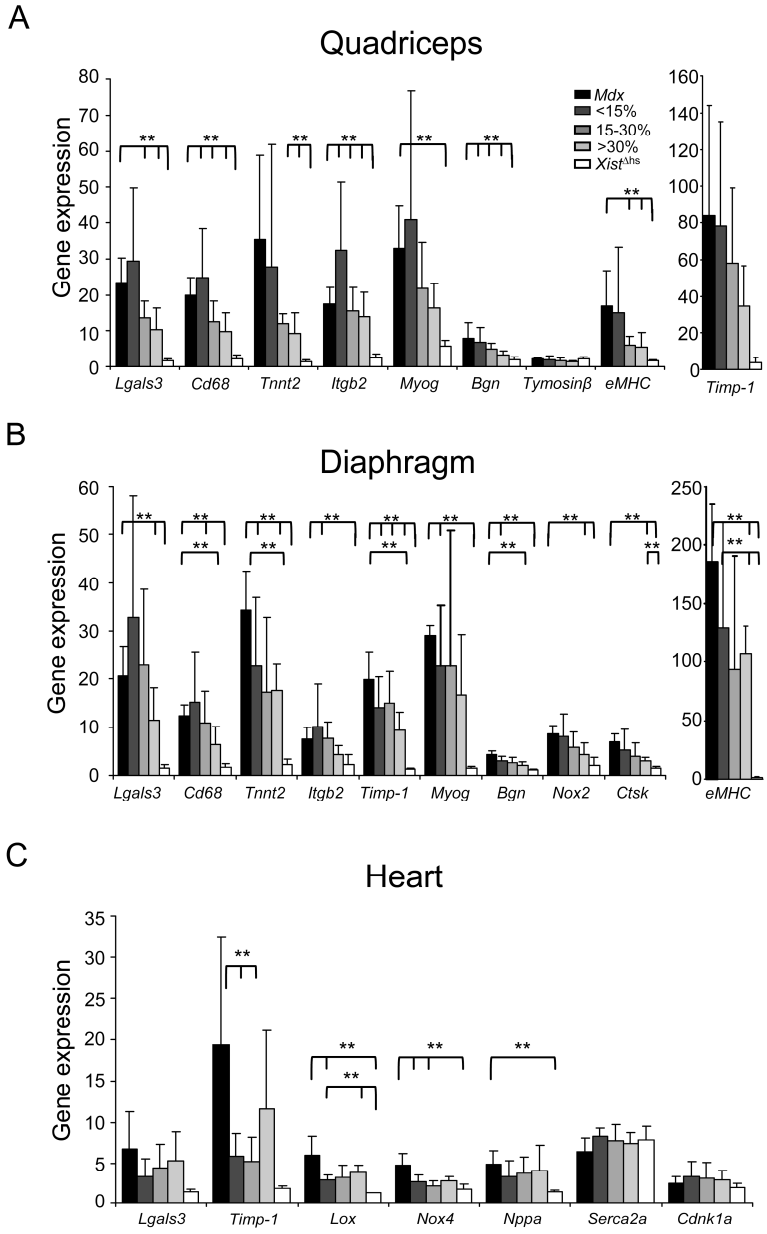


Figure 4. Expression of several genes involved in disease pathology. **A and B**. For most biomarkers a clear dystrophin level dependent restoration of gene expression levels was observed in the *mdx-Xist*$^{\Delta hs}$ mice, where intermediate dystrophin levels resulted in low expression of genes involved in disease pathology. For some genes, dystrophin levels <15% were enough to reduce gene expression while for other genes >30% was necessary. **C**. In the heart, even dystrophin levels of <15% decreased expression of fibrotic biomarkers like *Timp-1*. Since the mice were young, no difference in expression levels in heart function was observed, except for *Nppa*. Double asterisks indicate a $P<0.01$.

Dystrophin level dependent protection against exercise induced muscle damage

To determine the protective effect of low dystrophin levels on muscle integrity during chronic exercise, mice were forced to run three times a week on a horizontal treadmill. This was directly followed by a functional test to assess the influence of muscle fatigue on performance. We tested seven *mdx-Xist*$^{\Delta hs}$ mice which had an average dystrophin level of 21% (2%–45% median 25.8), six *mdx* and five C57BL/10ScSnJ females (the wild type sub-strain from which the *mdx* mouse was derived).

CK levels were assessed on Mondays before exercise (Figure 5B) and on Fridays directly after exercise (Figure 5C). For *mdx* and *mdx-Xist*$^{\Delta hs}$ mice CK levels increased significantly (P<0.01) upon exercise (4150 U/L before versus 11170 U/L after for *mdx* and 2070 U/L before versus 8850 U/L after for *mdx-Xist*$^{\Delta hs}$), whereas this was not observed for the wild type mice (250 U/L before versus 291 U/L after) (Figure 5A). CK levels of the *mdx-Xist*$^{\Delta hs}$ mice were significantly (P<0.05) lower compared to *mdx*, both before and after exercise. Wild type mice had significantly (P<0.01) lower CK levels than those of *mdx* and *mdx-Xist*$^{\Delta hs}$ mice. *Mdx-Xist*$^{\Delta hs}$ mice gained significantly (P<0.01) less weight over time than *mdx* mice, as they had a higher body weight at the start, but a similar body weight at the end of the test regime (data not shown). Wild type mice were significantly (P<0.01) less heavy than *mdx* mice, but did not significantly differ in weight from the *mdx-Xist*$^{\Delta hs}$ mice.

At an age of 8 and 14 weeks, serum levels of matrix metalloproteinase-9 (MMP-9), tissue inhibitors of matrix metalloproteinase-1 (TIMP-1) and osteopontin (OPN) were assessed. These markers have been identified as potential biomarkers to monitor disease progression in DMD patients (Nadarajah et al. 2011). For MMP-9, 8 week old *mdx* mice had significantly (P<0.05) higher levels when compared to wild type and *mdx-Xist*$^{\Delta hs}$ mice (Figure 5D).

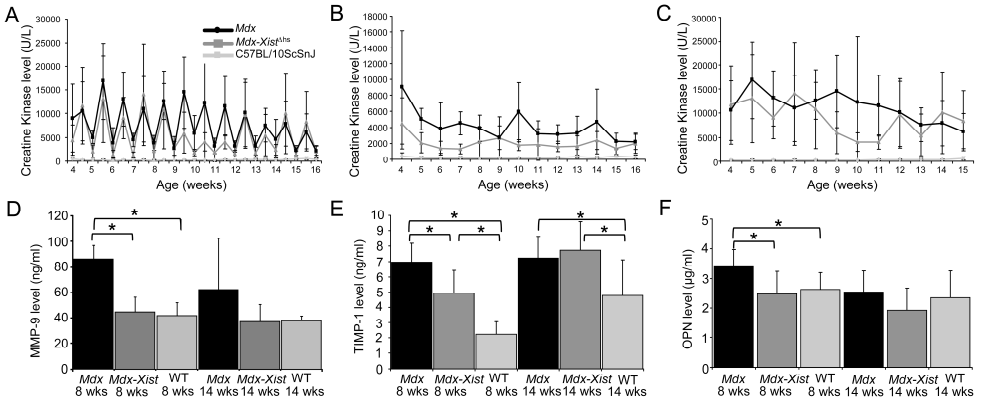


Figure 5. Serum and plasma biomarkers assessed before and directly after treadmill running. **A**. CK levels assessed before and directly after treadmill running. CK levels collected before exercise were significantly (P<0.01) lower than those collected directly after exercise in *mdx-Xist*$^{\Delta hs}$ and *mdx* mice. This exercise induced increase was absent in wild type mice. **B**. CK levels determined before exercise were significantly (P<0.01) elevated in *mdx* and *mdx-Xist*$^{\Delta hs}$ mice compared to wild type, but this was less pronounced for the *mdx-Xist*$^{\Delta hs}$ mice as *mdx* mice had significantly (P<0.05) higher CK levels. **C**. Plasma collected directly after exercise contained extremely high CK levels, in both *mdx* and *mdx-Xist*$^{\Delta hs}$ mice but not in wild type mice. **D**. Serum levels of MMP-9 were elevated in *mdx* mice compared to *Xist*$^{\Delta hs}$ mice at both 8 and 14 weeks of age, while levels were normalized in *mdx-Xist*$^{\Delta hs}$ mice. **E**. TIMP-1 levels were elevated in serum of both *mdx* and *mdx-Xist*$^{\Delta hs}$ mice. In wild type mice we found an age related increase of the serum TIMP-1 level. Interestingly, at the age of 8 weeks, levels of *mdx-Xist*$^{\Delta hs}$ mice were significantly lower than those of *mdx* mice. **F**. *Mdx* mice had significantly elevated OPN levels compared to both wild type and *mdx-Xist*$^{\Delta hs}$ at 8 weeks of age. Single asterisks indicate a P<0.05, average dystrophin level of *mdx-Xist*$^{\Delta hs}$ mice was 21% (2%–45% median 25.8).

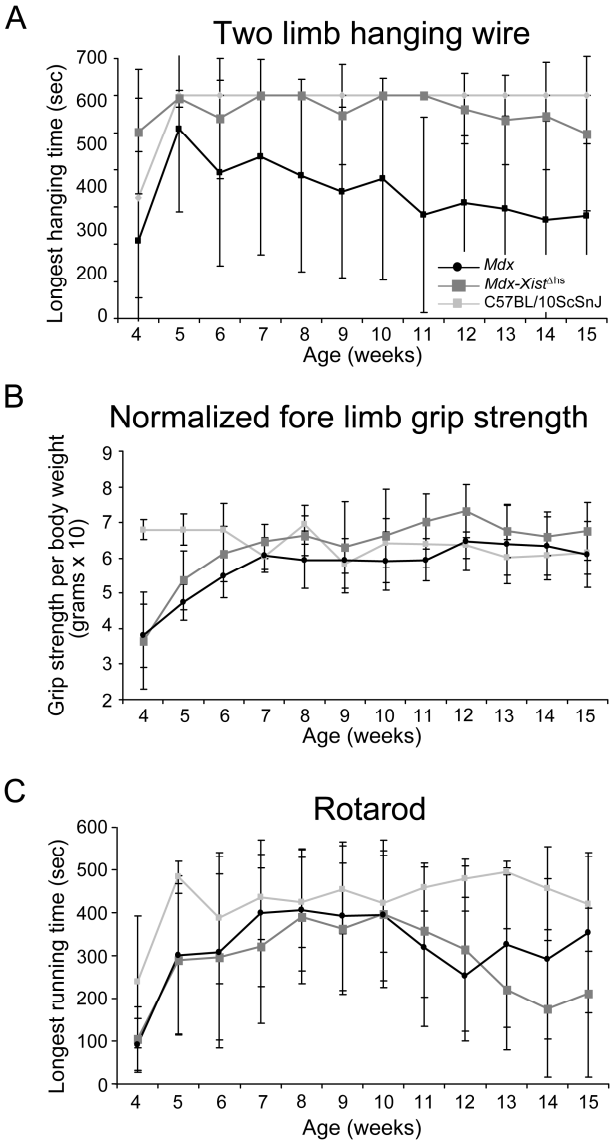


Figure 6. Functional performance measured directly after treadmill exercise. A. Longest hanging time with the two limb hanging test was achieved by wild type and *mdx-Xist*$^{\Delta hs}$ mice which both performed significantly (P<0.001) better than *mdx* mice. **B**. Fore limb grip strength of *mdx-Xist*$^{\Delta hs}$ mice was significantly (P<0.001) better than that of *mdx* mice. **C**. Wild type mice outperformed *mdx* and *mdx-Xist*$^{\Delta hs}$ mice on the rotarod, while no significant difference was observed between *mdx* and *mdx-Xist*$^{\Delta hs}$ mice. Average dystrophin level of *mdx-Xist*$^{\Delta hs}$ mice was 21% (2%–45% median 25.8).

No significant difference was observed between *mdx-Xist*$^{\Delta hs}$ and wild type mice. TIMP-1 levels were significantly (P<0.05) elevated in both *mdx* and *mdx-Xist*$^{\Delta hs}$ mice compared to wild type mice at the age of 8 and 14 weeks (Figure 5E). Interestingly, a significant (P<0.05) difference was also observed between *mdx* and *mdx-Xist*$^{\Delta hs}$ mice aged 8 weeks. OPN levels were significantly (P<0.05) elevated in *mdx* compared to both wild type and *mdx-Xist*$^{\Delta hs}$ at 8 weeks. This difference was not observed at 14 weeks of age (Figure 5F).

The chronic treadmill exercise protocol was completed by all mice without any problems. However, we later found that fibrosis was much worse in these exercised mice and that the low dystrophin levels were not enough to prevent worsening of the muscle's condition (see below). Directly after treadmill exercise, mice were subjected to two limb hanging wire test, fore limb grip strength or rotarod (Figure 6). For the two limb hanging wire test, the hanging time of

mdx mice decreased over time, and was significantly (P<0.001) lower than those of the *mdx-Xist*$^{\Delta hs}$ and wild type mice. The hanging time of the *mdx-Xist*$^{\Delta hs}$ and wild type mice did not differ significantly. Performance of the grip strength was consistently lower for the *mdx* mice (5.8) than for the other groups (*mdx-Xist*$^{\Delta hs}$ 6.3 and wild type 6.4). Wild type mice performed well at the start of the functional test regime, but their strength slightly decreased over time. Grip strength of *mdx* and *mdx-Xist*$^{\Delta hs}$ mice followed the same curve, and *mdx-Xist*$^{\Delta hs}$ mice performed significantly (P<0.001) better than *mdx* mice. Rotarod running time was significantly (P<0.001) higher in the wild type mice with an average running time of 430 seconds, which was generally 130 seconds longer than that of both dystrophic mouse strains. The performance of *mdx* and *mdx-Xist*$^{\Delta hs}$ mice did not significantly differ for this test.

Low dystrophin levels did not fully prevent exercise induced pathology

The effect of the chronic exercise regime on histopathology was assessed by measuring the percentage of fibrotic/necrotic tissue for the quadriceps. On average, 18% of the quadriceps of the *mdx* mice consisted of fibrotic/necrotic tissue, compared to less than 5% for wild type mice. *Mdx-Xist*$^{\Delta hs}$ mice had slightly more healthy tissue than *mdx* mice (Figure 7A). When compared to fibrosis observed in mice which underwent the functional test regime without treadmill running, histopathology was much worse. At the end of the chronic exercise regime, Evans blue dye was injected intravenously and the percentage of Evans blue dye positive fibers was manually counted for the quadriceps of all mice. Hardly any Evans blue dye positive fibers were detected in wild type muscle (0.41%), while both in *mdx* and *mdx-Xist*$^{\Delta hs}$ mice 11.11% and 9.23% of positive fibers were found. This suggests that while low dystrophin levels are sufficient to improve muscle function and muscle fiber integrity in the absence of chronic exercise, they apparently are not sufficient to protect against fiber damage induced by the chronic treadmill exercise regime.

The expression of some fibrosis, inflammation and regeneration biomarkers was assessed for the quadriceps. For most genes, *mdx* and *mdx-Xist*$^{\Delta hs}$ mice had significantly (P<0.05) increased expression when compared to wild type levels. However, between *mdx* and *mdx-Xist*$^{\Delta hs}$ mice no difference in expression was observed indicating that the dystrophin levels in these mice were not sufficient to prevent pathology induced by chronic exercise (Figure 7B). In addition, we were able to confirm the differences observed in serum for MMP-9, TIMP-1 and OPN (*Spp1*) on gene expression level.

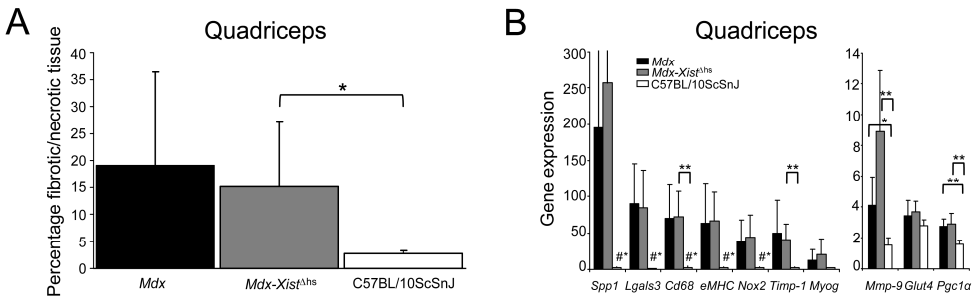


Figure 7. Exercise induced histopathology and biomarker gene expression. A. Wild type mice were less severely affected than *mdx* and *mdx-Xist*$^{\Delta hs}$ mice. Due to high variation between individual *mdx* mice, the difference between *mdx* and wild type mice was not significant. *Mdx-Xist*$^{\Delta hs}$ mice had slightly less fibrotic tissue than *mdx* mice. **B**. No difference in expression of genes involved in disease pathology was found between *mdx* and *mdx-Xist*$^{\Delta hs}$ mice. Both mouse strains did differ significantly from wild type mice, of which the expression levels were low. Single and double asterisks indicate a P<0.05 and P<0.01, respectively. # Indicates a significant difference from all other groups, average dystrophin levels of *mdx-Xist*$^{\Delta hs}$ mice was 21% (2%–45% median 25.8).

Discussion

With several potential therapeutic compounds being tested in clinical settings for DMD, there is an increasing need to gain detailed knowledge about which levels of dystrophin are of therapeutic value and which and/or how low dystrophin levels affect the different pathological pathways. This would help the optimization phase of pre-clinical research on therapeutic approaches aiming at dystrophin restoration. It will also facilitate providing patients and parents who are candidates to participate in clinical trials for these approaches with realistic expectations.

Several attempts to generate mice expressing low dystrophin levels have been undertaken previously, unfortunately without success since none of these strains expressed a wide variety of low dystrophin levels in the most interesting range. With no accessibility to a good model, current knowledge and rough estimations are based on human female DMD carriers, heterozygous *mdx* mice, generated transgenic mice expressing lower levels of full-length or truncated dystrophin of murine or human origin and antisense oligonucleotide (AON) treated *mdx* mice.

In this paper, we describe the easy to generate *mdx-Xist*$^{\Delta hs}$ mouse model, which facilitates assessment of the effects of different dystrophin levels on muscle performance and integrity. Mice with very low (<15%), low (15–30%) and moderate dystrophin (>30%) levels showed a dystrophin level dependent reduction of the homolog utrophin. All *mdx-Xist*$^{\Delta hs}$ mice had a normalized body weight and outperformed *mdx* mice in both hanging wire tests and in the grip strength test, indicating that even low dystrophin levels (<15%) can bring about improved performance in this mouse model. The improved functional performance observed is in concordance with that previously described in *mdx*^{3cv} mice and AON treated mice expressing low levels of dystrophin (Li et al. 2008;Sharp et al. 2011). Although, ~5% of dystrophin in the *mdx*^{3cv} mice resulted in increased specific tetanic force and partly resistance to eccentric contractions in young, but not in old mice, histopathology was not different from dystrophin negative *mdx*^{4cv} mice. This again is in line with our observation in *mdx-Xist*$^{\Delta hs}$ mice expressing <15% dystrophin, were we also found no histopathological improvements, while we did find improvements on motor function. Dystrophin levels >30% reduced CK levels significantly while for lower percentages only a non-significant trend was found. Also for the expression of pro-inflammatory biomarkers and histopathology, a dystrophin level dependent improvement was observed where for some genes >15% of dystrophin led to improvement while for other genes >30% dystrophin was needed. In chronically exercised mice with ~20% dystrophin, normalization towards wild type levels was observed for three different disease serum markers (CK, MMP-9 and TIMP-1). This confirms findings that MMP-9 and TIMP-1 are useful serum biomarkers to monitor disease pathology in DMD patients' serum (Nadarajah et al. 2011). Even after treadmill exercise the *mdx-Xist*$^{\Delta hs}$ mice performed significantly better than the *mdx* mice for the two limb hanging wire test and grip strength. However, the levels of fibrosis and Evans blue dye uptake were similar for *mdx-Xist*$^{\Delta hs}$ mice and *mdx* mice, indicating that ~20% of dystrophin is not sufficient to protect against forced exercise induced damage. Thus, while even dystrophin levels below 15% can improve pathology and performance, levels of >20% are needed to fully protect muscle fibers from exercise- induced damage.

The fact that most of our observations concur with those of other studies conducted in transgenic mice and AON treated mice confirms the usefulness of the *mdx-Xist*$^{\Delta hs}$ mouse as a dystrophic mouse strain. It should be noted that the *mdx-Xist*$^{\Delta hs}$ mouse expresses dystrophin in a random manner where nuclei either express wild type levels of dystrophin or no dystrophin at all. This is similar to the pattern what is expected for cell therapy, gene therapy and to what is observed in transverse cross sections after phosphorodiamidate morpholino oligomer (PMO)

administration (Cirak et al. 2011), but different from that of 2'-O-methyl phosphorothioate (2OMePS) (Goemans et al. 2011) or gentamicin administration (Malik et al. 2010), which result in a more evenly low dystrophin expression in nearly all fibers. With detailed knowledge lacking regarding the migration properties of AONs and dystrophin over the membrane, it is unknown whether the mosaic pattern seen in longitudinal cross sections of *mdx-Xist*$^{\Delta hs}$ mice could be expected upon PMO administration. The effect of differences in distribution of dystrophin has never been studied in great detail; i.e. whether 20% of dystrophin in all muscles is better than 100% dystrophin in 20% of muscle fibers. Previously, Phelps et al. showed that mice expressing dystrophin 10-fold greater than wild type levels in a mosaic manner had 34% of centralized nuclei, while mice expressing similar amounts uniformly only had 7% of central nuclei. More detailed studies especially in mice expressing low dystrophin levels are needed and could easily be conducted using our mouse model and comparing them to 2OMePS or gentamicin treated *mdx* mice (Phelps et al. 1995). Using the *mdx-Xist*$^{\Delta hs}$ mouse as study object is favored above treated *mdx* mice since no expensive treatment is needed to achieve a range of low dystrophin levels. Notably, we observed variation in pathology for mice with similar levels of dystrophin. This phenomenon is also anticipated for patients currently in clinical trials aiming at dystrophin restoration. Our mouse model will allow extended studies to elucidate this discrepancy.

In summary, the Gaussian distribution of low dystrophin levels obtained in the *mdx-Xist*$^{\Delta hs}$ mouse and the ease of generating large numbers of mice, make it a good mouse model for more detailed research on the effect of low levels of dystrophin on several aspects of DMD pathology and effects of future treatment strategies for dystrophinopathies.

Acknowledgments

We thank prof. Dr. Brockdorff and Tatyana Nesterova (MRC Clinical Sciences Center, London, UK, current affiliation Department of Biochemistry, University of Oxford, UK) for the *Xist*$^{\Delta hs}$ embryos and help with genotyping the mice. We thank Gert-Jan van Ommen for useful discussions and critically reading the manuscript. We are grateful to Jiyun Byun for her expert assistance with Mayachitra Imago.

Author Contributions

Conceived and designed the experiments: JTDD AAR PACH. Performed the experiments: MVP MH VDN SHVH EVH TM. Analyzed the data: MVP MVI PA. Contributed reagents/materials/analysis tools: MVI PA. Wrote the paper: MVP PACH AAR.

Supporting information

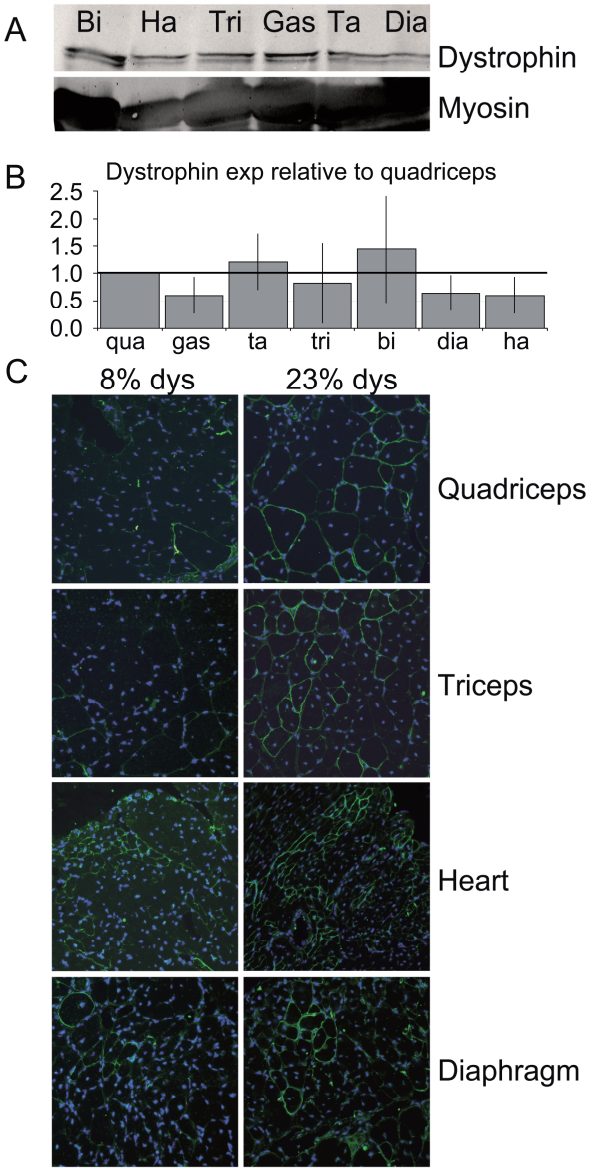


Figure S1 Dystrophin expression in *mdx-Xist*$^{\Delta hs}$ mice. A. Example of a Western blot of some skeletal muscles and heart. In order to determine the expression levels of the different muscles, a concentration curve was made of wild type samples from the corresponding muscle. Myosin was used as a loading control. **B**. Relative dystrophin levels of skeletal muscles compared to these of the quadriceps. Dystrophin levels of six *mdx-Xist*$^{\Delta hs}$ mice, with dystrophin levels of <15%, 15–30% and >30%, were assessed for skeletal muscles and heart by Western blot. Levels are expressed relative to the quadriceps. Those of gastrocnemius and triceps were similar to quadriceps levels, while those of the tibialis anterior and the biceps were slightly higher. Low levels were observed for the diaphragm and heart. qua: quadriceps, gas: gastrocnemius, ta: tibialis anterior, tri: triceps, bi: biceps, dia: diaphragm, ha: heart. **C**. Small groups of dystrophin positive fibers were randomly distributed over the muscles. Representative pictures of *mdx-Xist*$^{\Delta hs}$ mice with 8 and 23% dystrophin.

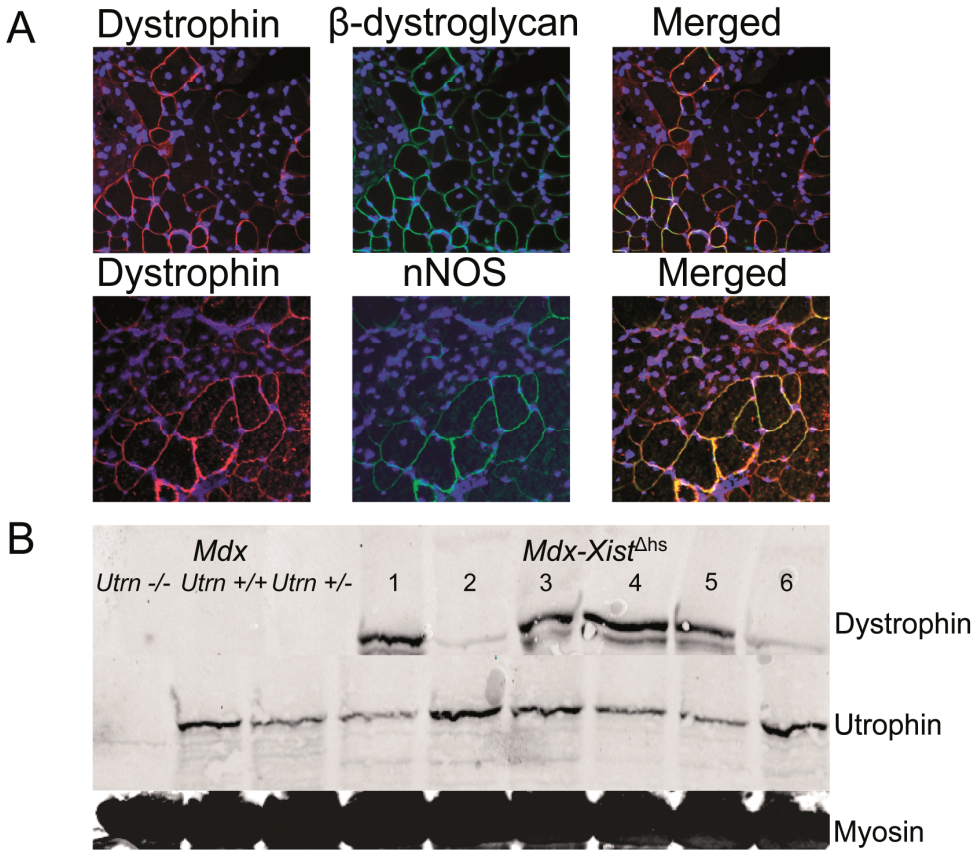


Figure S2 Dystrophin co-localisation with β-dystroglycan and nNOS in *mdx-Xist*$^{\Delta hs}$ mice. A. Dystrophin co- localises with β-dystroglycan (top) and nNOS (bottom). **B**. For *mdx-Xist*$^{\Delta hs}$ mice dystrophin levels previously determined on several Western blots (representative blot shown in Figure 1B) were compared to utrophin levels. The relative level of utrophin nicely correlated to that of dystrophin. Mice with intermediate dystrophin levels had decreased utrophin levels (lane 2 and 6) while mice with low dystrophin levels had higher utrophin levels (lane 1, 3–5). *Mdx/utrn* mice expressing utrophin on zero, one or two alleles were taken along as controls. Myosin was used as a loading control.

Chapter 6

Low dystrophin levels in heart are sufficient to delay heart failure in mdx mice

M. van Putten, E.M. van der Pijl, M. Hulsker, V.D. Nadarajah, I.E.C. Verhaart, L. van der Weerd, A.M. Aartsma-Rus

Submitted

Abstract

Aim: Duchenne muscular dystrophy is a muscular dystrophy caused by mutations that prevent synthesis of functional dystrophin. All patients develop dilated cardiomyopathy. Promising therapeutic approaches are underway that successfully restore dystrophin expression in skeletal muscle. However, their efficiency in heart is limited. Improved quality and function of only skeletal muscle potentially accelerates the development of cardiomyopathy. Our study aimed to elucidate which dystrophin levels in heart are required to prevent or delay cardiomyopathy in mice.

Methods and Results: Heart function and pathology assessed with magnetic resonance imaging, histology and gene expression analysis were compared between 2, 6 and 10-month-old *mdx-Xist*$^{\Delta hs}$ mice, expressing low dystrophin levels (3-15%) based on skewed X-inactivation, dystrophin-negative *mdx* mice, and wild type mice of corresponding genetic backgrounds.

Mdx mice developed severe dilated cardiomyopathy and hypertrophy, whereas the onset of heart pathology was delayed and function greatly improved in *mdx-Xist*$^{\Delta hs}$ mice. The ejection fraction, the most severely affected parameter for both ventricles, correlated to dystrophin expression and the percentage of fibrosis. Fibrosis was reduced from 9.8% in *mdx* to 5.4% in *mdx-Xist*$^{\Delta hs}$ mice. Additionally, expression of genes involved in heart pathology normalized towards wild type levels in older *mdx-Xist*$^{\Delta hs}$ mice.

Conclusions: These data suggest that mosaic expression of 3-15% dystrophin in heart is sufficient to delay the onset and ameliorate cardiomyopathy in mice.

Introduction

Duchenne muscular dystrophy (DMD) is the most common inherited neuromuscular disorder. It is characterized by severe and progressive muscle wasting and affects 1 in 3500 newborn boys. In DMD patients, the synthesis of functional dystrophin proteins is prevented by mutations in the *DMD* gene, located on the X-chromosome (Muntoni et al. 2003). Dystrophin is part of the dystrophin-associated protein complex, which links the actin cytoskeleton to the extracellular matrix and stabilizes the sarcolemma during muscle contractions (Blake et al. 2002). In DMD patients, this link is absent, making fibers vulnerable to exercise-induced damage, leading to repeated cycles of de- and regeneration. Upon exhaustion of the regenerative capacity, fibers are replaced by fibrotic and fat tissue, resulting in loss of ambulation in the second decade of life. Pre-clinical cardiac involvement is sometimes already observed in young patients (aged <6 years) and its frequency increases with age. Later in life, it progresses into clinically relevant cardiomyopathy affecting 40% of 10-year-old patients (Nigro et al. 1990). Old patients are dependent on assisted ventilation and at that stage the vast majority suffers from dilated and hypertrophic cardiomyopathy of the left ventricle, while the right ventricle and atrium remain unaffected (Connuck et al. 2008;van Bockel et al. 2009). Eventually, patients die of heart or respiratory failure in their third or fourth decade (Gulati et al. 2005).

Becker muscular dystrophy (BMD) is a milder form of muscular dystrophy, caused by in-frame mutations in the *DMD* gene, which result in reduced expression of dystrophin and/or internally truncated, but partly functional dystrophin. The skeletal muscle pathology is less severe than in DMD patients, and patients usually remain ambulant until later in life. However, in 70% of the BMD patients a more severe cardiomyopathy is observed at time of clinical presentation accounting for 50% of deaths (Connuck et al. 2008;Yilmaz et al. 2008;Kaspar et al. 2009). Especially BMD patients with very mildly affected skeletal muscles can develop severe cardiomyopathy (Melacini et al. 1996). Dilated cardiomyopathy is also found in DMD and BMD carriers, who express 50% of dystrophin in heart. Only 17% of the carriers exhibit some skeletal

muscle weakness, whereas 23% have dilated cardiomyopathy or left-ventricular dilation (Hoogerwaard et al. 1999).

There is no cure for DMD, but several potential therapies aiming at dystrophin restoration are under investigation in clinical trials (Bowles et al. 2012;Malik et al. 2010;Skuk et al. 2007), with antisense-mediated exon skipping being closest to clinical application (Goemans et al. 2011;Cirak et al. 2011). Unfortunately, the efficiency of targeting the heart seems less than for skeletal muscle for the exon skipping approaches currently tested in clinical trials (Alter et al. 2006;Bostick et al. 2009;Townsend et al. 2008;Heemskerk et al. 2010;Heemskerk et al. 2009;Malerba et al. 2011;Wu et al. 2011). Eventually, this might result in partial dystrophin restoration in skeletal muscle accompanied by improved function, but without restoration in the heart. Given that both BMD patients and DMD/BMD carriers exhibit more pronounced cardiomyopathy than DMD patients, increased physical activity is likely to put a larger workload on the heart, thereby potentially exacerbating the development of cardiomyopathy.

The most commonly used mouse model for DMD, the *mdx* mouse, also suffers from dilated cardiomyopathy. In non-treated *mdx* mice, increased activity (e.g. voluntary wheel running), accelerates the progression of dilated cardiomyopathy (Jearawiriyapaisarn et al. 2010;Quinlan et al. 2004;Spurney et al. 2008;Costas et al. 2010). In line with this, skeletal muscle restricted dystrophin restoration improves voluntary activities thereby increasing the workload of the heart and exacerbating heart pathology (Malerba et al. 2011;Townsend et al. 2008). By contrast, it has been shown that high dystrophin levels in skeletal muscles and diaphragm only, improve heart function in *mdx* mice (Crisp et al. 2011).

To study which dystrophin levels are needed to prevent or delay the onset of heart failure, we assessed heart function and pathology over time in *mdx-Xist*$^{\Delta hs}$ mice. These mice originate from crossing *Xist*$^{\Delta hs}$ females (expressing intact dystrophin but carrying a mutation in the promoter of the *Xist* gene which coordinates X-inactivation (Newall et al. 2001)), with dystrophic *mdx* males. In the female offspring (*mdx-Xist*$^{\Delta hs}$), the X-chromosome expressing the mutated *Xist* gene, but intact dystrophin, is preferentially inactivated, resulting in expression of varying, low dystrophin levels in skeletal muscle and heart (van Putten et al. 2012a). We show that dystrophin levels of 3-15% in heart are sufficient to delay the onset of dilated cardiomyopathy and reduce the severity of pathology in *mdx* mice.

Material and methods

Animal care

Breeding pairs of *mdx* (C57BL/10ScSn-mdx/J) males and *Xist*$^{\Delta hs}$ females gave birth to *mdx-Xist*$^{\Delta hs}$ females (van Putten et al. 2012a). The *Xist*$^{\Delta hs}$ model (Newall et al. 2001) was a kind gift from prof. Dr. Brockdorff (MRC Clinical Sciences Centre London, UK, current affiliation Department of Biochemistry, University of Oxford, UK). Genotyping was performed on DNA obtained from tail tips by PCR analysis. Mice were housed in individually ventilated cages with 12-h light-dark cycles and had *ad libitum* access to standard chow and water. All experiments were approved by the Animal Experimental Commission (DEC) of the LUMC and conforms with the Directive 2010/63/EU of the European Parliament.

MRI heart function analysis

MRI analysis was performed at the Faculty of Science of the University of Leiden to which the mice were transported a week before analysis to acclimatize. Mice were anaesthetized by inhalation of 2% isoflurane in a 1:1 mixture of pure oxygen and air. Mice were scanned in a vertical 9.4T magnet with 89 mm bore size, equipped with a 1 T/m gradient system (Bruker

BioSpin, Germany), using a quadrature birdcage coil (inner diameter 3 cm). Image acquisition was done with Bruker Paravision 5.0 software and took ~30 min including animal setup. A retrospectively-gated Intragate sequence was used with flip angle 10°; repetition time 8.5 ms; echo time 1.86 ms; field-of-view 2.56x2.56 cm^2; matrix 192x192; in-plane resolution 133 μm. We made 8-9 short-axis slices of the heart of 1 mm thick and 200 repetitions per slice. The navigator echo was placed in-slice. Images were reconstructed to 18 frames per heart cycle. Respiration rate was monitored with a respiratory pad and kept constant at 50-80 respirations per minute. Six of the 135 mice scanned were not used for analysis as the angle of the scan was incorrect.

MASS for MICE software (developed at the LUMC, Division of Image Processing (LKEB)) was used for image analysis (van der Geest and Reiber 1999). For each picture, endocardial and epicardial contours of both ventricles were drawn manually. The end diastolic and systolic phase was computed by the software and a maximum mass difference of 10% was accepted. When this criteria was met, End Diastolic and Systolic Volume (EDV and ESV, respectively) were determined and based on these values Stroke Volume (SV = EDV-ESV), Ejection Fraction (EF = (SV/EDV)*100%) and Cardiac Output (CO = SV*heart rate) were calculated automatically.

Serum biomarker level analysis

For analysis of cardiac Troponin I and N-terminal Pro Brain Natriuretic Peptide levels, blood (~1mL) was drawn from the anaesthetised mouse via the eye after which it was sacrificed by cervical dislocation. Blood was collected in a non-coated eppendorf tube, allowed to clot at room temperature for 10 min and stored on ice. Samples were centrifuged at 1700 *g* for 10 min at 4°C and stored at -80°C. Levels of cardiac Troponin I and NT-proBNP were measured using the High Sensitive Mouse Cardiac Troponin-I ELISA Kit (Life Diagnostics, USA) and the ELISA Kit for NT-proBNP (Uscn Life Science Inc, China) respectively.

Histological examination

Tissues were snap frozen in 2-methylbutane (Sigma Aldrich, the Netherlands) cooled in liquid nitrogen. Sections of 8 μm were made on Superfrost Plus slides (Thermo Fishes Scientific, Menzel-Gläser, Germany) with a Shandon cryotome (Thermo Fisher Scientific Co., USA) along the entire length of the heart with an interval of 240 μm between the sections. Excess tissue was used for protein and RNA isolation. Sections were stained with goat-anti-Collagen type 1 (dilution 1:100, 1310-01 Southern Biotech, USA), donkey-anti-goat Alexa594 (dilution 1:1000, Invitrogen, the Netherlands) and DAPI. A fluorescent microscope (Leica DM RA2) was used to examine the sections at a 16 times magnification and images covering the entire heart were captured with a Leica DC350FX snapshot camera. The percentage of fibrotic tissue was assessed with ImageJ software (Rasband W.S., ImageJ, U.S. National Institutes of Health, USA, http://rsb.info.nih.gov/ij/, 1997-2008).

Dystrophin determination by western blot

Heart and diaphragm muscles were homogenized and dystrophin levels quantified by western blotting using the Odyssey system as described previously (van Putten et al. 2012a). The lowest concentration in the standard curve was 3%.

Gene expression analysis with qPCR

Total RNA was isolated with TRIzole (Invitrogen, the Netherlands) in MagNA Lyser Green Beads tubes (Roche diagnostics Ltd, UK) and purified with the NucleoSpin RNA II kit (Bioke, the Netherlands). RNA integrity and concentration was determined with a total RNA nano-chip assay on a labchip bioanalyzer (Agilent, the Netherlands). Random hexamer primers were used for cDNA synthesis and gene expression was determined by Sybr Green based Real Time qPCR (95°C 10 sec, 60°C 30 sec, 72°C 20 sec for 45 cycli followed by melting curve analysis) on the Roche Lightcycler 480 (Roche diagnostics Ltd, UK). *Gapdh* was used as a reference gene. The C_p values were obtained with the second derivative maximum method and primer efficiencies and gene expression was determined with LinREgPCR version 11.1 (Ramakers et al. 2003). The expression of C57BL/10ScSnJ mice was set to one.

Statistics

Statistical analyses were performed using SPSS 17.0.2. (SPSS, Inc., Chicago, IL, USA). Heart function was compared over time with the two-way analysis of variance (ANOVA). In case of significance (P<0.05), a LSD correction for multiple testing was applied. Correlations for the 10-month-old *mdx-Xist*$^{\Delta hs}$ mice were tested with the Spearman correlation test. Values of P<0.05 were considered significant. The one-way ANOVA was conducted for comparison of the histological and gene expression data. In case of significance (P<0.05), the Bonferroni post hoc test was performed.

Results

Low dystrophin levels in heart prevent the age-dependent decline of heart function

To determine whether low dystrophin levels can prevent or delay the onset of dilated cardiomyopathy, heart function was determined by MRI in groups of female *mdx* (no dystrophin), *mdx-Xist*$^{\Delta hs}$ (low dystrophin), C57BL/10ScSnJ (wild type control) and *Xist*$^{\Delta hs}$ (wild type control) mice aged 2, 6 and 10 months. We chose a cross-sectional design to allow post-mortem histological validation. To assess the correlation between dystrophin levels and heart function in individual mice, 27 *mdx-Xist*$^{\Delta hs}$ mice were scanned per time point, while 6 mice were scanned for the control groups. Dystrophin levels in the heart of *mdx-Xist*$^{\Delta hs}$ mice varied between 3-15% and were similar for the different age groups (2 months; 3-13.8%, 6 months; 3-14.9%, 10 months; 3-12.1%) as assessed by western blot (Figure 1A-B). MRI scans were positioned on the left ventricle and the ejection fraction (EF), stroke volume (SV), end diastolic volume (EDV), cardiac output (CO) and end systolic mass of both ventricles were assessed.

Overall, the heart function of the two wild type strains was largely comparable, but differed slightly, probably due to differences in the genetic background. In *mdx* mice, heart function of both ventricles deteriorated with age, most evidently for the EF and SV, while it remained constant in both wild type models (Figure 1C-F, Table 1), as reported previously (Verhaart et al. 2011). Expression of 3-15% dystrophin in heart prevented EF and SV to drop in *mdx-Xist*$^{\Delta hs}$ mice as levels remained stable over time and were higher than *mdx* mice from the age of 6 months onwards (P<0.05). The EF and SV of *mdx-Xist*$^{\Delta hs}$ mice were similar to levels of the wild type stains at 6 months, and for the left ventricle only lower than 10-month-old *Xist*$^{\Delta hs}$ mice (P<0.05). The EDV and CO of both ventricles did not differ between the mouse models.

End systolic mass of both ventricles increased with age in all mice. However, the left ventricular mass of *mdx* mice was greater than that of all other mice regardless of their age (P<0.01), indicative of hypertrophy of the heart. In contrast, the expression of <15% dystrophin in *mdx-Xist*$^{\Delta hs}$ mice hearts completely prevented hypertrophy.

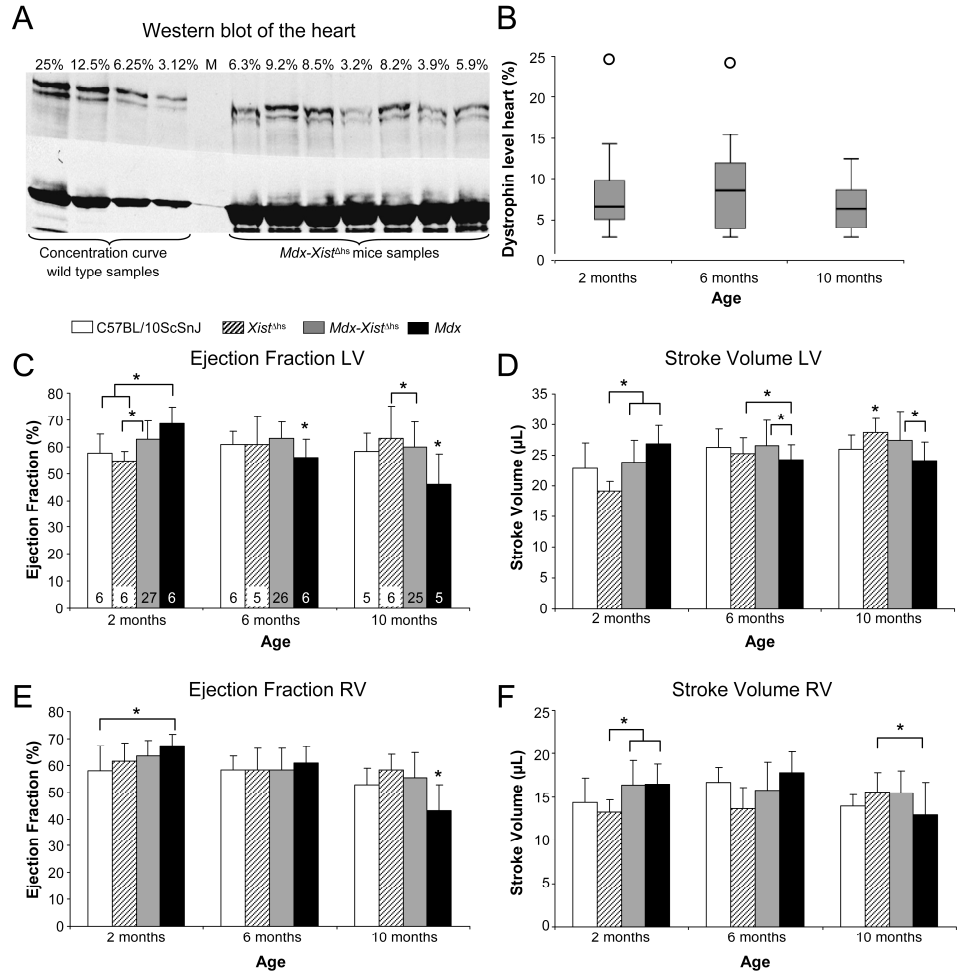


Figure 1. Dystrophin levels and heart function of *mdx-Xist*$^{\Delta hs}$ mice. (A) Dystrophin levels were assessed by western blot for all *mdx-Xist*$^{\Delta hs}$ mice, as shown in the representative blot. Myosin was used as a loading control. M=marker. **(B)** Dystrophin levels are plotted in the box plot. The line dissecting the box resembles the median, outer bars of the box resemble the lower and upper quartile. The bars show maximum and minimum values considered excepting outliers (indicated by ○). Dystrophin levels varied between 3-15%, n = 81 and no increment was observed in older animals. **(C-F)** The EF and SV of both ventricles remained stable in wild type mice, but declined in *mdx* mice, which was prevented in the *mdx-Xist*$^{\Delta hs}$ mice. LV=left ventricle, RV=right ventricle. Bars represent mean values and the standard deviation. Asterisks indicate a difference of P<0.05.

The right ventricular mass did not differ between *mdx* and C57BL/10ScSnJ mice, but was higher than that of *mdx-Xist*$^{\Delta hs}$ and *Xist*$^{\Delta hs}$ mice (P<0.01), which were comparable. This indicates that hypertrophy was restricted to the left ventricle. Heart rate increased in *mdx* mice with age (P<0.001), but remained stable over time for the other models. Heart rate of 2 months old *Xist*$^{\Delta hs}$ mice was higher than that of both *mdx* and *mdx-Xist*$^{\Delta hs}$ mice (P<0.01). In old *mdx* mice, heart rate was higher than that of both *mdx-Xist*$^{\Delta hs}$ and *Xist*$^{\Delta hs}$ mice (P<0.01).

Table 1. Heart function.

Age in months	2	2	2	2		6	6	6	6		10	10	10	10		
Mouse strain	Wt	*Xist*$^{\Delta hs}$	*Mdx-Xist*$^{\Delta hs}$	*Mdx*	Changes at 2 months	Wt	*Xist*$^{\Delta hs}$	*Mdx-Xist*$^{\Delta hs}$	*Mdx*	Changes at 6 months	Wt	*Xist*$^{\Delta hs}$	*Mdx-Xist*$^{\Delta hs}$	*Mdx*	Changes at 10 months	Change over time within strain
Left ventricle																
EF (%)	57.6±7.3	54.6±3.8	62.8±6.9	68.7±6.2	*mdx-Xist*$^{\Delta hs}$ vs *Xist*$^{\Delta hs}$ P<0.05 *mdx* vs wt P<0.05, *Xist*$^{\Delta hs}$ P<0.01	61.0±4.6	60.9±10.4	63.3±6.0	55.9±6.9	*mdx* vs wt P<0.05, *mdx-Xist*$^{\Delta hs}$ and *Xist*$^{\Delta hs}$ P<0.01	58.4±6.9	63.3±11.7	59.8±9.6	46.1±11.4	*mdx-Xist*$^{\Delta hs}$ vs *Xist*$^{\Delta hs}$ P<0.05 *mdx* vs all P<0.01	*mdx* decrease P<0.01 from 6 months onwards
SV (µl)	22.9±4.1	19.1±1.6	23.8±3.7	26.8±3.1	*Xist*$^{\Delta hs}$ vs *mdx-Xist*$^{\Delta hs}$ and *mdx* P<0.01	26.3±3.0	25.2±2.7	26.6±4.1	24.3±2.4	*mdx* vs *Xist*$^{\Delta hs}$ P<0.01, *mdx-Xist*$^{\Delta hs}$ P<0.05	26.0±2.3	28.8±2.3	27.4±4.7	24.2±3.0	*Xist*$^{\Delta hs}$ vs wt and *mdx-Xist*$^{\Delta hs}$ P<0.05, *mdx* P<0.01 *mdx* vs *mdx-Xist*$^{\Delta hs}$ P<0.05	*Xist*$^{\Delta hs}$ and *mdx-Xist*$^{\Delta hs}$ increase P<0.01 from 6 months onwards
EDV (µl)	39.8±5.3	35±2.4	38.1±4.5	39.4±6.6	NS	43.1±3.9	42.3±7.9	42.5±8.2	43.9±4.9	NS	45.1±6.9	47.8±15.7	46.5±8.7	54.4±11.7	NS	All strains increase P<0.01 from 6 months onwards
CO (µl/min)	8229±1801	7877±343	8506±1079	9403±2105	NS	9418±1758	10365±1754	10022±1421	8908±1587	NS	10995±2196	11762±1577	10178±2026	10637±1207	NS	All strains increase P<0.01 from 6 months onwards
ES mass (mg)	63.5±7.6	55.5±4.4	59.5±7.1	69.5±10.0	*mdx* vs all P<0.01	70.3±10.1	80.4±11.5	83.0±10.1	84.2±8.3	*mdx* vs all P<0.01	86.8±12.6	91.1±16.8	93.6±10.3	108±20.9	*mdx* vs all P<0.01	All strains increase P<0.01 from 6 months onwards
Right ventricle																
EF (%)	58.1±9.2	61.5±6.8	63.5±5.9	67.4±4.2	*mdx* vs wt P<0.05	58.2±5.3	58.2±8.1	58.3±7.9	60.9±6.3	NS	52.9±5.9	58.2±5.9	55.4±9.5	43.1±9.8	*mdx* vs all P<0.01	*mdx-Xist*$^{\Delta hs}$ decrease P<0.05 at 6 months and P<0.01 at 10 months *mdx* decrease P<0.01 at 10 months
SV (µl)	14.3±2.9	13.3±1.4	16.5±2.8	16.5±2.3	*Xist*$^{\Delta hs}$ vs *mdx-Xist*$^{\Delta hs}$ and *mdx* P<0.05	16.7±1.7	13.6±2.5	15.8±3.3	17.8±2.4	NS	14.0±1.3	15.6±2.3	15.5±2.5	12.9±3.8	*mdx* vs *Xist*$^{\Delta hs}$ P<0.05	*mdx* decrease P<0.05 at 10 months
EDV (µl)	25.1±6.0	21.9±3.4	26.0±4.7	24.6±4.2	NS	28.8±1.6	23.9±5.4	27.6±7.1	29.7±5.9	NS	26.5±1.7	27.1±5.7	28.9±7.1	30.8±9.4	NS	All strains increase P<0.01 at 6 months
CO (µl/min)	5166±1260	5492±426	5892±1050	5800±1373	NS	6002±1177	5640±1433	5938±1205	6448±919	NS	5859±665	6372±1173	5733±1056	5621±1365	NS	NS
ES mass (mg)	17.9±5.5	13.9±2.4	15.5±2.2	18.9±3.8	wt vs *Xist*$^{\Delta hs}$ P<0.05 *mdx* vs *Xist*$^{\Delta hs}$ and *mdx-Xist*$^{\Delta hs}$ P<0.01	20.3±1.7	19.2±5.4	19.4±4.7	22.8±2.2	wt vs *Xist*$^{\Delta hs}$ P<0.05 *mdx* vs *Xist*$^{\Delta hs}$ and *mdx-Xist*$^{\Delta hs}$ P<0.01	21.7±2.3	19.1±2.6	20.6±2.7	24.1±5.6	wt vs *Xist*$^{\Delta hs}$ P<0.05 *mdx* vs *Xist*$^{\Delta hs}$ and *mdx-Xist*$^{\Delta hs}$ P<0.01	All strains increase P<0.01 from 6 months onwards
Heart rate	362±58	414±18	363±34	352±49	*Xist*$^{\Delta hs}$ vs *mdx* and *mdx-Xist*$^{\Delta hs}$ P<0.01	388±24	410±38	383±39	364±33	NS	424±80	409±39	374±35	442±34	*mdx* vs *Xist*$^{\Delta hs}$ and *mdx-Xist*$^{\Delta hs}$ P<0.01	*mdx* increase with P<0.01 from 10 months onwards

Values are mean ± standard deviation. Wt indicates C57BL/10ScSnJ mice; EDV, end diastolic volume; CO, cardiac output; EF, ejection fraction; SV, stroke volume; ES mass, end systolic mass; NS, non significant; vs, versus.

Dystrophin levels of 10-month-old *mdx-Xist*$^{\Delta hs}$ mice correlated with the EF of both ventricles (left R=0.464 *P*=0.019, right R=0.471 *P*=0.017), which was also the most severely affected parameter in *mdx* mice (Figure 2A-B). As heart function has been described to normalize by dystrophin expression in the diaphragm (Crisp et al. 2011), we also assessed this for 10-month-old *mdx-Xist*$^{\Delta hs}$ mice. Dystrophin levels of the diaphragm varied between 1.5-38% (*mean* = 11.5% *stdev* = 8.8) and did not correlate to dystrophin levels in heart (R=0.04 *P*=0.849). Dystrophin levels in the diaphragm only correlated with the EDV of the right ventricle (R=0.492 *P*=0.017), however, the EDV did not differ between any of the models. We hypothesized that the combined presence of dystrophin in heart and diaphragm might have a cumulative beneficial effect on heart function (Figure 2C-D). To elucidate this, we grouped the EF of 10-month-old *mdx-Xist*$^{\Delta hs}$ mice based on their dystrophin levels in heart and diaphragm into the following groups; mice with <4% dystrophin in heart and >4% in diaphragm (heart; median 3.0% *stdev* = 0.29, diaphragm; median 8.67% *stdev* = 3.07, *n* = 7), >4% dystrophin in heart and <4% in diaphragm (heart; median 7.64% *stdev* = 1.13, diaphragm; median 2.63% *stdev* = 0.88, *n* = 5) and >4% dystrophin in heart and diaphragm (heart; median 6.31% *stdev* = 3.04, diaphragm; median 15.23% *stdev* = 9.31, *n* = 13) (there were no mice with <4% dystrophin in both heart and diaphragm). The EF of both ventricles of mice expressing <4% dystrophin in heart and >4% in diaphragm was as low as age-matched *mdx* mice. The EF of mice expressing >4% dystrophin in heart and <4% or >4% in diaphragm was higher than in *mdx* mice (*P*<0.05). This indicates that expression of >4% dystrophin in heart only improves EF of both ventricles, while expression of >4% (but less than 14%) dystrophin in diaphragm only does not.

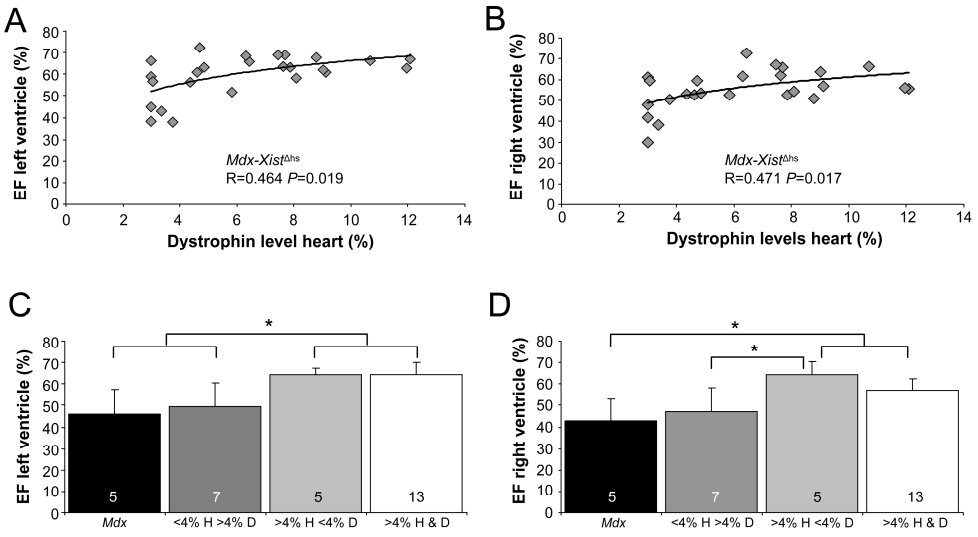


Figure 2. Correlation between dystrophin expression and heart function. (A-B) Dystrophin levels of the heart correlated to EF of both ventricles in 10-month-old *mdx-Xist*$^{\Delta hs}$ mice (left R=0.464 *P*=0.019 and right R=0.471 *P*=0.017). **(C-D)** <4% dystrophin in heart did not restore EF despite dystrophin expression in the diaphragm. EF levels were improved in mice expressing >4% dystrophin in heart regardless of expression levels in the diaphragm. H=heart, D=diaphragm. Bars represent mean values and the standard deviation. Asterisks indicate a difference of *P*<0.05.

We also assessed levels of potential serum biomarkers for heart failure; cardiac Troponin I and N-Terminal Pro Brain Natriuretic Peptide (NT-proBNP). Detectable concentrations of cardiac Troponin I were observed for some mice for all models and at all ages, but were slightly more often found in serum of dystrophic mice (Figure 3A). Cardiac Troponin I levels did not differ between *mdx* and *mdx-Xist*$^{\Delta hs}$ mice, nor did they correlate to heart dystrophin levels (R=0.004 *P*=0.986). Levels did correlate to CO and SV of the right ventricle (R= -0.535 *P*= 0.015 and R= -0.483 *P*=0.031 respectively). NT-proBNP levels were undetectable in any of the mouse models at any age.

Low dystrophin levels reduce fibrosis

Transverse cross-sections of the heart were stained with Collagen type I, to determine the percentage of fibrotic tissue (see Supplementary Figure 1 for representative examples). No fibrosis was detected in 2-month-old mice, whereas levels were elevated in 6-month-old *mdx* and *mdx-Xist*$^{\Delta hs}$ compared to wild type mice (2.4% and 3.4% vs 2%, Table 2). Due to high individual variation only the increment of the *mdx-Xist*$^{\Delta hs}$ mice reached significance (*P*<0.05). Fibrosis was most prominent in 10-month-old *mdx* mice, while its formation was partly prevented in *mdx-Xist*$^{\Delta hs}$ mice (9.8% vs 5.4%, *P*<0.01), although levels were still higher than wild type (*P*<0.01). Dystrophin levels in the *mdx-Xist*$^{\Delta hs}$ hearts did not correlate with fibrosis (R= -0.234 *P*=0.240, Figure 3B). Fibrosis negatively correlated to the EF of both ventricles (left R= -0.512 *P*=0.009, right R= -0.594 *P*=0.002) (Figure 3C-D). This concurs with the above described correlation between the EF of both ventricles and dystrophin levels Heart mass did not correlate with fibrosis (left R= 0.253 *P*= 0.222, right R= 0.285 *P*=0.167).

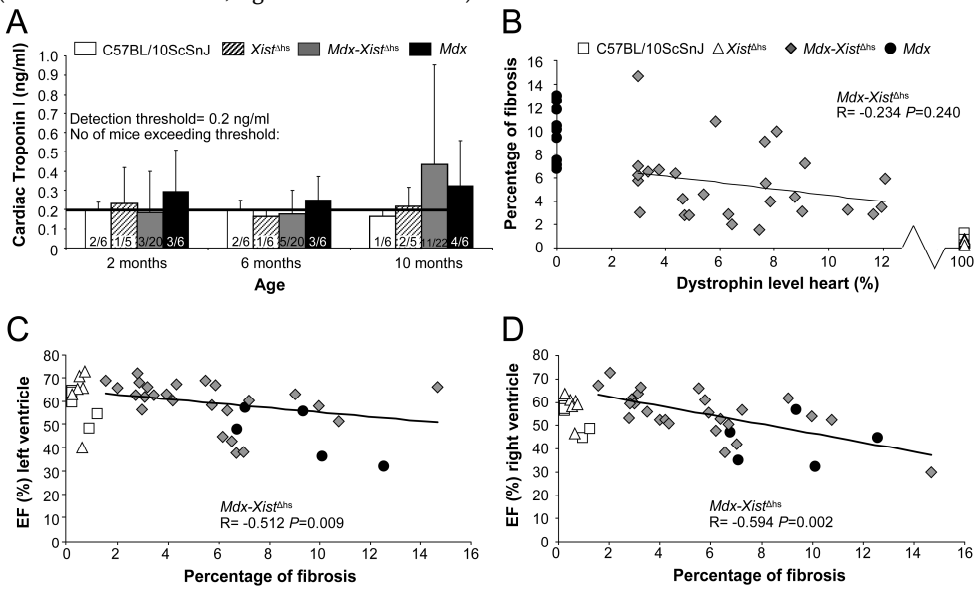


Figure 3. Cardiac Troponin I levels and correlation between fibrosis, dystrophin expression and heart function. Bars represent mean values and the standard deviation. **(A)** Serum cardiac Troponin I levels exceeded the detection threshold of 0.2 ng/µl in some samples from all models. Levels did not differ between models or correlate to dystrophin expression in the heart (R=0.004 *P*=0.986). **(B)** Scatter plot of the percentage of fibrosis versus dystrophin levels of the heart of 10-month-old mice. Although *mdx-Xist*$^{\Delta hs}$ mice had less fibrosis than *mdx* mice, dystrophin levels did not correlated to fibrosis (R= -0.234 *P*=0.240). **(C-D)** Fibrosis levels of 10-month-old *mdx-Xist*$^{\Delta hs}$ mice negatively correlated to EF of both ventricles (left R= -0.512 *P*=0.009, right R= -0.594 *P*=0.002).

Table 2. Fibrosis and gene expression of the heart.

Age in months	2	2	2	2		6	6	6	6		10	10	10	10	
Mouse strain	Wt	*Xist*$^{\Delta hs}$	*Mdx-Xist*$^{\Delta hs}$	*Mdx*	Changes at 2 months	Wt	*Xist*$^{\Delta hs}$	*Mdx-Xist*$^{\Delta hs}$	*Mdx*	Changes at 6 months	Wt	*Xist*$^{\Delta hs}$	*Mdx-Xist*$^{\Delta hs}$	*Mdx*	Changes at 10 months
Histopathology															
Fibrosis	0.57±0.15	0.47±0.25	1.06±1.07	1.34±1.12	NS	0.66±0.31	0.40±0.15	3.45±2.84	2.43±1.04	*mdx-Xist*$^{\Delta hs}$ vs wt $P<0.01$ and *Xist*$^{\Delta hs}$ $P<0.05$	0.54±0.37	0.55±0.18	5.43±3.01	9.84±2.35	*mdx-Xist*$^{\Delta hs}$ vs all $P<0.01$ *mdx* vs all $P<0.01$
Gene expression															
Lgals3	1±0.75	0.17±0.27	0.72±1.35	1.13±1.04	NS	1±0.77	1.02±0.25	4.06±3.93	3.07±3.16	NS	1±0.51	0.87±0.77	2.65±1.85	4.09±2.75	*mdx* vs wt and *Xist*$^{\Delta hs}$ $P<0.01$
Cd68	1±0.22	1.12±0.21	1.38±1.05	1.63±0.97	NS	1±0.36	1.08±0.47	2.33±1.51	1.17±0.29	*mdx-Xist*$^{\Delta hs}$ vs wt $P<0.05$	1±0.29	0.88±0.11	2.00±0.86	1.76±0.71	*mdx-Xist*$^{\Delta hs}$ vs wt and *Xist*$^{\Delta hs}$ $P<0.01$
Ctgf	1±0.46	1.63±0.50	1.89±0.83	1.48±0.65	*mdx-Xist*$^{\Delta hs}$ vs wt $P<0.05$	1±0.48	1.83±0.65	2.13±0.74	1.12±0.43	*mdx-Xist*$^{\Delta hs}$ vs wt and *mdx* $P<0.01$	1±0.36	0.88±0.26	1.20±0.41	1.79±0.72	*mdx* vs wt and *Xist*$^{\Delta hs}$ $P<0.01$, vs *mdx-Xist*$^{\Delta hs}$ $P<0.05$
Nox4	1±0.32	0.62±0.31	0.84±0.30	0.82±0.22	NS	1±0.51	0.85±0.20	1.63±0.88	1.85±0.50	NS	1±0.50	0.58±0.20	2.06±0.86	3.39±1.29	*mdx-Xist*$^{\Delta hs}$ vs wt $P<0.05$ and *Xist*$^{\Delta hs}$ $P<0.01$ *mdx* vs all $P<0.01$
Serca2a	1±0.14	1.21±0.17	1.17±0.37	1.10±0.26	NS	1±0.20	1.01±0.14	0.80±0.18	0.75±0.24	NS	1±0.30	1.47±0.22	0.94±0.33	0.28±0.19	*Xist*$^{\Delta hs}$ vs wt $P<0.05$ and *mdx-Xist*$^{\Delta hs}$ $P<0.01$ *mdx* vs all $P<0.01$
Nppa	1±0.51	0.47±0.31	0.79±0.56	0.93±0.29	NS	1±0.74	0.67±0.25	0.95±0.55	1.70±0.67	*mdx* vs *Xist*$^{\Delta hs}$ and *mdx-Xist*$^{\Delta hs}$ $P<0.05$	1±0.73	0.77±0.24	1.37±0.78	3.99±2.11	*mdx* vs all $P<0.01$

Values are mean ± standard deviation. Wt indicates C57BL/10ScSnJ mice; NS, non significant; vs, versus.

Concurring with histopathological and functional data, expression levels of 2-month-old dystrophic mice were not elevated except for *Ctgf*, which was increased in *mdx-Xist*$^{\Delta hs}$ compared to C57BL/10ScSnJ mice. With age, expression of several genes increased in *mdx* mice, but to a lesser extent in *mdx-Xist*$^{\Delta hs}$ mice. In 6-month-old *mdx* mice, expression of *Nppa* was elevated. Gene expression of 10-month-old *mdx* mice was greatly increased, while levels of *mdx-Xist*$^{\Delta hs}$ mice fell between those of *mdx* and wild type mice for most genes. By contrast, levels of *Serca2a* dropped in *mdx* mice, but were similar for *mdx-Xist*$^{\Delta hs}$ and C57BL/10ScSnJ mice.

Discussion

Potential therapeutic strategies for DMD are currently tested in clinical trials and encouraging results have been published for dystrophin restoration in skeletal muscles (Cirak et al. 2011;Goemans et al. 2011). Unfortunately, the heart seems to be a less efficient target as several therapeutic approaches fail to restore dystrophin expression in this organ or are less efficient in heart than skeletal muscle (Bowles et al. 2012;Cirak et al. 2011;Goemans et al. 2011;Malik et al. 2010;Skuk et al. 2007). Studies in *mdx* mice suggest that functional improvement in skeletal muscles may worsen cardiomyopathy (Malerba et al. 2011;Townsend et al. 2008). It is, however, unknown whether low dystrophin levels can preserve function and prevent or delay heart pathology.

We used skewed X-inactivation as a tool to generate mice with low dystrophin levels in heart and skeletal muscles. Heart function of *mdx* mice progressively declines with age, resulting in severe dilation of both ventricles in 10-month-old mice (Quinlan et al. 2004;Spurney et al. 2008;Verhaart et al. 2011;Zhang et al. 2008). With age, they develop severe fibrosis and upregulate genes involved in pathology and function, whereas this remains stable in wild type mice (Au et al. 2011;Li et al. 2009). Interestingly, expression of 3-15% dystrophin in 10-month-old *mdx-Xist*$^{\Delta hs}$ mice ameliorates the age-dependent loss of heart function and pathology, as heart function parameters, fibrosis and gene expression partly normalize towards wild type levels. Whereas EF and SV are affected already in *mdx* mice aged 6 months, this is observed later (10 months) and to a lesser extent in *mdx-Xist*$^{\Delta hs}$ mice.

It was hypothesized that the combined expression of dystrophin in heart and diaphragm might cumulatively improve heart function, as others observed beneficial effects of dystrophin expression in diaphragm on heart function (Crisp et al. 2011). Expression of >4% dystrophin in diaphragm does not improve heart function (EF, the most affected parameter) in *mdx-Xist*$^{\Delta hs}$ mice, whereas similar levels in heart do. Expression of >4% dystrophin in both heart and diaphragm does not further improve heart function indicating that the cumulative beneficial effect of dystrophin expression in diaphragm on heart function is limited. The discrepancy between our findings and those reported by Crisp et al. might be caused by the low dystrophin levels in diaphragm in this study compared to the high dystrophin levels in their study. This suggests that for a protective effect on heart function probably high dystrophin levels in diaphragm are needed.

Dystrophin levels of the *mdx-Xist*$^{\Delta hs}$ mice do not correlate with fibrosis, whereas, fibrosis correlates to the EF of both ventricles, which is in concordance with literature (Li et al. 2009). It should be stressed that *mdx-Xist*$^{\Delta hs}$ mice also express low dystrophin levels in skeletal muscle leading to improved muscle quality and function, which has been reported to increase the workload for the heart, thereby potentially worsening cardiomyopathy. Whether 3-15% dystrophin in heart is still protective when forced strenuous exercise is applied remains to be elucidated. Hearts of *mdx* mice are hypertrophic from the age of 2 months onwards, a pathological feature which is not observed in any of the *mdx-Xist*$^{\Delta hs}$ mice. Our finding (assessing

the mass of the entire ventricle) concurs with the report of Costas et al. (assessing ventricular wall thickness (Costas et al. 2010)), but is in contrast with work from others who observe hypertrophy from 6 months onwards (measuring heart to body weight ratios) (Bia et al. 1999;Quinlan et al. 2004). The difference in age of onset might be caused by differences in sensitivity of the quantification methods used.

The applicability of cardiac Troponin I and NT-proBNP as biomarkers for heart failure was also assessed. Cardiac Troponin I has previously been used for detection of cardiac infarcts and was reported to be a useful marker for heart function in DMD and BMD patients (Matsumura et al. 2007). Additionally, cardiac Troponin I levels of idebenone treated *mdx* mice have been reported to normalize towards wild type levels (Buyse et al. 2009). Unexpectedly, serum cardiac Troponin I values observed in our study did not correspond with those obtained by Buyse et al. However, personal communication revealed that their values were in the in pg/ml range instead of the published ng/ml, making their observations fall in the same range as ours. Although heart function of *mdx* mice is severely impaired, serum cardiac Troponin I levels barely exceeds the detection threshold of the kit. Thus, we feel the usefulness of cardiac Troponin I as a biomarker for cardiomyopathy in dystrophic mouse models is limited. Based on literature, the applicability of NT-proBNP is questionable as well, as positive and negative correlations with heart function in DMD and BMD patients have been published (van Bockel et al. 2009;Schade van Westrum et al. 2006). In our hands, NT-proBNP levels are undetectable even in 10-month-old *mdx* mice. Therefore we propose this marker not suitable for the assessment of heart failure in *mdx* mice younger than 10 months.

Our study is partly limited by the fact that scans only entirely cover the left ventricle, while the top part of the right ventricle is not scanned. At initiation of this study, our primary focus was the left ventricle, but with interesting findings published on the right ventricle meanwhile, we also analysed MRI data available for the right ventricle. All scans were analysed in the same manner and up to exactly the same height in the right ventricle to ensure comparability. However, the top part of the right ventricle was not scanned and analysed, which resulted in a lower CO for the right compared to the left ventricle. It may also be the reason that we observe a more severe phenotype for the left than the right ventricle, while others have reported the opposite (Crisp et al. 2011;Verhaart et al. 2011).

In summary, we have shown that expression of 3-15% dystrophin not only delays the onset of cardiomyopathy, but also largely ameliorates its severity in 10-month-old *mdx* mice. These observations suggest that treatments restoring only low dystrophin levels in the heart of DMD patients may have benefits on heart function.

Funding

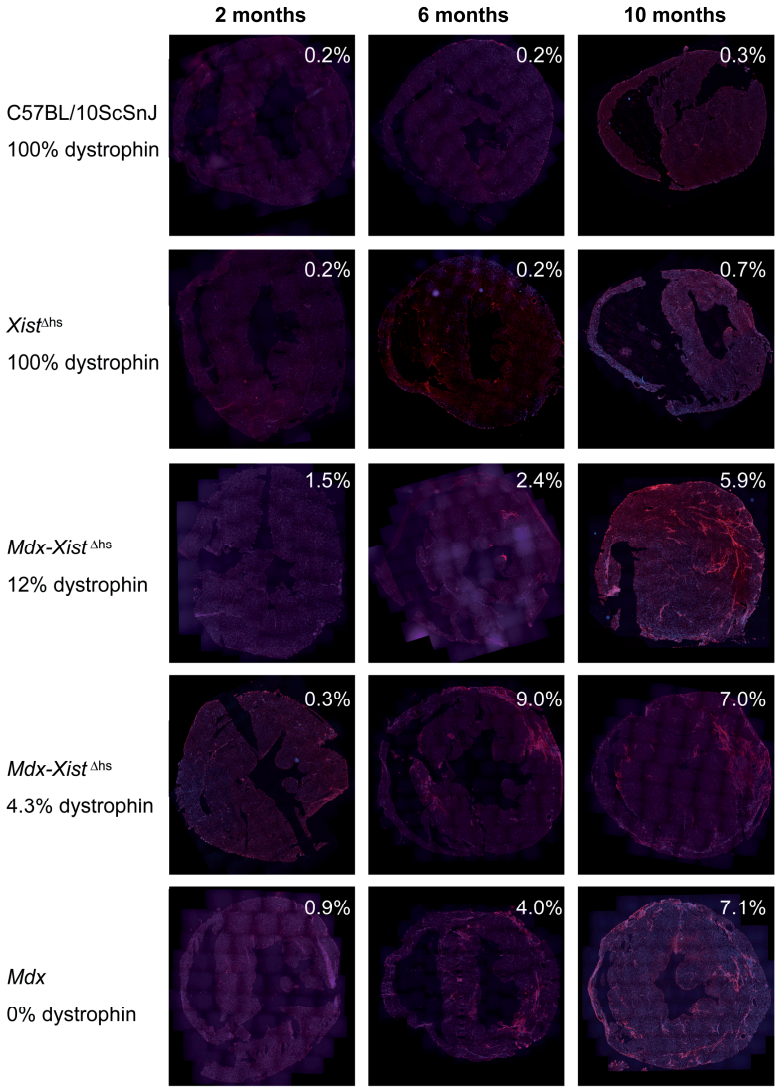
This work was supported by a ZonNW (Zorg Onderzoek Nederland Medische Wetenschappen) grant [grant number 43200002].

Acknowledgements

We are grateful to Dr. R.J. van der Geest of the Division of Image Processing (LKEB), Department of Radiology for his assistance with MASS for mice software.

Conflict of Interest

None declared



Supplementary Figure 1. Representative pictures of fibrosis in the heart. Mean dystrophin levels are indicated for each model and the percentage of fibrosis is given for each picture. No fibrosis was evident in any of the models aged 2 months, nor in wild type mice regardless of their age. From 6 months onwards, increased levels of fibrosis were observed in *mdx* and *mdx-Xist*$^{\Delta hs}$ mice. Ten months old *mdx* mice had extensive areas of fibrosis, covering ~10% of the heart, whereas this was partly prevented in *mdx-Xist*$^{\Delta hs}$ mice. The blue spots are stitching artifacts.

Chapter 7

Low dystrophin levels increase survival and improve muscle pathology and function in dystrophin/utrophin double knockout mice

M. van Putten, M. Hulsker, C. Young, V.D. Nadarajah, H. Heemskerk, L. van der Weerd, P.A.C. 't Hoen, G.J.B. van Ommen, A.M. Aartsma-Rus

Submitted

Abstract

Duchenne muscular dystrophy is a severe muscle wasting disorder caused by the lack of functional dystrophin. There is no cure, but several clinical trials are underway aimed at restoring the synthesis of functional dystrophin. The dystrophin levels needed for improvement of muscle pathology, function and overall vitality are unknown. Here, we describe the *mdx/utrn*$^{-/-}$*/Xist*$^{\Delta hs}$ mouse model, which expresses a range of low dystrophin levels depending on the degree of skewing of X-inactivation in a utrophin negative background. *Mdx/utrn*$^{-/-}$ mice develop severe muscle weakness, kyphosis, respiratory and heart failure and premature death closely resembling DMD pathology. We show that dystrophin levels below 4% already greatly improve survival and motor function in these animals. In mice expressing more than 4% dystrophin, histopathology is ameliorated as well. This suggests that the dystrophin levels needed to benefit vitality and functioning of DMD patients might be lower than those needed for full protection against muscle damage.

Introduction

Duchenne muscular dystrophy (DMD) is the most common inherited neuromuscular disorder. It is caused by mutations which disrupt the reading frame of the *DMD* gene located on the X-chromosome. These mutations result in a premature stop codon, which prevents the synthesis of functional dystrophin (Hoffman et al. 1987). Dystrophin provides muscle fiber stability during contraction by anchoring the extracellular matrix to actin filaments. When this connection is absent, fibers are vulnerable to exercise-induced damage and, upon exhaustion of the regenerative capacity, they will be replaced by fibrotic and fat tissue. The continuous loss of muscle tissue results in loss of ambulation generally in the second decade of the patient's life. Due to improved care including corticosteroid treatment, spinal surgery and assisted ventilation, patients now survive till the third or forth decade in the Western world (Muntoni et al. 2003;Kohler et al. 2009). Mutations that do not disrupt the reading frame are found in Becker muscular dystrophy patients (BMD). These patients express dystrophin of lower quantity and/or of different quality (generally internally deleted) that is partly functional, resulting in a milder phenotype.

The *mdx* mouse is the most commonly used mouse model for basic and therapy research for DMD. It carries a nonsense/stop mutation in exon 23 of the mouse *Dmd* gene and consequently, like DMD patients, lacks functional dystrophin. The phenotype of this mouse is, however, less severe than that of DMD patients and the life span is nearly normal (Sicinski et al. 1989;Stedman et al. 1991). This is likely due to a better regenerative capacity than human muscle, as suggested by the upregulation of muscle transcription factors. Also the dystrophin homologue utrophin, in the mouse, seems better capable of replacing dystrophin. *Mdx/utrn*$^{-/-}$ mice, lacking both dystrophin and utrophin, mimic the DMD patients' phenotype more closely, since they are severely affected, develop kyphosis, show breathing difficulties and do not live beyond 3 months (Deconinck et al. 1997b, Grady et al. 1997a).

There is no cure for DMD, but several therapeutic approaches, aiming to restore the expression of functional dystrophin, are currently under investigation in clinical trials (Goemans et al. 2011;Cirak et al. 2011;Bowles et al. 2011;Malik et al. 2010;Skuk et al. 2006). It is, however, unknown which dystrophin levels are needed to obtain a beneficial effect in DMD patients and whether correction of muscle function, histopathology and overall vitality require similar dystrophin levels.

Previously, two attempts have been undertaken to elucidate this. The *mdx*^{3cv} mice (expressing ~5% of truncated dystrophin lacking exon 65/66) were crossed into two different utrophin negative backgrounds (Rafael et al. 1999;Li et al. 2010). In the first study, these mice

were as severely affected as *mdx/utrn*$^{-/-}$ mice and no increase in the 12-week life span was observed. By contrast, (Li et al. 2010) the other study reported mice with a median survival of 79 weeks. Despite discrepancies between these models, their common drawback is that dystrophin expression is limited to <5% of a compromised dystrophin in the *mdx*^{3cv} model, whereas expression of a broader range of a partially functional dystrophin is preferred.

We here determined the effects of a broad range of low dystrophin levels against an *utrn*$^{-/-}$ background on muscle integrity, pathology, function and overall viability in the *mdx/utrn*$^{-/-}$*/Xist*$^{\Delta hs}$ mouse model. These mice have mutations in the *Xist* gene of one X-chromosome leading to skewed X-inactivation, combined with a defective dystrophin on the other X-chromosome, resulting in low dystrophin levels (Newall et al. 2001). Introducing low, but varying, dystrophin levels resulted in improvements in life span and pathology, ranging from that of severely affected *mdx/utrn*$^{-/-}$ to almost wild type mice. Dystrophin expression correlated with survival and severity of pathology: where <4% dystrophin already significantly improved life span and muscle function, levels of >4% dystrophin not only further improved this, but also protected muscles against damage.

Materials and methods

Animal care

All mice participating in this study were bred at the animal facility at the LUMC where they were housed in groups in individually ventilated cages with 12-h light-dark cycles. Mice were given standard chow and water *ad libitum*. The generation of *mdx/utrn*$^{-/-}$*/Xist*$^{\Delta hs}$ mice was performed in two steps. First, we crossed *Xist*$^{\Delta hs}$ females (Newall et al. 2001) with *hDMD*$^{+/-}$*utrn*$^{-/-}$ males. The *hDMD* mouse has an intact and functional copy of the human dystrophin gene, which can functionally compensate for the lack of mouse dystrophin ('t Hoen et al. 2008). Offspring were genotyped, and *utrn*$^{+/-}$*/Xist*$^{\Delta hs}$ mice lacking the *hDMD* gene were interbred to generate *utrn*$^{-/-}$*/Xist*$^{\Delta hs}$ mice. *Utrn*$^{-/-}$*/Xist*$^{\Delta hs}$ males were then crossed with *mdx/utrn*$^{+/-}$ females, giving rise to female *mdx/utrn*$^{-/-}$*/Xist*$^{\Delta hs}$ mice, which were used for experiments (Fig. 1A). The *Xist*$^{\Delta hs}$ mice were a kind gift from Prof. Brockdorff (MRC Clinical Sciences Centre London, UK, current affiliation Department of Biochemistry, University of Oxford, UK). Genotyping was performed on DNA obtained from ear biopsies by PCR analysis (primers and PCR conditions available on request). All experiments were approved by the Animal Experimental Committee (DEC) of the LUMC. Mice that became too severely affected (body weight drop of >15% within two days) were sacrificed. All mice used in the study were females, except for the *mdx/utrn*$^{-/-}$ mice of which both genders were used.

Determination of functional performance

To assess forelimb grip strength, mice were suspended above the grid of a strength meter (Columbus Instruments, USA), which they instinctively grasped and were then pulled backwards forcing release of the grid. Five measurements were made in a row and the average of the three highest measured values was divided by the body weight in grams and used for further analysis.

To determine running performance on the rotarod (Ugo Basile, Italy), mice were placed on the rotating tube, which accelerated from 5 to 45 rotations per min within 15 sec. Mice had to run for a maximum of 500 sec without falling. Individuals that fell off earlier were given two more tries. The longest running time was used for analysis.

The two limb hanging wire test was conducted with a metal cloth hanger that was secured above a cage filled with bedding. Mice had to grasp the wire with the two forelimbs and were then released. During the 10 min session, all limbs and the tail were used depending on the

functional ability of the mouse. Mice that were not able to hang for the maximum time were allowed two more tries. Maximum hanging time was used for analysis.

For the four limb hanging wire test, mice were placed on a grid, which was turned upside down above a cage filled with bedding, forcing mice to hang using four limbs from the start of the test onwards. The session ended when the mice had hung for 10 min or otherwise after three sessions. Maximum hanging time was used for analysis. When possible, standardized operating procedures from the TREAT-NMD network were implemented (http://www.treat-nmd.eu/resources/research-resources/dmd-sops/).

Blood biomarker analysis

At the age of 8 and 14 weeks blood was collected via the tail to determine serum biomarker levels of matrix metallopeptidase-9 (MMP-9), tissue inhibitor of metalloproteinases-1 (TIMP-1) and vascular endothelial growth factor (VEGF) (Nadarajah et al. 2011;Saito et al. 2009). The mouse MMP-9 (total) immunoassay kit (catalog number MMPT90), mouse TIMP-1 immunoassay kit (catalog number MTM100) and mouse VEGF immunoassay kit (catalog number MMV00) were purchased from R&D systems (UK). Collected blood was allowed to clot at room temperature for 10 min before centrifuging (1700 x *g* for 10 min at 4°C) and stored at -80°C, before use. Age and gender-matched C57BL/10ScSnJ ($n = 4$) and *mdx/utrn*$^{-/-}$ mice ($n = 4$) were used as controls.

Plasma creatine kinase (CK) levels were determined in blood that was obtained via the tail and collected in a Minicollect tube (0.8ml Lithium Heparin Sep, Greiner bio-one, Austria). CK levels were determined with Reflotron CK test strips in the Reflotron plus machine (Roche diagnostics Ltd, UK).

Heart function assessment

Mice were transported to the Faculty of Science at the University of Leiden where they were housed for at least one week to acclimatize. Heart function was assessed by Magnetic Resonance Imaging (MRI) in a vertical 9.4T magnet with 89 mm bore size, equipped with a 1 T/m gradient system (Bruker BioSpin, Germany), using a quadrature birdcage coil with an inner diameter of 30 mm. Mice were anesthetized by inhalation of 2% isoflurane in a 1:1 mixture of oxygen and air. Respiratory rate was monitored during the scan with a respiratory pad and kept between 50-80 respirations per minute. Image acquisition was done with Bruker Paravision 5.0 software and took approximately 30 min per mouse including animal setup. A retrospectively-gated Intragate sequence was used with flip angle 10º; repetition time 8.5 ms; echo time 1.86 ms; field-of-view 2.56x2.56 cm^2; matrix 192x192; in-plane resolution 133 μm. We made 8-9 short-axis slices of the heart with a slice thickness of 1 mm and 200 repetitions per slice. The navigator echo was placed in-slice. Images were reconstructed to 18 frames per heart cycle. Scans were oriented on the left ventricle (Verhaart et al. 2011). Mice were sacrificed by cervical dislocation after completion of the scans. The scans were analyzed with MASS for MICE software (developed at the LUMC, Division of Image Processing (LKEB))(van der Geest et al. 1997;van der Geest and Reiber 1999). The endo and epicardial contours of both ventricles were drawn manually for each image. The end diastolic and systolic phase was computed by the software and a maximum mass difference of 10% was accepted for both ventricles. When this criterion was met, end diastolic and systolic volume were determined and based on these values stroke volume (end diastolic volume – end systolic volume), ejection fraction (stroke volume/end diastolic volume*100%) and cardiac output (stroke volume*heart rate) were calculated automatically. One *mdx/utrn*$^{-/-}$*/Xist*$^{\Delta hs}$ mouse was left out of the analysis as the scan was made with an incorrect angle.

Western blot analysis

Protein was isolated from the quadriceps and heart in 1 ml buffer (1.25 M Tris-HCl pH 6.8, 20% (v/v) glycerol and 25% (w/v) SDS) in MagNA Lyser green beads in the MagNA Lyser (Roche Diagnostics, the Netherlands). The BCA protein assay kit (Thermoscientific, Il, USA) was used according to the manufacturer's instructions to determine protein concentration. Subsequently, the protein solution was complemented with 5% (v/v) β-mercaptoethanol and 0.001% (w/v) bromophenol blue. The Trans-blot Turbo system (BioRad, the Netherlands) was used for Western blotting (Hulsker et al. manuscript in preparation). Samples (30 µg) were heated at 95°C for 5 min and 20 µl was loaded on 1.0 mm thick native PAGE Tris acetate (polyacrylamide) gels, with a linear resolving gel gradient of 3-8% (BioRad, the Netherlands). The gels were run on ice for 1 hr at 75 V (0.07 A) and 2 hrs at 150 V (0.12 A) in the running buffer (XT Tricine; BioRad; the Netherlands). When changing voltage, running buffer was refreshed to maintain pH. Proteins were blotted to membrane using the ready to use Trans-Blot Turbo transfer packs and the Trans-Blot Turbo transfer system at 2.5 A (25 V) for 10 min. Membranes were blocked for 1 hr with 5% (w/v) non-fat dried milk (Campina Melkunie, the Netherlands) in TBS and washed three times with TBST for 10 min. Primary dystrophin antibody NCL-DYS1 (dilution 1:125 in TBS, Novacastra, UK) and loading control α-actinin (dilution 1:5000 in TBS, AB72592, Abcam) were incubated overnight at 4°C. After the membranes were rinsed three times with TBS for 10 min, they were incubated for 1 hr with fluorescent IRDye 800CW goat-anti-mouse (dilution 1:5000, Li-Cor, NE, USA) and IRDye 650LT donkey-anti-rabbit (1:10,000, Li-Cor, NE, USA). Protein quantification was performed with the Odyssey system and software (Li-Cor, NE, USA).

Histological examination

After sacrifice, skeletal muscles and heart were dissected and snap frozen in 2-methylbutane (Sigma-Aldrich, The Netherlands) cooled in liquid nitrogen. For the quadriceps and heart, sections of 8 µm were cut along the entire length of the muscle with a Shandon cryotome (Thermo Fisher Scientific Co., Pittsburgh, PA, USA) with an interval of 240 µm between the sections. Sections of the quadriceps were stained with Harris Haematoxylin and Eosin (H&E), according to conventional histological procedures. From the middle section of the muscle, images covering the entire muscle were captured with a light microscope (Leica DM LB, Leica Microsystems, The Netherlands) and a Leica DC500 camera with Leica IM50 software (Leica Microsystems, The Netherlands) at a 5 times magnification. Blending and background correction was performed with Adobe Photoshop CS3 version 10.0.1. Freely available ImageJ software with the H&E colour deconvolution plugin (Rasband, W.S., ImageJ, U. S. National Institutes of Health, Bethesda, Maryland, USA, http://rsb.info.nih.gov/ij/) was used to determine the fibrotic/necrotic percentage of the entire cross-section by two individuals in a double blinded manner, as described previously (van Putten et al. 2010).

Fiber size and the percentage of centralized nuclei were determined with Mayachitra Imago 1 (http://www.mayachitra.com/imago/) (van Putten et al. manuscript in preparation) on five randomly captured images of the quadriceps stained with dystrophin (dilution 1:50, C-20, Santa Cruz, Germany) and laminin (dilution 1:50, ab11575, Abcam, UK) where donkey-anti-goat Alexa 594 and donkey-anti-rabbit Alexa 488 (dilution 1:1000, Invitrogen, the Netherlands) were respectively used as a secondary antibody. Slides were mounted with Vectashield mounting medium including DAPI (Vector Labs, Germany).

Cryosections of the heart were stained with goat-anti-Collagen type 1 (dilution 1:100, 1310-01 Southern Biotech, USA), rabbit-anti-goat Alexa 594 (dilution 1:1000, Invitrogen, The Netherlands) and DAPI. Sections were examined with a Leica DM RA2 fluorescent microscope at

a 16 times magnification and images covering the entire heart were captured with a Leica DC350FX snapshot camera. The percentage of fibrosis was quantified with ImageJ software (Rasband, W.S., ImageJ, U. S. National Institutes of Health, Bethesda, Maryland, USA, http://rsb.info.nih.gov/ij/).
Co-localization of dystrophin and β-dystroglycan was performed on a transverse cross-section of the quadriceps, stained with dystrophin (dilution 1:50, C-20, Santa Cruz, Germany) and β-dystroglycan (dilution 1:50, NCL β-DG, Novocastra UK). The staining was completed with donkey-anti-rabbit Alexa 488 (dilution 1:1000, Invitrogen, the Netherlands) and Fluorescein Avidin solution of the MOM kit (Vector Laboratories, UK), respectively.

RT-qPCR analysis

For total RNA isolation, tissue was disrupted in MagNA Lyser Green Beads tubes (Roche diagnostics Ltd, UK) with Tripure isolation reagent (Roche diagnostics Ltd, USA). Isolation was performed with chloroform, and RNA precipitated with isopropanol. The NucleoSpin RNA II kit including a DNAse digestion (Bioke, the Netherlands) was used for RNA purification. RNA integrity and concentration was checked with a total RNA nano-chip assay on a labchip bioanalyzer (Agilent, The Netherlands) and used for cDNA synthesis with random hexamer primers. Expression of genes involved in regeneration (*Myog*, *eMHC3*), inflammation (*Cd68*, *Lgals3*), fibrosis (*Lox*, *Timp-1, Nox4, Ctgf*) and heart function (*Serca2a*, *Nppa*) was determined by Sybr Green based Real Time qPCR (95°C 10 sec, 60°C 30 sec, 72°C 20 sec, 45 cycles followed by melting curve analysis) on the Roche Lightcycler 480 (Roche diagnostics Ltd., UK). *Gapdh* was used as a reference gene, since the expression of this gene did not differ between different muscles and mouse strains or over time. Primer efficiencies were determined and analysis was performed with LinREgPCR version 11.1 (Ramakers et al. 2003).

Statistics

Statistical analyses were performed with statistical software in R (package 2.11.1) and SPSS 17.0.2. (SPSS, Inc., Chicago, IL, USA). Cox regression analysis was used to test for differences in survival between groups (Fig. 1C and 2D). Figures 1, 3, 5 and 7 summarize the data, i.e. showing the mean and standard error of the mean per genotype and age. We applied an analysis of covariance (ANCOVA) to the temporal functional performance and CK level data, to overcome applying separate tests for each age between genotypes as this suffers from multiple testing and ignores the age trend. Age was used as a continuous variable and genotype as a categorical variable. Comparisons between *mdx/utrn*$^{-/-}$ mice with the other strains were performed on data obtained between the age of 4 and 11 weeks, while for comparisons between the other strains, data from all ages was taken into account. In choosing the appropriate model we applied the principle of parsimony. Given the application of tests for several different variables, we considered $P<0.01$ as significant. A one-way ANOVA was used to analyze the serum biomarkers, the percentage of fibrosis, central nucleation and the gene expression data, followed by the Bonferroni post-hoc test in case of significance. For the fiber size distributions, the one-way ANOVA test was applied on the median of all fibers of each mouse and in case of significance ($P<0.05$) followed by a Bonferroni post hoc test. Spearman correlation was used to test for correlations. The heart function data were analyzed with the one-way ANOVA in case of significance ($P<0.05$) a LSD post hoc test was applied. For all these tests a $P<0.05$ was considered significant.

Results

Low dystrophin levels improve muscle function

Mdx/utrn$^{-/-}$*/Xist*$^{\Delta hs}$ females were bred and used to study the potential of low dystrophin levels to improve motor function in the absence of utrophin (fig. 1A). *Mdx/utrn*$^{-/-}$*/Xist*$^{\Delta hs}$ (n = 20) and *mdx/utrn*$^{-/-}$ (n = 9) mice underwent a functional test regime consisting of four different tests per week for a maximum of 12 weeks (van Putten et al. 2010). Mice were sacrificed when the burden of the phenotype was moderate/severe, or at completion of the functional test regime (aged 16 weeks). Post mortem dystrophin levels of the quadriceps were determined by western blot. No dystrophin was observed for *mdx/utrn*$^{-/-}$ mice, while for *mdx/utrn*$^{-/-}$*/Xist*$^{\Delta hs}$ mice levels varied between 3-16.2% (fig. 1B). In cross-sections of *mdx/utrn*$^{-/-}$*/Xist*$^{\Delta hs}$ mice, dystrophin co-localized with β-dystroglycan, suggesting that the dystrophin-glycoprotein complex was restored (For a representative see picture fig. S1A).

Mdx/utrn$^{-/-}$*/Xist*$^{\Delta hs}$ mice were divided into two groups based on dystrophin levels either below or above the median dystrophin level observed (3.9%). Most strikingly, 14 out of 20 *mdx/utrn*$^{-/-}$*/Xist*$^{\Delta hs}$ mice survived the entire test period, while none of the *mdx/utrn*$^{-/-}$ mice did (P<0.0001, fig. 1C). Mice with >4% dystrophin outlived mice with <4% dystrophin (P<0.001).

Creatine kinase (CK) levels reduced in a dystrophin level dependent manner (fig. 1D). Mice with >4% dystrophin had lower CK levels than mice with <4% dystrophin (average 2604 U/L vs 3860 U/L, P<0.05), but levels did not completely normalize to wild type (<500 U/L, P<0.0001).

Maximum times obtained in the two limb hanging wire test for *mdx/utrn*$^{-/-}$*/Xist*$^{\Delta hs}$ mice were higher than those for *mdx/utrn*$^{-/-}$ mice (>4% 404 sec and <4% 298 sec, vs 71 sec for *mdx/utrn*$^{-/-}$, P<0.0001, fig. 1E). Mice with >4% dystrophin outperformed mice with <4% dystrophin (P<0.01). However, performance was not completely restored to wild type (594 sec, P<0.0001). A similar pattern was obtained for the four limb hanging wire test, in which all *mdx/utrn*$^{-/-}$*/Xist*$^{\Delta hs}$ mice outperformed *mdx/utrn*$^{-/-}$ mice (>4% 496 sec and <4% 407 sec, vs 163 sec for *mdx/utrn*$^{-/-}$, P<0.01, fig. 1F). Expression of >4% dystrophin improved outcome over <4% dystrophin (P<0.001), but did not completely restore it to wild type (586 sec, P<0.001). Normalized forelimb grip strength of *mdx/utrn*$^{-/-}$*/Xist*$^{\Delta hs}$ mice was greater than *mdx/utrn*$^{-/-}$ mice (>4% 59 grams and <4% 58 grams, vs 38 gram for *mdx/utrn*$^{-/-}$, P<0.0001), and lower than wild type mice (79 grams, P<0.0001, fig. 1G). *Mdx/utrn*$^{-/-}$*/Xist*$^{\Delta hs}$ mice outperformed *mdx/utrn*$^{-/-}$ mice on the rotarod (>4% 260 sec and <4% 222 sec, vs 51 sec for *mdx/utrn*$^{-/-}$, P<0.0001, fig. 1H), but performance did not differ between them. In our experience, wild type mice (*Xist*$^{\Delta hs}$ and C57BL/10ScSnJ) do not perform well on the rotarod (van Putten et al. 2012a;van Putten et al. 2012b). *Xist*$^{\Delta hs}$ mice ran longer than *mdx/utrn*$^{-/-}$ mice (183 sec vs 51 sec, P<0.0001), but shorter than *mdx/utrn*$^{-/-}$*/Xist*$^{\Delta hs}$ mice. In summary, for all functional tests, <4% dystrophin already substantially improves motor function compared to *mdx/utrn*$^{-/-}$ mice, while >4% dystrophin further improves hanging performance.

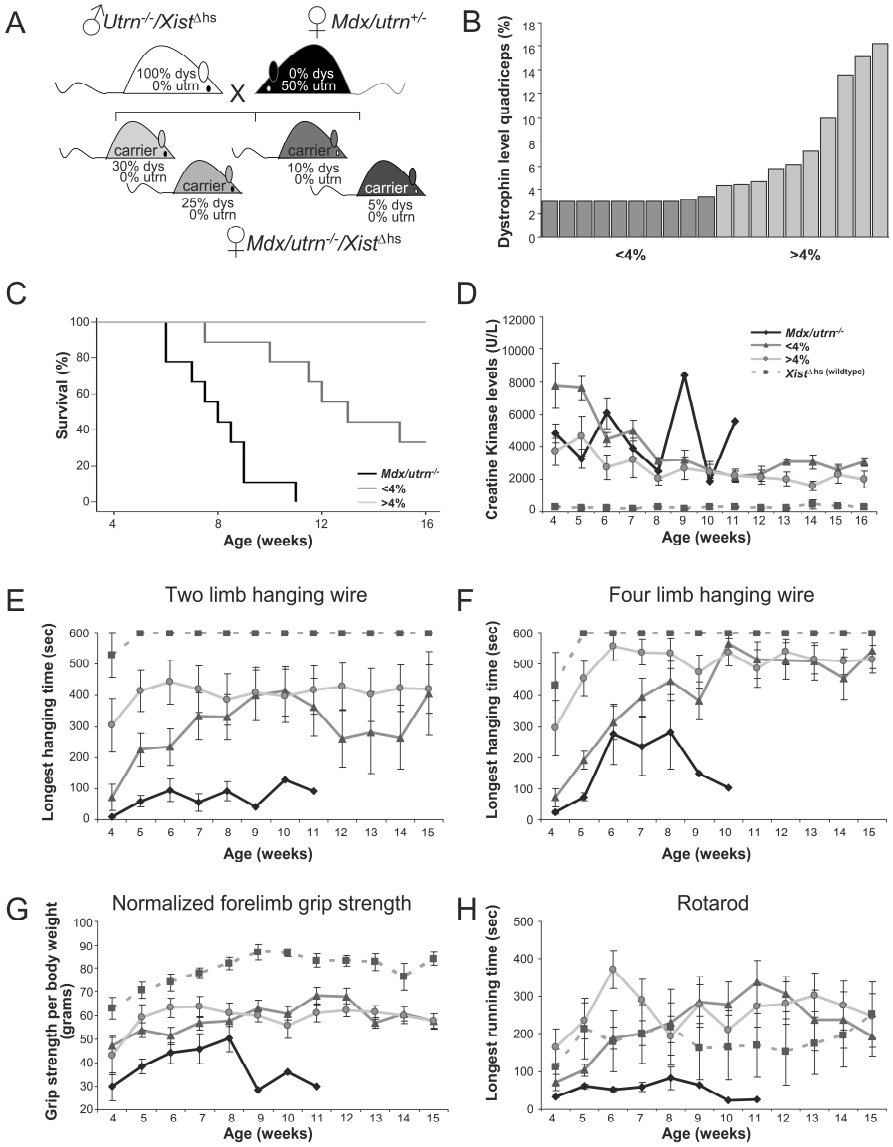
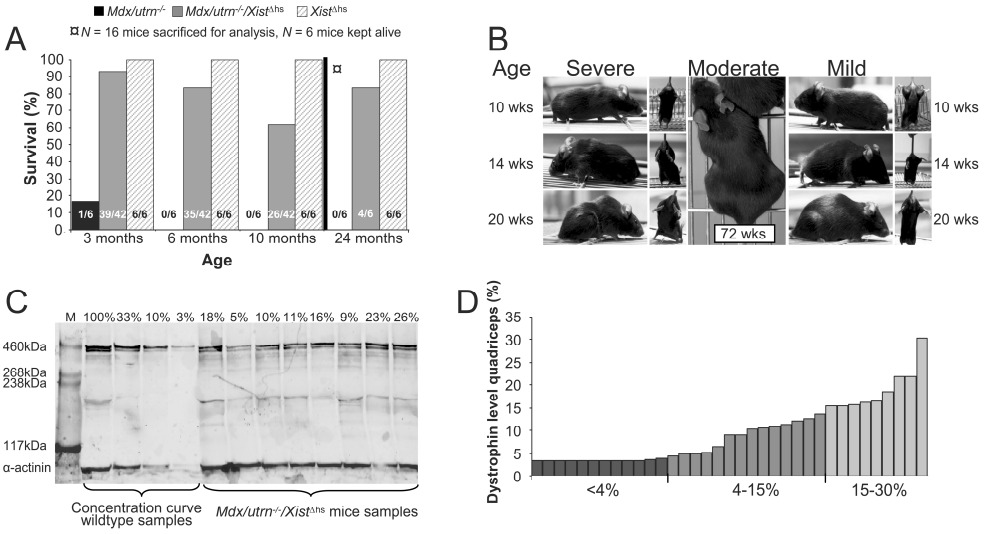
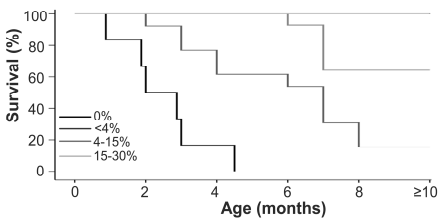


Fig. 1. Survival and functional performance of *mdx/utrn*$^{-/-}$/*Xist*$^{\Delta hs}$ mice. (**A**). *Mdx/utrn*$^{-/-}$ females expressing low dystrophin levels due to skewed X-inactivation were bred by crossing *utrn*$^{-/-}$/*Xist*$^{\Delta hs}$ males with *mdx/utrn*$^{+/-}$ females. (**B**). *Mdx/utrn*$^{-/-}$/*Xist*$^{\Delta hs}$ mice were grouped based on dystrophin levels of the quadriceps, which varied between 3 and 16.2%. (**C**). Levels <4% dystrophin increased life span in *mdx/utrn*$^{-/-}$/*Xist*$^{\Delta hs}$ mice (P<0.0001), while all *mdx/utrn*$^{-/-}$ mice died prematurely. Expression of >4% dystrophin prevented premature death. (**D**). CK levels decreased in a dystrophin level dependent manner in *mdx/utrn*$^{-/-}$/*Xist*$^{\Delta hs}$ mice, but did not completely normalize to wild type levels. (**E**). *Mdx/utrn*$^{-/-}$/*Xist*$^{\Delta hs}$ mice outperformed *mdx/utrn*$^{-/-}$ mice in the two limb hanging wire test, but performed worse compared to wild type mice (P<0.0001). >4% dystrophin resulted in better hanging times than <4% dystrophin (P<0.01). (**F**). *Mdx/utrn*$^{-/-}$/*Xist*$^{\Delta hs}$ mice hang longer compared to *mdx/utrn*$^{-/-}$ mice in the four limb hanging wire test. Expression of >4% dystrophin further increased performance (P<0.001), although it was worse than wild type mice (P<0.001). (**G**). *Mdx/utrn*$^{-/-}$/*Xist*$^{\Delta hs}$ mice had a greater forelimb grip strength than *mdx/utrn*$^{-/-}$ mice (P<0.0001). (**H**). Rotarod running times of *mdx/utrn*$^{-/-}$/*Xist*$^{\Delta hs}$ mice exceeded those of *mdx/utrn*$^{-/-}$ and wild type mice (P<0.0001). Data are represented as mean±SEM.



E

	Phenotype			
Dys level		Severe	Moderate	Mild
	<4%	46%	23%	23%
	4-15%	7%	28%	64%
	15-30%	0%	0%	100%



G

Mouse	Dys level	Phenotype	Life span (months)	Cause of death
1	3%	Severe	17	Muscular dystrophy
2	27%	Moderate	24.5	Muscular dystrophy
3	35%	Mild	17.5	Black gall bladder, pale liver
4	55%	Mild	25.7	Agressive tumor
5	N.D.	Mild	25	Natural cause; ageing
6	N.D.	Mild	26	Alive at time of submission

Fig. 2. Long term survival of *mdx/utrn*$^{-/-}$*/Xist*$^{\Delta hs}$ mice. (**A**). *Mdx/utrn*$^{-/-}$*/Xist*$^{\Delta hs}$ mice significantly outlived *mdx/utrn*$^{-/-}$ mice, which all died prematurely, as at the age of 10 months, 26 out of 42 mice were still alive. Sixteen mice were sacrificed for analysis before the age of one year and six mice were allowed to life, of which four were still alive at the age of two years. (**B**). *Mdx/utrn*$^{-/-}$*/Xist*$^{\Delta hs}$ mice could be discriminated into three phenotypically distinct groups based on disease severity. Severely affected mice developed similar symptoms as *mdx/utrn*$^{-/-}$ mice although at a much older age. Moderately affected mice developed malformations of the hips possibly combined with kyphosis, while mildly affected mice were similar to wild type mice. (**C**). Representative western blot of the quadriceps. The percentage of individual mice was assessed using a concentration curve made from wild type samples. (**D**). Dystrophin levels of the quadriceps ranged from 3-30.4%, which was used to divide mice into three groups. (**E**). Dystrophin expression correlated to the phenotype of the mice. (**F**). Dystrophin expression correlated to phenotypic appearance and life span (R=0.718 $P<0.0001$). Levels of <4% dystrophin improved life span, with 63% of these mice still alive at the age of 6 months ($P<0.01$). Expression of higher dystrophin levels further improved life span. (**G**) Overview of the dystrophin levels of the quadriceps, clinical features, life span and cause of death of six *mdx/utrn*$^{-/-}$*/Xist*$^{\Delta hs}$ mice that were kept alive. Data are represented as mean.

Dystrophin levels of <4% improve long term survival

To more thoroughly investigate life span of *mdx/utrn*$^{-/-}$*/Xist*$^{\Delta hs}$ mice, a longer survival study was performed in 42 *mdx/utrn*$^{-/-}$*/Xist*$^{\Delta hs}$ and 6 *mdx/utrn*$^{-/-}$ mice. Several other aspects of skeletal muscle and heart function were assessed along with histopathology. *Mdx/utrn*$^{-/-}$ mice again became severely affected as they developed kyphosis, could not spread their hindlimbs and had difficulties moving and breathing, leading to death generally before the age of 12 weeks (fig. 2A). Disease severity of *mdx/utrn*$^{-/-}$*/Xist*$^{\Delta hs}$ mice could be divided into three phenotypically distinct subgroups (fig. 2B). The first subgroup developed similar symptoms as *mdx/utrn*$^{-/-}$ mice, including severe muscle weakness, kyphosis and inability to spread their hindlimbs. Notably, these mice exhibited these pathological features at an older age than *mdx/utrn*$^{-/-}$ mice and had a similar appearance to wild type mice before onset. Mice of the second subgroup had a moderate phenotype; they developed malformations of the hips, leading to an unnatural way of walking (video available on request). This was observed either in presence or absence of kyphosis. The last subgroup exhibited a mild phenotype and appeared comparable to wild type mice. The age of death depended on the age at onset of pathology and the degree of severity. Generally, mice with a moderate or mild phenotype outlived those with a severe phenotype.

For each mouse studied, post mortem dystrophin levels of the quadriceps were determined by western blot (fig. 2C). Levels varied between 3-30.4% and were higher than those observed for animals sacrificed after 16 weeks. We attribute this to selection of dystrophin positive fibers over time (Danko et al. 1992;Karpati et al. 1990), or transcriptional rate exceeding protein turnover rate, causing accumulation of protein over time. Based on the dystrophin level, mice were divided into three groups (fig 2D). *Mdx/utrn*$^{-/-}$*/Xist*$^{\Delta hs}$ mice belonging to the severe phenotype mostly had <4% dystrophin (fig 2E). Of these, 62% were still alive at the age of 6 months, reflecting an improved life span compared to *mdx/utrn*$^{-/-}$ mice (P<0.01). Dystrophin levels between 4-15% generally resulted in a moderate or mild phenotype and increased survival compared to *mdx/utrn*$^{-/-}$ mice (P<0.0001). Of these mice 100% were still alive after 6 months and 64% after 10 months (fig 2F). Notably, their life span was further improved over the mice with <4% dystrophin (P<0.01). All mice with 15-30% dystrophin survived until the age of 10 months after which they were sacrificed for analysis, extending their life span yet further than all other mice (P<0.05). The Spearman correlation test confirmed a very strong positive correlation between dystrophin expression and life span (R=0.718 P<0.0001).

Six *mdx/utrn*$^{-/-}$*/Xist*$^{\Delta hs}$ mice were kept alive (fig 2G). At the time of submission, one mouse aged 26 months, is still alive, looking similar to age-matched wild type mice. Three out of the five remaining mice died of non-muscle related causes, aged 17.5, 25 and 25.7 months and expressing >35% dystrophin. The other two mice died as a consequence of their muscular dystrophy aged 17 (fig. S1B) and 24.5 months (fig. S1C). These mice had a severe and moderate phenotype and expressed 3% and 27% dystrophin respectively.

Low dystrophin levels improve muscle function and normalize serum biomarker levels

During the survival study, all mice were subjected to two limb hanging wire and forelimb grip strength tests once every 6 weeks (van Putten et al. 2010). Hanging performance clearly depended on dystrophin expression. Mice with <4% dystrophin hung shorter than mice with 4-15% dystrophin (135 vs 369 sec, P<0.0001, fig 3A), while mice with 15-30% dystrophin hung even longer (499 sec, P<0.01). Forelimb grip strength of mice with <4% dystrophin was lower than that of mice with 4-15% dystrophin (55 grams vs 60 grams, P<0.05, fig. 3B), which were as strong as mice with 15-30% dystrophin (63 grams, P=0.16).

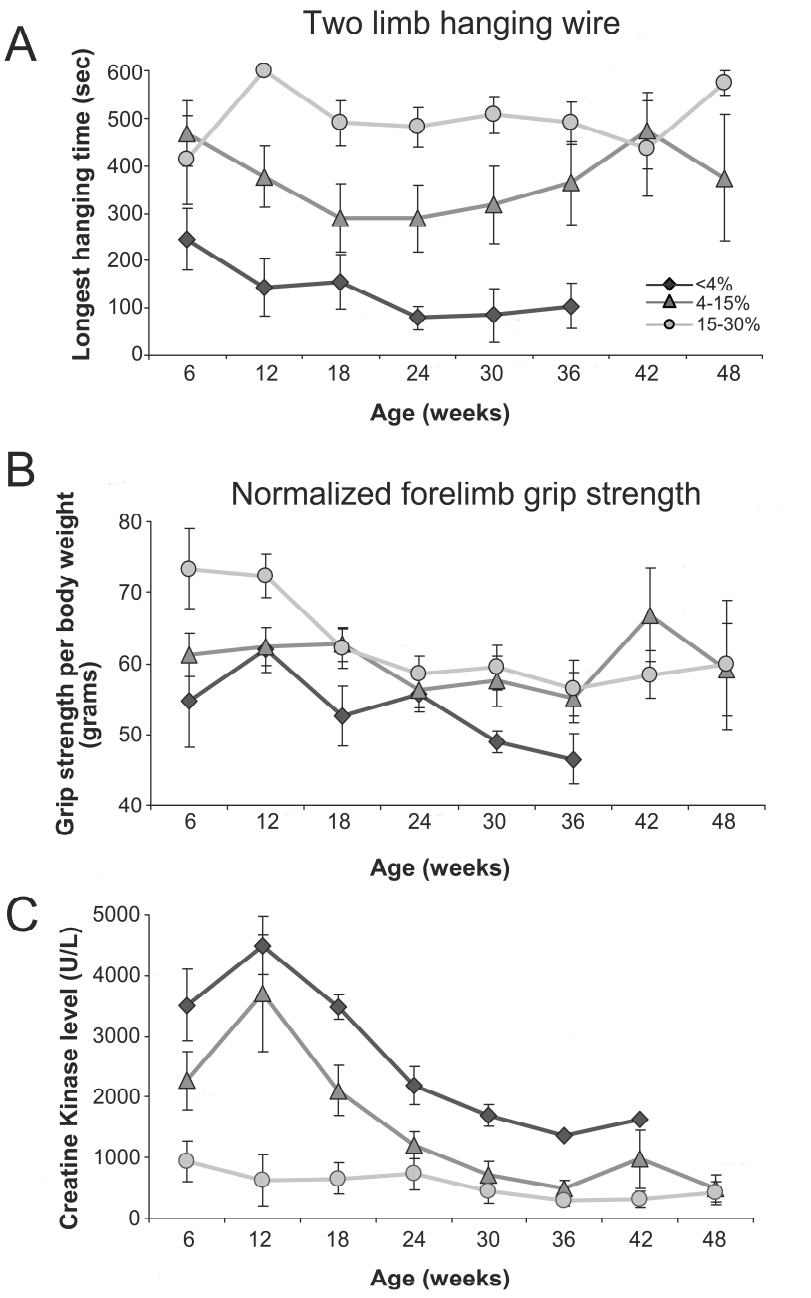


Fig. 3. Functional performance and plasma CK levels. (**A**). Two limb hanging wire performance was impaired in mice with <4% dystrophin compared to mice with 4-15% dystrophin (P<0.001), and mice expressing 15-30% dystrophin (P<0.001). (**B**). Mice with 4-15% dystrophin had a larger normalized forelimb grip strength than mice with <4% dystrophin (P<0.05). Strength did not further improve in mice with 15-30% dystrophin. (**C**). CK levels were elevated in mice with <4% dystrophin compared to mice with >4% dystrophin. For all mice, levels dropped over time and reached wild type levels from 30 weeks of age onwards. Data are represented as mean±SEM.

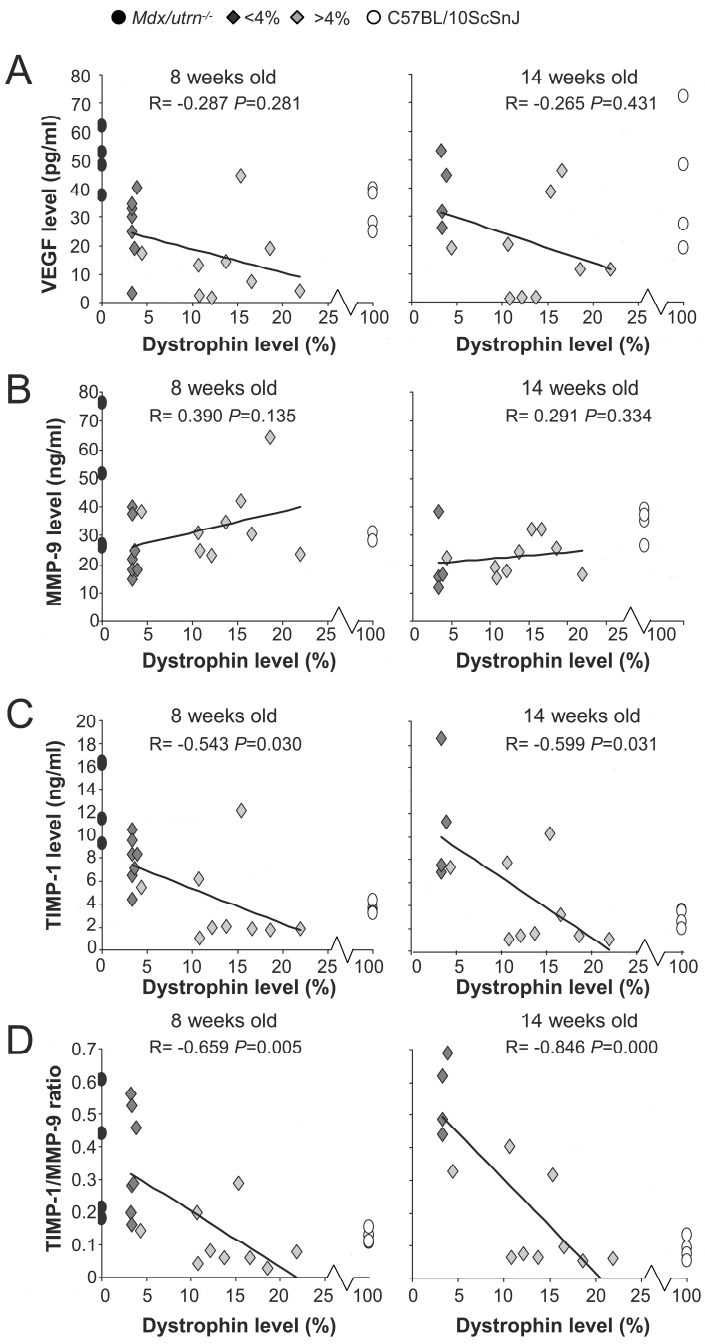


Fig. 4. Serum levels of VEGF, MMP-9 and TIMP-1 at 8 and 14 weeks of age. (**A**). VEGF levels already decreased in mice with <4% dystrophin. (**B**). MMP-9 levels normalized in mice with <4% dystrophin. (**C**). TIMP-1 levels showed a clear dystrophin level dependent normalization. Already <4% dystrophin decreased levels compared to *mdx/utrn*$^{-/-}$ mice while >4% dystrophin resulted in further decrement. (**D**). The TIMP-1/MMP-9 ratio normalized to wild type levels in mice with >4% dystrophin.

Plasma CK levels, assessed every 6 weeks throughout the study, clearly fell in all mice over time. Mice with <4% dystrophin had higher CK levels than mice with 4-15% dystrophin (3251 vs 1785 U/L, $P<0.0001$, fig. 3C). CK levels fell further in mice with 15-30% dystrophin, reaching wild type levels from 30 weeks onwards (554 U/L, $P<0.0001$).

Serum levels of VEGF (angiogenesis (Saito et al. 2009)), MMP-9 and TIMP-1 (tissue integrity (Nadarajah et al. 2011;van Putten et al. 2012a)) were analyzed on a group of 20 *mdx/utrn*$^{-/-}$/*Xist*$^{\Delta hs}$, 4 *mdx/utrn*$^{-/-}$ and 4 C57BL/10ScSnJ mice at the age of 8 and 14 weeks (fig. 4). Levels of all biomarkers were elevated in *mdx/utrn*$^{-/-}$ compared to wild type mice. At 8 weeks, VEGF levels were already decreased with < 4% dystrophin ($P<0.05$), whereas >4% dystrophin also normalized TIMP-1 and the TIMP-1/MMP-9 ratio to wild type levels. At 14 weeks, <4% dystrophin decreased VEGF and MMP-9 levels, whereas >4% dystrophin also normalized TIMP-1 levels and the TIMP-1/MMP-9 ratio. At both ages, dystrophin expression significantly correlated to TIMP-1 levels (8 weeks R= -0.543 $P=0.03$, 14 weeks R= -0.599 $P=0.03$) and the TIMP-1/MMP-9 ratio (8 weeks R= -0.659 $P=0.005$, 14 weeks R= -0.846 $P<0.001$).

Low dystrophin levels improve muscle pathology

A strong negative correlation was observed between dystrophin expression and the percentage of fibrosis and necrosis (R= -0.616 $P<0.0001$, fig. 5A). *Mdx/utrn*$^{-/-}$/*Xist*$^{\Delta hs}$ mice with <4% dystrophin had more fibrosis and necrosis than *mdx/utrn*$^{-/-}$ mice ($P<0.05$). This is possibly due to the age difference of the two groups (6-9 weeks and 7-40 weeks). Levels of fibrosis and necrosis dropped in mice expressing >4% dystrophin ($P<0.01$) and did not differ from wild type levels.

Fiber size distribution and the percentage of centrally nucleated fibers also normalized towards wild type levels in a dystrophin level dependent manner in mice expressing >4% dystrophin (fig. 5B-C). Dystrophin expression also correlated to the median of fiber surface area (R=0.779 $P<0.0001$) and central nucleation (R= -0.675, $P<0.0001$).

Finally, we quantified the expression of some biomarker genes involved in inflammation (*Cd68*, *Lgals3*), fibrosis (*Lox*, *Timp-1*) and regeneration (*eMHC3*, *Myog*) for the quadriceps (fig. 5D-F). Although the high inter group variation only occasionally resulted in significant differences, there is a clear pattern, in line with the histological data, that gene expression of *mdx/utrn*$^{-/-}$/*Xist*$^{\Delta hs}$ mice with <4% dystrophin is higher than *mdx/utrn*$^{-/-}$ mice, while >4% dystrophin results in a clear dystrophin level dependent normalization towards wild type levels.

Dystrophin level dependent improvement of heart pathology

At the age of 10 months, heart function of *mdx/utrn*$^{-/-}$/*Xist*$^{\Delta hs}$ mice ($n = 10$) was analyzed with Magnetic Resonance Imaging and compared with age and gender-matched *mdx*, *Xist*$^{\Delta hs}$ and C57BL/10ScSnJ mice ($n = 5$). Dystrophin levels of the heart ranged from 2.5-49.2% (median = 13.7, *stdev* = 17.3) and mice were divided into a low (2.5-10.9%, median = 4.3, *stdev* = 3.3), and high dystrophin level group (16.4-49.2%, median = 29.7, *stdev* = 14.3). Left ventricular ejection fraction of mice with low dystrophin levels was severely hampered, but improved in mice expressing higher dystrophin levels ($P<0.05$), although not to wild type levels ($P<0.01$, fig. 6).
Also stroke volume was significantly decreased ($P<0.05$) in all *mdx/utrn*$^{-/-}$/*Xist*$^{\Delta hs}$ mice. Right ventricular function was not affected in *mdx/utrn*$^{-/-}$/*Xist*$^{\Delta hs}$ mice. Dystrophin expression correlated to the ejection fraction of both ventricles (left R=0.817 $P=0.007$, right R=0.717 $P=0.03$).

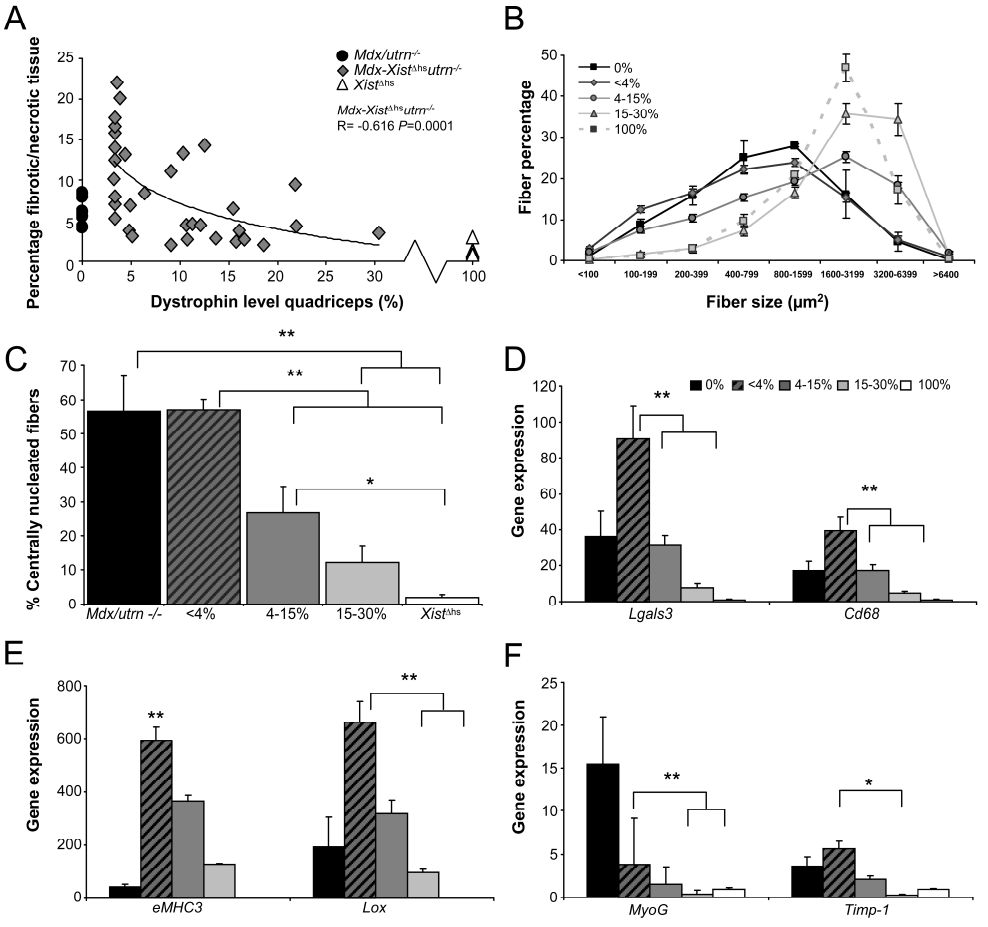


Fig. 5. Dystrophin levels and histopathology. Note that not all mice are of similar age; *mdx/utrn*$^{-/-}$ mice did not live beyond 12 weeks, while the age of *mdx/utrn*$^{-/-}$*/Xist*$^{\Delta hs}$ mice ranges from 7 weeks to 1 year. Data of *Xist*$^{\Delta hs}$ mice are from 16 week old animals. (**A**). Dystrophin expression negatively correlated to the percentage of fibrotic/necrotic tissue (R= -0.518 *P*<0.002). Mice with <4% dystrophin had more fibrotic/necrotic tissue compared to *mdx/utrn*$^{-/-}$ mice (*P*<0.05). (**B**). Fiber size distribution of mice with <4% dystrophin was comparable to that of *mdx/utrn*$^{-/-}$ mice, whereas 4-15% dystrophin reduced the number of small recently regenerated fibers. Distribution pattern of mice with 15-30% dystrophin closely resembled that of wild type mice. (**C**). Central nucleation was comparable for *mdx/utrn*$^{-/-}$ mice and mice with <4% dystrophin. Higher dystrophin levels resulted in a drop (*P*<0.01) although levels were still considerably higher than wild type. (**D-F**). Expression levels of genes involved in inflammation (*Lgals3, Cd68*), regeneration (*eMHC3, Myog*) and fibrosis (*Lox, Timp-1*) were upregulated in mice with <4% dystrophin compared to *mdx/utrn*$^{-/-}$ mice, whereas a dystrophin level dependent normalization was observed for the other groups. Single and double asterisks represent a *P*-value of <0.05 and <0.01 respectively. Data are represented as mean±SEM.

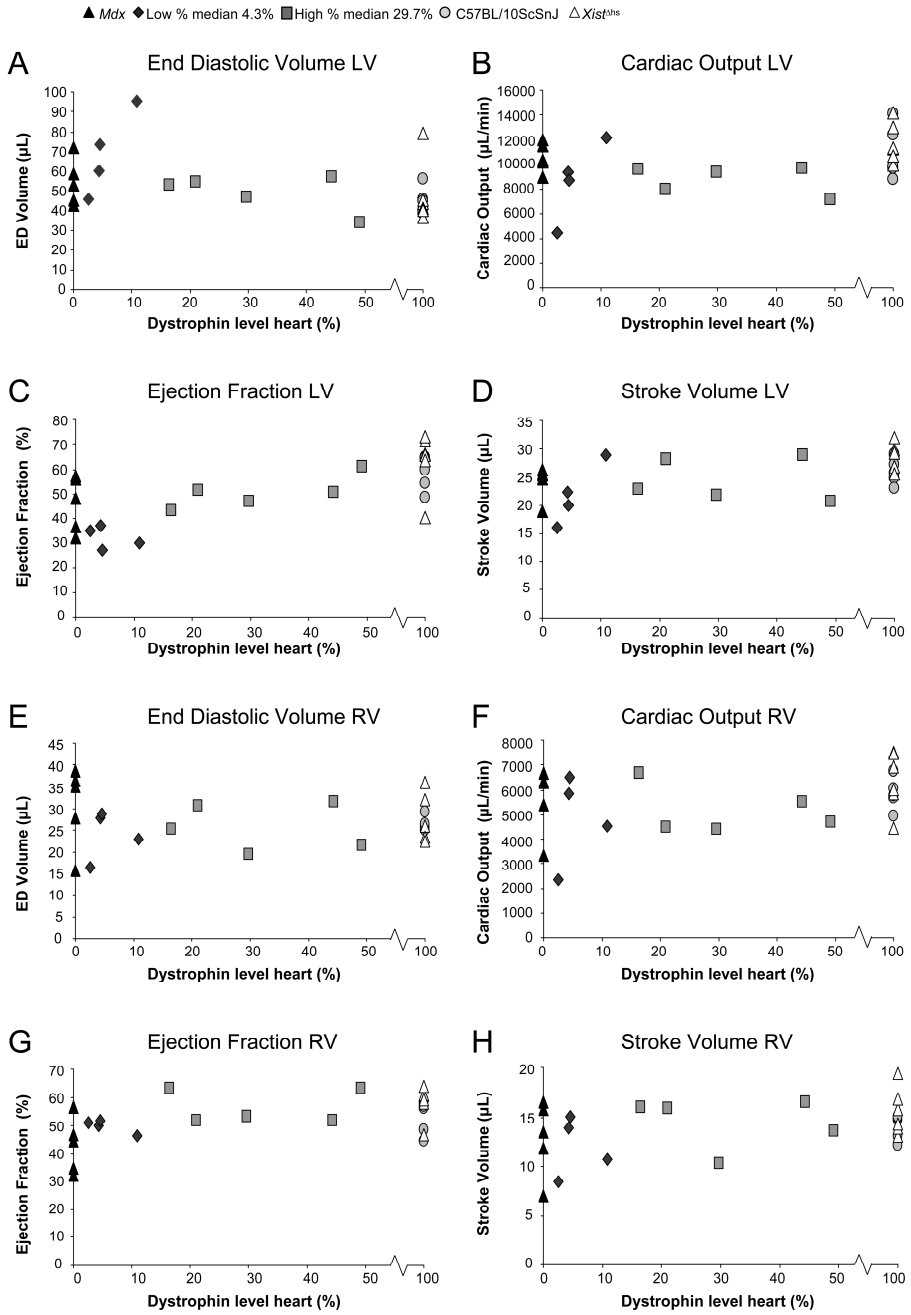


Fig. 6. Heart function. (**A-D**). Heart function of the left ventricle (LV). Ejection fraction and stroke volume of *mdx/utrn*$^{-/-}$*/Xist*$^{\Delta hs}$ mice with low dystrophin levels were severely hampered. This was restored by expression of high dystrophin levels, although not completely to wild type levels. (**E-H**). Heart function of the right ventricle (RV) was not affected in any of the *mdx/utrn*$^{-/-}$*/Xist*$^{\Delta hs}$ mice. Ejection fraction of *mdx* mice was significantly (P<0.05) smaller than that of wild type strains and mice with high dystrophin levels.

Dystrophin expression also negatively correlated to the extent of fibrosis (R= -0.733 $P<0.05$). The extensive fibrosis in mice with low dystrophin levels was markedly reduced in mice with higher levels of dystrophin ($P<0.05$, fig. 7A and S1D) although still exceeding wild type ($P<0.01$).

Expression of genes involved in inflammation, fibrosis and heart function was elevated in hearts of all dystrophic mice compared to wild type, except for *Serca2a*, of which levels are known to be down regulated in dystrophic mice (fig. 7B). In line with the histological data, gene expression levels of mice high dystrophin levels was normalized, although still exceeded wild type levels.

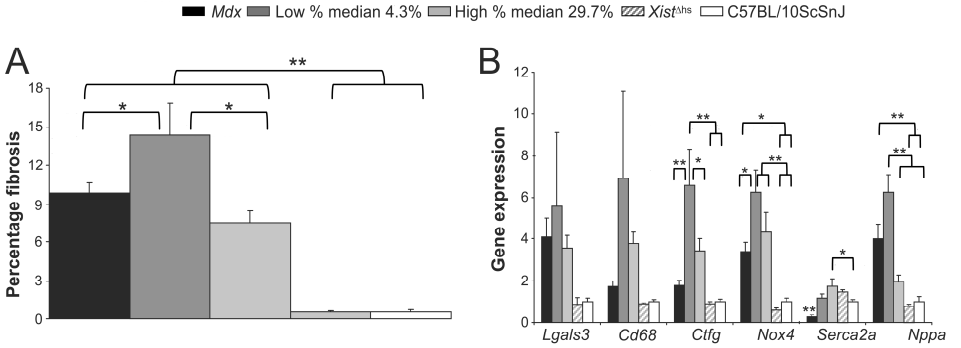


Fig. 7. Heart pathology. (**A**). The percentage of fibrotic tissue in mice with low dystrophin levels was higher than mice with higher dystrophin levels and *mdx* mice ($P<0.05$). Wild type mice had lower levels compared to dystrophic mice ($P<0.01$). (**B**). Expression of genes involved in heart pathology and function matched that found for histopathology. Gene expression of *mdx/utrn*$^{-/-}$*/Xist*$^{\Delta hs}$ mice with low dystrophin levels was higher compared to those of mice with higher dystrophin levels, *mdx* and wild type mice. Single and double asterisks represent a *P*-value of <0.05 and <0.01 respectively. Data are represented as mean±SEM.

Discussion

Over the last couple of years, several therapeutic strategies for DMD have progressed into clinical trials, aiming to restore functional dystrophin (Cirak et al. 2011;Goemans et al. 2011;Malik et al. 2010;Bowles et al. 2011;Skuk et al. 2006). Most likely, these strategies will not result in full restoration of dystrophin to healthy control levels. However, based on the mild disease of BMD patients and DMD/BMD carriers expressing low dystrophin levels, this is probably not necessary to provide benefit,

Our study describes the *mdx/utrn*$^{-/-}$*/Xist*$^{\Delta hs}$ mouse, which expresses a variety of low dystrophin levels in a utrophin negative background based on skewed X-inactivation. In these mice, <4% of the wild type dystrophin level already greatly improved life span and performance in functional tests. Higher dystrophin levels (4-15%) yet further increased survival and functional performance in hanging wire tests, but not in grip strength and rotarod running. This suggests that maintenance of vitality and functionality of the front and hind paw musculature requires less dystrophin than the larger limb and trunk muscles do.

Over time, *mdx/utrn*$^{-/-}$*/Xist*$^{\Delta hs}$ mice expressing <4% dystrophin develop severe pathology, with high levels of fibrosis, central nucleation and upregulation of genes involved in pathology . We attribute the fact that the pathology of *mdx/utrn*$^{-/-}$ mice was in fact less severe, to the lack of time to develop more severe muscle damage prior to their early death (van Putten et al. 2012b). Thus, while expression of <4% dystrophin allowed for a longer life span and improved muscle function, it could not yet prevent severe muscle damage. In contrast, expression of >4% dystrophin, besides further improving life span and muscle function, also protected muscles against damage.

We also assessed the potential of several biomarkers to monitor disease progression over time. Although plasma CK levels decreased in a dystrophin dependent manner in *mdx/utrn*$^{-/-}$*/Xist*$^{\Delta hs}$ mice, they reached wild type levels after 30 weeks, hampering the usefulness of this biomarker. Both serum TIMP-1 levels and the TIMP-1/MMP-9 ratio correlated to dystrophin expression and showed a clear dystrophin level dependent normalization towards wild type levels. We therefore propose these as useful biomarkers to monitor therapeutic effects for dystrophin-restoring approaches in mice and possibly humans (Nadarajah et al. 2011). Although levels of MMP-9 and VEGF were elevated in *mdx/utrn*$^{-/-}$ compared to wild type mice, levels in *mdx/utrn*$^{-/-}$*/Xist*$^{\Delta hs}$ mice were similar to, or lower than wild type mice. This implies that, at least in mice, MMP-9 and VEGF are less suitable serum biomarkers.

Ten-month-old *mdx/utrn*$^{-/-}$*/Xist*$^{\Delta hs}$ mice expressing low dystrophin levels (median 4.3%) suffered from a more severe cardiomyopathy than mice expressing higher dystrophin levels (median 29.7%). This suggests that prolonged life span and functionality in these mice leads to a high workload for which the lower dystrophin levels in the heart can not entirely compensate. A small limitation of this experiment is that the scans only entirely covered the left ventricle, which was our main focus at initiation of the study. Interesting findings published on the right ventricle meanwhile encouraged us to also analyze this ventricle. Comparability was ensured by analyzing all scans in the same manner and exactly to the same height. However, as the top part of the right ventricle was not scanned and measured, this resulted in a lower cardiac output, and underestimation of end diastolic volume. This may also explain that in this study the left ventricle was more severely affected, while others have reported the opposite (Crisp et al. 2011;Verhaart et al. 2011).

It should be noted that *mdx/utrn*$^{-/-}$*/Xist*$^{\Delta hs}$ mice have low dystrophin levels in a mosaic manner from birth onwards, protecting them during extensive cycles of regeneration and degeneration occurring early in life. Studies treating *mdx/utrn*$^{-/-}$ mice postnatally are limited to a starting age of at least 10 days (Goyenvalle et al. 2010;Goyenvalle et al. 2012;Kawano et al. 2008). Generally, dystrophin levels needed to improve life span exceeded 25% in these studies. We observe that 4-15% dystrophin not only greatly improves life span and muscle function, but also prevents histopathological damage. This indicates that, at least in mice, dystrophin restoration has larger protective effects when initialized very early after birth, or even before. Whether similar effects on disease pathology can also be expected for DMD patients is unknown.

To summarize, the *mdx/utrn*$^{-/-}$*/Xist*$^{\Delta hs}$ mouse model described here expresses a range of low dystrophin levels in a utrophin negative background. Major improvement in life span and functional performance is obtained even with expression of <4% dystrophin, while further improvement in life span and performance as well as protection against muscle damage is achieved when >4% dystrophin is expressed. These data indicate that very low dystrophin levels, like they are currently generated in several therapeutic trials, may already have substantial beneficial effects in DMD patients, which is encouraging for therapies aiming at dystrophin restoration. Especially worth noting is the striking effect on survival. This is probably due to general effects on condition and resilience, which are not otherwise measurable so far. If this pertains to DMD in humans as well, extension of the life span may be amongst the main benefits of therapies currently in development. This puts special emphasis of the urgent need to develop additional, and more refined therapeutic readouts than those based on ambulation.

Acknowledgements

We thank prof. Neil Brockdorff and dr. Tatyana Nesterova (MRC Clinical Sciences Center, London, UK, current affiliation Department of Biochemistry, University of Oxford, UK) for the *Xist*$^{\Delta hs}$ embryos and help with genotyping the mice, and prof. Kay Davies (Department of Physiology, Anatomy and Genetics, University of Oxford) for providing us with the *mdx/utrn*$^{-/-}$ mouse. We are grateful to Maarten van Iterson and Jelle Goeman for their help with statistical analyses. **Funding:** This work is supported by the FP6 funded TREAT-NMD network of excellence (LSHM-CT-2006-036825), the Dutch organization for scientific research (NWO/ZonMW, grant number 43200002), and the Dutch Duchenne Parent Project and utilizes the infrastructure of the Center for Biomedical Genetics (the Netherlands) and the Center for Medical Systems Biology (the Netherlands). **Author contributions:** Conceived and designed the experiments: LVDW, PACH, GJBVO, AAR. Performed the experiments: MVP, MH, CY, VDN, HH. Analyzed the data: MVP, MH, VDN, AAR. Wrote the paper: MVP, AAR. **Competing interests:** The authors declare no conflict of interest. **Data and materials availability:** The data are archived in an approved database and will be available for every reader. The *Xist*$^{\Delta hs}$ model was shared by Neil Brockdorff; requests for sharing (MTA) should be addressed to him.

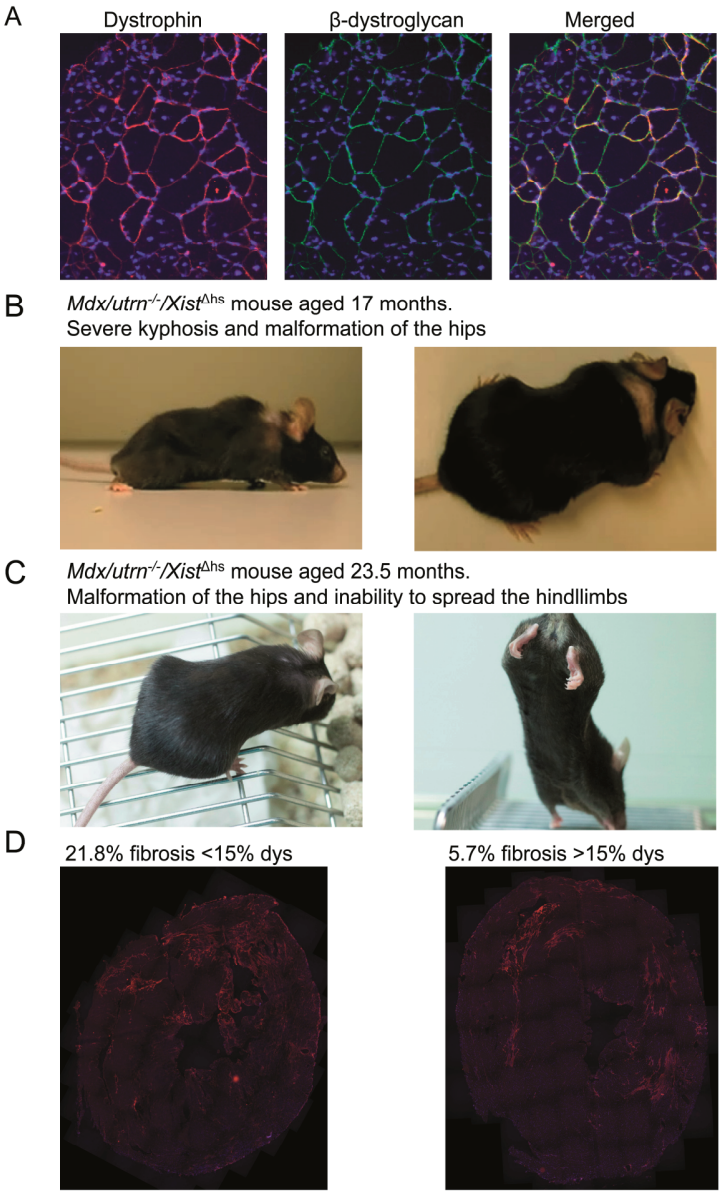


Fig. S1. Characterization of the *mdx/utrn*$^{-/-}$*/Xist*$^{\Delta hs}$ mouse. (**A**). Transverse cross-section of the quadriceps stained with dystrophin that nicely co-localizes with β-dystroglycan, a member of the dystrophin-associated protein complex. (**B**). *Mdx/utrn*$^{-/-}$*/Xist*$^{\Delta hs}$ mouse exhibiting severe kyphosis and malformations of the hips at the age of 17 months. Both phenotypical characteristics were developed later in life. This mouse was found dead at the age of 17 months, probably caused by respiratory or heart failure as body weight only slightly dropped in the week prior to death. This mouse expressed 3% dystrophin in the quadriceps. (**C**). *Mdx/utrn*$^{-/-}$*/Xist*$^{\Delta hs}$ mouse exhibiting a minor degree of kyphosis and severe malformations of the hips at the age of 23.5 months, which was developed later in life. This mouse was sacrificed at the age of 24.5 months, after it slowly but progressively lost weight. The mouse expressed 27% dystrophin in the quadriceps. (**D**). Representative pictures of a transverse cross-section of the heart stained with Collagen Type I from 10 months old *mdx/utrn*$^{-/-}$*/Xist*$^{\Delta hs}$ mice with either <15% or >15% dystrophin, which resulted in 21.8 and 5.7% fibrosis respectively.

References

't Hoen PA, van der Wees CG, Aartsma-Rus A, Turk R, Goyenvalle A, Danos O, Garcia L, van Ommen GJ, den Dunnen JT, van Deutekom JC (2006) Gene expression profiling to monitor therapeutic and adverse effects of antisense therapies for Duchenne muscular dystrophy. Pharmacogenomics 7:281-297

't Hoen PA, de Meijer EJ, Boer JM, Vossen RH, Turk R, Maatman RG, Davies KE, van Ommen GJ, van Deutekom C, den Dunnen JT (2008) Generation and characterization of transgenic mice with the full-length human DMD gene. J Biol Chem 283:5899-5907

Aartsma-Rus A (2010) Antisense-mediated modulation of splicing: therapeutic implications for Duchenne muscular dystrophy. RNA Biol 7:453-461

Aartsma-Rus A, den Dunnen JT, van Ommen GJ (2010) New insights in gene-derived therapy: the example of Duchenne muscular dystrophy. Ann N Y Acad Sci 1214:199-212

Aartsma-Rus A, Fokkema I, Verschuuren J, Ginjaar I, van Deutekom JC, van Ommen GJ, den Dunnen JT (2009) Theoretic applicability of antisense-mediated exon skipping for Duchenne muscular dystrophy mutations. Hum Mutat 30:293-299

Aartsma-Rus A, Janson AA, Kaman WE, Bremmer-Bout M, den Dunnen JT, Baas F, van Ommen GJ, van Deutekom JC (2003) Therapeutic antisense-induced exon skipping in cultured muscle cells from six different DMD patients. Hum Mol Genet 12:907-914

Aartsma-Rus A, Janson AA, Kaman WE, Bremmer-Bout M, van Ommen GJ, den Dunnen JT, van Deutekom JC (2004a) Antisense-induced multiexon skipping for Duchenne muscular dystrophy makes more sense. Am J Hum Genet 74:83-92

Aartsma-Rus A, Janson AA, van Ommen GJ, van Deutekom JC (2007) Antisense-induced exon skipping for duplications in Duchenne muscular dystrophy. BMC Med Genet 8:43

Aartsma-Rus A, Kaman WE, Bremmer-Bout M, Janson AA, den Dunnen JT, van Ommen GJ, van Deutekom JC (2004b) Comparative analysis of antisense oligonucleotide analogs for targeted DMD exon 46 skipping in muscle cells. Gene Ther 11:1391-1398

Aartsma-Rus A, van Deutekom JC, Fokkema IF, van Ommen GJ, den Dunnen JT (2006) Entries in the Leiden Duchenne muscular dystrophy mutation database: an overview of mutation types and paradoxical cases that confirm the reading-frame rule. Muscle Nerve 34:135-144

Aartsma-Rus A, van Ommen GJ (2010) Progress in therapeutic antisense applications for neuromusculardisorders. Eur J Hum Genet 18:146-153

Allen DG, Gervasio OL, Yeung EW, Whitehead NP (2010) Calcium and the damage pathways in muscular dystrophy. Can J Physiol Pharmacol 88:83-91

Alter J, Lou F, Rabinowitz A, Yin H, Rosenfeld J, Wilton SD, Partridge TA, Lu QL (2006) Systemic delivery of morpholino oligonucleotide restores dystrophin expression bodywide and improves dystrophic pathology. Nat Med 12:175-177

Amantana A, Iversen PL (2005) Pharmacokinetics and biodistribution of phosphorodiamidate morpholino antisense oligomers. Curr Opin Pharmacol 5:550-555

Angelini C (2007) The role of corticosteroids in muscular dystrophy: a critical appraisal. Muscle Nerve 36:424-435

Aoki Y, Nakamura A, Yokota T, Saito T, Okazawa H, Nagata T, Takeda S (2010) In-frame dystrophin following exon 51-skipping improves muscle pathology and function in the exon 52-deficient *mdx* mouse. Mol Ther 18:1995-2005

Apel ED, Roberds SL, Campbell KP, Merlie JP (1995) Rapsyn may function as a link between the acetylcholine receptor and the agrin-binding dystrophin-associated glycoprotein complex. Neuron 15:115-126

Araki E, Nakamura K, Nakao K, Kameya S, Kobayashi O, Nonaka I, Kobayashi T, Katsuki M (1997) Targeted disruption of exon 52 in the mouse dystrophin gene induced muscle degeneration similar to that observed in Duchenne muscular dystrophy. Biochem Biophys Res Commun 238:492-497

Archer JD, Vargas CC, Anderson JE (2006) Persistent and improved functional gain in *mdx* dystrophic mice after treatment with L-arginine and deflazacort. FASEB J 20:738-740

Au CG, Butler TL, Sherwood MC, Egan JR, North KN, Winlaw DS (2011) Increased connective tissue growth factor associated with cardiac fibrosis in the *mdx* mouse model of dystrophic cardiomyopathy. Int J Exp Pathol 92:57-65

Azofeifa J, Voit T, Hubner C, Cremer M (1995) X-chromosome methylation in manifesting and healthy carriers of dystrophinopathies: concordance of activation ratios among first degree female relatives and skewed inactivation as cause of the affected phenotypes. Hum Genet 96:167-176

Baar K, Wende AR, Jones TE, Marison M, Nolte LA, Chen M, Kelly DP, Holloszy JO (2002) Adaptations of skeletal muscle to exercise: rapid increase in the transcriptional coactivator PGC-1. FASEB J 16:1879-1886

Baban D, Davies KE (2008) Microarray analysis of *mdx* mice expressing high levels of utrophin: therapeutic implications for dystrophin deficiency. Neuromuscul Disord 18:239-247

Beastrom N, Lu H, Macke A, Canan BD, Johnson EK, Penton CM, Kaspar BK, Rodino-Klapac LR, Zhou L, Janssen PM, Montanaro F (2011) *mdx*^{cv} mice manifest more severe muscle dysfunction and diaphragm force deficits than do *mdx* mice. Am J Pathol 179:2464-2474

Beggs AH, Hoffman EP, Snyder JR, Arahata K, Specht L, Shapiro F, Angelini C, Sugita H, Kunkel LM (1991) Exploring the molecular basis for variability among patients with Becker muscular dystrophy: dystrophin gene and protein studies. Am J Hum Genet 49:54-67

Bia BL, Cassidy PJ, Young ME, Rafael JA, Leighton B, Davies KE, Radda GK, Clarke K (1999) Decreased myocardial nNOS, increased iNOS and abnormal ECGs in mouse models of Duchenne muscular dystrophy. J Mol Cell Cardiol 31:1857-1862

Billard C, Gillet P, Signoret JL, Uicaut E, Bertrand P, Fardeau M, Barthez-Carpentier MA, Santini JJ (1992) Cognitive functions in Duchenne muscular dystrophy: a reappraisal and comparison with spinal muscular atrophy. Neuromuscul Disord 2:371-378

Bjerglund NL, Nielsen IM (1984) Turner's syndrome and Duchenne muscular dystrophy in a girl with an X; autosome translocation. Ann Genet 27:173-177

Blake DJ, Weir A, Newey SE, Davies KE (2002) Function and genetics of dystrophin and dystrophin-related proteins in muscle. Physiol Rev 82:291-329

Bobet J, Mooney RF, Gordon T (1998) Force and stiffness of old dystrophic *mdx* mouse skeletal muscles. Muscle Nerve 21:536-539

Borrelli O, Salvia G, Mancini V, Santoro L, Tagliente F, Romeo EF, Cucchiara S (2005) Evolution of gastric electrical features and gastric emptying in children with Duchenne and Becker muscular dystrophy. Am J Gastroenterol 100:695-702

Bostick B, Yue Y, Duan D (2010) Gender influences cardiac function in the *mdx* model of Duchenne cardiomyopathy. Muscle Nerve 42:600-603

Bostick B, Yue Y, Long C, Duan D (2008) Prevention of dystrophin-deficient cardiomyopathy in twenty-one-month-old carrier mice by mosaic dystrophin expression or complementary dystrophin/utrophin expression. Circ Res 102:121-130

Bostick B, Yue Y, Long C, Marschalk N, Fine DM, Chen J, and Duan D (2009). Cardiac expression of a mini-dystrophin that normalizes skeletal muscle force only partially restores heart function in aged *mdx* mice. Mol. Ther 17:253-261

Bothwell JH, Griffin JL (2011) An introduction to biological nuclear magnetic resonance spectroscopy. Biol Rev Camb Philos Soc 86:493-510

Bowles DE, McPhee SW, Li C, Gray SJ, Samulski JJ, Camp AS, Li J, Wang B, Monahan PE, Rabinowitz JE, Grieger JC, Govindasamy L, Agbandje-McKenna M, Xiao X, Samulski RJ (2011) Phase 1 Gene Therapy for Duchenne Muscular Dystrophy Using a Translational Optimized AAV Vector. Mol Ther 20:443-455

Boyd Y, Buckle V, Holt S, Munro E, Hunter D, Craig I (1986) Muscular dystrophy in girls with X;autosome translocations. J Med Genet 23:484-490

Brockdorff N, Ashworth A, Kay GF, Cooper P, Smith S, McCabe VM, Norris DP, Penny GD, Patel D, Rastan S (1991) Conservation of position and exclusive expression of mouse Xist from the inactive X chromosome. Nature 351:329-331

Brunelli S, Sciorati C, D'Antona G, Innocenzi A, Covarello D, Galvez BG, Perrotta C, Monopoli A, Sanvito F, Bottinelli R, Ongini E, Cossu G, Clementi E (2007) Nitric oxide release combined with nonsteroidal antiinflammatory activity prevents muscular dystrophy pathology and enhances stem cell therapy. Proc Natl Acad Sci USA 104:264-269

Brussee V, Tardif F, Tremblay JP (1997) Muscle fibers of *mdx* mice are more vulnerable to exercise than those of normal mice. Neuromuscul Disord 7:487-492

Brunner S, Kim JO, Methe H (2010) Relation of matrix metalloproteinase-9/tissue inhibitor of metalloproteinase-1 ratio in peripheral circulating CD14+ monocytes to progression of coronary artery disease. Am J Cardiol 105:429-434

Bulfield G, Siller WG, Wight PA, Moore KJ (1984) X chromosome-linked muscular dystrophy *mdx* in the mouse. Proc Natl Acad Sci USA 81:1189-1192

Burton EA, Tinsley JM, Holzfeind PJ, Rodrigues NR, Davies KE (1999) A second promoter provides an alternative target for therapeutic up-regulation of utrophin in Duchenne muscular dystrophy. Proc Natl Acad Sci USA 96:14025-14030

Bushby K, Lochmuller H, Lynn S, Straub V (2009) Interventions for muscular dystrophy: molecular medicines entering the clinic. Lancet 374:1849-1856

Buyse GM, Van der Mieren G, Erb M, D'hooge J, Herijgers P, Verbeken E, Jara A, Van Den Bergh A, Mertens L, Courdier-Fruh I, Barzaghi P, and Meier T (2009) Long-term blinded placebo-controlled study of SNT-MC17/idebenone in the dystrophin deficient *mdx* mouse: cardiac protection and improved exercise performance. Eur. Heart J 30:116-124

Cacchiarelli D, Martone J, Girardi E, Cesana M, Incitti T, Morlando M, Nicoletti C, Santini T, Sthandier O, Barberi L, Auricchio A, Musaro A, Bozzoni I (2010) MicroRNAs involved in molecular circuitries relevant for the Duchenne muscular dystrophy pathogenesis are controlled by the dystrophin/nNOS pathway. Cell Metab 12:341-351

Call JA, Ervasti JM, Lowe DA (2011) TAT-muUtrophin mitigates the pathophysiology of dystrophin and utrophin double-knockout mice. J Appl Physiol 111:200-205

Call JA, McKeehen JN, Novotny SA, Lowe DA (2010) Progressive resistance voluntary wheel running in the *mdx* mouse. Muscle Nerve 42:871-880

Carter GT, Abresch RT, Fowler WM, Jr. (2002) Adaptations to exercise training and contraction-induced muscle injury in animal models of muscular dystrophy. Am J Phys Med Rehabil 81:S151-S161

Carter GT, Wineinger MA, Walsh SA, Horasek SJ, Abresch RT, Fowler WM, Jr. (1995) Effect of voluntary wheel-running exercise on muscles of the *mdx* mouse. Neuromuscul Disord 5:323-332

Castellano G, Malaponte G, Mazzarino MC, Figini M, Marchese F, Gangemi P, Travali S, Stivala F, Canevari S, Libra M (2008) Activation of the osteopontin/matrix metalloproteinase-9 pathway correlates with prostate cancer progression. Clin Cancer Res 14:7470-7480

Chamberlain JS (1997) Dystrophin levels required for genetic correction of duchenne muscular dystrophy. Basic and Applied Myology 7:251-255

Chamberlain JS, Metzger J, Reyes M, Townsend D, Faulkner JA (2007) Dystrophin-deficient *mdx* mice display a reduced life span and are susceptible to spontaneous rhabdomyosarcoma. FASEB J 21:2195-2204

Chan S, Head SI (2011) The role of branched fibres in the pathogenesis of Duchenne muscular dystrophy. Exp Physiol 96:564-571

Chan S, Head SI, Morley JW (2007) Branched fibers in dystrophic *mdx* muscle are associated with a loss of force following lengthening contractions. Am J Physiol Cell Physiol 293:C985-C992

Chapillon P, Lalonde R, Jones N, Caston J (1998) Early development of synchronized walking on the rotorod in rats. Effects of training and handling. Behav Brain Res 93:77-81

Chapman VM, Miller DR, Armstrong D, Caskey CT (1989) Recovery of induced mutations for X chromosome-linked muscular dystrophy in mice. Proc Natl Acad Sci USA 86:1292-1296

Chelly J, Marlhens F, Le MB, Jeanpierre M, Lambert M, Hamard G, Dutrillaux B, Kaplan JC (1986) De novo DNA microdeletion in a girl with Turner syndrome and Duchenne muscular dystrophy. Hum Genet 74:193-196

Chen YW, Nagaraju K, Bakay M, McIntyre O, Rawat R, Shi R, Hoffman EP (2005) Early onset of inflammation and later involvement of TGFbeta in Duchenne muscular dystrophy. Neurology 65:826-834

Chen YW, Zhao P, Borup R, Hoffman EP (2000) Expression profiling in the muscular dystrophies: identification of novel aspects of molecular pathophysiology. J Cell Biol 151:1321-1336

Chun JL, O'Brien R, Berry SE (2012) Cardiac dysfunction and pathology in the dystrophin and utrophin-deficient mouse during development of dilated cardiomyopathy. Neuromuscul Disord 22:368-379

Cirak S, Arechavala-Gomeza V, Guglieri M, Feng L, Torelli S, Anthony K, Abbs S, Garralda ME, Bourke J, Wells DJ, Dickson G, Wood MJ, Wilton SD, Straub V, Kole R, Shrewsbury SB, Sewry C, Morgan JE, Bushby K, Muntoni F (2011) Exon skipping and dystrophin restoration in patients with Duchenne muscular dystrophy after systemic phosphorodiamidate morpholino oligomer treatment: an open-label, phase 2, dose-escalation study. Lancet 378:595-605

Clerk A, Morris GE, Dubowitz V, Davies KE, Sewry CA (1993) Dystrophin-related protein, utrophin, in normal and dystrophic human fetal skeletal muscle. Histochem J 25:554-561

Connolly AM, Keeling RM, Mehta S, Pestronk A, Sanes JR (2001) Three mouse models of muscular dystrophy: the natural history of strength and fatigue in dystrophin-, dystrophin/utrophin-, and laminin alpha2-deficient mice. Neuromuscul Disord 11:703-712

Connuck DM, Sleeper LA, Colan SD, Cox GF, Towbin JA, Lowe AM, Wilkinson JD, Orav EJ, Cuniberti L, Salbert BA, and Lipshultz SE (2008) Characteristics and outcomes of cardiomyopathy in children with Duchenne or Becker muscular dystrophy: a comparative study from the Pediatric Cardiomyopathy Registry Am Heart J 155:998-1005

Consolino CM, Brooks SV (2004) Susceptibility to sarcomere injury induced by single stretches of maximally activated muscles of *mdx* mice. J Appl Physiol 96:633-638

Costa MF, Oliveira AG, Feitosa-Santana C, Zatz M, Ventura DF (2007) Red-green color vision impairment in Duchenne muscular dystrophy. Am J Hum Genet 80:1064-1075

Costas JM, Nye DJ, Henley JB, Plochocki JH (2010) Voluntary exercise induces structural remodeling in the hearts of dystrophin-deficient mice. Muscle Nerve 42:881-885

Cox GA, Phelps SF, Chapman VM, Chamberlain JS (1993) New *mdx* mutation disrupts expression of muscle and nonmuscle isoforms of dystrophin. Nat Genet 4:87-93

Crisp A, Yin H, Goyenvalle A, Betts C, Moulton HM, Seow Y, Babbs A, Merritt T, Saleh AF, Gait MJ, Stuckey DJ, Clarke K, Davies KE, Wood MJ (2011) Diaphragm rescue alone prevents heart dysfunction in dystrophic mice. Hum Mol Genet 20:413-421

Danko I, Chapman V, Wolff JA (1992) The frequency of revertants in *mdx* mouse genetic models for Duchenne muscular dystrophy. Pediatr Res 32:128-131

De Luca A, Nico B, Liantonio A, Didonna MP, Fraysse B, Pierno S, Burdi R, Mangieri D, Rolland JF, Camerino C, Zallone A, Confalonieri P, Andreetta F, Arnoldi E, Courdier-Fruh I, Magyar JP, Frigeri A, Pisoni M, Svelto M, Conte CD (2005) A multidisciplinary evaluation of the effectiveness of cyclosporine a in dystrophic *mdx* mice. Am J Pathol 166:477-489

De Luca A, Nico B, Rolland JF, Cozzoli A, Burdi R, Mangieri D, Giannuzzi V, Liantonio A, Cippone V, De Bellis M, Nicchia GP, Camerino GM, Frigeri A, Svelto M, Camerino DC (2008) Gentamicin treatment in exercised *mdx* mice: Identification of dystrophin-sensitive pathways and evaluation of efficacy in work-loaded dystrophic muscle. Neurobiol Dis 32:243-253

De Luca A, Pierno S, Liantonio A, Cetrone M, Camerino C, Fraysse B, Mirabella M, Servidei S, Ruegg UT, Conte CD (2003) Enhanced dystrophic progression in *mdx* mice by exercise and beneficial effects of taurine and insulin-like growth factor-1. J Pharmacol Exp Ther 304:453-463

De Paiva CS, Corrales RM, Villarreal AL, Farley WJ, Li DQ, Stern ME, Pflugfelder SC (2006) Corticosteroid and doxycycline suppress MMP-9 and inflammatory cytokine expression, MAPK activation in the corneal epithelium in experimental dry eye. Exp Eye Res 83:526-535

Deconinck AE, Potter AC, Tinsley JM, Wood SJ, Vater R, Young C, Metzinger L, Vincent A, Slater CR, Davies KE (1997a) Postsynaptic abnormalities at the neuromuscular junctions of utrophin-deficient mice. J Cell Biol 136:883-894

Deconinck AE, Rafael JA, Skinner JA, Brown SC, Potter AC, Metzinger L, Watt DJ, Dickson JG, Tinsley JM, Davies KE (1997b) Utrophin-dystrophin-deficient mice as a model for Duchenne muscular dystrophy. Cell 90:717-727

Deconinck N, Dan B (2007) Pathophysiology of duchenne muscular dystrophy: current hypotheses. Pediatr Neurol 36:1-7

Deconinck N, Rafael JA, Beckers-Bleukx G, Kahn D, Deconinck AE, Davies KE, Gillis JM (1998) Consequences of the combined deficiency in dystrophin and utrophin on the mechanical properties and myosin composition of some limb and respiratory muscles of the mouse. Neuromuscul Disord 8:362-370

Deconinck N, Tinsley J, De BF, Fisher R, Kahn D, Phelps S, Davies K, Gillis JM (1997c) Expression of truncated utrophin leads to major functional improvements in dystrophin-deficient muscles of mice. Nat Med 3:1216-1221

den Dunnen JT, Grootscholten PM, Bakker E, Blonden LA, Ginjaar HB, Wapenaar MC, van Paassen HM, van Broeckhoven C, Pearson PL, van Ommen GJ (1989) Topography of the Duchenne muscular dystrophy (DMD) gene: FIGE and cDNA analysis of 194 cases reveals 115 deletions and 13 duplications. Am J Hum Genet 45:835-847

Dellorusso C, Crawford RW, Chamberlain JS, Brooks SV (2001) Tibialis anterior muscles in *mdx* mice are highly susceptible to contraction-induced injury. J Muscle Res Cell Motil 22:467-475

Dennis CL, Tinsley JM, Deconinck AE, Davies KE (1996) Molecular and functional analysis of the utrophin promoter. Nucleic Acids Res 24:1646-1652

Duchenne GB (1868) Recherches sur la paralysie musculaire pseudohypertrophique ou paralysie myo-sclérosique. Arch Gen Med 11:178, 305, 421, 552

Dunant P, Larochelle N, Thirion C, Stucka R, Ursu D, Petrof BJ, Wolf E, Lochmuller H (2003) Expression of dystrophin driven by the 1.35-kb MCK promoter ameliorates muscular dystrophy in fast, but not in slow muscles of transgenic *mdx* mice. Mol Ther 8:80-89

Dunckley MG, Manoharan M, Villiet P, Eperon IC, Dickson G (1998) Modification of splicing in the dystrophin gene in cultured *mdx* muscle cells by antisense oligoribonucleotides. Hum Mol Genet 7:1083-1090

Dupont-Versteegden EE, McCarter RJ, Katz MS (1994) Voluntary exercise decreases progression of muscular dystrophy in diaphragm of *mdx* mice. J Appl Physiol 77:1736-1741

Eagle M, Bourke J, Bullock R, Gibson M, Mehta J, Giddings D, Straub V, Bushby K (2007) Managing Duchenne muscular dystrophy--the additive effect of spinal surgery and home nocturnal ventilation in improving survival. Neuromuscul Disord 17:470-475

Ehmsen J, Poon E, Davies K (2002) The dystrophin-associated protein complex. J Cell Sci 115:2801-2803

Emery AE (1993) Duchenne muscular dystrophy--Meryon's disease. Neuromuscul Disord 3:263-266

Emery AE, Muntoni F (2003) Duchenne Muscular Dystrophy. Oxford University Press USA; 3rd edition

England SB, Nicholson LV, Johnson MA, Forrest SM, Love DR, Zubrzycka-Gaarn EE, Bulman DE, Harris JB, Davies KE (1990) Very mild muscular dystrophy associated with the deletion of 46% of dystrophin. Nature 343:180-182

Faist V, Konig J, Hoger H, Elmadfa I (2001) Decreased mitochondrial oxygen consumption and antioxidant enzyme activities in skeletal muscle of dystrophic mice after low-intensity exercise. Ann Nutr Metab 45:58-66

Ferretti R, Neto HS, Marques MJ (2011) Expression of utrophin at dystrophin-deficient neuromuscular synapses of *mdx* mice: a study of protected and affected muscles. Anat Rec (Hoboken) 294:283-286

Ferrier P, Bamatter F, Klein D (1965) Muscular dystrophy (Duchenne) in a girl with Turner's syndrome. J Med Genet 2:38-46

Finsterer J, Stollberger C (2003) The heart in human dystrophinopathies. Cardiology 99:1-19

Garrood P, Hollingsworth KG, Eagle M, Aribisala BS, Birchall D, Bushby K, Straub V (2009) MR imaging in Duchenne muscular dystrophy: quantification of T1-weighted signal, contrast uptake, and the effects of exercise. J Magn Reson Imaging 30:1130-1138

Ghedini PC, Viel TA, Honda L, Avellar MC, Godinho RO, Lima-Landman MT, Lapa AJ, Souccar C (2008) Increased expression of acetylcholine receptors in the diaphragm muscle of *mdx* mice. Muscle Nerve 38:1585-1594

Goemans NM, Tulinius M, van den Akker JT, Burm BE, Ekhart PF, Heuvelmans N, Holling T, Janson AA, Platenburg GJ, Sipkens JA, Sitsen JM, Aartsma-Rus A, van Ommen GJ, Buyse G, Darin N, Verschuuren JJ, Campion GV, de Kimpe SJ, van Deutekom JC (2011) Systemic administration of PRO051 in Duchenne's muscular dystrophy. N Engl J Med 364:1513-1522

Goleva E, Hauk PJ, Boguniewicz J, Martin RJ, Leung DY (2007) Airway remodeling and lack of bronchodilator response in steroid-resistant asthma. J Allergy Clin Immunol 120:1065-1072

Golumbek PT, Keeling RM, Connolly AM (2007) Strength and corticosteroid responsiveness of *mdx* mice is unchanged by RAG2 gene knockout. Neuromuscul Disord 17:376-384

Gorecki DC, Monaco AP, Derry JM, Walker AP, Barnard EA, Barnard PJ (1992) Expression of four alternative dystrophin transcripts in brain regions regulated by different promoters. Hum Mol Genet 1:505-510

Gowers WE (1879) Pseudo-hypertrophic muscular paralysis. A clinical lecture. J. & A. Churchill, New burlington street, London

Goyenvalle A, Babbs A, Powell D, Kole R, Fletcher S, Wilton SD, Davies KE (2010) Prevention of dystrophic pathology in severely affected dystrophin/utrophin-deficient mice by morpholino-oligomer-mediated exon-skipping. Mol Ther 18:198-205

Goyenvalle A, Babbs A, Wright J, Wilkins V, Powell D, Garcia L, Davies KE (2012) Rescue of severely affected dystrophin/utrophin-deficient mice through scAAV-U7snRNA-mediated exon skipping. Hum Mol Genet

Grady RM, Merlie JP, Sanes JR (1997a) Subtle neuromuscular defects in utrophin-deficient mice. J Cell Biol 136:871-882

Grady RM, Teng H, Nichol MC, Cunningham JC, Wilkinson RS, Sanes JR (1997b) Skeletal and cardiac myopathies in mice lacking utrophin and dystrophin: a model for Duchenne muscular dystrophy. Cell 90:729-738

Grady RM, Zhou H, Cunningham JM, Henry MD, Campbell KP, Sanes JR (2000) Maturation and maintenance of the neuromuscular synapse: genetic evidence for roles of the dystrophin--glycoprotein complex. Neuron 25:279-293

Granchelli JA, Pollina C, Hudecki MS (2000) Pre-clinical screening of drugs using the *mdx* mouse. Neuromuscul Disord 10:235-239

Gregorevic P, Meznarich NA, Blankinship MJ, Crawford RW, Chamberlain JS (2008) Fluorophore-labeled myosin-specific antibodies simplify muscle-fiber phenotyping. Muscle Nerve 37:104-106

Grounds MD, Radley HG, Lynch GS, Nagaraju K, De Luca A (2008) Towards developing standard operating procedures for pre-clinical testing in the *mdx* mouse model of Duchenne muscular dystrophy. Neurobiol Dis 31:1-19

Grounds MD, Shavlakadze T (2011) Growing muscle has different sarcolemmal properties from adult muscle: a proposal with scientific and clinical implications: reasons to reassess skeletal muscle molecular dynamics, cellular responses and suitability of experimental models of muscle disorders. Bioessays 33:458-468

Gulati S, Saxena A, Kumar V, and Kalra V (2005) Duchenne muscular dystrophy: prevalence and patterns of cardiac involvement. Indian J Pediatr 72:389-393

Haenggi T, Fritschy JM (2006) Role of dystrophin and utrophin for assembly and function of the dystrophin glycoprotein complex in non-muscle tissue. Cell Mol Life Sci 63:1614-1631

Hainsey TA, Senapati S, Kuhn DE, Rafael JA (2003) Cardiomyopathic features associated with muscular dystrophy are independent of dystrophin absence in cardiovasculature. Neuromuscul Disord 13:294-302

Hakim CH, Duan D (2012) Gender differences in contractile and passive properties of *mdx* extensor digitorum longus muscle. Muscle Nerve 45:250-256

Hara H, Nolan PM, Scott MO, Bucan M, Wakayama Y, Fischbeck KH (2002) Running endurance abnormality in *mdx* mice. Muscle Nerve 25:207-211

Haslett JN, Sanoudou D, Kho AT, Bennett RR, Greenberg SA, Kohane IS, Beggs AH, Kunkel LM (2002) Gene expression comparison of biopsies from Duchenne muscular dystrophy (DMD) and normal skeletal muscle. Proc Natl Acad Sci USA 99:15000-15005

Hauser MA, Amalfitano A, Kumar-Singh R, Hauschka SD, Chamberlain JS (1997) Improved adenoviral vectors for gene therapy of Duchenne muscular dystrophy. Neuromuscul Disord 7:277-283

Hayes A, Williams DA (1996) Beneficial effects of voluntary wheel running on the properties of dystrophic mouse muscle. J Appl Physiol 80:670-679

Hayes A, Williams DA (1998) Contractile function and low-intensity exercise effects of old dystrophic *mdx* mice. Am J Physiol 274:C1138-C1144

Head SI, Williams DA, Stephenson DG (1992) Abnormalities in structure and function of limb skeletal muscle fibres of dystrophic *mdx* mice. Proc Biol Sci 248:163-169

Heemskerk HA, de Winter CL, de Kimpe SJ, van Kuik-Romeijn P, Heuvelmans N, Platenburg GJ, van Ommen GJ, van Deutekom JC, Aartsma-Rus A (2009) In vivo comparison of 2'-O-methyl phosphorothioate and morpholino antisense oligonucleotides for Duchenne muscular dystrophy exon skipping. J Gene Med 11:257-266

Heemskerk H, de Winter CL, van Kuik P, Heuvelmans N, Sabatelli P, Rimessi P, Braghetta P, van Ommen GJ, de Kimpe S, Ferlini A, Aartsma-Rus A, van Deutekom JC (2010) Preclinical PK and PD studies on 2'-O-methyl-phosphorothioate RNA antisense oligonucleotides in the *mdx* mouse model. Mol Ther 18:1210-1217

Heemskerk H, de Winter CL, van Ommen GJ, van Deutekom JC, Aartsma-Rus A (2009) Development of antisense-mediated exon skipping as a treatment for duchenne muscular dystrophy. Ann N Y Acad Sci 1175:71-79

Helderman-van den Enden A, Straathof CS, Aartsma-Rus A, den Dunnen JT, Verbist BM, Bakker E, Verschuuren JJ, Ginjaar HB (2010) Becker muscular dystrophy patients with deletions around exon 51; a promising outlook for exon skipping therapy in Duchenne patients. Neuromuscul Disord 20:251-254

Hernandez-Gonzalez EO, Mornet D, Rendon A, Martinez-Rojas D (2005) Absence of Dp71 in *mdx*^{3cv} mouse spermatozoa alters flagellar morphology and the distribution of ion channels and nNOS. J Cell Sci 118:137-145

Hirawat S, Welch EM, Elfring GL, Northcutt VJ, Paushkin S, Hwang S, Leonard EM, Almstead NG, Ju W, Peltz SW, Miller LL (2007) Safety, tolerability, and pharmacokinetics of PTC124, a nonaminoglycoside nonsense mutation suppressor, following single- and multiple-dose administration to healthy male and female adult volunteers. J Clin Pharmacol 47:430-444

Hoffman EP, Brown RH, Jr, Kunkel LM (1987) Dystrophin: the protein product of the Duchenne muscular dystrophy locus. Cell 51:919-928

Hoffman EP, Fischbeck KH, Brown RH, Johnson M, Medori R, Loike JD, Harris JB, Waterston R, Brooke M, Specht L (1988) Characterization of dystrophin in muscle-biopsy specimens from patients with Duchenne's or Becker's muscular dystrophy. N Engl J Med 318:1363-1368

Hoffman EP, Kunkel LM, Angelini C, Clarke A, Johnson M, Harris JB (1989) Improved diagnosis of Becker muscular dystrophy by dystrophin testing. Neurology 39:1011-1017

Hoffman EP, Morgan JE, Watkins SC, Partridge TA (1990) Somatic reversion/suppression of the mouse *mdx* phenotype in vivo. J Neurol Sci 99:9-25

Holmes KC (1996) Muscle proteins--their actions and interactions. Curr Opin Struct Biol 6:781-789

Hoogerwaard EM, Bakker E, Ippel PF, Oosterwijk JC, Majoor-Krakauer DF, Leschot NJ, Van Essen AJ, Brunner HG, van der Wouw PA, Wilde AA, de Visser M (1999) Signs and symptoms of Duchenne muscular dystrophy and Becker muscular dystrophy among carriers in The Netherlands: a cohort study. Lancet 353:2116-2119

Howard PL, Dally GY, Wong MH, Ho A, Weleber RG, Pillers DA, Ray PN (1998) Localization of dystrophin isoform Dp71 to the inner limiting membrane of the retina suggests a unique functional contribution of Dp71 in the retina. Hum Mol Genet 7:1385-1391

Huang P, Cheng G, Lu H, Aronica M, Ransohoff RM, Zhou L (2011) Impaired respiratory function in *mdx* and *mdx/utrn* +/- mice. Muscle Nerve 43:263-267

Hurst JW (1998) Naming of the waves in the ECG, with a brief account of their genesis. Circulation 98:1937-1942

Im WB, Phelps SF, Copen EH, Adams EG, Slightom JL, Chamberlain JS (1996) Differential expression of dystrophin isoforms in strains of *mdx* mice with different mutations. Hum Mol Genet 5:1149-1153

Ishizaki M, Suga T, Kimura E, Shiota T, Kawano R, Uchida Y, Uchino K, Yamashita S, Maeda Y, Uchino M (2008) *Mdx* respiratory impairment following fibrosis of the diaphragm. Neuromuscul Disord 18:342-348

Janssen PM, Hiranandani N, Mays TA, Rafael-Fortney JA (2005) Utrophin deficiency worsens cardiac contractile dysfunction present in dystrophin-deficient *mdx* mice. Am J Physiol Heart Circ Physiol 289:H2373-H2378

Jearawiriyapaisarn N, Moulton HM, Sazani P, Kole R, and Willis MS (2010) Long-term improvement in *mdx* cardiomyopathy after therapy with peptide-conjugated morpholino oligomers. Cardiovasc. Res. 85:444-453.

Johnson MA, Polgar J, Weightman D, Appleton D (1973) Data on the distribution of fibre types in thirty-six human muscles. An autopsy study. J Neurol Sci 18:111-129

Kaja S, Todorov B, van de Ven RC, Ferrari MD, Frants RR, van den Maagdenberg AM, Plomp JJ (2007) Redundancy of Cav2.1 channel accessory subunits in transmitter release at the mouse neuromuscular junction. Brain Res 1143:92-101

Karpati G, Carpenter S, Prescott S (1988) Small-caliber skeletal muscle fibers do not suffer necrosis in *mdx* mouse dystrophy. Muscle Nerve 11:795-803

Karpati G, Zubrzycka-Gaarn EE, Carpenter S, Bulman DE, Ray PN, Worton RG (1990) Age-related conversion of dystrophin-negative to -positive fiber segments of skeletal but not cardiac muscle fibers in heterozygote *mdx* mice. J Neuropathol Exp Neurol 49:96-105

Kaspar RW, Allen HD, Ray WC, Alvarez CE, Kissel JT, Pestronk A, Weiss RB, Flanigan KM, Mendell JR, and Montanaro F (2009). Analysis of dystrophin deletion mutations predicts age of cardiomyopathy onset in becker muscular dystrophy. Circ. Cardiovasc. Genet. 2, 544-551.

Kawano R, Ishizaki M, Maeda Y, Uchida Y, Kimura E, Uchino M (2008) Transduction of full-length dystrophin to multiple skeletal muscles improves motor performance and life span in utrophin/dystrophin double knockout mice. Mol Ther 16:825-831

Khurana TS, Prendergast RA, Alameddine HS, Tome FM, Fardeau M, Arahata K, Sugita H, Kunkel LM (1995) Absence of extraocular muscle pathology in Duchenne's muscular dystrophy: role for calcium homeostasis in extraocular muscle sparing. J Exp Med 182:467-475

Kinali M, Arechavala-Gomeza V, Feng L, Cirak S, Hunt D, Adkin C, Guglieri M, Ashton E, Abbs S, Nihoyannopoulos P, Garralda ME, Rutherford M, McCulley C, Popplewell L, Graham IR, Dickson G, Wood MJ, Wells DJ, Wilton SD, Kole R, Straub V, Bushby K, Sewry C, Morgan JE, Muntoni F (2009) Local restoration of dystrophin expression with the morpholino oligomer AVI-4658 in Duchenne muscular dystrophy: a single-blind, placebo-controlled, dose-escalation, proof-of-concept study. Lancet Neurol 8:918-928

Klein CJ, Coovert DD, Bulman DE, Ray PN, Mendell JR, Burghes AH (1992) Somatic reversion/suppression in Duchenne muscular dystrophy (DMD): evidence supporting a frame-restoring mechanism in rare dystrophin-positive fibers. Am J Hum Genet 50:950-959

Kleopa KA, Drousiotou A, Mavrikiou E, Ormiston A, Kyriakides T (2006) Naturally occurring utrophin correlates with disease severity in Duchenne muscular dystrophy. Hum Mol Genet 15:1623-1628

Knuesel I, Bornhauser BC, Zuellig RA, Heller F, Schaub MC, Fritschy JM (2000) Differential expression of utrophin and dystrophin in CNS neurons: an in situ hybridization and immunohistochemical study. J Comp Neurol 422:594-611

Kobayashi YM, Rader EP, Crawford RW, Iyengar NK, Thedens DR, Faulkner JA, Parikh SV, Weiss RM, Chamberlain JS, Moore SA, Campbell KP (2008) Sarcolemma-localized nNOS is required to maintain activity after mild exercise. Nature 456:511-515

Koenig M, Hoffman EP, Bertelson CJ, Monaco AP, Feener C, Kunkel LM (1987) Complete cloning of the Duchenne muscular dystrophy (DMD) cDNA and preliminary genomic organization of the DMD gene in normal and affected individuals. Cell 50:509-517

Koenig M, Kunkel LM (1990) Detailed analysis of the repeat domain of dystrophin reveals four potential hinge segments that may confer flexibility. J Biol Chem 265:4560-4566

Koenig M, Monaco AP, Kunkel LM (1988) The complete sequence of dystrophin predicts a rod-shaped cytoskeletal protein. Cell 53:219-228

Kohler M, Clarenbach CF, Boni L, Brack T, Russi EW, Bloch KE (2005) Quality of life, physical disability, and respiratory impairment in Duchenne muscular dystrophy. Am J Respir Crit Care Med 172:1032-1036

Kohler M, Clarenbach CF, Bahler C, Brack T, Russi EW, Bloch KE (2009) Disability and survival in Duchenne muscular dystrophy. J Neurol Neurosurg Psychiatry 80:320-325

Konhilas JP, Widegren U, Allen DL, Paul AC, Cleary A, Leinwand LA (2005) Loaded wheel running and muscle adaptation in the mouse. Am J Physiol Heart Circ Physiol 289:H455-H465

Lai Y, Thomas GD, Yue Y, Yang HT, Li D, Long C, Judge L, Bostick B, Chamberlain JS, Terjung RL, Duan D (2009) Dystrophins carrying spectrin-like repeats 16 and 17 anchor nNOS to the sarcolemma and enhance exercise performance in a mouse model of muscular dystrophy. J Clin Invest 119:624-635

Landisch RM, Kosir AM, Nelson SA, Baltgalvis KA, Lowe DA (2008) Adaptive and nonadaptive responses to voluntary wheel running by *mdx* mice. Muscle Nerve 38:1290-1303

Law DJ, Tidball JG (1993) Dystrophin deficiency is associated with myotendinous junction defects in prenecrotic and fully regenerated skeletal muscle. Am J Pathol 142:1513-1523

Lee CC, Pons F, Jones PG, Bies RD, Schlang AM, Leger JJ, Caskey CT (1993) *Mdx* transgenic mouse: restoration of recombinant dystrophin to the dystrophic muscle. Hum Gene Ther 4:273-281

Lewis C, Ohlendieck K (2010) Proteomic profiling of naturally protected extraocular muscles from the dystrophin-deficient *mdx* mouse. Biochem Biophys Res Commun 396:1024-1029

Li D, Yue Y, Duan D (2008) Preservation of muscle force in *Mdx*^{3cv} mice correlates with low-level expression of a near full-length dystrophin protein. Am J Pathol 172:1332-1341

Li D, Yue Y, Duan D (2010) Marginal level dystrophin expression improves clinical outcome in a strain of dystrophin/utrophin double knockout mice. PLoS One 5:e15286

Li H, Mittal A, Makonchuk DY, Bhatnagar S, Kumar A (2009) Matrix metalloproteinase-9 inhibition ameliorates pathogenesis and improves skeletal muscle regeneration in muscular dystrophy. Hum Mol Genet 18:2584-2598

Li W, Liu W, Zhong J, Yu X (2009) Early manifestation of alteration in cardiac function in dystrophin deficient *mdx* mouse using 3D CMR tagging. J Cardiovasc Magn Reson 11:40

Lidov HG (1996) Dystrophin in the nervous system. Brain Pathol 6:63-77

Lindenbaum RH, Clarke G, Patel C, Moncrieff M, Hughes JT (1979) Muscular dystrophy in an X; 1 ranslocation female suggests that Duchenne locus is on X chromosome short arm. J Med Genet 16:389-392

Lo Mauro A, D'Angelo MG, Romei M, Motta F, Colombo D, Comi GP, Pedotti A, Marchi E, Turconi AC, Bresolin N, Aliverti A (2010) Abdominal volume contribution to tidal volume as an early indicator of respiratory impairment in Duchenne muscular dystrophy. Eur Respir J 35:1118-1125

Love DR, Forrest SM, Smith TJ, England S, Flint T, Davies KE, Speer A (1989a) Molecular analysis of Duchenne and Becker muscular dystrophies. Br Med Bull 45:659-680

Love DR, Hill DF, Dickson G, Spurr NK, Byth BC, Marsden RF, Walsh FS, Edwards YH, Davies KE (1989b) An autosomal transcript in skeletal muscle with homology to dystrophin. Nature 339:55-58

Lovering RM, Michaelson L, Ward CW (2009) Malformed *mdx* myofibers have normal cytoskeletal architecture yet altered EC coupling and stress-induced Ca2+ signaling. Am J Physiol Cell Physiol 297:C571-C580

Lu QL, Mann CJ, Lou F, Bou-Gharios G, Morris GE, Xue SA, Fletcher S, Partridge TA, Wilton SD (2003) Functional amounts of dystrophin produced by skipping the mutated exon in the *mdx* dystrophic mouse. Nat Med 9:1009-1014

Lu QL, Morris GE, Wilton SD, Ly T, Artem'yeva OV, Strong P, Partridge TA (2000) Massive idiosyncratic exon skipping corrects the nonsense mutation in dystrophic mouse muscle and produces functional revertant fibers by clonal expansion. J Cell Biol 148:985-996

Lu QL, Rabinowitz A, Chen YC, Yokota T, Yin H, Alter J, Jadoon A, Bou-Gharios G, Partridge T (2005) Systemic delivery of antisense oligoribonucleotide restores dystrophin expression in body-wide skeletal muscles. Proc Natl Acad Sci USA 102:198-203

Lupski JR, Garcia CA, Zoghbi HY, Hoffman EP, Fenwick RG (1991) Discordance of muscular dystrophy in monozygotic female twins: evidence supporting asymmetric splitting of the inner cell mass in a manifesting carrier of Duchenne dystrophy. Am J Med Genet 40:354-364

Lynch GS, Hinkle RT, Chamberlain JS, Brooks SV, Faulkner JA (2001) Force and power output of fast and slow skeletal muscles from *mdx* mice 6-28 months old. J Physiol 535:591-600

Lyon M (1961) Gene action in the X-chromosome of the mouse (Mus musculus L.). Nature 190:372-373

Lyons PR, Slater CR (1991) Structure and function of the neuromuscular junction in young adult *mdx* mice. J Neurocytol 20:969-981

Maciver DH, Townsend M (2008) A novel mechanism of heart failure with normal ejection fraction. Heart 94:446-449

Malerba A, Boldrin L, Dickson G (2011a) Long-term systemic administration of unconjugated morpholino oligomers for therapeutic expression of dystrophin by exon skipping in skeletal muscle: implications for cardiac muscle integrity. Nucleic Acid Ther 21:293-298

Malerba A, Sharp PS, Graham IR, Arechavala-Gomeza V, Foster K, Muntoni F, Wells DJ, Dickson G (2011b) Chronic systemic therapy with low-dose morpholino oligomers ameliorates the pathology and normalizes locomotor behavior in *mdx* mice. Mol Ther 19:345-354

Malerba A, Thorogood FC, Dickson G, Graham IR (2009) Dosing regimen has a significant impact on the efficiency of morpholino oligomer-induced exon skipping in *mdx* mice. Hum Gene Ther 20:955-965

Malik V, Rodino-Klapac LR, Viollet L, Wall C, King W, Al-Dahhak R, Lewis S, Shilling CJ, Kota J, Serrano-Munuera C, Hayes J, Mahan JD, Campbell KJ, Banwell B, Dasouki M, Watts V, Sivakumar K, Bien-Willner R, Flanigan KM, Sahenk Z, Barohn RJ, Walker CM, Mendell JR (2010) Gentamicin-induced readthrough of stop codons in Duchenne muscular dystrophy. Ann Neurol 67:771-780

Manzur AY, Kinali M, Muntoni F (2008) Update on the management of Duchenne muscular dystrophy. Arch Dis Child 93:986-990

Marden FA, Connolly AM, Siegel MJ, Rubin DA (2005) Compositional analysis of muscle in boys with Duchenne muscular dystrophy using MR imaging. Skeletal Radiol 34:140-148

Marshall PA, Williams PE, Goldspink G (1989) Accumulation of collagen and altered fiber-type ratios as indicators of abnormal muscle gene expression in the *mdx* dystrophic mouse. Muscle Nerve 12:528-537

Martigne L, Salleron J, Mayer M, Cuisset JM, Carpentier A, Neve V, Tiffreau V, Guimber D, Gottrand F (2011) Natural evolution of weight status in Duchenne muscular dystrophy: a retrospective audit. Br.J.Nutr. 105:1486-1491

Matsumura T, Saito T, Fujimura H, and Shinno S (2007). Cardiac troponin I for accurate evaluation of cardiac status in myopathic patients. Brain Dev. 29, 496-501.

Mazzone ES, Messina S, Vasco G, Main M, Eagle M, D'Amico A, Doglio L, Politano L, Cavallaro F, Frosini S, Bello L, Magri F, Corlatti A, Zucchini E, Brancalion B, Rossi F, Ferretti M, Motta MG, Cecio MR, Berardinelli A, Alfieri P, Mongini T, Pini A, Astrea G, Battini R, Comi G, Pegoraro E, Morandi L, Pane M, Angelini C, Bruno C, Villanova M, Vita G, Donati MA, Bertini E, Mercuri E (2009) Reliability of the North Star Ambulatory Assessment in a multicentric setting. Neuromuscul Disord 19:458-461

Melacini P, Fanin M, Danieli GA, Villanova C, Martinello F, Miorin M, Freda MP, Miorelli M, Mostacciuolo ML, Fasoli G, Angelini C, and Dalla VS (1996). Myocardial involvement is very frequent among patients affected with subclinical Becker's muscular dystrophy. Circulation 94, 3168-3175.

Melis MA, Cau M, Muntoni F, Mateddu A, Galanello R, Boccone L, Deidda F, Loi D, Cao A (1998) Elevation of serum creatine kinase as the only manifestation of an intragenic deletion of the dystrophin gene in three unrelated families. Eur J Paediatr Neurol 2:255-261

Mendell JR, Campbell K, Rodino-Klapac L, Sahenk Z, Shilling C, Lewis S, Bowles D, Gray S, Li C, Galloway G, Malik V, Coley B, Clark KR, Li J, Xiao X, Samulski J, McPhee SW, Samulski RJ, Walker CM (2010) Dystrophin immunity in Duchenne's muscular dystrophy. N Engl J Med 363:1429-1437

Meryon E (1852) On Granular and Fatty Degeneration of the Voluntary Muscles. Med Chir Trans 35:73-84

Miike T, Miyatake M, Zhao J, Yoshioka K, Uchino M (1989) Immunohistochemical dystrophin reaction in synaptic regions. Brain Dev 11:344-346

Miike T, Sugino S, Ohtani Y, Taku K, Yoshioka K (1987) Vascular endothelial cell injury and platelet embolism in Duchenne muscular dystrophy at the preclinical stage. J Neurol Sci 82:67-80

Minetti GC, Colussi C, Adami R, Serra C, Mozzetta C, Parente V, Fortuni S, Straino S, Sampaolesi M, Di PM, Illi B, Gallinari P, Steinkuhler C, Capogrossi MC, Sartorelli V, Bottinelli R, Gaetano C, Puri PL (2006) Functional and morphological recovery of dystrophic muscles in mice treated with deacetylase inhibitors. Nat Med 12:1147-1150

Mirowska D, Wicha W, Czlonkowski A, Czlonkowska A, Weber F (2004) Increase of matrix metalloproteinase-9 in peripheral blood of multiple sclerosis patients treated with high doses of methylprednisolone. J Neuroimmunol 146:171-175

Mizuno Y, Nonaka I, Hirai S, Ozawa E (1993) Reciprocal expression of dystrophin and utrophin in muscles of Duchenne muscular dystrophy patients, female DMD-carriers and control subjects. J Neurol Sci 119:43-52

Monaco AP, Bertelson CJ, Liechti-Gallati S, Moser H, Kunkel LM (1988) An explanation for the phenotypic differences between patients bearing partial deletions of the DMD locus. Genomics 2:90-95

Moulton HM, Wu B, Jearawiriyapaisarn N, Sazani P, Lu QL, Kole R (2009) Peptide-morpholino conjugate: a promising therapeutic for Duchenne muscular dystrophy. Ann N Y Acad Sci 1175:55-60

Muntoni F, Mateddu A, Marchei F, Clerk A, Serra G (1993) Muscular weakness in the *mdx* mouse. J Neurol Sci 120:71-77

Muntoni F, Torelli S, Brockington M (2008) Muscular dystrophies due to glycosylation defects. Neurotherapeutics 5:627-632

Muntoni F, Torelli S, Ferlini A (2003) Dystrophin and mutations: one gene, several proteins, multiple phenotypes. Lancet Neurol 2:731-740

Mysliwiec J, Adamczyk M, Pawlowski P, Nikolajuk A, Gorska M (2007) Serum gelatinases (MMP-2 and MMP-9) and VCAM-1 as a guideline in a therapeutic approach in Graves' ophthalmopathy. Endokrynol Pol 58:105-109

Nadarajah VD, van Putten M, Chaouch A, Garrood P, Straub V, Lochmuller H, Ginjaar HB, Aartsma-Rus AM, van Ommen GJ, den Dunnen JT, 't Hoen PA (2011) Serum matrix metalloproteinase-9 (MMP-9) as a biomarker for monitoring disease progression in Duchenne muscular dystrophy (DMD). Neuromuscul Disord 21:569-578

Nakamura A, Yoshida K, Takeda S, Dohi N, Ikeda S (2002) Progression of dystrophic features and activation of mitogen-activated protein kinases and calcineurin by physical exercise, in hearts of *mdx* mice. FEBS Lett 520:18-24

Narita S, Yorifuji H (1999) Centrally nucleated fibers (CNFs) compensate the fragility of myofibers in *mdx* mouse. Neuroreport 10:3233-3235

Neri M, Torelli S, Brown S, Ugo I, Sabatelli P, Merlini L, Spitali P, Rimessi P, Gualandi F, Sewry C, Ferlini A, Muntoni F (2007) Dystrophin levels as low as 30% are sufficient to avoid muscular dystrophy in the human. Neuromuscul Disord 17:913-918

Newall AE, Duthie S, Formstone E, Nesterova T, Alexiou M, Johnston C, Caparros ML, Brockdorff N (2001) Primary non-random X inactivation associated with disruption of Xist promoter regulation. Hum Mol Genet 10:581-589

Ng K, Pullirsch D, Leeb M, Wutz A (2007) Xist and the order of silencing. EMBO Rep 8:34-39

Nguyen TM, Ellis JM, Love DR, Davies KE, Gatter KC, Dickson G, Morris GE (1991) Localization of the DMDL gene-encoded dystrophin-related protein using a panel of nineteen monoclonal antibodies: presence at neuromuscular junctions, in the sarcolemma of dystrophic skeletal muscle, in vascular and other smooth muscles, and in proliferating brain cell lines. J Cell Biol 115:1695-1700

Nicholson LV, Johnson MA, Bushby KM, Gardner-Medwin D (1993) Functional significance of dystrophin positive fibres in Duchenne muscular dystrophy. Arch Dis Child 68:632-636

Nigro G, Comi LI, Politano L, and Bain RJ (1990). The incidence and evolution of cardiomyopathy in Duchenne muscular dystrophy. Int. J. Cardiol. 26, 271-277.

Oda T, Shimizu N, Yonenobu K, Ono K, Nabeshima T, Kyoh S (1993) Longitudinal study of spinal deformity in Duchenne muscular dystrophy. J Pediatr Orthop 13:478-488

Ogata H, Nakagawa H, Hamabe K, Hattori A, Ishikawa Y, Ishikawa Y, Saito M, Minami R (2000) A female carrier of Duchenne muscular dystrophy complicated with cardiomyopathy. Intern Med 39:34-38

Ohlendieck K, Ervasti JM, Matsumura K, Kahl SD, Leveille CJ, Campbell KP (1991) Dystrophin-related protein is localized to neuromuscular junctions of adult skeletal muscle. Neuron 7:499-508

Payne ET, Yasuda N, Bourgeois JM, Devries MC, Rodriguez MC, Yousuf J, Tarnopolsky MA (2006) Nutritional therapy improves function and complements corticosteroid intervention in *mdx* mice. Muscle Nerve 33:66-77

Pearce M, Blake DJ, Tinsley JM, Byth BC, Campbell L, Monaco AP, Davies KE (1993) The utrophin and dystrophin genes share similarities in genomic structure. Hum Mol Genet 2:1765-1772

Pegoraro E, Hoffman EP, Piva L, Gavassini BF, Cagnin S, Ermani M, Bello L, Soraru G, Pacchioni B, Bonifati MD, Lanfranchi G, Angelini C, Kesari A, Lee I, Gordish-Dressman H, Devaney JM, McDonald CM (2011) SPP1 genotype is a determinant of disease severity in Duchenne muscular dystrophy. Neurology 76:219-226

Pegoraro E, Schimke RN, Garcia C, Stern H, Cadaldini M, Angelini C, Barbosa E, Carroll J, Marks WA, Neville HE, Marks H, Appleton S, Toriello H, Wessel HB, Donnelly J, Bernes SM, Taber JW, Weiss L, Hoffman EP (1995) Genetic and biochemical normalization in female carriers of Duchenne muscular dystrophy: evidence for failure of dystrophin production in dystrophin-competent myonuclei. Neurology 45:677-690

Perkins KJ, Davies KE (2002) The role of utrophin in the potential therapy of Duchenne muscular dystrophy. Neuromuscul Disord 12 Suppl 1:S78-S89

Perronnet C, Vaillend C (2010) Dystrophins, utrophins, and associated scaffolding complexes: role in mammalian brain and implications for therapeutic strategies. J Biomed Biotechnol 2010:849426

Pescatori M, Broccolini A, Minetti C, Bertini E, Bruno C, D'Amico A, Bernardini C, Mirabella M, Silvestri G, Giglio V, Modoni A, Pedemonte M, Tasca G, Galluzzi G, Mercuri E, Tonali PA, Ricci E (2007) Gene expression profiling in the early phases of DMD: a constant molecular signature characterizes DMD muscle from early postnatal life throughout disease progression. FASEB J 21:1210-1226

Phelps SF, Hauser MA, Cole NM, Rafael JA, Hinkle RT, Faulkner JA, Chamberlain JS (1995) Expression of full-length and truncated dystrophin mini-genes in transgenic *mdx* mice. Hum Mol Genet 4:1251-1258

Pierno S, Nico B, Burdi R, Liantonio A, Didonna MP, Cippone V, Fraysse B, Rolland JF, Mangieri D, Andreetta F, Ferro P, Camerino C, Zallone A, Confalonieri P, De Luca A (2007) Role of tumour necrosis factor alpha, but not of cyclo-oxygenase-2-derived eicosanoids, on functional and morphological indices of dystrophic progression in *mdx* mice: a pharmacological approach. Neuropathol Appl Neurobiol 33:344-359

Pilgram GS, Potikanond S, Baines RA, Fradkin LG, Noordermeer JN (2010) The roles of the dystrophin-associated glycoprotein complex at the synapse. Mol Neurobiol 41:1-21

Pillers DA, Fitzgerald KM, Duncan NM, Rash SM, White RA, Dwinnell SJ, Powell BR, Schnur RE, Ray PN, Cibis GW, Weleber RG (1999) Duchenne/Becker muscular dystrophy: correlation of phenotype by electroretinography with sites of dystrophin mutations. Hum Genet 105:2-9

Pillers DA, Weleber RG, Woodward WR, Green DG, Chapman VM, Ray PN (1995) *mdx*^{Cv3} mouse is a model for electroretinography of Duchenne/Becker muscular dystrophy. Invest Ophthalmol Vis Sci 36:462-466

Pons F, Nicholson LV, Robert A, Voit T, Leger JJ (1993) Dystrophin and dystrophin-related protein (utrophin) distribution in normal and dystrophin-deficient skeletal muscles. Neuromuscul Disord 3:507-514

Porter JD (1998) Commentary: extraocular muscle sparing in muscular dystrophy: a critical evaluation of potential protective mechanisms. Neuromuscul Disord 8:198-203

Porter JD, Rafael JA, Ragusa RJ, Brueckner JK, Trickett JI, Davies KE (1998) The sparing of extraocular muscle in dystrophinopathy is lost in mice lacking utrophin and dystrophin. J Cell Sci 111 (Pt 13):1801-1811

Quinlan JG, Hahn HS, Wong BL, Lorenz JN, Wenisch AS, and Levin LS (2004). Evolution of the *mdx* mouse cardiomyopathy: physiological and morphological findings. Neuromuscul Disord 14, 491-496.

Radley HG, Davies MJ, Grounds MD (2008) Reduced muscle necrosis and long-term benefits in dystrophic *mdx* mice after cV1q (blockade of TNF) treatment. Neuromuscul Disord 18:227-238

Radley HG, Grounds MD (2006) Cromolyn administration (to block mast cell degranulation) reduces necrosis of dystrophic muscle in *mdx* mice. Neurobiol Dis 23:387-397

Rafael JA, Sunada Y, Cole NM, Campbell KP, Faulkner JA, Chamberlain JS (1994) Prevention of dystrophic pathology in *mdx* mice by a truncated dystrophin isoform. Hum Mol Genet 3:1725-1733

Rafael JA, Tinsley JM, Potter AC, Deconinck AE, Davies KE (1998) Skeletal muscle-specific expression of a utrophin transgene rescues utrophin-dystrophin deficient mice. Nat Genet 19:79-82

Rafael JA, Townsend ER, Squire SE, Potter AC, Chamberlain JS, Davies KE (2000) Dystrophin and utrophin influence fiber type composition and post-synaptic membrane structure. Hum Mol Genet 9:1357-1367

Rafael JA, Trickett JI, Potter AC, Davies KE (1999) Dystrophin and utrophin do not play crucial roles in nonmuscle tissues in mice. Muscle Nerve 22:517-519

Rafael-Fortney JA, Chimanji NS, Schill KE, Martin CD, Murray JD, Ganguly R, Stangland JE, Tran T, Xu Y, Canan BD, Mays TA, Delfin DA, Janssen PM, Raman SV (2011) Early treatment with lisinopril and spironolactone preserves cardiac and skeletal muscle in duchenne muscular dystrophy mice. Circulation 124:582-588

Raffetto JD, Khalil RA (2008) Matrix metalloproteinases and their inhibitors in vascular remodeling and vascular disease. Biochem Pharmacol 75:346-359

Ramakers C, Ruijter JM, Deprez RH, Moorman AF (2003) Assumption-free analysis of quantitative real-time polymerase chain reaction (PCR) data. Neurosci Lett 339:62-66

Raymackers JM, Debaix H, Colson-Van SM, De Backer F, Tajeddine N, Schwaller B, Gailly P, Gillis JM (2003) Consequence of parvalbumin deficiency in the *mdx* mouse: histological, biochemical and mechanical phenotype of a new double mutant. Neuromuscul Disord 13:376-387

Richards CS, Watkins SC, Hoffman EP, Schneider NR, Milsark IW, Katz KS, Cook JD, Kunkel LM, Cortada JM (1990) Skewed X inactivation in a female MZ twin results in Duchenne muscular dystrophy. Am J Hum Genet 46:672-681

Rifai N, Gillette MA, Carr SA (2006) Protein biomarker discovery and validation: the long and uncertain path to clinical utility. Nat Biotechnol 24:971-983

Roberts RG, Coffey AJ, Bobrow M, Bentley DR (1993) Exon structure of the human dystrophin gene. Genomics 16:536-538

Ruifrok AC, Katz RL, Johnston DA (2003) Comparison of quantification of histochemical staining by hue-saturation-intensity (HSI) transformation and color-deconvolution. Appl Immunohistochem Mol Morphol 11:85-91

Rybakova IN, Amann KJ, Ervasti JM (1996) A new model for the interaction of dystrophin with F-actin. J Cell Biol 135:661-672

Saito T, Yamamoto Y, Matsumura T, Nozaki S, Fujimura H, Shinno S (2005) Coagulation system activated in Duchenne muscular dystrophy patients with cardiac dysfunction. Brain Dev 27:415-418

Saito T, Yamamoto Y, Matsumura T, Fujimura H, Shinno S (2009) Serum levels of vascular endothelial growth factor elevated in patients with muscular dystrophy. Brain Dev 31:612-617

Sander M, Chavoshan B, Harris SA, Iannaccone ST, Stull JT, Thomas GD, Victor RG (2000) Functional muscle ischemia in neuronal nitric oxide synthase-deficient skeletal muscle of children with Duchenne muscular dystrophy. Proc Natl Acad Sci USA 97:13818-13823

Sazani P, Blouch R, Weller D, Leow S, Kole R, Shrewsbury SB (2009) AVI 5038: Initial efficacy and safety evaluation in cynomolgus monkeys. Treat-NMD/NIH Conference

Schade van Westrum, SM, Dekker L, Endert E, de Haan RJ, Wilde AAM, de Visser M, and van der Kooi AJ (2006) NT-proBNP is not associated with dilated cardiomyopathy in Becker and Duchenne muscular dystrophies. Neuromuscul Disord Ref Type: Abstract

Schiaffino S, Gorza L, Sartore S, Saggin L, Ausoni S, Vianello M, Gundersen K, Lomo T (1989) Three myosin heavy chain isoforms in type 2 skeletal muscle fibres. J Muscle Res Cell Motil 10:197-205

Schmidt-Achert M, Fischer P, Muller-Felber W, Mudra H, Pongratz D (1993) Heterozygotic gene expression in endomyocardial biopsies: a new diagnostic tool confirms the Duchenne carrier status. Clin Investig 71:247-253

Schneider JE, Cassidy PJ, Lygate C, Tyler DJ, Wiesmann F, Grieve SM, Hulbert K, Clarke K, Neubauer S (2003) Fast, high-resolution in vivo cine magnetic resonance imaging in normal and failing mouse hearts on a vertical 11.7 T system. J Magn Reson Imaging 18:691-701

Sciandra F, Bozzi M, Bianchi M, Pavoni E, Giardina B, Brancaccio A (2003) Dystroglycan and muscular dystrophies related to the dystrophin-glycoprotein complex. Ann Ist Super Sanita 39:173-181

Senner CE, Brockdorff N (2009) Xist gene regulation at the onset of X inactivation. Curr Opin Genet Dev 19:122-126

Sharp PS, Jee H, Wells DJ (2011) Physiological characterization of muscle strength with variable levels of dystrophin restoration in *mdx* mice following local antisense therapy. Mol Ther 19:165-171

Sicinski P, Geng Y, Ryder-Cook AS, Barnard EA, Darlison MG, Barnard PJ (1989) The molecular basis of muscular dystrophy in the *mdx* mouse: a point mutation. Science 244:1578-1580

Skuk D, Goulet M, Roy B, Chapdelaine P, Bouchard JP, Roy R, Dugre FJ, Sylvain M, Lachance JG, Deschenes L, Senay H, Tremblay JP (2006) Dystrophin expression in muscles of duchenne muscular dystrophy patients after high-density injections of normal myogenic cells. J Neuropathol Exp Neurol 65:371-386

Skuk D, Goulet M, Roy B, Piette V, Cote CH, Chapdelaine P, Hogrel JY, Paradis M, Bouchard JP, Sylvain M, Lachance JG, and Tremblay JP (2007) First test of a "high-density injection" protocol for myogenic cell transplantation throughout large volumes of muscles in a Duchenne muscular dystrophy patient: eighteen months follow-up. Neuromuscul Disord 17:38-46

Soltanzadeh P, Friez MJ, Dunn D, von NA, Gurvich OL, Swoboda KJ, Sampson JB, Pestronk A, Connolly AM, Florence JM, Finkel RS, Bonnemann CG, Medne L, Mendell JR, Mathews KD, Wong BL, Sussman MD, Zonana J, Kovak K, Gospe SM, Jr, Gappmaier E, Taylor LE, Howard MT, Weiss RB, Flanigan KM (2010) Clinical and genetic characterization of manifesting carriers of DMD mutations. Neuromuscul Disord 20:499-504

Spurney CF, Gordish-Dressman H, Guerron AD, Sali A, Pandey GS, Rawat R, van der Meulen JH, Cha HJ, Pistilli EE, Partridge TA, Hoffman EP, Nagaraju K (2009) Preclinical drug trials in the *mdx* mouse: assessment of reliable and sensitive outcome measures. Muscle Nerve 39:591-602

Spurney CF, Knoblach S, Pistilli EE, Nagaraju K, Martin GR, Hoffman EP (2008) Dystrophin-deficient cardiomyopathy in mouse: expression of Nox4 and Lox are associated with fibrosis and altered functional parameters in the heart. Neuromuscul Disord 18:371-381

Squire S, Raymackers JM, Vandebrouck C, Potter A, Tinsley J, Fisher R, Gillis JM, Davies KE (2002) Prevention of pathology in *mdx* mice by expression of utrophin: analysis using an inducible transgenic expression system. Hum Mol Genet 11:3333-3344

Stedman HH, Sweeney HL, Shrager JB, Maguire HC, Panettieri RA, Petrof B, Narusawa M, Leferovich JM, Sladky JT, Kelly AM (1991) The *mdx* mouse diaphragm reproduces the degenerative changes of Duchenne muscular dystrophy. Nature 352:536-539

Stillwell E, Vitale J, Zhao Q, Beck A, Schneider J, Khadim F, Elson G, Altaf A, Yehia G, Dong JH, Liu J, Mark W, Bhaumik M, Grange R, Fraidenraich D (2009) Blastocyst injection of wild type embryonic stem cells induces global corrections in *mdx* mice. PLoS One 4:e4759

Summerton J, Weller D (1997) Morpholino antisense oligomers: design, preparation, and properties. Antisense Nucleic Acid Drug Dev 7:187-195

Sun G, Haginoya K, Chiba Y, Uematsu M, Hino-Fukuyo N, Tanaka S, Onuma A, Iinuma K, Tsuchiya S (2010) Elevated plasma levels of tissue inhibitors of metalloproteinase-1 and their overexpression in muscle in human and mouse muscular dystrophy. J Neurol Sci 297:19-28

Sun GL, Zhao S, Li P, Jiang HK (2006) Expression of tissue inhibitor of metalloproteinase-1 in progression muscular dystrophy. Neurosci Bull 22:85-90

Takeshima Y, Wada H, Yagi M, Ishikawa Y, Ishikawa Y, Minami R, Nakamura H, Matsuo M (2001) Oligonucleotides against a splicing enhancer sequence led to dystrophin production in muscle cells from a Duchenne muscular dystrophy patient. Brain Dev 23:788-790

Tanaka H, Ikeya K, Ozawa E (1990) Difference in the expression pattern of dystrophin on the surface membrane between the skeletal and cardiac muscles of *mdx* carrier mice. Histochemistry 93:447-452

Tennyson CN, Klamut HJ, Worton RG (1995) The human dystrophin gene requires 16 hours to be transcribed and is cotranscriptionally spliced. Nat Genet 9:184-190

Thanh LT, Nguyen TM, Helliwell TR, Morris GE (1995) Characterization of revertant muscle fibers in Duchenne muscular dystrophy, using exon-specific monoclonal antibodies against dystrophin. Am J Hum Genet 56:725-731

Thomas LB, Joseph GL, Adkins TD, Andrade FH, Stemple JC (2008) Laryngeal muscles are spared in the dystrophin deficient *mdx* mouse. J Speech Lang Hear Res 51:586-595

Tinsley J, Deconinck N, Fisher R, Kahn D, Phelps S, Gillis JM, Davies K (1998) Expression of full-length utrophin prevents muscular dystrophy in *mdx* mice. Nat Med 4:1441-1444

Tinsley JM, Potter AC, Phelps SR, Fisher R, Trickett JI, Davies KE (1996) Amelioration of the dystrophic phenotype of *mdx* mice using a truncated utrophin transgene. Nature 384:349-353

Torres LF, Duchen LW (1987) The mutant *mdx*: inherited myopathy in the mouse. Morphological studies of nerves, muscles and end-plates. Brain 110 (Pt 2):269-299

Torriani M, Townsend E, Thomas BJ, Bredella MA, Ghomi RH, Tseng BS (2011) Lower leg muscle involvement in Duchenne muscular dystrophy: an MR imaging and spectroscopy study. Skeletal Radiol 41:437-445

Townsend D, Yasuda S, Li S, Chamberlain JS, Metzger JM (2008) Emergent dilated cardiomyopathy caused by targeted repair of dystrophic skeletal muscle. Mol Ther 16:832-835

Turgeman T, Hagai Y, Huebner K, Jassal DS, Anderson JE, Genin O, Nagler A, Halevy O, Pines M (2008) Prevention of muscle fibrosis and improvement in muscle performance in the *mdx* mouse by halofuginone. Neuromuscul Disord 18:857-868

Turk R, Sterrenburg E, de Meijer EJ, van Ommen GJ, den Dunnen JT, 't Hoen PA (2005) Muscle regeneration in dystrophin-deficient *mdx* mice studied by gene expression profiling. BMC Genomics 6:98

Turk R, Sterrenburg E, van der Wees CG, de Meijer EJ, de Menezes RX, Groh S, Campbell KP, Noguchi S, van Ommen GJ, den Dunnen JT, 't Hoen PA (2006) Common pathological mechanisms in mouse models for muscular dystrophies. FASEB J 20:127-129

Vaillend C, Billard JM, Claudepierre T, Rendon A, Dutar P, Ungerer A (1998) Spatial discrimination learning and CA1 hippocampal synaptic plasticity in *mdx* and *mdx*3cv mice lacking dystrophin gene products. Neuroscience 86:53-66

Vaillend C, Rendon A, Misslin R, Ungerer A (1995) Influence of dystrophin-gene mutation on *mdx* mouse behavior. I. Retention deficits at long delays in spontaneous alternation and bar-pressing tasks. Behav Genet 25:569-579

Vaillend C, Ungerer A (1999) Behavioral characterization of *mdx*3cv mice deficient in C-terminal dystrophins. Neuromuscul Disord 9:296-304

van Bockel EA, Lind JS, Zijlstra JG, Wijkstra PJ, Meijer PM, van den Berg MP, Slart RH, Aarts LP, and Tulleken JE (2009) Cardiac assessment of patients with late stage Duchenne muscular dystrophy. Neth. Heart J. 17:232-237

van der Geest RJ, Buller VG, Jansen E, Lamb HJ, Baur LH, van der Wall EE, de RA, Reiber JH (1997) Comparison between manual and semiautomated analysis of left ventricular volume parameters from short-axis MR images. J Comput Assist Tomogr 21:756-765

van der Geest RJ, Reiber JH (1999) Quantification in cardiac MRI. J Magn Reson Imaging 10:602-608

van Deutekom JC, Bremmer-Bout M, Janson AA, Ginjaar IB, Baas F, den Dunnen JT, van Ommen GJ (2001) Antisense-induced exon skipping restores dystrophin expression in DMD patient derived muscle cells. Hum Mol Genet 10:1547-1554

van Deutekom JC, Janson AA, Ginjaar IB, Frankhuizen WS, Aartsma-Rus A, Bremmer-Bout M, den Dunnen JT, Koop K, van der Kooi AJ, Goemans NM, de Kimpe SJ, Ekhart PF, Venneker EH, Platenburg GJ, Verschuuren JJ, van Ommen GJ (2007) Local dystrophin restoration with antisense oligonucleotide PRO051. N Engl J Med 357:2677-2686

van Erp C, Loch D, Laws N, Trebbin A, Hoey AJ (2010) Timeline of cardiac dystrophy in 3-18-month-old *mdx* mice. Muscle Nerve 42:504-513

van Putten M, de Winter CL, van Roon-Mom W, van Ommen GJ, 't Hoen PA, Aartsma-Rus A (2010) A 3 months mild functional test regime does not affect disease parameters in young *mdx* mice. Neuromuscul Disord 20:273-280

van Putten M, Hulsker M, Nadarajah VD, van Heiningen SH, van Huizen E, van Iterson M, Admiraal P, Messemaker T, den Dunnen JT, 't Hoen PA, Aartsma-Rus A (2012a) The effects of low levels of dystrophin on mouse muscle function and pathology. PLoS One 7:e31937

van Putten M, Kumar D, Hulsker M, Hoogaars WM, Plomp JJ, van Opstal A, van Iterson M, Admiraal P, van Ommen GJ, 't Hoen PA, Aartsma-Rus A (2012b) Comparison of skeletal muscle pathology and motor function of dystrophin and utrophin deficient mouse strains. Neuromuscul Disord 5:406-417

Verhaart IE, Heemskerk H, Karnaoukh TG, Kolfschoten IG, Vroon A, van Ommen GJ, van Deutekom JC, Aartsma-Rus A (2012) Prednisolone Treatment Does Not Interfere with 2'-O-Methyl Phosphorothioate Antisense-Mediated Exon Skipping in Duchenne Muscular Dystrophy. Hum Gene Ther 3:262-273

Verhaart IE, van Duijn RJ, den Adel B, Roest AA, Verschuuren JJ, Aartsma-Rus A, van der Weerd L (2011) Assessment of cardiac function in three mouse dystrophinopathies by magnetic resonance imaging. Neuromuscul Disord 5:418-426

Vetrone SA, Montecino-Rodriguez E, Kudryashova E, Kramerova I, Hoffman EP, Liu SD, Miceli MC, Spencer MJ (2009) Osteopontin promotes fibrosis in dystrophic mouse muscle by modulating immune cell subsets and intramuscular TGF-beta. J Clin Invest 119:1583-1594

Vilquin JT, Brussee V, Asselin I, Kinoshita I, Gingras M, Tremblay JP (1998) Evidence of *mdx* mouse skeletal muscle fragility in vivo by eccentric running exercise. Muscle Nerve 21:567-576

Webster C, Silberstein L, Hays AP, Blau HM (1988) Fast muscle fibers are preferentially affected in Duchenne muscular dystrophy. Cell 52:503-513

Weller B, Karpati G, Carpenter S (1990) Dystrophin-deficient *mdx* muscle fibers are preferentially vulnerable to necrosis induced by experimental lengthening contractions. J Neurol Sci 100:9-13

Wells DJ, Wells KE, Asante EA, Turner G, Sunada Y, Campbell KP, Walsh FS, Dickson G (1995) Expression of human full-length and minidystrophin in transgenic *mdx* mice: implications for gene therapy of Duchenne muscular dystrophy. Hum Mol Genet 4:1245-1250

Wersinger E, Bordais A, Schwab Y, Sene A, Benard R, Alunni V, Sahel JA, Rendon A, Roux MJ (2011) Re-Evaluation of Dystrophins Localization in the Mouse Retina. Invest Ophthalmol Vis Sci 11:7901-7908

Whitehead NP, Yeung EW, Allen DG (2006) Muscle damage in *mdx* (dystrophic) mice: role of calcium and reactive oxygen species. Clin Exp Pharmacol Physiol 33:657-662

Wiesen MH, Bogdanovich S, Agarkova I, Perriard JC, Khurana TS (2007) Identification and characterization of layer-specific differences in extraocular muscle m-bands. Invest Ophthalmol Vis Sci 48:1119-1127

Willmann R, De Luca A, Benatar M, Grounds M, Dubach J, Raymackers JM, Nagaraju K (2011) Enhancing translation: Guidelines for standard pre-clinical experiments in *mdx* mice. Neuromuscul Disord 1:43-49

Willmann R, Possekel S, Dubach-Powell J, Meier T, Ruegg MA (2009) Mammalian animal models for Duchenne muscular dystrophy. Neuromuscul Disord 19:241-249

Wilson J, Putt W, Jimenez C, Edwards YH (1999) Up71 and up140, two novel transcripts of utrophin that are homologues of short forms of dystrophin. Hum Mol Genet 8:1271-1278

Wilton SD, Lloyd F, Carville K, Fletcher S, Honeyman K, Agrawal S, Kole R (1999) Specific removal of the nonsense mutation from the *mdx* dystrophin mRNA using antisense oligonucleotides. Neuromuscul Disord 9:330-338

Winder SJ, Gibson TJ, Kendrick-Jones J (1995) Dystrophin and utrophin: the missing links! FEBS Lett 369:27-33

Wooddell CI, Zhang G, Griffin JB, Hegge JO, Huss T, Wolff JA (2010) Use of Evans blue dye to compare limb muscles in exercised young and old *mdx* mice. Muscle Nerve 41:487-499

Wu B, Xiao B, Cloer C, Shaban M, Sali A, Lu P, Li J, Nagaraju K, Xiao X, and Lu QL (2011) One-year treatment of morpholino antisense oligomer improves skeletal and cardiac muscle functions in dystrophic *mdx* mice. Mol Ther 19:576-583

Wu ZS, Wu Q, Yang JH, Wang HQ, Ding XD, Yang F, Xu XC (2008) Prognostic significance of MMP-9 and TIMP-1 serum and tissue expression in breast cancer. Int J Cancer 122:2050-2056

Yilmaz A, Gdynia HJ, Baccouche H, Mahrholdt H, Meinhardt G, Basso C, Thiene G, Sperfeld AD, Ludolph AC, and Sechtem U (2008) Cardiac involvement in patients with Becker muscular dystrophy: new diagnostic and pathophysiological insights by a CMR approach. J Cardiovasc Magn Reson 10,50

Yin H, Moulton HM, Betts C, Merritt T, Seow Y, Ashraf S, Wang Q, Boutilier J, Wood MJ (2010) Functional rescue of dystrophin-deficient *mdx* mice by a chimeric peptide-PMO. Mol Ther 18:1822-1829

Yin H, Moulton HM, Betts C, Seow Y, Boutilier J, Iverson PL, Wood MJ (2009) A fusion peptide directs enhanced systemic dystrophin exon skipping and functional restoration in dystrophin-deficient *mdx* mice. Hum Mol Genet 18:4405-4414

Yin H, Moulton HM, Seow Y, Boyd C, Boutilier J, Iverson P, Wood MJ (2008) Cell-penetrating peptide-conjugated antisense oligonucleotides restore systemic muscle and cardiac dystrophin expression and function. Hum Mol Genet 17:3909-3918

Yin H, Saleh AF, Betts C, Camelliti P, Seow Y, Ashraf S, Arzumanov A, Hammond S, Merritt T, Gait MJ, Wood MJ (2011) Pip5 transduction peptides direct high efficiency oligonucleotide-mediated dystrophin exon skipping in heart and phenotypic correction in *mdx* mice. Mol Ther 19:1295-1303

Yokota T, Lu QL, Morgan JE, Davies KE, Fisher R, Takeda S, Partridge TA (2006) Expansion of revertant fibers in dystrophic *mdx* muscles reflects activity of muscle precursor cells and serves as an index of muscle regeneration. J Cell Sci 119:2679-2687

Yokota T, Lu QL, Partridge T, Kobayashi M, Nakamura A, Takeda S, Hoffman E (2009) Efficacy of systemic morpholino exon-skipping in Duchenne dystrophy dogs. Ann Neurol 65:667-676

Yue Y, Liu M, Duan D (2006) C-terminal-truncated microdystrophin recruits dystrobrevin and syntrophin to the dystrophin-associated glycoprotein complex and reduces muscular dystrophy in symptomatic utrophin/dystrophin double-knockout mice. Mol Ther 14:79-87

Zhang W, ten Hove M, Schneider JE, Stuckey DJ, Sebag-Montefiore L, Bia BL, Radda GK, Davies KE, Neubauer S, Clarke K (2008) Abnormal cardiac morphology, function and energy metabolism in the dystrophic *mdx* mouse: an MRI and MRS study. J Mol Cell Cardiol 45:754-760

Zhou L, Rafael-Fortney JA, Huang P, Zhao XS, Cheng G, Zhou X, Kaminski HJ, Liu L, Ransohoff RM (2008) Haploinsufficiency of utrophin gene worsens skeletal muscle inflammation and fibrosis in *mdx* mice. J Neurol Sci 264:106-111

Discussion

With several clinical trials ongoing aiming to restore dystrophin synthesis, more attention has been drawn to answering the most tempting question; how much dystrophin is needed to delay and/or prevent disease pathology and improve muscle function in DMD patients? The definite answer to this is rather complex as many factors need to be considered. This thesis covers many of these aspects, although several more still remain to be answered.

First of all, the amount of dystrophin needed depends on whether the newly synthesized dystrophin protein will be full-length, which might be achieved with e.g. stem cell therapy, or whether it is an internally truncated dystrophin obtained by e.g. gene therapy or AON-mediated exon skipping. In mice, full-length dystrophin is more effective than truncated dystrophin. Differences in efficacy between different truncated dystrophins are also expected, as the phenotype of BMD patients expressing different truncated dystrophin also varies between individuals.

Second, the way in which dystrophin will be expressed differs between the different types of treatment. Stem cell, PMO-mediated exon skipping and gene therapy result in dystrophin expression in a mosaic manner, whereas gentamycin administration and 2OMePS-mediated exon skipping result in a more uniformly expressed dystrophin pattern. Additionally, although stem cell therapy results in fibers expressing dystrophin at wild type intensities, the other therapies will likely result in intensities that are significantly lower and that might differ from muscle to muscle. Both the type and levels of dystrophin expression largely influences its ability to protect fibers against pathology. Especially when dystrophin is expressed in a mosaic manner, the distribution of dystrophin within a fiber will probably largely influence its protective effect. Large dystrophin negative clusters might still be prone to injury and are likely to be replaced by either smaller dystrophin negative clusters or more homogenous dispersion. Nevertheless it seems that dystrophin positive fibers create a beneficial environment for dystrophin negative ones and thereby enhance their survival. There might however be a threshold to the number of dystrophin positive parts within a fiber needed to ensure such an environment. Interestingly, limited studies in *mdx* mice have shown that a uniform expression will probably protect fibers better than when similar amounts of total protein are expressed in a mosaic manner. Extensive studies addressing these issues are lacking. In the same line, it is also interesting to know how much dystrophin can migrate over the membrane away from its transcription side.

The levels of dystrophin needed might also vary between different skeletal muscles. It is likely that slow fibers require less dystrophin than fast fibers to ensure protection against pathology. Likewise, muscles undergoing great workloads might be more demanding.

So far, the heart appeared to be very challenging to target. Dystrophin restoration in skeletal muscle potentially results in higher activity levels in DMD patients, which subsequently increases the workload for the heart. As DMD patients already suffer from dilated cardiomyopathy this might worsen its progression. The few publications available on this topic showed that 50% of dystrophin is sufficient to prevent heart failure, but based on our study we know that levels <22% already improve heart function significantly. Others have shown that low

dystrophin levels in the diaphragm also partly prevent against heart failure in mice. With the studies described in this thesis and those performed by others more insight has been obtained regarding the protective effect of low dystrophin levels in several mouse models for DMD. So far, conclusions based on mouse studies show strong similarities with the limited amount of human case reports available and with results obtained from gentamycin upregulation. This indicates that results obtained in mice are probably useful in translation to conclusions with respect to the dystrophin levels needed in humans. It is however unknown which effect size in mice is needed (e.g. improvement of 30% in the hanging wire test) to obtain clinically relevant effects in DMD patients. It might be that specific improvements obtained with low dystrophin levels in mice do have a less benefit in the larger muscles of the human body. Undoubtedly, the timing of initiation of dystrophin expression will largely influence the efficacy of the therapy. Ongoing clinical trials will probably gives more insight in these matters.

Summary

Duchenne muscular dystrophy (DMD) is the most prevalent neuromuscular disorder, affecting 1:4000 boys. The first symptoms, consisting of difficulties in running, climbing stairs and standing from the ground become apparent by the age of three. Loss of muscle fibers leads to wheelchair dependency from the age of 12 years onwards. Patients die due to respiratory and heart failure around the age of 30. Although symptomatic treatment has significantly improved life expectancy in the Western world, no therapy is available yet.

DMD is caused by mutations in the *DMD* gene which encodes the protein dystrophin. Dystrophin forms a bridge between the sarcolemma and the extracellular matrix and provides stability to muscle fibers during contractions. In the absence of dystrophin, fibers are more prone to exercise-induced damage. This leads to continuous necrosis of muscle fibers which is compensated for by regeneration. Upon exhaustion of the regenerative capacity fibers are replaced by fibrotic and fat tissue, leading to a loss of muscle function.

In healthy individuals the *DMD* gene transcribes dystrophin according to a reading frame in which three mRNA nucleotides contain information for one amino acid (THE DOG BIT THE CAT). Reading frame disrupting mutations, like those found in DMD patients, result in premature termination of protein synthesis (THE DOG BIT HEC AT). In-frame mutations result in transcription of a shortened, but functional protein as both begin and end regions are conserved (THE DOG BIT CAT). These mutations are present in Becker muscular dystrophy (BMD) patients, which express low levels of dystrophin that generally results in a milder phenotype.

Using antisense oligonucleotides (AON) the disrupted reading frame in DMD patients can be restored, allowing synthesis of shorter but partly functional BMD-like dystrophin. At best, this and other clinical interventions result in the expression of low dystrophin levels. Fortunately, expression of wild type levels is not needed, as both humans and mice expressing ~50% of dystrophin do not show pathology. Even expression of ~30% of dystrophin has been found to result in a mild phenotype. Detailed studies on which levels of dystrophin are needed to increase muscle integrity, prevent muscle damage and improve muscle function have been performed in this thesis.

To do so we first had to set up good outcome measures. To assess motor function in *mdx* mice without interfering with the natural course of the disease a functional test regime consisting of four different functional tests was designed. In Chapter 2 we show that this type of exercise indeed did not interfere with disease pathology. Thereupon, we determined motor function in several mouse models for DMD (Chapter 3). We observed that motor function in mice that either did not express utrophin or in a monoallelic manner is significantly impaired compared to that of *mdx* mice. Additionally we identified MMP-9 and TIMP-1 as suitable serum biomarkers to monitor disease progression in both human and mouse samples (Chapter 4). Having good biomarkers is essential as patients need to be repeatedly treated with AONs whereas treatment efficacy cannot be determined on biopsies on a regular basis.

These tools were further validated and used in two new innovative mouse models expressing low levels of dystrophin. The first model was generated by crossing mice with a

mutation in the *Xist* gene (*Xist*$^{\Delta hs}$) with *mdx* mice. In female *mdx-Xist*$^{\Delta hs}$ embryos X-chromosomes that carried the mutated *Xist* gene but expressed intact dystrophin were preferably inactivated. This resulted in the expression of low dystrophin levels in a utrophin positive background (Chapter 5). We observed that dystrophin levels <15% already resulted in significantly improved muscle performance, while histopathology was largely prevented in mice expressing >15% dystrophin. Higher dystrophin levels (>22%) were needed to protect muscles from damage initiated by chronic treadmill exercise. So far, AON delivery to skeletal muscle is much easier to achieve than to the heart which appears to be a very difficult target. In mice, partly restored dystrophin expression in skeletal muscle increases voluntary activities thereby increasing the workload for the heart. The *mdx-Xist*$^{\Delta hs}$ mouse was used to study whether low dystrophin levels in heart can delay or prevent the onset of dilated cardiomyopathy (Chapter 6). Dystrophin levels between 3 and 21% already prevented the development of dilated cardiomyopathy in 10 months old dystrophic mice.

Mdx mice are less severely affected than DMD patients due to over expression of the dystrophin homologue utrophin, which compensates for its absence. Mice lacking both proteins mimic the human phenotype and die before the age of 12 weeks. To determine the effect of low dystrophin levels in these mice *mdx/utrn*$^{+/-}$ mice were crossed with *utrn*$^{-/-}$ *Xist*$^{\Delta hs}$ mice (Chapter 7). Again, based on skewed X-inactivation these mice expressed dystrophin levels <50%. In these mice, <10% dystrophin already significantly improved life expectancy and muscle function. To reduce histopathology >10% dystrophin was needed.

Based on these results it can be concluded that <10% dystrophin already improves the dystrophic phenotype to some extent, but >10% is needed to protect muscles from disease pathology. These findings are encouraging for ongoing and future clinical trails.

Samenvatting voor niet ingewijden

Duchenne spierdystrofie (DMD) is de meest voorkomende neuromusculaire aandoening die 1 op de 4000 jongens treft. De eerste symptomen zijn zichtbaar vanaf het 3e levensjaar en omvatten moeite met rennen, traplopen en opstaan. Door verlies van spiervezels worden de jongens rond hun 12e rolstoelafhankelijk en overlijden ze rond hun 30e veelal als gevolg van ademhalings en hartfalen. Ondanks dat de levensverwachting in de Westerse wereld is gestegen door verbeterde zorg en in het bijzonder beademingsondersteuning, is er tot op heden geen therapie.

DMD wordt veroorzaakt door mutaties in het *DMD* gen welke codeert voor het eiwit dystrofine. Dystrofine vormt een brug tussen het sarcolemma en de extracellulaire matrix en geef zo stabiliteit aan spiervezels tijdens contracties. In afwezigheid van dystrofine zijn deze vatbaarder voor schade tijdens beweging. Dit resulteert in een chronisch verlies van spiervezels wat tot op zekere hoogte wordt opgevangen door regeneratie. Wanneer de regeneratie capaciteit van de spier is uitgeput worden ze vervangen door bindweefsel en vet.

In gezonde personen wordt het *DMD* gen afgeschreven volgens een leesraam waarbij elke drie mRNA bouwstenen de informatie bevatten voor één aminozuur (LEO EET EEN KIP). DMD patiënten hebben mutaties die het leesraam vertoren wat leidt tot een voortijdige stop van de eiwit synthese (LEO EET ENK IP). Mutaties waarbij het leesraam intact blijft, zoals die bij Becker spierdystrofie (BMD) patiënten, resulteren in de synthese van een kleiner maar functioneel eiwit gezien zowel het begin als eind van het eiwit aanwezig is (LEO EET KIP). BMD patiënten brengen kleine hoeveelheden dystrofine tot expressie en zijn daardoor minder ernstig aangedaan.

In DMD patiënten kan met behulp van antisense oligonucleotiden (AON) het leesraam worden hersteld waardoor een korter maar deels functioneel Becker-achtig dystrofine wordt aangemaakt. Hoogstwaarschijnlijk zullen deze en andere klinische interventies niet resulteren in het herstel van dystrofine expressie op wild type niveau. Gelukkig is dat waarschijnlijk ook niet nodig gezien zowel mensen als muizen die ~50% dystrofine tot expressie brengen niet zijn aangedaan. Op basis van een case report is het bekend dat zelfs 30% dystrofine kan leiden tot een mild fenotype. Gedetailleerde studies naar welke hoeveelheden dystrofine leiden tot verbeterde spier integriteit, bescherming tegen spierschade en verbetering van spierfunctie zijn beschreven in dit proefschrift.

Allereerst hebben we een functioneel test regime opgezet bestaande uit vier functionele testen om spierfunctie in *mdx* muizen te bepalen zonder daarbij het natuurlijk ziektebeloop te beïnvloeden (Hoofdstuk 2). Met behulp hiervan hebben we de spierfunctie van verschillende muismodellen voor DMD bepaald (Hoofdstuk 3). We zagen dat de spierfunctie van muizen die geen utrofine tot expressie brengen of op één allel een significant slechtere spierfunctie hebben in vergelijking tot *mdx* muizen. Daarnaast hebben we bewezen dat MMP-9 en TIMP-1 geschikte serum biomarkers zijn om het ziektebeloop in mens en muis te bepalen (Hoofdstuk 4). Gezien patiënten herhaaldelijk moeten worden behandeld met AONs en het effect van behandeling niet continu via biopten kan worden bepaald is het essentieel om te beschikken over goede biomarkers.

Zowel het functionele test regime als de serum biomarkers werden vervolgens gevalideerd en gebruikt in twee nieuwe innovatieve muis modellen die lage hoeveelheden dystrofine tot expressie brengen. Het eerste model werd gegenereerd door muizen met een mutatie in het *Xist* gen (*Xist*$^{\Delta hs}$) te kruizen met *mdx* muizen. In de vrouwelijke *mdx-Xist*$^{\Delta hs}$ embryo's werd voornamelijk het X-chromosoom geïnactiveerd dat het gemuteerde *Xist* gen bevatte, maar dat intact dystrofine tot expressie bracht. Dit resulteerde in expressie van een laag percentage dystrofine in een utrofine positieve achtergrond (Hoofdstuk 5). We zagen dat spierfunctie significant verbeterde in muizen met <15% dystrofine, terwijl histopathologie sterk afnam bij >15% dystrofine. Meer dystrofine (>22%) is nodig om spieren te beschermen tegen schade die wordt geïnduceerd door blootstelling aan rennen op een loopband op een chronische basis. Hoewel AONs succesvol opgenomen worden door skeletspieren blijkt het hart moeilijker te behandelen. Deels herstelde dystrofine expressie in skeletspieren verhoogt vrijwillige activiteit in muizen wat voor een grotere belasting voor het hart zorgt. In *mdx-Xist*$^{\Delta hs}$ muizen werd bepaald of lage hoeveelheden dystrofine in het hart het ontstaan van gedilateerde cardiomyopathie kan uitstellen of zelfs voorkomen (Hoofdstuk 6). Tussen de 3 en 21% dystrofine was al afdoende om gedilateerde cardiomyopathie te voorkomen op een leeftijd van 10 maanden.

Mdx muizen zijn veel minder ernstig aangedaan dan DMD patiënten doordat zij de dystrofine homoloog utrofine tot overexpressie brengen, wat compenseert voor de afwezigheid van dystrofine. Muizen die beide eiwitten missen hebben een vergelijkbaar fenotype als DMD patiënten en sterven al voor ze de leeftijd van 12 weken bereiken. Om te bepalen wat het effect van lage hoeveelheden dystrofine in deze muizen is hebben we *mdx/utrn* $^{+/-}$ muizen gekruist met *utrn* $^{-/-}$ *Xist*$^{\Delta hs}$ muizen (Hoofdstuk 7). Ook bij deze muizen resulteert niet-random X-inactivatie in dystrofine levels van <50%. We observeerden dat <10% dystrofine levensverwachting en spierfunctie verbeterd in deze muizen. Om histopathologie te verbeteren was >10% dystrofine nodig.

Gebaseerd op deze resultaten kan worden geconcludeerd dat <10% dystrofine het fenotype al tot op zekere hoogte verbeterd. Echter is >10% dystrofine noodzakelijk om spieren te beschermen tegen pathologie. Deze bevindingen zijn zeer bemoedigend voor gaande en toekomstige klinische studies.

Bibliography

M. Hulsker, **M. van Putten**, A.M. Aartsma-Rus. *A new and quick Western blot system for dystrophin detection.* Manuscript in preparation

M. van Putten, M. Hulsker, C. Young, V.D. Nadarajah, H. Heemskerk, L. van der Weerd, G.J.B. van Ommen, A.M. Aartsma-Rus. *Low dystrophin levels increase survival and improve muscle pathology and function in dystrophin/utrophin double knockout mice.* Submitted

M. van Putten, E.M. van der Pijl, M. Hulsker, V.D. Nadarajah, I.E. Verhaart, L. van der Weerd, A.M. Aartsma-Rus. *Low dystrophin levels in heart are sufficient to delay heart failure in mdx mice.* Submitted

C.L. Tanganyika-de Winter, H. Heemskerk, T.G. Karnaoukh, **M. van Putten**, S.J. de Kimpe, J. van Deutekom and A.M. Aartsma-Rus. *Long term exon skipping studies with 2'-O-methyl phosphorothioate antisense oligonucleotides in dystrophic mouse models.* Molecular Therapy–Nucleic Acids. 2012

M. van Putten, M. Hulsker, V.D. Nadarajah, S.H. van Heiningen, E. van Huizen, M. van Iterson, P. Admiraal, T. Messemaker, J.T. den Dunnen, P.A.C. 't Hoen, A.M. Aartsma-Rus. *The effects of low levels of dystrophin on mouse muscle function and pathology.* PLoS One. 2012

M. van Putten, D. Kumar, M. Hulsker, W.M.H. Hoogaars, J.J. Plomp, A. van Opstal, M. van Iterson, P. Admiraal, G.J.B. van Ommen, P.A.C. 't Hoen, A.M. Aartsma-Rus. *Comparison of skeletal muscle pathology and motor function of dystrophin and utrophin deficient mouse strains.* Neuromuscular Disord. 2012

M. van Putten, A.M. Aartsma-Rus. *Opportunities and challenges for the development of antisense treatment in neuromuscular disorders.* Expert Opin Biol Ther. 2011

V.D. Nadarajah, **M. van Putten**, A. Chaouch, P. Garrood, V. Straub, H. Lochmüller, H.B. Ginjaar, A.M. Aartsma-Rus, G.J.B. van Ommen, J.T. den Dunnen, P.A.C. 't Hoen. *Serum matrix metalloproteinase-9 (MMP-9) as a biomarker for monitoring disease progression in Duchenne muscular dystrophy (DMD).* Neuromuscul Disord. 2011

T.J. van Dooren, H.A. van Goor, **M. van Putten**. *Handedness and asymmetry in scale-eating cichlids: antisymmetries of different strength.* Evolution. 2010

M. van Putten, C. de Winter, W.M. van Roon-Mom, G.J.B. van Ommen, P.A.C. 't Hoen, A.M. Aartsma-Rus. *A 3 months mild functional test regime does not affect disease parameters in young mdx mice.* Neuromuscul Disord. 2010

Curriculum Vitae

Maaike van Putten was born on January 11th 1984 in Haarlem, the Netherlands. She attended Lyceum Sancta Maria, and obtained her HAVO degree in 2001. Subsequently, she attended Biology and Medical Laboratory Sciences at the Hogeschool Leiden, where she specialized in working with experimental animals (art.12). Her bachelor internship focussed on the role of dietary folic acid and DNA methylation in utero on vascular damage and was conducted at the department of Human Genetics of the Leiden University Medical Center under supervision of Prof.dr J.A.P. Willems van Dijk. She continued working as a research technician in the summer after graduating for her Bachelor degree in 2005.

Based on her strong interest for animals, she started the Master Animal Biology at the Leiden University and conducted two internships. First, she studied the effect of daily show performances on behaviour and vocalisation of bottlenose dolphins under supervision of Dr. S. Kuczaj and Prof.dr. C. ten Cate (dept. Animal Behaviour, Leiden University) at the Marine Mammal and Cognition Laboratory of the University of Southern Mississippi (USA). Her second internship was completed under supervision of Dr. T.J.M. van Dooren at the Animal Ecology department of the Leiden University where she investigated the role of foraging behaviour on the ability of adaptation in mouth opening asymmetry in scale-eating cichlids. She graduated for her Master degree in 2007.

In September 2007, she started her PhD research at the department of Human Genetics ot the Leiden University Medical Center under supervision of Prof.dr. G.J.B. van Ommen and Dr. A.M. Aartsma-Rus. The results of the work conducted are presented in this thesis. During her PhD, Maaike was a working group member of the TREAT-NMD network of excellence and the Wellstone Center. She developed standard operating procedures to unify experimental protocols used to test the effects of new treatments in animal models for DMD.

With the personal financial support she received from the Bontius Fellowship, Maaike has investigated physiological parameters in *mdx-Xist*$^{\Delta hs}$ and *mdx-utrn* $^{-/-}$*/Xist*$^{\Delta hs}$ mice in the group of Prof.dr. D.J. Wells at the Royal Veterinary College in London. Currently, she continues her work as a post doctoral researcher at the department of Human Genetics of the Leiden University Medical Center.

Acknowledgements

Ik heb een ontzettend leuke tijd gehad tijdens mijn promotie onderzoek en zou iedereen willen bedanken die op enige wijze heeft bijgedragen aan de totstandkoming van mijn proefschrift.

Gert-Jan, bedankt voor je betrokkenheid bij mijn onderzoek, je suggesties tijdens de experimenten en je kritische kijk op mijn manuscripten. Jouw input heb ik altijd als zeer waardevol beschouwd.

Annemieke, jouw inzet en enthousiasme voor het onderzoek werkten zeer inspirerend en je was mijn rots in de branding als ik het even niet meer zag zitten. Bedankt voor je vertrouwen, je begeleiding en dat je mij de mogelijkheid bood deel uit te maken van de (inter)nationale 'Duchenne familie'.

Margriet, jouw bijdrage aan dit proefschrift is enorm. Dank voor al je inzet en hulp; als er iemand gedreven is dan ben jij het wel, zowel in het lab als in de fotografie. Het was zeer plezierig om met je samen te werken en ik kijk ernaar uit om deze samenwerking voort te zetten.

Ook wil ik graag mijn (oud) kamer genoten bedanken; Hans, Christa, Dwi, Emile, Laura, Pietro, Silvana, Stijn en Monica. Door jullie ben ik elke dag met veel plezier naar mijn werk gegaan. Ik heb een ontzettend leuke tijd op onze koe-kamer gehad, waar ik mij al vanaf de eerste dag op m'n plek voelde. Ik kon altijd bij jullie terecht met mijn vragen en frustraties en het was fijn mijn enthousiasme over o.a. leuke resultaten met jullie te kunnen delen. Ik zal in de toekomst proberen om vaker samen met jullie lunchen in plaats van achter de computer te blijven zitten ☺. Daarnaast wil ik ook de andere exon-skippers; Isabella, Ingrid, Marcel, Willem, Nisha en Peter-Bram bedanken voor jullie hulp met de muizen, de statistiek en elk ander gebied.

Verder wil ik de rest van Lab-J en de afdeling Humane Genetica bedanken voor de hulp en gezelligheid. Het is zeer plezierig en stimulerend om in zo'n hechte onderzoeksgroep en afdeling te mogen werken, waar iedereen open staat voor elkaar en bereid is elkaar te helpen.

I also learned a lot from my students Tobias, Lincy, Darshan, Ella, Peter, Annemarieke, Lizette and Courtney. Thank you all for the work and dedication you put into your projects. You taught me how to be a better teacher.

Naast mijn collega's heb ik ook veel gehad aan de afleiding die mijn vrienden mij boden. Voornamelijk mijn voormalige HBO-labmaatjes Karijn, Ramona en Marthe hebben mij enorm gesteund. Maar ook de gezellige avonden/weekenden met Danique, Marije, Daniëlle, Susan en mijn Jovink en Normaal moaties waren onvergetelijk.

Ook wil ik graag mijn familie bedanken; Ookal ging het soms boven jullie pet en was het lastig te begrijpen wat alles inhield, jullie interesse in mijn onderzoek bleef bestaan.

In het bijzonder wil ik Oma van Putten bedanken; het is fijn om een passie voor dieren en natuur met iemand te delen die er hetzelfde over denkt. En opa en oma Rutte; dank dat jullie in mij geloofden en hebben voorgehouden dat je ergens voor moet gaan zonder ooit op te geven. Jullie toonden altijd interesse in mijn bezigheden op school. Ik weet zeker dat jullie daar boven trots op me zijn!

Stef en Lana, bedankt voor alle steun die ik van jullie heb gehad; jullie waren er altijd voor mij en betekenen veel voor me.

Ruud en Rini, de weg die heeft geleidt tot dit boekje had ik niet zonder jullie kunnen bewandelen. Jullie hebben aan één blik genoeg om te weten hoe ik mij voel, kennen mij door en door en sturen mij waar nodig. Dank voor al jullie steun en vertrouwen.

Ze zeggen wel eens, je moet het beste voor het laatste bewaren. In mijn leven is dat Bas. Lief, ik wil je bedanken voor al je geduld, je hulp en luisterend oor en het eten dat s'avonds op tafel stond koud te worden omdat ik nog 'even' wat op het lab af moest maken. Jij hebt mij enorm gesteund in mijn werk, probeerde altijd oplossingen voor problemen te vinden, en maakte het mij mogelijk om uiteindelijk tot dit eindresultaat te komen. Ik vind het geweldig dat jij in me gelooft, ookal betekende dat bijvoorbeeld dat je me dit jaar bijna niet hebt gezien. Die onvoorwaardelijke steun houdt me op de been en ik put er veel geluk en warmte uit.

Bedankt voor alles.

Maaike